

**Regulation of Basidiomycete Small Molecules during
Co-culturing**

Dissertation

To Fulfill the
Requirements for the Degree of
“Doctor of Philosophy” (PhD)

**Submitted to the Council of the Faculty of
Biology and Pharmacy
of the Friedrich Schiller University Jena**

by James Patrick Tauber, M.Sc.

**born on January 23, 1989
in Washington, D.C., USA**

Die Arbeiten zur Erlangung des akademischen Doctor of Philosophy (PhD) wurden im Zeitraum von Oktober 2014 bis September 2017 am Lehrstuhl für Pharmazeutische Mikrobiologie der Friedrich-Schiller-Universität Jena unter der Leitung von Prof. Dr. Dirk Hoffmeister angefertigt. Die Arbeitsgruppe ist mit dem Leibniz-Institut für Naturstoff-Forschung und Infektionsbiologie, Hans-Knöll Institut Jena, assoziiert.

Dissertation, Friedrich-Schiller-University, Jena, 2018

Tag der öffentlichen Verteidigung: 05/11/2018

Gutachter 1: Prof. Dr. Dirk Hoffmeister (Friedrich-Schiller-University, Jena, Germany)

Gutachter 2: Prof. Dr. Erika Kothe (Friedrich-Schiller-University, Jena, Germany)

Gutachter extern: Prof. Jonathan S. Schilling (University of Minnesota, USA)

Table of contents

Summary.....	1
Zusammenfassung.....	3
1. Introduction	5
1.1. Fungal Natural product research.....	5
1.2. Classification of natural products.....	6
1.3. Nonribosomal peptide synthetase-like enzymes and compounds	9
1.3.1. Nonribosomal peptide synthetase-like overview	9
1.3.2. Atromentin	11
1.4. Overview of atromentin-derived pigments	12
1.5. Fungal chromophoric compounds in natural contexts	14
1.5.1. The ecological role of chromophoric compounds for basidiomycetes.....	15
1.5.2. Other fungal defense mechanisms	19
1.6. Aims and justification of this research	19
2. Manuscripts.....	21
2.1. Three Redundant Synthetases Secure Redox-Active Pigment Production in the Basidiomycete <i>Paxillus involutus</i>	21
2.2. A Fivefold Parallelized Biosynthetic Process Secures Chlorination of <i>Armillaria mellea</i> (Honey Mushroom) Toxins	46
2.3. Bacteria induce pigment formation in the basidiomycete <i>Serpula lacrymans</i>.....	60
2.4. Dissimilar pigment regulation in <i>Serpula lacrymans</i> and <i>Paxillus involutus</i> during inter-kingdom interactions	89
2.5. Analysis of basidiomycete pigments <i>in situ</i> by Raman spectroscopy	135
3. Unpublished results.....	168
3.1. RNA-sequencing of <i>Serpula lacrymans</i> – <i>Bacillus subtilis</i>.....	168
3.1.1. Methods	168
3.1.2. Results	170
3.2. Spectroscopic (MALDI-TOF-MS & MS²) analyses of pigments	176
3.2.1. Methods	177
3.2.2. Results	178
4. Discussion	184
4.1. Role and induction of natural products during co-culturing	184
4.2. Genetic regulation and bioprospecting of natural products in co-cultures.....	189
4.3. Bioinformatics and cellular regulation of natural product gene clusters.....	194
5. References.....	204
6. Acknowledgments	225

Summary

There is an increasing interest in microbial biological systems, the competition or cooperation within, and ensuing natural products that may be produced or suppressed. The focus of this work was to understand the role and regulation of basidiomycete natural products in co-cultures. Ecologically relevant model basidiomycetes like *Serpula lacrymans* and *Paxillus involutus*, whose genomes contain an unusually high number of yet to be characterized natural product genes, are ideal for such studies. Because basidiomycetes have not been extensively studied in this regard, our main objective was to shed new light into such basidiomycete biotic interactions and the ensuing natural products. Listed here are the main results from this dissertation:

- At least 13 different bacteria stimulated the production of atromentin-derived pigments (e.g. variegatic acid) in the brown-rotter *Serpula lacrymans*;
- Correspondingly, the atromentin gene cluster was induced;
- Pigment induction by bacteria was not observed in the taxonomically related, but mycorrhizae-forming fungus, *Paxillus involutus*;
- Enzymatic, but not mechanical, damage to *S. lacrymans* also induced pigmentation;
- Congruently, protease-inhibited *Bacillus subtilis* did not cause pigment induction;
- Variegatic acid from *S. lacrymans* inhibited movement of *B. subtilis* but did not kill the bacterium;

- Promoter motifs preceding key atromentin biosynthesis genes were found highly conserved in basidiomycetes, while certain motifs varied depending on lifestyle (brown-rotter vs. mycorrhizae);
- RNA-sequencing data from *S. lacrymans* - *B. subtilis* co-cultures provided additional insight into other simultaneously up-regulated genes that are involved in natural product biosynthesis, iron movement and stress;
- Raman spectroscopy was applied to facilitate the study of pigment induction in various multi-partner cultures by non-destructively fingerprinting compounds in the interaction zone; and
- Putatively new pigments were also preliminarily described.

This work provided the first experimental evidence that a basidiomycete natural product gene cluster (*i.e.*, atromentin) was inducible and co-regulated during trans-kingdom co-incubations. The combined results set the stage to study unexplored basidiomycete natural product regulatory processes using the atromentin gene cluster as a model.

Zusammenfassung

Es gibt ein zunehmendes Interesse an biologischen Systemen, den ihnen zugrunde liegenden Interaktionen, und Naturstoffe, die unter solchen Umständen induziert oder unterdrückt werden können. Der Schwerpunkt dieser Arbeit lag darin, die Rolle und Regulierung von Basidiomyceten-Naturstoffe in Co-Kulturen zu verstehen. Ökologische relevante Modell-Basidiomyceten wie *Serpula lacrymans* und *Paxillus involutus*, deren Genome für eine untypische hohe Anzahl von uncharakterisierten Naturstoffgenen kodieren, sind für solche Studien ideal. Da Basidiomyceten in dieser Hinsicht nicht ausgiebig untersucht wurden, war es unser Hauptziel, solche Interaktionen der Basidiomyceten und die resultierenden Naturstoffe zu identifizieren. Im Folgenden sind die wichtigsten Ergebnisse dieser Dissertation aufgeführt:

- Mindestens 13 verschiedene Bakterien könnten die Produktion von Atromentin-abgeleiteten Pigmenten in dem Braunfäuleerreger *Serpula lacrymans* stimulieren;
- Die Induktion durch Bakterien wurde jedoch nicht im Mykorrhiza-Pilz *Paxillus involutus* beobachtet, obwohl der Pilz taxonomisch verwandt war;
- Enzymatische, aber nicht mechanische, Beschädigung von *S. lacrymans* induzierte ebenfalls Pigmentierung;
- Zwei Pigmente aus *S. lacrymans* hemmten die Motilität von *Bacillus subtilis*, töteten aber nicht die Bakterien;
- Eine stark konservierte Promotorsequenz wurde vor den Atromentin-Biosynthesegenen gefunden. Weitere zwei Promotorsequenzen wurden

gefunden, deren An- oder Abwesenheit mit dem Lebensstil korrelierte (Braunfäuleerreger vs. Mykorrhiza);

- RNA-seq Daten von den Co-Kulturen *S. lacrymans* - *B. subtilis*- zeigten zusätzliche Einblicke in induzierte Stress- und Eisen-Genen;
- Raman-Spektroskopie wurde angewendet, um die Untersuchung der Pigmentinduktion in verschiedenen Multipartner-Kulturen zu erforschen; und
- Neue Pigmente wurde vorläufig beschrieben.

Unsere Arbeit erbrachte den ersten experimentellen Beweis, dass ein Naturstoff-Gen-cluster von einem Basidiomycete durch Co-Inkubationen induziert und co-reguliert wurde. Unsere Ergebnisse bereiten den Weg, um die bislang unerforschte Regulation von Naturstoffgenen in Basidiomyceten mit dem Atromentin-Gencluster modellhaft zu untersuchen.

1. Introduction

1.1. Fungal natural product research

Although estimations of the number of fungal species on Earth vary, an estimation by O'Brien and colleagues puts this number between 3.5 and 5.1 million species or more (1), with fungi encompassing all seven continents (2), and science has only described species mostly from the Ascomycota and Basidiomycota divisions, namely 98% of all described fungi (3). Aside from their global presence and ecological roles in nutrient cycling (4), a century of isolating and describing natural products from fungi has secured human's interest in them (5). The exemplar discovery in the early 20th century of the antibiotic penicillin produced by the fungus *Penicillium notatum* has ever since been critical in the advancement of medicine (6). Moreover, massive sequencing efforts have brought significant attention to the catalytic potential of basidiomycete fungi, in addition to the significant roles fungi play in natural systems (e.g. element cycling; (7, 8)). Although the basidiomycetes have entered the spotlight, lack of or reliable genetic manipulation and gene silencing techniques, as well as growth limitations (particularly for rust fungi and obligate mycorrhizae), have led to more research using other organisms (9). Despite the limitations, the future in natural product research on the underrepresented basidiomycetes has never been so promising as the amount of sequence data increases, the accessibility and technology of analytic chemistry improves (10, 11), new techniques for genetic manipulations become available (e.g. CRISPR/Cas9; (12)), and the interest in natural products with regard to natural systems continues to rise (13-15).

1.2. Classification of natural products

Natural products that are produced from living organisms can be categorized into 'primary metabolites' that are absolutely required for growth of an organism (e.g. fatty acids, nucleotides and amino acids), and 'secondary metabolites' that are not absolutely required for growth, although they speculatively increase an organism's fitness that confers a selective advantage (16). Alternatively, compounds can be categorized into 'basic integrated metabolism' that are the basis for all further produced compounds, 'supporting metabolism' that give "vitality" to the organism, and 'speculative metabolism' that we conventionally consider 'secondary metabolites' (17, 18).

Secondary metabolites are particularly interesting. This is because the enzymatic machinery behind their production can produce highly diverse and functionalized compounds (e.g. antibacterial, antifungal and cytotoxic compounds), thus providing or inspiring new drugs as well as increased interest in chemical ecology. Secondary metabolites thus fit into an evolutionary perspective when a species faces severe challenges. In response to such pressures that would essentially force a species to evolve, secondary metabolites should then come about at a higher rate than the metabolites that merely sustain or support growth. This has to occur at a low/reasonable cost (*i.e.*, structure-function cost), with a purpose (*i.e.*, functional), and all together increase the organisms' fitness in 'reasonable time' (18). Therefore, these diverse metabolites modulate various ways in which organisms have come to survive such as biofilm formation, metal acquisition, microbial communication (e.g. in diverse communities and within a population), morphological differentiation, virulence

(e.g., host-pathogen interactions), and growth competition (e.g., antimicrobials; (19, 20)).

Secondary metabolites are classified (albeit sometimes with disagreeing nomenclature) into i) terpenoids; ii) polyketides (PKs); iii) nonribosomal peptides (NRPs); iv) alkaloids; v) ribosomally synthesized and post-translationally modified peptides (RiPPs); and vi) combinations of the former: PKS-NRPS hybrid produced compounds, meroterpenoids (polyketide and terpenoid moieties), or NRPS-Dimethylallyl Tryptophan (DMAT) produced compounds (21, 22). These categories are not exhaustive, and as the synthetic synthesis of natural products as well as the discovery of new natural products progresses, there will be even more described chemical categories (23).

The canonical building units and enzymatic catalysis (excluding any post-synthesized tailoring) for the aforementioned categories follow suit: i) isoprene subunits via terpene synthases; ii) malonyl-CoA extender subunits via polyketide synthases (PKSs); iii) amino acids subunits via nonribosomal peptide synthetases (NRPSs); iv) aromatic amino acid subunits via NRPS-like enzymes; and v) peptides translated via ribosomes. The genes for these enzymes usually reside adjacent to other genes involved in the formation or regulation of the natural product (*i.e.*, they reside in a gene cluster), and these enzymes are considered the “backbone” of the cluster and are used to identify gene clusters in a genome (24).

Adding complexity to secondary metabolite production, the canonical catalyses noted above can vary. For example, NRPSs can incorporate non-proteinogenic amino acid, fatty acid and carboxylic acid building blocks (25, 26). Alkaloids like the medically-relevant muscarine, an ammonium quaternary alkaloid, and psilocybin, a tryptamine alkaloid, would in fact be missed if only seeking NRPS(-like) genes because their

biosynthesis is not dependent on such machinery (27, 28). As another example, PKSs may be iterative and/or highly-reducing which makes structure predictions very difficult (29, 30).

Figure 1-1 demonstrates the structural diversity of secondary metabolites from microorganisms using model examples from each category.

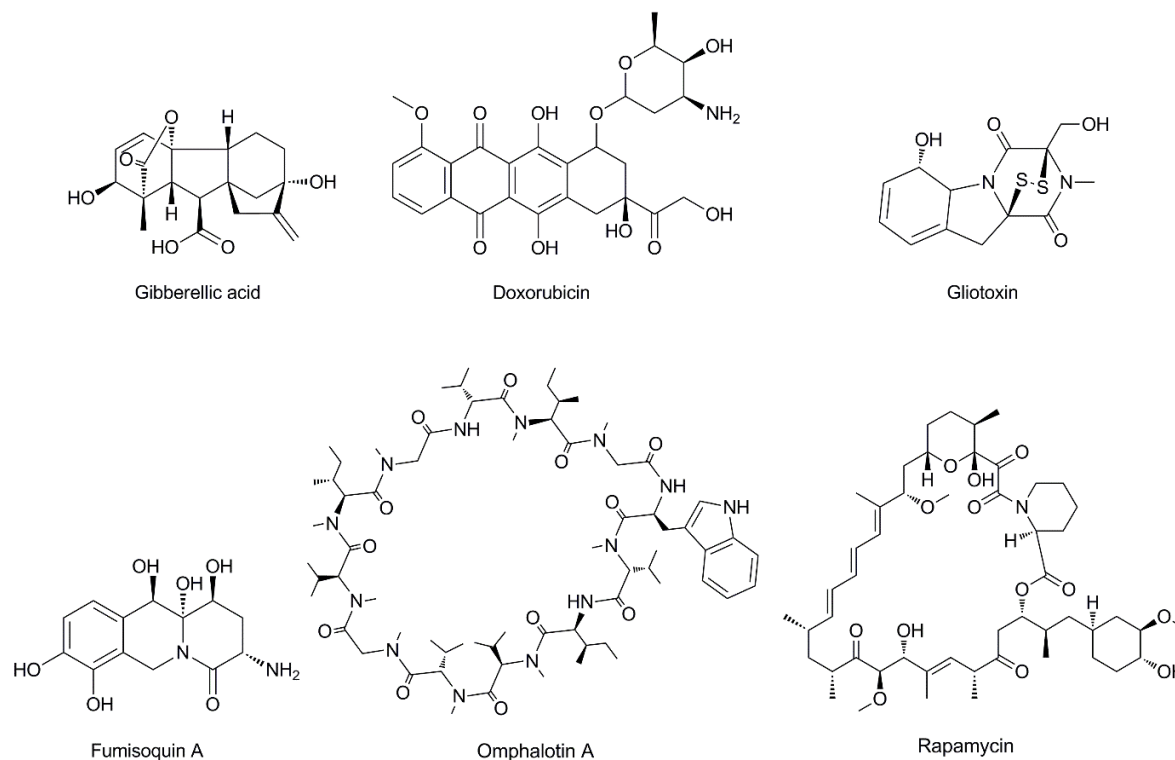


Figure 1-1: Structures of well-known secondary metabolites and an example per compound category: i) gibberellic acid, a hormone diterpenoid from *Aspergillus fumigatus* (31); ii) doxorubicin, an antibacterial polyketide from *Streptomyces peucetius* var. *caesius* (32); iii) gliotoxin, an immunosuppressant nonribosomal peptide from *A. fumigatus* (33); iv) fumisoquin A, an isoquinoline NRPS-like derived alkaloid from *Aspergillus fumigatus* (34); v) omphalotin A, a nematotoxic RiPP from *Omphalotus olearius* (35, 36); vi) rapamycin, a macrolide immunosuppressive PKS-NRPS produced compound from *Streptomyces hygroscopicus* (37, 38).

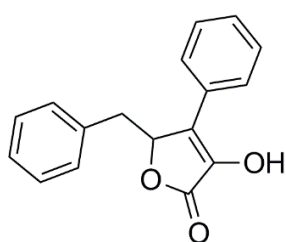
1.3. Nonribosomal peptide synthetase-like enzymes and compounds

1.3.1. Nonribosomal peptide synthetase-like overview

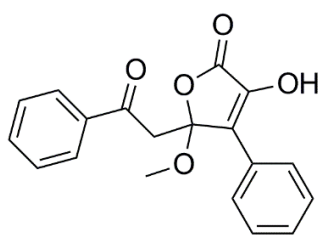
Fungal nonribosomal peptide synthetases are large, multi-domain proteins that canonically and minimally consist of a module with an adenylation domain (A), thiolation/peptidyl carrier protein domain (T/PCP), and a condensation domain (C; (24)). In short, the domain architecture follows an A-T-C setup. Using this minimalistic model, a compound is catalyzed as follows: the building block is adenylated by the A domain using ATP to form an aminoacyl-adenylate, which is transferred to the free thiol group of the T/PCP domain to form an aminoacyl-S-T, and then the C domain condenses two substrates (*i.e.*, the downstream growing peptidyl-S-T is combined with an upstream monomer and thus the product is elongated; (39)). While the final release step of the product from the enzyme in bacteria is typified by a final thioesterase (TE) domain in the final module, which releases by hydrolysis, cyclization or oligomerization (40), product release in fungi has evolved to use specialized C domains which can release the product by reduction (41) or cyclization (42).

NRPS-like dedicated enzymes are those that have a non-typical condensation domain while still retaining the canonical didomain (A-T-X). This is exemplified for adenylate-forming (NADPH-) reductases (A-T-R) which are characterized by modifying a substrate, rather than amide bond condensation, and a reductive release of the final product (43, 44). Prominent examples include LYS2 for L-lysine biosynthesis in *Saccharomyces cerevisiae* or SafA/SafB for saframycin biosynthesis

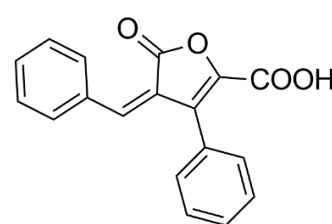
in *Myxococcus xanthus* (39, 45-47). Alternatively, the terminating domain may be a thioesterase domain (A-T-TE) whereby peptide formation and off-loading without a C domain is nonetheless possible. NRPS-like enzymes that have this module configuration are known to accept identical α -keto acids as substrates, and catalyze the formation of terphenylquinones and furanones (Figure 1-2; (48)). For terphenylquinone or bis-indolylquinone formation, carbon-carbon bond formation via Claisen- / Dieckmann-type reactions occurs, followed by release (49, 50). For furanone formation, a carbon-carbon- α bond is formed via an aldol condensation, followed by lactonization via a carbon-oxygen bond, and lastly released (50, 51). Interestingly, these compounds are derived from amino acids, but do not contain peptide bonds in their final structures.



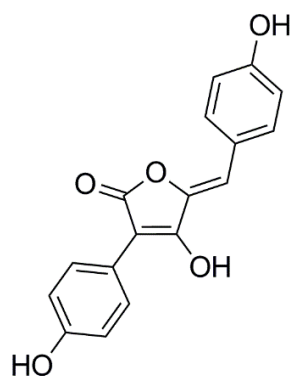
Xenofuranone B



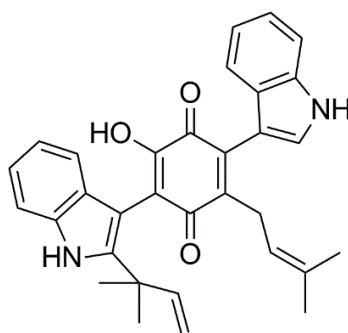
Allantofuranone



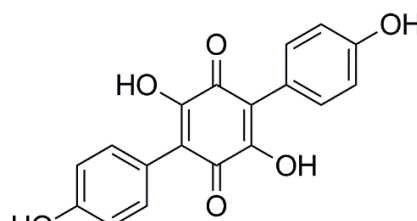
Ralfuranone I



Aspulvinone E



Terrequinone A



Atromentin

Figure 1-2: Examples of furanones and two quinone natural products. Furanones include: xenofuranone B from *Xenorhabdus szentirmaii* (Proteobacteria; (52)); allantofuranone from *Allantophomopsis lycopodina* (ascomycete; (53)); ralfuranone I from *Ralstonia solanacearum* (Proteobacteria; (51)); and aspulvinone E from *Aspergillus terreus* (ascomycete; (48)). Examples of quinones include the bis-indolylquinone terrequinone A from *Aspergillus nidulans* (ascomycete; (54)); and the terphenylquinone atromentin from *Tapinella panuoides* (basidiomycete; (49)).

1.3.2. Atromentin

Atromentin is an example of a hydroxylated *para*-terphenylquinone compound that is synthesized via NRPS-like machinery and is a focus of this doctoral work. The chemical, genetic and enzymatic basis of its production is well described (49, 55-58).

Atromentin and other similar *para*-terphenyl compounds (e.g. polyporic acid, leucomelone, and muscarufin) derive from the shikimate–chorismate pathway, that is, derive from arylpyruvic acids. Stable-isotope feeding experiments with L-Tyrosine showed that atromentin was indeed derived from this amino acid (58, 59).

Terrequinone A biosynthesis in *Aspergillus nidulans* from the asterriquinone synthetase TdiA, which catalyzes two Claisen-type condensations of 3-Indolylpyruvic acid, was the inspiration for the investigation into the genetic and enzymatic basis for atromentin production, which follows a similar catalysis (60). *Tapinella (Paxillus) panuoides* was used as the model organism (49). Atromentin biosynthesis was supported through overexpression of the putative atromentin/quinone synthetase gene (*atrA*) and adjacent putative L-tyrosine:2-oxoglutarate aminotransferase gene

(*atrD*) and then subsequent enzyme assays. *In vitro* reactions showed that L-Tyrosine was deaminated by AtrD to produce 4-hydroxyphenylpyruvic acid (4-HPP), and two 4-HPP monomers were condensed by AtrA to form atromentin.

Using different model basidiomycetes, other atromentin synthetases were characterized: GreA from *Suillus grevillei* (56); InvA1, 2 and 5 from *Paxillus involutus* (55); and NPS3 from *Serpula lacrymans* (57).

As noted before, the biosynthetic genes for atromentin were found adjacent to one another (49), and this was then observed for 23 atromentin-producing basidiomycetes whose genomes or cosmid libraries were available (57). Lastly, a gene encoding an alcohol dehydrogenase/oxidoreductase is also observed in between the atromentin synthetase and aminotransferase genes and its function in atromentin biosynthesis remains unknown, and atromentin is a precursor to many other pigments whose genetic and enzymatic basis has yet to be described. These atromentin-derived pigments are discussed in the following sections.

1.4. Overview of atromentin-derived pigments

Much interest in isolating fungal natural products came from the vibrancy of the mushrooms (61). Before DNA-based identification, the pigments were even a useful chemotaxonomic tool for classifying *Boletales*, *Agaricales* and ensuing genera within, especially with advancements in analytical chemistry and mass spectrometry for pigment identification (reviewed (62, 63)). Pigments were originally identified by TLC (thin layer chromatography), and later by HPLC (High-performance liquid chromatography), thus improving research of fungal pigments (62, 64).

Extensive research of atromentin-derived pigments from basidiomycetes has been done for about 50 years, even though atromentin was first isolated and published in 1878 (58, 65). Stable-isotope feeding experiments of atromentin showed that it is the precursor of many derivatives, such as the pulvinic acid-type pigments and the 2,5-diarylcyclopentenones (55, 58, 59). The interest in various basidiomycete pigments, including atromentin-derived pigments, is evident from extensive reviews (“Pigments of Fungi (Macromycetes)”) for over three decades (5, 58, 66, 67).

Various modifications of atromentin form a multitude of pigments, both vibrant and colorless (Figure 1-3). Herein, three atromentin-derived classes are described: i) atromentin relatives; ii) pulvinic acid-type family; and iii) 2,5-diarylcyclopentenone (“cyclopentenones”). Atromentin relatives involve only reduction and esterification modifications to functional groups attached to atromentin’s quinone and thus represent compounds maintaining the central quinone ring. Enzymatic oxidation and loss of water of the central ring that produces a heterocyclic butenolide ring will make the pulvinic acid-type family. The pulvinic acid-type family is mainly produced from fungi in the genera *Tapinella*, *Gomphidius*, *Hygrophoropsis*, *Coniophora*, *Leucogyrophana*, *Rhizopogon*, *Serpula*, *Boletus*, *Xerocomus*, and even in a distantly related genus, *Omphalotus* (68). If the ring undergoes an oxidative ring contraction and becomes a 5-membered carbon ring, the resulting pigments are known as the cyclopentenones. Following suit of chemotaxonomic classification, the cyclopentenones are mainly found in the genera *Paxillus*, *Gyrodon*, *Gyroporus*, *Chamonixia*, and *Leccinum* (68). Although no direct evidence supports the grevillin family as atromentin-derived, a contraction of two 4-hydroxyphenylpyruvic acids or an oxidation of atromentin will likely produce the yellow to red colored grevillin family (58). These pigments are characteristic of the genus *Suillus*.

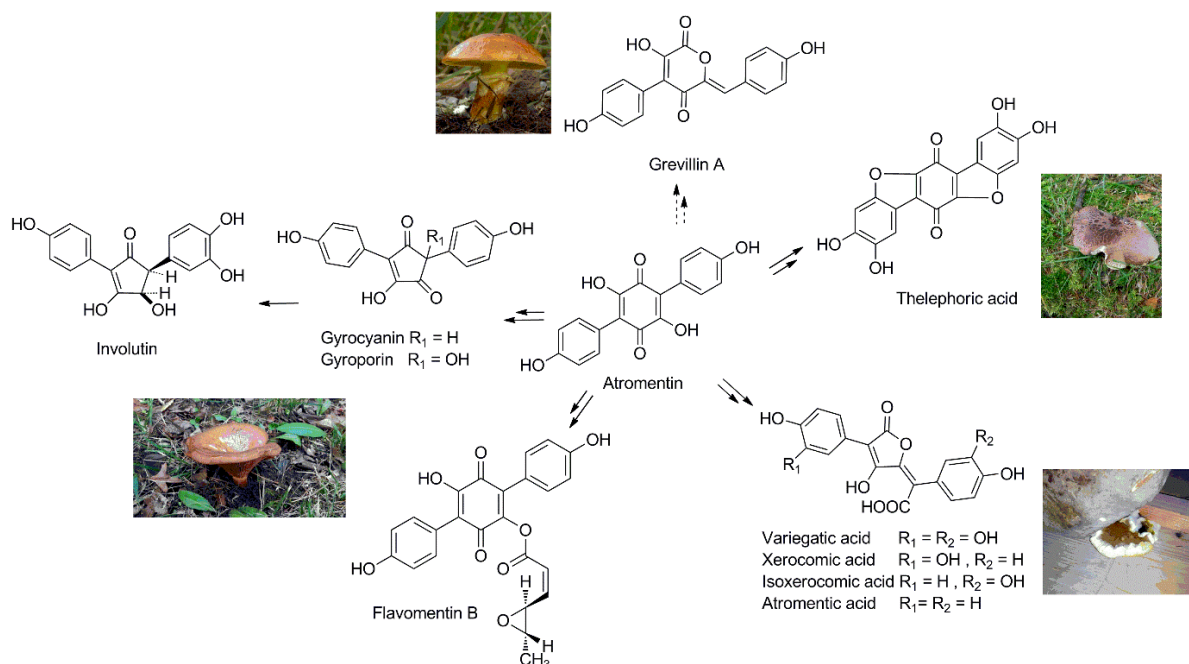


Figure 1-3: The diversity of atromentin-derived pigments and associated mushrooms. Exemplified pigments by compound class are: i) atromentin relatives: flavomentin B (*Paxillus* spp.), and thelephoric acid (*Thelephora* spp.); ii) pulvinic acid-type family: variegatic, (iso)xerocomic, and atromentic acids (*Serpula lacrymans*); and iii) cyclopentenones: gyrocyanin, gyroporin, and involutin (*Paxillus involutus*). Grevillin A (*Suillus* spp.) is shown, and although atromentin may be a precursor, no experimental evidence exists unlike for the other pigment families. Most photographs are compliments of Prof. Dirk Hoffmeister.

1.5. Fungal chromophoric compounds in natural contexts

In a natural context, basidiomycetes are faced with either persisting or changing abiotic and biotic factors, and as such they must adapt and respond. Many biotic and abiotic factors are recognized by fungi and dealt with accordingly, including as defense responses, and such factors include ambient pH, nutrients, temperature, iron

availability, light, wounding, predators, and microbial signaling/communication (69). One such response is the biosynthesis of secondary metabolites, and more specifically, compounds featuring chromophores (*i.e.*, pigments; (15, 69)). For instance, pigments can absorb wavelengths for protection from ultraviolet light damage or even for phototropism; attract or repel fungivores; scavenge oxidative radicals; act as antibiotics or antifungals; or mediate communication for symbiosis, antagonism or pathogenicity (69-72). Here the focus is on pigments, in particular atromentin-derived pigments, and their known or speculative role(s) for the basidiomycetes in nature.

1.5.1. The ecological role of chromophoric compounds for basidiomycetes

Pigments may act as defense compounds. Regarding atromentin-derived pigments, variegatic acid, involutin and gyroporin are of particular interest. From the bruising of some *Boletales* that produce at least one of these compounds, there then comes an intense coloration, presumably a defensive reaction. Variegatic acid from *Suillus variegatus*, involutin from *Paxillus involutus*, and gyroporin from *Gyroporus cyanescens* were identified as the causative agents of this intense coloration (73-75). For example, after *S. variegatus* is bruised, variegatic acid is transformed into quinone methides likely via oxidase enzymes. Although this reaction to injury has no definitively known ecological significance (70), other quinone methides are antimicrobial (76). In line with physical injury to *Boletales*, pests can injure a fungus by feeding. Interestingly, a long observed phenomenon is that the fungus *Paxillus atrotomentosus* remains seemingly free of insects in nature (77, 78). It was determined that atromentin itself was not the antifeedant, but rather a seemingly

energy-intensive, wound-activated defense strategy had evolved. Leucomentins and flavomentins, which are derivatives of atromentin, are ester hydrolyzed back to atromentin and other further hydrolyzed antifeedants that are known as butenolide and (-)-osmundalactone (77, 79). Other examples of defensive compounds are anthraquinones that are laxatives, in the case that their vibrant colors had not already dissuaded the predator from feeding on the fungus (80); antilarval PKS-derived polyenes from a taxonomically undetermined basidiomycete, BY1 (81); and the antifungal 2-chloro-4-nitrophenol from the basidiomycete carrot truffle *Stephanospora caroticolor*, which is derived from the orange-colored precursor stephanosporin (82). Indeed, given the catalytic potential of basidiomycetes and the fact that these fungi naturally face competition, allelochemicals produced by basidiomycetes are interesting not only for potential pest management, but also for understanding chemical ecology (83).

Chromophoric compounds are also involved in securing environmental elements that are necessary for the fungus to survive. This is also a basis for inter-organismal competition or cooperation. As an example, iron is an extremely fought after element in nature. Iron complexes in nature which forms stable ferric oxide hydrates, and this causes depletion of freely available iron that is necessary for an organism's survival (84). One mechanism to acquire iron is the secretion of siderophores, which can become pigmented when complexed with iron but are otherwise not when deferrated. One example of a basidiomycete siderophore is ferrichrome A from *Ustilago sphaerogena* (85, 86). The genetic basis for ferrichrome A was later characterized from *Omphalotus olearius* that revealed it is a NRPS-derived compound (87). There is, however, no true ecological significance described for basidiomycete siderophores. Therefore, we must rely on knowledge obtained from studying siderophores secreted from ascomycete fungi. Siderophores have been well studied in *Aspergillus* spp. and

have been implicated in microbial interactions and virulence (reviewed; (88, 89)). Given that siderophore production in *A. fumigatus* was induced by *Pseudomonas aeruginosa* during competition (90), and that siderophores help fungi outcompete other organisms during colonization (70), one can extrapolate that basidiomycete siderophores function similarly during inter-organismal competition.

Another environmental element is carbon, particularly carbon “trapped” in dead plant matter. Obtaining this carbon has been an interest for generating cellulosic bioethanol (91). However, for basidiomycetes that degrade wood or plant litter, this derived carbon is likely a special food source because it is generally inaccessible to other organisms. This is evident when testing plant substrate utilization by the brown-rot fungus *Gloeophyllum trabeum*, whereby ethanol production was severely limited because the fungus was in fact consuming the derived sugars (91). Also, evidence suggests that pigments such as variegatic acid and involutin are iron-reductants involved in the initial attack of wood for cellulose decomposition (92, 93). The degradation of cellulose and hemicellulose is considered a “brown-rot” mechanism. Variegatic acid and involutin from the brown-rotter *Serpula lacrymans* and ectomycorrhiza-forming *Paxillus involutus*, respectively, were secreted when the fungus was introduced to high organic nitrogen content (92, 94). For example, the induction of variegatic acid is speculated to coincide with when the fungus arrives at a new food source like wood. *P. involutus* is particularly interesting because the fungus is a symbiont that can exchange nutrients with a plant partner, and at one time it was speculated to be devoid of brown-rot mechanisms. However, *P. involutus* still retains reduced brown-rot capabilities, and the released carbon is speculated to be further modified by commensal microbes (95). During the initial attack at the recalcitrant, polymeric plant cellulose, these pigments are involved in creating hydroxyl radicals in conjunction with oxidoreductases and hydrogen peroxide. This

site is at first inaccessible to extracellular hydrolase enzymes (e.g. cellulases). Afterwards, the hydrolase enzymes are able to penetrate to their attack site, and they are the actual main machinery that degrade the plant matter. The redox process is termed Fenton chemistry and follows the reaction: $\text{Fe}^{2+} + \text{H}_2\text{O}_2 + \text{H}^+ \rightarrow \text{Fe}^{3+} + \cdot\text{OH} + \text{H}_2\text{O}$ (94).

Besides securing a carbon source, the release of nitrogen from plant matter is of particular interest for an ectomycorrhizal fungus like *P. involutus*. This nitrogen is taken up by the ectomycorrhizal fungus which is in return exchanged with the associated plant for additional carbon (95).

Another atromentin-derived pigment that can bind to and move other elements is norbadione A. Norbadione A from *Xerocomus badius* binds to caesium metal ions and potassium, the former being a similar cation to the latter and thus likely an unwanted reaction as the mushroom attempts to uptake biologically essential potassium (96, 97).

A compound that is antioxidant has the ability to bind to free radicals in biological systems, and antioxidants gain a lot of attention in the interest of human health. Terphenylquinones are compounds that are well known to be antioxidants (67). Indeed, variegatic acid was described as a strong antioxidant (98), and this property may contribute to the health of the mushroom. Overall, pigments, in particular atromentin-derived compounds, appear to have a variety of important ecological functions for mushrooms.

1.5.2. Other fungal defense mechanisms

Mushrooms have other protective mechanisms than besides natural products (71). Using just a few examples, the mushroom of *P. involutus* has an involute (curled) mature mushroom structure that reduces predatory attacks (99), and *Psilocybe* spp. have gelatinous pileipellis that may repel fungivores (100). As part of the fungus' innate defense system, proteins can also protect the fungus. One example is lectins, carbohydrate-binding proteins that are toxic against nematodes (101).

1.6. Aims and justification of this research

The goal of the research presented here was to describe the role and regulation of basidiomycete secondary metabolites in the context of microbial interactions. In particular, the goal was to gain first insight into the (co-)regulation of a basidiomycete natural product gene cluster, and to identify basidiomycete chemical mediators that could influence a mushroom's surrounding community. It is generally undisputed that there is a knowledge gap between researching basidiomycete and ascomycete natural products that are involved in microbial interactions.

For example, the model basidiomycete *Serpula lacrymans* is not only known a current economic burden (102), but this fungus is also recognized for its enormous natural product potential (92). The genome of *S. lacrymans* contains at least 24 natural product genes, and only one was characterized to have a direct link between enzyme and final product (57, 92). Additionally, only three classes of compounds have been described from the genus. Thus, *S. lacrymans* is an excellent candidate

for natural product bioprospecting, especially using methods such as co-culturing in order to induce natural product production (103), and also for improving our knowledge on the role and regulation of natural products in natural contexts.

The workflow involved co-incubation of basidiomycetes with bacteria or other fungi, identification and titer assessment of produced secondary metabolites in the co-cultures followed by identification and transcription profiling of the responsible natural product genes. The inducible secondary metabolites were screened for bioactivity to determine their potential role in an inter-microbial context. Two taxonomically related model basidiomycetes that follow different lifestyles, which allowed for comparisons, were used: the brown-rotter *Serpula lacrymans* and the ectomycorrhiza-forming *Paxillus involutus*. Each's genome contains an unusually high number of natural product genes, thus making these fungi excellent candidates to both discover new compounds or to shed new light on known natural products.

2. Manuscripts

Manuscripts are listed chronologically, and include four published manuscripts and one manuscript that was prepared for submission.

2.1. Three Redundant Synthetases Secure Redox-Active Pigment Production in the Basidiomycete *Paxillus involutus*

Braesel, J., Götze, S., Shah, F., Heine, D., Tauber, J., Hertweck, C., and Hoffmeister, D.

Published manuscript (55).

Chem. Biol. (2015) 22: 1325–1334.

Summary and importance

Atromentin is a pigment and precursor to many other pigments produced by basidiomycetes. Although feeding experiments have already unequivocally determined that atromentin is a precursor to certain pigments, other pigments were only speculated to be derived therefrom. One such speculated pigment class was the

cyclopentenones, which may derive from atromentin, gyrocyanin or atromentic acid. This study was pivotal in providing evidence that showed atromentin is the most likely precursor to this class, including involutin. This study also showed that atromentin was produced in redundancy; of six atromentin synthetase enzymes, three were found functional to secure atromentin biosynthesis. This redundancy highlights the mushroom's role in forest carbon cycling as involutin is indirectly involved in the breakdown of plant matter.

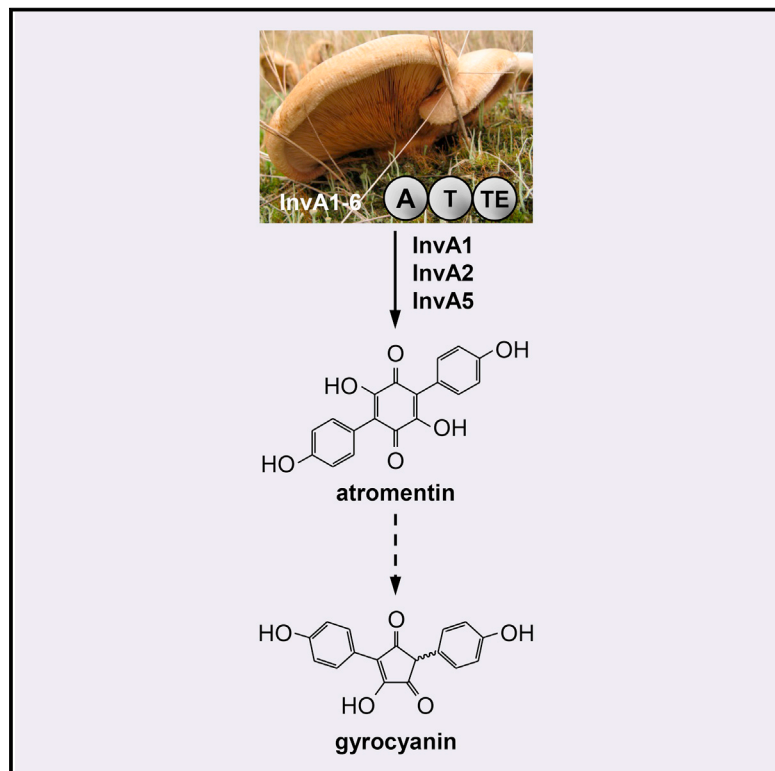
Contribution to the manuscript

James Tauber contributed to the manuscript by cloning *invA6*, over-expressing the gene *invA6*, and testing the purified enzyme in an assay with J.B. In the context of the entire paper, the other authors worked on: i) five other similar genes and enzymatic assays, including all chromatography; ii) transcriptomic work (extractions, data acquisition and analyses); iii) sequence alignments of NRPS-like domains; iv) all culturing and isotope feeding work; and v) wrote the majority of the manuscript, including figures. James Tauber wrote his respective section for the manuscript as well as reviewed and edited the entire manuscript draft.

Chemistry & Biology

Three Redundant Synthetases Secure Redox-Active Pigment Production in the Basidiomycete *Paxillus involutus*

Graphical Abstract



Authors

Jana Braesel, Sebastian Götze, Firoz Shah, ..., Anders Tunlid, Pierre Stallforth, Dirk Hoffmeister

Correspondence

dirk.hoffmeister@hki-jena.de

In Brief

Diarylcyclopentenones, produced by the symbiotic fungus *Paxillus involutus*, are redox-active metabolites involved in carbon cycling as they serve Fenton-based decomposition of lignocellulose in forest ecosystems. Braesel et al. show that the fungus uses three enzymes in parallel to secure the key step in diarylcyclopentenone biosynthesis.

Highlights

- Diarylcyclopentenone biosynthesis proceeds via atromentin as precursor
- Atromentin biosynthesis in *Paxillus involutus* is a parallelized process
- A thioesterase signature sequence indicative for quinone formation was identified
- Quinone synthetases are amenable to engineering by domain swaps



Three Redundant Synthetases Secure Redox-Active Pigment Production in the Basidiomycete *Paxillus involutus*

Jana Braesel,¹ Sebastian Götze,² Firoz Shah,³ Daniel Heine,⁴ James Tauber,¹ Christian Hertweck,⁴ Anders Tunlid,³ Pierre Stallforth,² and Dirk Hoffmeister^{1,*}

¹Department of Pharmaceutical Microbiology, Hans Knöll Institute, Friedrich-Schiller-University Jena, Beutenbergstrasse 11a, 07745 Jena, Germany

²Junior Group Chemistry of Microbial Communication, Leibniz Institute for Natural Product Research and Infection Biology, Hans Knöll Institute, Beutenbergstrasse 11a, 07745 Jena, Germany

³Department of Biology, Lund University, Sölvegatan 37, 221 00 Lund, Sweden

⁴Department of Biomolecular Chemistry, Leibniz Institute for Natural Product Research and Infection Biology, Hans Knöll Institute, Beutenbergstrasse 11a, 07745 Jena, Germany

*Correspondence: dirk.hoffmeister@hki-jena.de
<http://dx.doi.org/10.1016/j.chembiol.2015.08.016>

SUMMARY

The symbiotic fungus *Paxillus involutus* serves a critical role in maintaining forest ecosystems, which are carbon sinks of global importance. *P. involutus* produces involutin and other 2,5-diarylcyclopentenone pigments that presumably assist in the oxidative degradation of lignocellulose via Fenton chemistry. Their precise biosynthetic pathways, however, remain obscure. Using a combination of biochemical, genetic, and transcriptomic analyses, in addition to stable-isotope labeling with synthetic precursors, we show that atromentin is the key intermediate. Atromentin is made by tridomain synthetases of high similarity: InvA1, InvA2, and InvA5. An inactive atromentin synthetase, InvA3, gained activity after a domain swap that replaced its native thioesterase domain with that of InvA5. The found degree of multiplex biosynthetic capacity is unprecedented with fungi, and highlights the great importance of the metabolite for the producer.

INTRODUCTION

The basidiomycete model fungus *Paxillus involutus* (poison pax mushroom, *Boletales*) displays a Janus-faced existence. It can cause a deadly hemolytic autoimmune reaction, infamously known as Paxillus syndrome, upon repeated ingestion of its carpophores. On the other hand, this species is of critical ecological importance, and thus represents one of the best-studied symbiotic fungi on a molecular, physiological, and environmental level. It forms symbiotic associations, so-called ectomycorrhizae, with various trees in managed and unmanaged forests, among them dominant and both silviculturally and economically important species such as spruce, pine, birch, poplar, and beech (Wallander and Söderström, 1999). A remarkable feature of

P. involutus and numerous other species within the *Boletales* is their capacity to synthesize brightly colored aromatic pigments. These natural products fall into various subclasses, among them the pulvinic acids and the 2,5-diarylcyclopentenones, e.g., involutin and gyrocyanin (Edwards et al., 1967; Edwards and Gill, 1973; Besl et al., 1973; Steglich et al., 1977; Figure 1). These pigments display redox activity and are assumed to play a crucial role in the reduction of Fe³⁺ during the Fenton-based decomposition of litter material by *P. involutus* (Eastwood et al., 2011; Shah, 2014). Decomposition of such material by ectomycorrhizal fungi are thought to play a key role in mobilizing nutrients embedded in recalcitrant organic matter complexes, thereby making them accessible to the host plant (Lindahl and Tunlid, 2015).

Details of the pigment biosynthesis have been profoundly studied on a chemical level (reviewed by Gill and Steglich, 1987 and Zhou and Liu, 2010). Stable-isotope labeling confirmed L-tyrosine as the metabolic origin and that the terphenylquinone atromentin (Figure 1) is the direct precursor of the pulvinic acids (Hermann, 1980; Gill and Steglich, 1987). However, the biogenesis of 2,5-diarylcyclopentenones has remained enigmatic, as two routes are conceivable that either include an atromentin-independent direct condensation of 4-hydroxyphenylpyruvic acid (Figure 1, route 1) or involve atromentin formation (route 2), which then undergoes oxidative ring contraction or conversion to atromentic acid to form the cyclopentenone skeleton.

Here, we report on the biosynthesis of diarylcyclopentenone pigments in *P. involutus* and show that atromentin is their metabolic precursor, which is biosynthesized in a multiplexed process. Evidence comes from (1) in vitro characterization of six wild-type and two artificially created chimeric quinone synthetases, (2) transcriptomic data, and (3) stable-isotope labeling to track the turnover of precursors by *P. involutus*. The chimeric quinone synthetases demonstrate that successful engineering of these enzymes by replacing an entire domain is feasible. We also characterized the *P. involutus* phosphopantetheinyl transferase PptA, which converts the above quinone synthetases from the inactive *apo* into their functional *holo* forms.

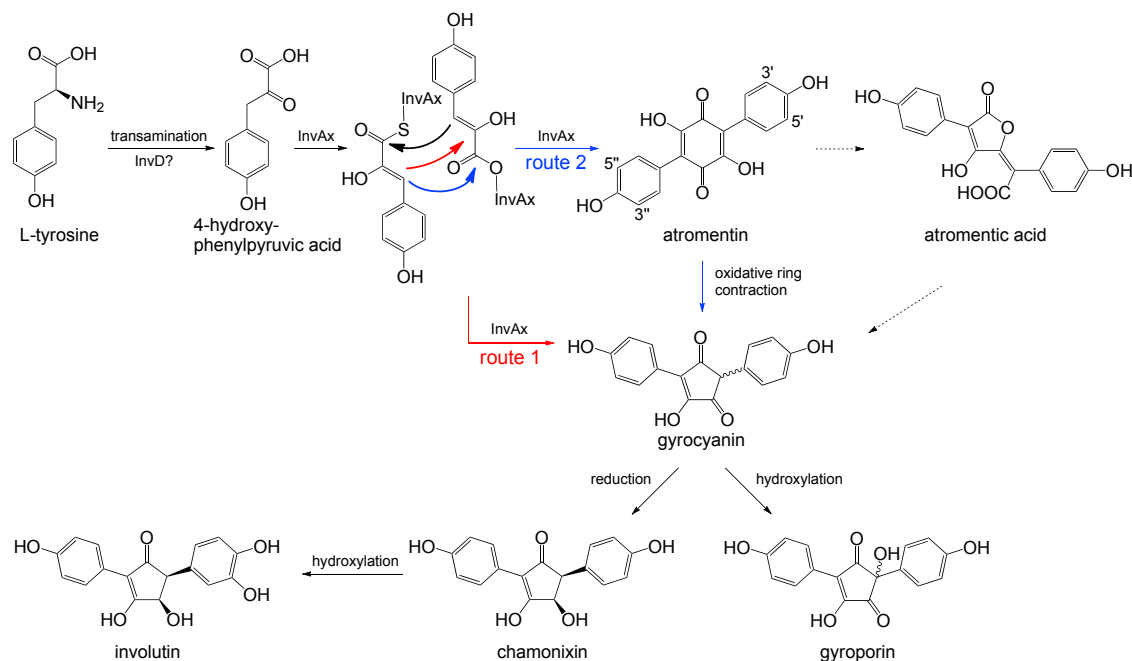


Figure 1. L-Tyrosine-Derived *Paxillus* Pigments

Schematic of pigment biosynthesis. L-Tyrosine is deaminated to 4-hydroxyphenylpyruvic acid by a PLP-dependent transaminase, followed by covalent tethering as a thioester and oxoester onto the thiolation and thioesterase domains, respectively, of the InvAx synthetases ($x = 1, 2, 5$). Two alternative theoretical routes may complete cyclopentenone biosynthesis. Route 1 (red) includes direct decarboxylative condensation (black and red arrows between 4-hydroxyphenylpyruvic acid units) into gyrocyanin, i.e., the common diarylcyclopentenone intermediate. Experimentally verified route 2 (blue) involves symmetric condensation (black and blue arrows between 4-hydroxyphenylpyruvic acid units) into atromentin, followed by oxidative ring contraction to yield gyrocyanin. Dotted arrows indicate a possible shunt within route 2 via atromentic acid.

RESULTS AND DISCUSSION

Genetic and Transcriptional Characterization of *invA* Genes

Diarylcyclopentenone natural products originate from the shikimic acid pathway that is likely extended by an AtrD-like transaminase activity (Schneider et al., 2008) to produce 4-hydroxyphenylpyruvic acid from L-tyrosine. However, the mechanistic basis for the condensation of two 4-hydroxyphenylpyruvic acid units into the diarylcyclopentenone scaffold has remained obscure. Two routes appear plausible (Figure 1, routes 1 and 2), which either require or bypass atromentin as a precursor. In the atromentin-dependent scenario that requires atromentin synthetase activity (route 2), atromentin may undergo oxidative ring contraction to yield the cyclopentenone scaffold in a one-step process, or is converted into atromentic acid, i.e., a butenolide, which then serves as intermediate for cyclopentenone formation (Gill and Steglich, 1987). An alternative biosynthetic scenario (route 1) includes a direct condensation of 4-hydroxyphenylpyruvate (Gruber et al., 2014), thereby bypassing an atromentin intermediate but still requiring enzymatic activation, most likely through adenylate formation. To shed more light onto the biogenesis of fungal diarylcyclopentenones, we searched the genome of the basidiomycete *P. involutus* ATCC 200175 (Kohler et al., 2015) for genes encoding adenylating multidomain enzymes, as they were shown to catalyze formation of carbon-carbon or carbon-oxygen bonds between aromatic α -keto acid

building blocks (Schneider et al., 2008; Wackler et al., 2012). Six candidate genes were identified, hereafter referred to as *invA1* to *invA6* (Figure 2A). These genes encode putative tridomain monomeric synthetases, each featuring an adenylation (A), a thiolation (T), and a thioesterase (TE) domain (Figure 2B). The signature motifs of these domains followed the established consensus (Schwarzer et al., 2003). *InvA1*–*A6* are 955, 953, 949, 950, 953, and 952 amino acids long, respectively, with theoretical molecular masses of 104.8, 104.6, 104.4, 105.0, 104.6, and 104.7 kDa. The sequences shared 74%–83% identical amino acids with the *Suillus grevillei* atromentin synthetase GreA (protein accession NCBI: AFB76152.1), and 67%–76% with the *Tapinella panuoides* atromentin synthetase AtrA (ACH 90386.1). The Joint Genome Institute protein IDs for *InvA1*–*A6* are JGI: 166672, 69019, 127833, 127875, 77684, and 69028, respectively.

The gene *invA5* is located on scaffold 16 of the *P. involutus* genome, while all other *invA* genes are encoded on scaffold 4 (Figure 2A). The *invA2* and *invA3* genes are encoded in the vicinity of a putative aminotransferase gene, which is referred to as *invD*. It is hypothesized to encode the gateway enzyme for terphenylquinone/atromentin biosynthesis, as other highly similar fungal enzymes, TdiD and AtrD, were shown to be responsible for the first step in bis-indolylquinone and terphenylquinone formation (Schneider et al., 2007, 2008). Scaffold 4 also encodes other genes that are potentially involved in secondary metabolism, encoding four transporters of the major facilitator

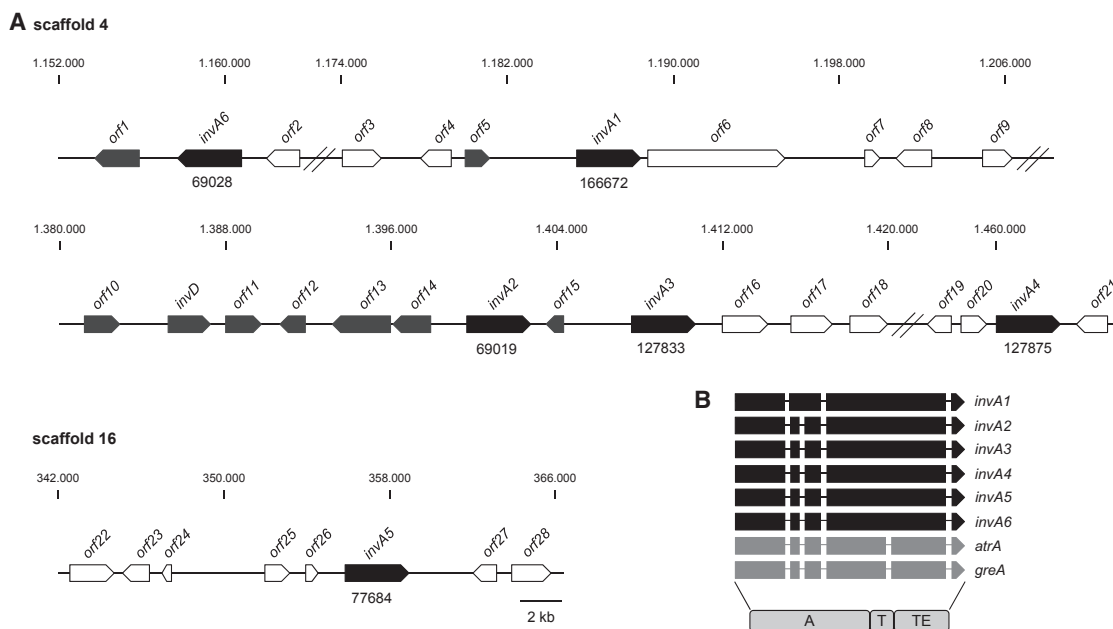


Figure 2. Physical Map of Biosynthetic Genes and Synthetase Gene Structures

(A) Genes *invA1*–*invA6* (black arrows) and adjacent reading frames are located on scaffolds 4 and 16 in the genome of *P. involutus*. Open arrows represent hypothetical reading frames; gray arrows represent putative transporter and biosynthesis genes. Protein IDs for InvA1 to InvA6 are indicated below the respective arrows, and base counts of the scaffolds are indicated above the genes. For clarity, introns are not shown.

(B) Comparison of the structures of *P. involutus* synthetase genes *invA1*–*A6* (black) and basidiomycete orthologs *atrA* of *Tapinella panuoides* and *greA* of *Suillus grevillei* (gray). Lines represent introns. The domain setup of InvA1–A6, AtrA, and GreA is shown below the genes. A, adenylation domain; T, thiolation domain; TE, thioesterase domain.

superfamily (*orf11*, *orf13*–*orf15*), an oxidoreductase (*orf1*), a glycosyltransferase (*orf5*), an aldo-keto reductase (*orf10*), and an alcohol dehydrogenase (*orf12*).

Transcriptomic analysis identified *invA1* to *invA6* as expressed genes, when the fungus is grown in axenic culture, regardless of the media tested. Analysis of relative transcript levels showed a high abundance of *invA1*, *invA2*, and *invA5* transcripts, and moderate levels of *invA6* mRNA. In contrast, *invA3* and *invA4* were only poorly expressed. When using media containing organic nitrogen, we found a more than 13-fold and 15-fold higher number of transcripts encoding *invA1* and *invA5*, respectively, compared with *invA3* or *invA4*. The transcripts of *invA1* and *invA5* were about 5-fold more abundant than those of *invA6*, and 1.4-fold and 2-fold higher compared with *invA2*. The experimentally verified cDNA sequences for *invA1* and *invA3* deviate from the predicted sequences deposited on the JGI server. For these genes, additional 673- and 595-bp introns, respectively, were erroneously predicted in the center portion of the reading frame. By amplification of partial sequences of genomic and cDNA, we showed that the protein sequence of InvA3 is one amino acid shorter than predicted.

The genes *invA1* possesses three and *invA2*–*A6* four introns, which are between 50 and 61 bp in length (Figure 2B). The intron positions are conserved in the *invA* orthologs *atrA* and *greA*. However, these genes are interrupted by a fifth intron in their 3'-terminal portions. For *invA3* and *invA6*, erroneously spliced transcripts were found that either included retained introns or erroneously removed exonic sequences. The resulting shifted reading frames lead to premature stop codons and, conse-

quently, non-functional proteins. Transcript variants of a gene may be interpreted as a posttranscriptional regulatory mechanism (Conti and Izaurralde, 2005) and are also described for the basidiomycetes *Phanerochaete chrysosporium* and *Armillaria mellea* (Larrondo et al., 2004; Misiek and Hoffmeister, 2008).

P. involutus 4'-Phosphopantetheinyl Transferase

For enzymatic activity, multidomain biosynthesis enzymes, such as peptide and quinone synthetases, strictly require posttranslational modification by 4'-phosphopantetheinyl (4'-PPT) transfer to a conserved serine residue within the T domain. This 4'-PPT transfer is catalyzed by dedicated transferases (so-called Sfp-type 4'-PPTase). As no such enzyme of basidiomycete origin has yet been described or characterized, we carried out a tblastn search across the *P. involutus* genome, using the sequence of *Aspergillus nidulans* 4'-PPTase NpgA (Keszenman-Pereyra et al., 2003) as query. A gene encoding a 263-amino-acid putative Sfp-type 4'-PPTase (OMIM: 174503) was identified on scaffold 3 of the *P. involutus* genome. The 1,004-bp gene includes four introns and is referred to as *pptA* hereafter. PptA shares 54% identical amino acids with a predicted 4'-phosphopantetheinyl transferase of *Gloeophyllum trabeum* ATCC 11539 (accession number NCBI: XP_007861898).

Biochemical Characterization of Putative Synthetases

The apo-proteins InvA1–A6 were heterologously produced in *Escherichia coli* KRX and SoluBL as N-terminally hexahistidine-tagged fusion proteins (Figure S1). Substrate specificity, temperature, and pH optima of the A domains of apo-InvA1–A6 were

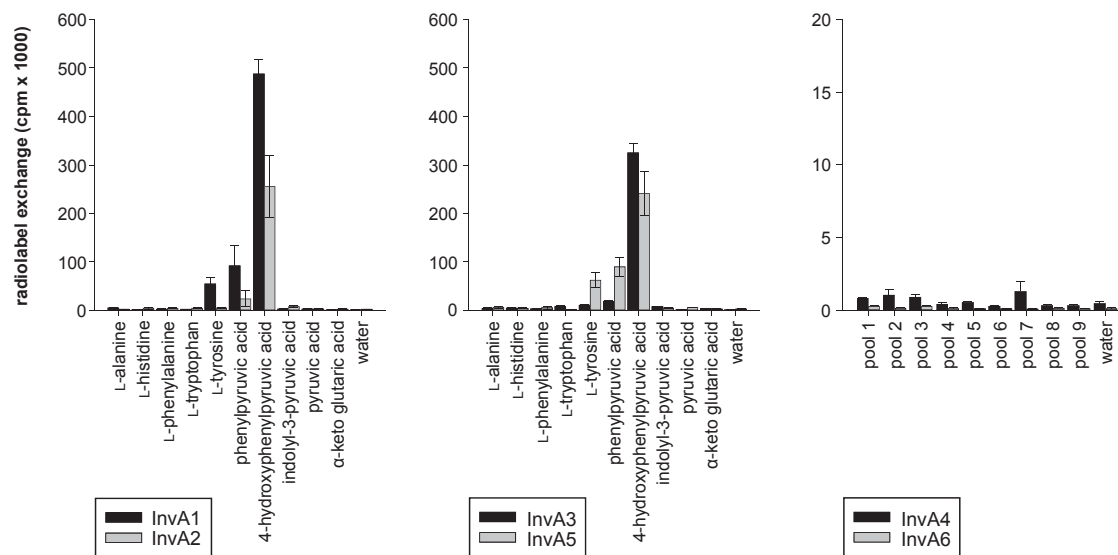


Figure 3. Substrate Specificity of the Adenylation Domains InvA1 to InvA6

Substrate specificity was determined *in vitro* using the substrate-dependent ATP-[32 P]pyrophosphate exchange assay. Error bars indicate SD. Left: InvA1 and InvA2; center: InvA3 and InvA5; right: InvA4 and InvA6. The latter enzymes were tested with 37 substrates, combined in nine pools (Table S2). Polyacrylamide gels of purified proteins and initial substrate screens are shown in Figure S1.

characterized using the ATP-[32 P]pyrophosphate radiolabel exchange assay.

As *Paxillus* pigments originate from the shikimic acid pathway, aromatic 2-oxo acids and aromatic L-amino acids were tested as potential substrates, along with pyruvic acid and L-alanine as controls. Strongest pyrophosphate exchange by InvA1–A3 and InvA5 was observed with 4-hydroxyphenylpyruvic acid (InvA1: 487,600 cpm; InvA2: 255,600 cpm; InvA3: 325,200 cpm; InvA5: 241,100 cpm; Figure 3). 4-Hydroxyphenylpyruvic acid is the expected initial building block for diarylcyclopentenones, irrespective of the biosynthetic route. With the pyrophosphate exchange normalized with respect to 4-hydroxyphenylpyruvic acid, phenylpyruvic acid was turned over between 5.8% and 37.4%, and L-tyrosine between 2.1% and 26%, respectively. However, these compounds and a subsequently tested extended set of potential substrates, i.e., pools comprising 37 compounds (L-amino acids, α -keto acids, and aromatic carboxylic acids, Table S2) were rejected by InvA4 and InvA6 (<2,000 cpm; Figures 3 and S1). Therefore, their substrate preferences remain unknown but are incongruent with those of the other tested InvA enzymes. Alternatively, InvA4 and InvA6 may have lost enzymatic activity. Crystallography and biochemical evidence have established ten key amino acid residues within the primary amino acid sequence of A domains that are most likely involved in substrate recognition (Stachelhaus et al., 1999). This sequence signature, also referred to as non-ribosomal code, of the InvA enzymes is V-A-E-F-S-G-G-A-C-K, except for InvA4, whose signature bears a glycine instead of a glutamic acid at the third position (V-A-G-F-S-G-G-A-C-K). This signature is conserved in the biochemically characterized atromentin synthetases AtrA and GreA (Schneider et al., 2008; Wackler et al., 2012). Therefore, our biochemical results confirm this signature as specific non-ribosomal code for aromatic α -keto acid-activating synthetases. Optimal pyrophosphate exchange with

InvA1–A3 and InvA5 took place at 20°C (InvA2, InvA3) and 25°C (InvA1, InvA5), and at pH 7.2, 7.6, 6.8, 7.4 for InvA1, InvA2, InvA3, and InvA5, respectively.

InvA1–A3 and InvA5 were treated *in vitro* with the heterologously produced 4'-PPTases Svp (Sanchez et al., 2001) and, in separate reactions, with *P. involutus* PptA (Figure S1), to produce the *holo*-enzyme. *Holo*-InvA enzymes were separately incubated with 1.8 mM 4-hydroxyphenylpyruvic acid under optimum conditions in Mg $^{2+}$ -containing Tris buffer and 2.5 mM ATP. After 16 hr of incubation, the reactions containing InvA1, InvA2, and InvA5, respectively, turned violet, irrespective of the 4'-PPTase used for priming.

In negative controls without ATP or a 4'-PPTase, this coloration was not observed. The UV-visible spectrum, high-resolution mass (found m/z 323.0555 [M – H] $^-$, calculated for C $_{18}$ H $_{12}$ O $_6$: m/z 323.0561 [M – H] $^-$), and retention time of the colored compound were identical to an authentic atromentin sample (Figure 4). We therefore conclude that InvA1, InvA2, and InvA5 are atromentin synthetases, which is consistent with earlier reports that *P. involutus* does have the capacity to produce atromentin (Bresinsky and Rennschmidt, 1971; Bresinsky, 1974).

Usually, fungi rely on one set of small-molecule biosynthetic pathway genes per haploid genome. A three-fold redundantly secured natural product biosynthesis pathway is unprecedented with fungi, but points to an indispensable ecological role of the diarylcyclopentenone products, likely to degrade organic matter in forest ecosystems. This feature is somewhat reminiscent of a duplicated cluster of genes in *Aspergillus flavus*, which encode the production of the same set of piperazines that are essential for sclerotia formation (Forseth et al., 2013).

Product formation was not observed with InvA3, whereas the ATP-[32 P]pyrophosphate exchange assay verified that the A domain is active and adenylates 4-hydroxyphenylpyruvic acid. Therefore, we hypothesized that the TE domain that would

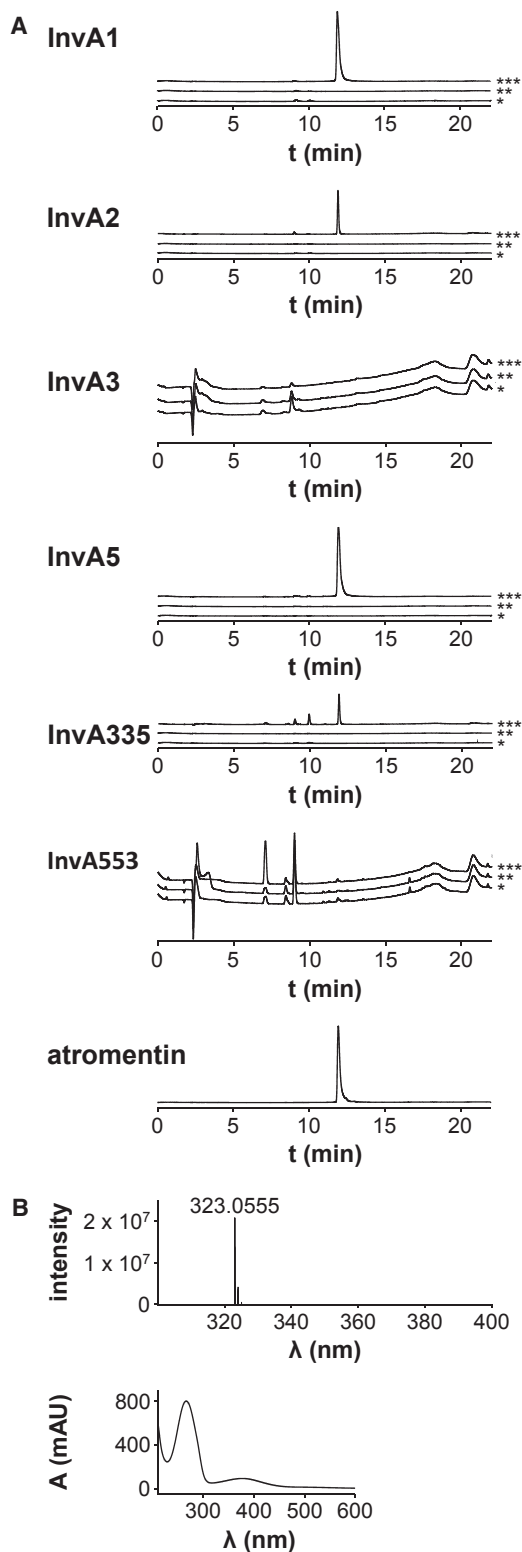


Figure 4. Chromatographic Analysis of InvA-Mediated In Vitro Synthesis of Atromentin by PptA-Primed Synthetases

(A) Enzymatic reactions and authentic atromentin standard. Single asterisk indicates control without ATP, double asterisk control without PPTase, and triple asterisk the reaction. Absorption of the signal at $t_R = 11.9$ min is: InvA1,

catalyze symmetric condensation of two 4-hydroxyphenylpyruvic acid units into a substituted benzoquinone may be inactive. Furthermore, we assumed that replacing the InvA3 TE domain by a TE domain of an active *P. involutus* atromentin synthetase might reconstitute its functionality. To test this hypothesis, we constructed a chimeric gene (*invA335*) that encoded the InvA3 A-T didomain fused to the InvA5 TE domain. For negative control, we also created the inverse chimera, termed *invA553*, encoding a synthetase composed of the InvA5 A-T didomain and the InvA3 TE domain. For product formation, either chimera was heterologously produced as hexahistidine fusion in *E. coli* (for SDS gel picture, see Figure S1), converted in vitro into the *holo* form by 4'-PPTases Svp or PptA, and incubated under optimum conditions, as described above.

High-performance liquid chromatography (HPLC) analysis clearly showed atromentin production in vitro by the chimera InvA335, whereas the chimeric synthetase InvA553 did not produce atromentin, or any other compound, in detectable amounts (Figure 4). This result demonstrates that the wild-type InvA3 enzyme is inactive because of its non-functional TE domain, and gains full functionality when the TE domain is replaced. Engineering of quinone synthetases has not been reported as yet. Our results demonstrate that they are amenable to domain swaps. This finding may open up new avenues of research to engineer multimodular enzymes, as quinone synthetases represent a simple model for the study of interdomain interactions that involve TE domains.

Signature Sequence of Quinone-Forming Thioesterase Domains

Numerous non-ribosomal peptide synthetases (NRPSs) rely on a TE domain for product release (Schwarzer et al., 2003). Crystallographic analysis of the surfactin A synthetase SrfA-C and bioinformatics analyses revealed that TE domains belong to the α/β -hydrolase superfamily (Bruner et al., 2002; Samel et al., 2006; Cantu et al., 2010). The TE domain catalytic triad is composed of the residues Ser80, Asp107, and His207 (numbering according to Bruner et al., 2002). The InvA synthetases show strictly conserved serine and histidine residues, with the second residue of the triad being variable (Table 1). InvA3, InvA4, and InvA6 harbor the conserved aspartate residue. In those enzymes that showed quinone synthetase activity, i.e., InvA1, InvA2, and InvA5, this residue was replaced by an asparagine (Table 1). We compared the sequences of all characterized quinone and furanone synthetases available from the literature, which include NPS3, TdiA, AtrA, GreA, BthI10204, EchA, RalA, and MicA (Eastwood et al., 2011; Schneider et al., 2007, 2008; Wackler et al., 2011, 2012; Biggins et al., 2011; Zhu et al., 2014; Yeh et al., 2012), along with TE domains of multimodular NRPSs, and identified a dichotomous motif pattern. Quinone synthetases, including InvA1, InvA2, and InvA5, consistently

661 mAU; InvA2, 394 mAU; InvA5, 635 mAU; InvA335, 258 mAU; standard, 745 mAU. The signals at $t_R = 9.0$ and 9.5 min represent unconverted substrates. Maximum absorption in InvA3 and InvA553 chromatograms was <20 mAU; for all other chromatograms the maximum absorption was 800 mAU.

(B) High-resolution mass spectrometry profile and UV-visible spectrum of authentic atromentin. These spectra were also found in enzymatic reactions. Detection wavelength was $\lambda = 254$ nm.

Table 1. Catalytic Triads of InvA1–A6, Other NRPS-like Enzymes, and NRPSs, Based on Alignment of Their TE Domains with GENEIOUS Software, Version 7.1.4, Using SrfTE as Reference

Protein	Species	Catalytic Triad ^a	Product	Protein Accession #/NCBI Reference
InvA3	<i>Paxillus involutus</i>	G Y S Y G ... V I D - - - I I ... G H H Y T	unknown	127833
InvA4	<i>Paxillus involutus</i>	G Y S Y G ... I I D - - - M I ... G H H Y T		127875
InvA6	<i>Paxillus involutus</i>	G Y S Y G ... L V D I P P H I ... G H H D T		69028
InvA1	<i>Paxillus involutus</i>	G Y S Y G ... L I N I P P H I ... G Q H Y T	quinone	166672
InvA2	<i>Paxillus involutus</i>	G Y S Y G ... L I N I P P H I ... G Q H Y T		69019
InvA5	<i>Paxillus involutus</i>	G Y S Y G ... L I N I P P N I ... G Q H Y T		77684
AtrA	<i>Tapinella panuoides</i>	G Y S Y G ... L I N I P P H I ... G Q H Y T		ACH90386.1
GreA	<i>Suillus grevillei</i>	G Y S Y G ... L I N I P P H I ... G Q H Y T		AFB76152
Nps3 ^a	<i>Serpula lacrymans</i>	G Y S Y G ... L I N I P P H I ... G R H Y T		EGO23141.1
TdiA	<i>Aspergillus nidulans</i>	G Y S F G ... S W N L P P H I ... G A H Y T		CBF80711.1
BthII0204 ^b	<i>Burkholderia pseudomallei</i>	G Y S Y G ... S F N L P P H I ... G E H Y T		CAH37575
EchA	<i>Streptomyces</i> sp. LZ35	G Y S Y G ... S F N L P P H I ... P G H Y T		YP_008789943
MicA ^b	<i>Aspergillus nidulans</i>	G Y S L G ... S I D Y P P H I ... G I H A K	furanone	XP_661000.1
RalA	<i>Ralstonia solanacearum</i>	G Y S Y G ... S I D A P P V I ... G E H H T		AEC03968.1
GrsB	<i>Bacillus brevis</i>	G Y S S G ... L F D V - - Y W ... G A H S N	ester/ peptide	CAA43838
TycC	<i>Bacillus brevis</i>	G Y S S G ... L F D S - - Y W ... G I H S R	(macro-cycles)	O30409
FenB	<i>Bacillus subtilis</i>	G Y S A G ... I V D A - - Y K ... G A H K D		AAB00093.1
SrfA-C	<i>Bacillus subtilis</i>	G Y S A G ... M V D S - - Y K ... G T H A E		WP_029878554

After Bruner et al. (2002).

^aThe residues of the catalytic triad Ser80, Asp107, and His207 (numbering according to SrfTE) are marked in bold.

^bEnzymatic function deduced from indirect evidence, as these enzymes have not yet been characterized biochemically.

showed a Ser/Asn/His triad, with the asparagine being followed by a branched-chain aliphatic amino acid (leucine or isoleucine) and two proline residues. Synthetases catalyzing furanone assembly (RalA and MicA) and thioesterases of macrolacton/macrolactam forming peptide synthetases SrfTE, FenTE, TycTE, and GrsTE (Bruner et al., 2002; Samel et al., 2006; Trauger et al., 2000; Hoyer et al., 2007) showed the regular Ser/Asp/His triad (Table 1). The aspartate residue within the catalytic triad hydrogen bonds and polarizes the histidine. A recent report describes an engineered catalytic triad of a *Listeria monocytogenes* caseinolytic protease (CipP). The authors report that substituting the naturally occurring asparagine by aspartate increased hydrolysis, favored oligomerization, and impacted on an adjacent Asp/Arg oligomerization sensor sequence (Zeiler et al., 2013) which is, however, not present in any of the aforementioned natural product TE domains. Furthermore, the presence of a sequence motif composed of an aliphatic residue and a double proline that immediately follows the asparagine seems restricted to synthetases that condense two monomers into a quinone natural product scaffold, i.e., rather small products, compared with the macrocycle-forming NRPSs. Although the functional role of the neutral asparagine, combined with the above motif, remains elusive in the context of these synthetases, it appears critical for quinone formation from aromatic α -keto acids and helps selectively recognize quinone synthetases. Notably, the inactive *Paxillus* synthetases, InvA3 and InvA4, lack the double proline motif (Table 1). InvA6 is also inactive and also shows an aspartic acid residue, like InvA3 and InvA4, but has the Ile-Pro-Pro motif. A chimeric enzyme, encoded by the *invA556* gene and comprising the InvA5 A-T didomain fused to the InvA6 TE

domain, was used to test whether the InvA6 thioesterase is functional. InvA556 adenylated 4-hydroxyphenylpyruvic acid but did not show product formation (data not shown). We therefore conclude that the adenylation and thioesterase domains of InvA6 are inactive. Taken together, these findings support our in vitro data of InvA3, InvA4, and InvA6 as not being relevant for atromentin production.

Stable-Isotope Labeling

InvA1, InvA2, and InvA5 were shown to possess atromentin synthetase activity, while InvA3 turned functional only after artificially replacing its TE domain, probably because of the aforementioned deviating TE motifs. InvA4 and InvA6 did not accept 4-hydroxyphenylpyruvic acid. Hence, InvA3, InvA4, and InvA6 could be excluded as not being relevant for biosynthesis of 2,5-diarylcyclopentenone or their likely biosynthetic precursor atromentin. However, we could still not discount a scenario of direct cyclopentenone formation by any of these enzymes in vivo via route 1 (Figure 1), thereby altogether bypassing atromentin as intermediate. Therefore, we carried out feeding experiments with stable-isotope-labeled atromentin, followed by HPLC and mass spectrometry analysis. When 3',3'',5',5''-D₄-atromentin was administered to the homogenized mycelium, the deuterium label clearly appeared in two cyclopentenones, gyrocyanin and its oxidation product gyroporin (Figure 5), whose masses were found to increase by four mass units (gyrocyano: *m/z* 295.0615; D₄-gyrocyano: *m/z* 299.0861; gyroporin: *m/z* 311.0558; D₄-gyroporin: *m/z* 315.0813 [M – H][–]), thereby demonstrating that atromentin serves as cyclopentenone precursor. Gyrocyano was identified by comparison of

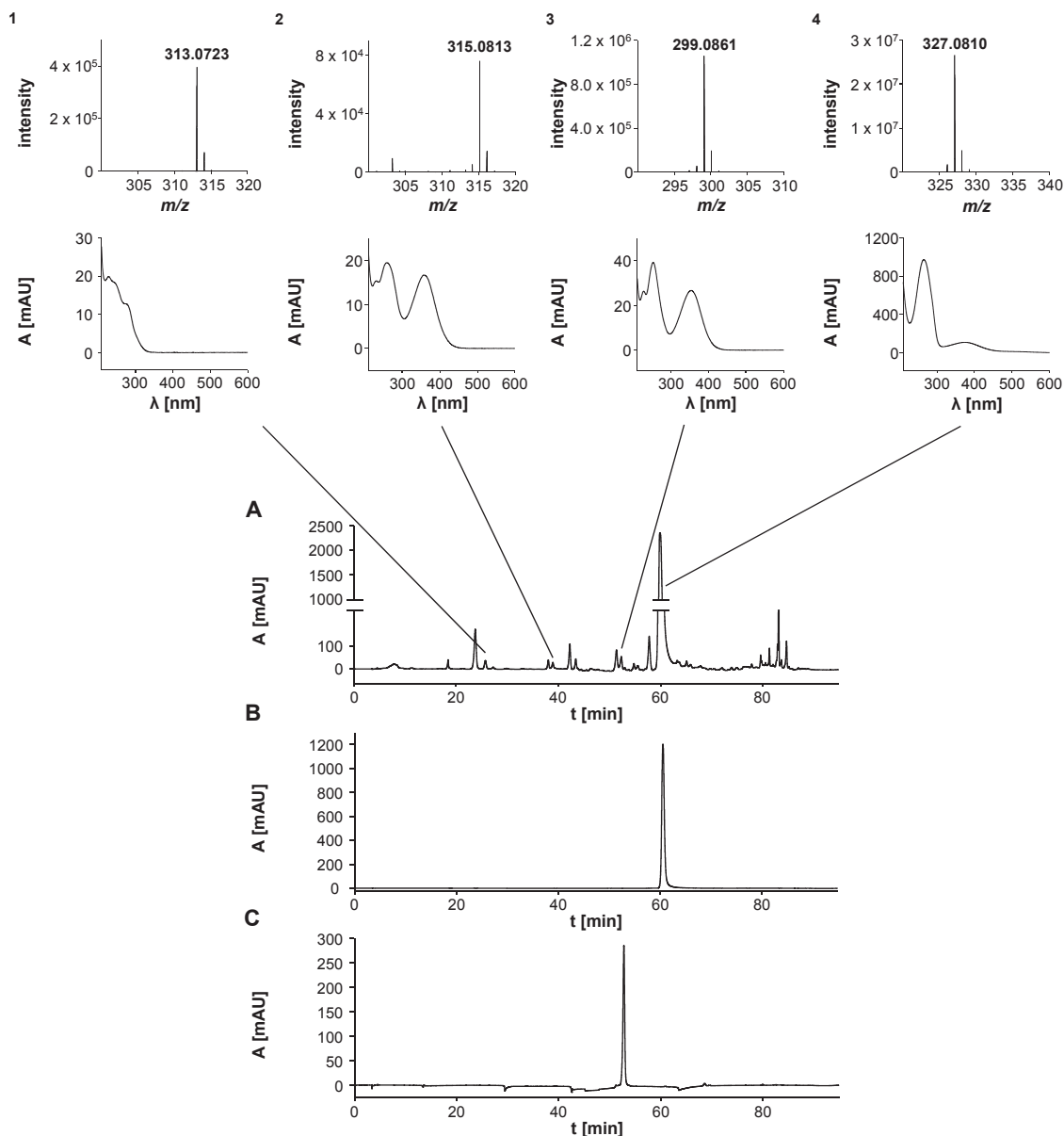


Figure 5. Chromatographic Analysis of the Isotope-Labeling Experiment

(A) Tetradeuterated atromentin, added to *P. involutus* mycelial homogenate.

(B and C) Authentic atromentin (B) and synthetic gyrocyanin (C). Chromatographic signals: $t_R = 25.7$ min for involutin (compound 1); $t_R = 38.9$ min for gyroporin (2); $t_R = 52.3$ min for gyrocyanin (3); $t_R = 60.4$ min for atromentin (4). Detection wavelength was $\lambda = 254$ nm. Mass spectra of mycelial homogenate supplemented with unlabeled atromentin are shown in Figure S2.

chromatographic and mass spectrometric characteristics with a synthetic reference (see Supplemental Experimental Procedures). Involutin was found only in non-deuterated form (m/z 313.0723 $[M - H]^-$), likely due to the mycelial homogenate failing to reduce gyrocyanin into chamonixin (Figure 1), with the latter only being detectable in negligible traces and in non-deuterated form by mass spectrometry.

$3',3'',5',5''$ -D₄-atromentin was also added to intact *P. involutus* cultures at 1.5 mM final concentration. As fungi usually secrete atromentin and/or its follow-up products out of the cells and given the competing cellular biosynthesis of non-labeled atro-

mentin, we expected very minor quantities of deuterated atromentin being taken up and catalytically converted by the cells, and being secreted back into the medium. We therefore resorted to single-ion monitoring high-resolution electrospray ionization mass spectrometry (HRESI-MS) for analysis. The mass spectrometric data (Figure S2) supported the above findings, as they demonstrated the presence of tetradeuterated gyrocyanin and gyroporin as well. We also detected the mass (m/z 301.1017 $[M - H]^-$) of tetradeuterated chamonixin (Besl et al., 1980), the biosynthetic follow-up product downstream of gyrocyanin. Unlabeled involutin, which is three biosynthetic steps away from

atromentin, and atromentic acid, which is a direct follow-up product of atromentin, were present in traces (Figure S2). Our data cannot fully rule out a route involving atromentic acid, i.e., a butenolide intermediate. However, our data strongly favor the latter model, since merely traces of atromentic acid were detectable by HRESI-MS, and diarylcyclopentenone biosynthesis in *P. involutus* proceeds through the terphenylquinone atromentin. This compound represents the common intermediate of both the atromentic acid/pulvinic acid and the thelephoric acid family of fungal pigments. Our results expand its significance by adding the cyclopentenones as another atromentin-derived class of ecologically relevant basidiomycete natural products.

SIGNIFICANCE

The basidiomycete *P. involutus* represents a model organism for ectomycorrhizae. These tree-fungus symbioses are critical for functional forest ecosystems, which are carbon sinks of global importance. To mobilize nutrients embedded in forest litter material, this fungus relies on Fenton chemistry to help degrade complex organic biomass and, thus, maintain carbon cycling. This chemistry requires redox-active 2,5-diarylcyclopentenone pigments, e.g., involutin. Our study demonstrates that the biosynthetic key intermediate is the terphenylquinone atromentin, which is supplied in a parallelized physiological process. The highly and simultaneously expressed genes *invA1*, *invA2*, and *invA5* encode functional three-domain quinone synthetases to secure atromentin biosynthesis. A three-fold multiplex natural product pathway is unprecedented with fungi, yet underlines the ecological significance of environmentally relevant redox-active cyclopentenones.

EXPERIMENTAL PROCEDURES

General Procedures and Culture Conditions

P. involutus ATCC 200175 was routinely grown at 23°C as still culture on liquid modified Melin-Norkrans (MMN) medium. Molecular genetic procedures were carried out according to the manufacturers' instructions (Fermentas, NEB, Promega) or as described below. Chemicals were purchased from Alfa Aesar, Sigma-Aldrich, Roth, and VWR, except [³²P]pyrophosphate, which was obtained from PerkinElmer, and deuterated L-tyrosine (ring-3,5-D₂, 98%), which was purchased from Cambridge Isotope Laboratories. The genomic sequence of *P. involutus* ATCC 200175 is available through the MycoCosm genome portal at the Joint Genome Institute (Kohler et al., 2015).

Cloning of *invA1–invA6* and *pptA* cDNAs

The SV total RNA isolation system (Promega) was used to purify total RNA from *P. involutus* mycelium. First-strand synthesis was primed with a 16-mer oligo(dT)-primer (40 pmol) and carried out in the supplied buffer, with MgCl₂ (2 mM), dinucleotide triphosphates (dNTPs) (0.5 mM each), and ImProm reverse transcriptase, in a total volume of 20 μl. A portion of the first-strand reaction (3 μl) was used as template in subsequent PCRs. The reactions (50 μl) to amplify cDNAs of *invA1*, *invA3*, and *invA6* consisted of 3 mM MgCl₂, 0.2 mM each dNTP, 40 pmol (each) primer (Table S1), and 1 U Phusion DNA polymerase in the buffer supplied with the enzyme and using the following thermal cycling parameters: 30 s at 98°C; 30–35 cycles of 98°C for 10 s, 59°C–66.5°C for 20 s, and 72°C for 105 s; and a terminal hold for 5 min at 72°C. The cDNAs of genes *invA4* and *invA5* were amplified with 4 mM MgSO₄, 0.2 mM each dNTP, 40 pmol (each) primer (Table S1), and 1.5 U pfu DNA polymerase in the buffer supplied with the enzyme, in a total volume of 50 μl. Thermocycling conditions were initial denaturation: 2 min at 95°C; amplification: 35 cycles (95°C for 30 s, 60°C–65°C for 30 s, 72°C for 8 min); terminal

hold: 10 min at 72°C. The primers introduced restriction sites into the PCR products, which were cloned into expression vectors pET28b and pRSETb, respectively, to create plasmids pJB051 (to express *invA5*), pJB064 (*invA4*), pJB078 (*invA1*), pJB080 (*invA6*), and pJB082 (*invA3*). Codon-optimized cDNAs of *invA2*, *invA3*, *invA6*, and *pptA* were synthesized by a commercial vendor (GenScript). The cDNAs of *invA2* and *pptA* were ligated to the *Nde*I and *Bam*HI sites of pET28b to create pJB053 (to express *invA2*) and pJB062 (*pptA*), respectively. The *invA6* cDNA was ligated to the *Nde*I and *Bam*HI sites of pET28b, to create plasmid pJB066, and later excised and ligated into equally cut pCold-I to generate plasmid pJT026. The *invA3* cDNA was cloned into the *Nhe*I and *Bam*HI sites of expression vector pRSETb to create plasmid pJB063.

Construction of Chimeric Genes

The codon-optimized version of gene *invA3* was inserted into the *Nhe*I and *Bam*HI sites of expression vector pET28b to create plasmid pJB059. Subsequently, the portion of pJB059 encoding the TE domain of *InvA3* was replaced by the corresponding portion of *InvA5* (taken from plasmid pJB051) using the *Kpn*I and *Bam*HI restriction sites. The created chimeric gene *invA335* was cloned into expression vector pRSETb to create pJB074. It encodes a chimeric synthetase composed of the *InvA3* adenylation-thiolation (A-T) didomain and the *InvA5* thioesterase (TE) domain. A gene for the inverse chimera (*InvA553*, *InvA5* A-T didomain fused to the *InvA3* TE domain) was constructed using the Gibson Assembly Master Mix (New England Biolabs) using plasmids pJB051 and pJB059 as templates, to yield plasmid pJB075. The reactions (50 μl) consisted of 1.5–2.5 mM MgCl₂, 0.2 mM each dNTP, 20 pmol (each) primer (Table S1), and 1 U Phusion DNA polymerase in the supplied buffer and with the following thermocycling parameters, to create plasmid pJB075: 30 s at 98°C; 30 cycles of 98°C for 10 s, 48°C, 57°C, and 64.5°C, respectively, for 15 s, and 72°C for 45 s (*InvA3* TE domain), 90 s (*InvA5* A-T didomain), and 3 min (pET28b); and a terminal hold for 5 min at 72°C. To create the chimeric gene *invA556* (encoding the *InvA5* A-T didomain fused to the *InvA6* TE domain), plasmid pJB048 (*invA5*, cloned into pRSETb) was used. The gene portion encoding the TE domain of *invA6* was excised by *Cla*I and *Bam*HI restriction from pJB066 and ligated to pJB048, cut equally, to yield pJB071. The complete chimeric gene *invA556* was then cloned between the *Nde*I and *Bam*HI sites of pET28b, which yielded the final expression plasmid pJB072.

Heterologous Gene Expression and In Vitro Enzyme Characterization

N-Terminally hexahistidine-tagged *InvA2*, *InvA4*, *InvA5*, *InvA553*, *InvA556*, and *PptA* were produced in *E. coli* KRX, transformed with plasmids pJB053, pJB064, pJB051, pJB075, pJB072, and pJB062, respectively. Expression of genes *invA1*, *invA3*, *invA6*, and *invA335* was accomplished in *E. coli* SoluBL transformed with plasmids pJB078, pJB063, pJT026, and pJB074, respectively. For details on gene expression and protein purification, see Supplemental Experimental Procedures. To characterize the *InvA1–A6* adenylation domains, the ATP-[³²P]pyrophosphate exchange assay was used as described by Schneider et al. (2008). 4-Hydroxyphenylpyruvate, or other substrates (Table S2) to determine substrate specificities, were added at 1 mM final concentration. To determine optima, the temperature was varied from 10°C to 35°C, and the pH from 6.0 to 8.2 with phosphate or Tris buffers, covering overlapping pH ranges.

In Vitro Biotransformation

Conversion of *apo*-enzymes into their *holo* form was catalyzed by the phosphotransferase Svp (Sanchez et al., 2001) or *PptA*. 0.5 μM of the respective *apo*-enzyme and 0.5 μM Svp or *PptA* were incubated for 30 min at 20°C–25°C in 75 mM Tris-HCl buffer (pH 6.8–7.6), and 120 μM coenzyme A as donor substrate. Product formation was accomplished in 500-μl reactions, containing 75 mM Tris-HCl buffer (pH 6.8–7.6, according to the optimum conditions), 5 mM MgCl₂, 125 nM EDTA, 2.5 mM ATP, 0.5 μM *InvA*, and 1.8 mM 4-hydroxyphenylpyruvic acid, at 20°C–25°C for 16 hr. The reaction mixtures were extracted twice with an equal volume of ethyl acetate, and the organic extract was concentrated under reduced pressure. For analytical HPLC (see below), the extracts were dissolved in methanol.

Synthesis of Deuterated Atromentin

The synthesis of deuterated 4-hydroxyphenylpyruvic acid was carried out according to a described method (Munde et al., 2013). The synthesis of

deuterated atromentin was carried out in analogy to the in vitro atromentin formation (see above). A reaction mixture (8 ml) consisted of 75 mM Tris-HCl buffer (pH 7.2), 10 mM MgCl₂, 125 nM EDTA, 5 mM ATP, 4 μM InvA1, 4 μM Svp, 114 μM coenzyme A, and 3 mM deuterated 4-hydroxyphenylpyruvic acid. It was incubated for 16 hr at 25°C and subsequently extracted three times with an equal volume of ethyl acetate. The extract was dissolved in methanol, and purification was accomplished by preparative HPLC (see below).

Stable-Isotope Labeling

For supplementation with stable-isotope-labeled atromentin, *P. involutus* was grown in Petri dishes on a layer of glass beads immersed in liquid medium (van Schöll et al., 2006). A monolayer of autoclaved 4-mm glass beads was poured into the bottom of a 9-cm Petri dish and 10 ml of MMN medium was added. A mycelial plug was cut from the mycelial margin of a culture actively growing on MMN agar and transferred to the center of the glass-bead plate. After 9 days of incubation at 18°C–20°C in the dark, the MMN medium was removed. The glass beads and the mycelium were washed with sterile MilliQ water, and 10 ml of MMN medium without a nitrogen source was added. After 24 hr, the mycelium was washed with sterile MilliQ water. Subsequently, 10 ml of maize hot extract supplemented with glucose (final concentration 2.5 g/l; pH 4) was added (Rineau et al., 2012; Shah et al., 2013). The culture was incubated for another 7 days at 18°C–20°C in the dark. For the first feeding experiment with homogenized mycelium, ten plates of *P. involutus* were cultivated as described above. The mycelium was then homogenized in 100 ml of 75 mM Tris-HCl buffer (pH 7.2) supplemented with 1 mM PMSF, using an Ultra-Turrax T25 basic (IKA). Unlabeled or 3',3'',5',5''-D₄-atromentin was added to 30 ml of homogenized mycelium at a final concentration of 1 mM. As control, another 30 ml was left without any labeled compounds. The reactions were incubated for 24 hr at room temperature and then extracted three times with 30 ml of ethyl acetate. The organic extracts were concentrated under reduced pressure. The extracts were redissolved in methanol for analytical HPLC (see below). For the second labeling experiment, six plates of *P. involutus* were cultivated as described above. Two plates were supplemented with 3',3'',5',5''-D₄-atromentin (final concentration: 1.5 mM, added together with the maize hot extract). Another two plates without labeled compounds served as control. The cultures were incubated for another 7 days at 18°C–20°C in the dark, before the media were extracted three times with ethyl acetate and further processed as described above.

Chromatography and Mass Spectrometry

HPLC analysis of in vitro product formation was performed on an Agilent 1200 system equipped with a Zorbax Eclipse XDB-C₁₈ column (4.6 × 150 mm, 5 μm particle size). Solvent A was 0.1% (v/v) trifluoroacetic acid in water, and solvent B was methanol. The solvent gradient was: initial hold at 5% B, for 0.5 min, linear gradient from 5% to 90% B within 14.5 min, held at 90% B for 2 min, increased to 100% B within 0.5 min, and held for 4.5 min, at a flow rate of 1.0 ml/min. The detection wavelength range was 200–600 nm; chromatograms were extracted at λ = 254 nm. HPLC to analyze compounds after stable-isotope feeding was carried out as described above, but using a Nucleosil 100-5 C₁₈ column (4.6 × 250 mm, 5 μm particle size) and the following gradient: initial hold at 5% B for 10 min, linear gradient 5%–50% B within 60 min, then increased to 100% B within 10 min, then held for another 5 min, at a flow rate of 1.0 ml/min.

High-resolution mass spectra were recorded on an Exactive Orbitrap mass spectrometer (Thermo) in the negative mode using electrospray ionization and equipped with a Betasil C₁₈ column (Thermo, 2.1 × 150 mm; 3 μm particle size). Solvent A was 0.1% (v/v) formic acid in water, and solvent B was 0.1% (v/v) formic acid in acetonitrile. The solvent gradient was: initial hold at 5% B, for 1 min, linear gradient from 5% to 98% B within 15 min, then held at 98% B for 3 min, at a flow rate of 0.2 ml/min.

Preparative HPLC to purify deuterated atromentin was performed on an Agilent 1260 Infinity System, equipped with a Zorbax Eclipse XDB-C₈ column (21.2 × 250 mm; 7 μm particle size), at a flow rate of 25 ml/min. Solvent A was 0.1% (v/v) trifluoroacetic acid in water, and solvent B was acetonitrile. The gradient was: linear increase from 5% to 80% B within 20 min, increased to 100% in 1 min, and held for another 1 min. The detection wavelength range was λ = 200–600 nm.

Transcriptomic Analysis

Fungal mycelia were grown as described above, but using BSA (16% [w/w] N) as sole nitrogen source, or organic matter extracts (forest hot extract, maize hot extract, and maize compost). For each treatment there were three biological replicates with three Petri dishes per replicate. The biomass was collected and immediately dropped into a clean mortar filled with liquid nitrogen, and homogenized using a pestle. Total RNA was isolated using the RNeasy Plant Mini Kit (Qiagen) with the RLC buffer and the on-column DNase treatment according to the manufacturer. Total RNA was eluted in diethylpyrocarbonate-treated H₂O and stored at –20°C until use. For quality assessments, all samples were inspected using an RNA 6000 Nano kit on an Agilent 2100 Bioanalyzer. The microarray analysis was performed using already published data including six biological replicates on the reference MMN medium that are available at NCBI GEO (accession numbers NCBI-GEO: GSM848412–GSM848414 and GSM848421–GSM848423), as well as three replicates each for forest hot extract (GSM848415–GSM848417), maize hot extract (GSM848418–GSM848420), maize compost (GSM848424–GSM84842), and BSA (GSE47838) (Rineau et al., 2012; Shah et al., 2013).

SUPPLEMENTAL INFORMATION

Supplemental Information includes Supplemental Experimental Procedures, two figures, and two tables and can be found with this article online at <http://dx.doi.org/10.1016/j.chembiol.2015.08.016>.

AUTHOR CONTRIBUTIONS

J.B. performed molecular biological and biochemical experiments and chromatographic analyses; S.G. synthesized gyrocyanin; F.S. and A.T. generated and interpreted the transcriptomic data; D. Heine provided critical input on the synthesis of deuterated atromentin; J.T. cloned and expressed the *invA6* gene; D. Hoffmeister designed the study and co-wrote the paper together with C.H., P.S., and A.T.

ACKNOWLEDGMENTS

This work was supported by the Deutsche Forschungsgemeinschaft (DFG grant HO2515/4-1 to D. Hoffmeister). A stipend of the Studienstiftung des deutschen Volkes to D. Heine is gratefully acknowledged. P.S. is grateful to the Daimler und Benz Stiftung for a Research Scholarship, and J. T. acknowledges funding by the Collaborative Research Center ChemBioSys (SFB1127/1). We thank Andrea Perner and Heike Heinecke (Leibniz Institute for Natural Product Research and Infection Biology, Hans Knöll Institute, Jena, Germany) for recording mass and NMR spectra, respectively.

Received: June 7, 2015

Revised: August 17, 2015

Accepted: August 27, 2015

Published: October 22, 2015

REFERENCES

- Besl, H., Bresinsky, A., Steglich, W., and Zipfel, K. (1973). Pilzpigmente XVII. Über Gyrocyanin, das blauende Prinzip des Korbblumenröhrchens (*Gyroporus cyanescens*) und eine oxidative Ringverengung des Atromentins. *Chem. Ber.* 106, 3223–3229.
- Besl, H., Bresinsky, A., Herrmann, R., and Steglich, W. (1980). Chamonixin and involutin, two chemosystematically interesting cyclopentanediones from *Gyrodon lividus*. *Z. Naturforsch.* 35C, 824–825.
- Biggins, J.B., Liu, X., Feng, Z., and Brady, S.F. (2011). Metabolites from the induced expression of cryptic single operons found in the genome of *Burkholderia pseudomallei*. *J. Am. Chem. Soc.* 133, 1638–1641.
- Bresinsky, A. (1974). Zur Frage der taxonomischen Relevanz chemischer Merkmale bei Höheren Pilzen. *Bull. Soc. Linnéenne Lyon*, 61–84.
- Bresinsky, A., and Rennschmidt, A. (1971). Pigmentmerkmale, Organisationsstufen und systematische Gruppen bei höheren Pilzen. *Ber. Dtsch. Bot. Ges.* 84, 313–329.

- Bruner, S.D., Weber, T., Kohli, R.M., Schwarzer, D., Marahiel, M.A., Walsh, C.T., and Stubbs, M.T. (2002). Structural basis for the cyclization of the lipopeptide antibiotic surfactin by the thioesterase domain SrfTE. *Structure* 10, 301–310.
- Cantu, D.C., Chen, Y., and Reilly, P.J. (2010). Thioesterases: a new perspective based on their primary and tertiary structures. *Protein Sci.* 19, 1281–1295.
- Conti, E., and Izaurralde, E. (2005). Nonsense-mediated mRNA decay: molecular insights and mechanistic variations across species. *Curr. Opin. Cell Biol.* 17, 316–325.
- Eastwood, D.C., Floudas, D., Binder, M., Majcherczyk, A., Schneider, P., Aerts, A., Asiegbu, F.O., Baker, S.E., Barry, K., Bendiksby, M., et al. (2011). The plant cell wall-decomposing machinery underlies the functional diversity of forest fungi. *Science* 333, 762–765.
- Edwards, R.L., and Gill, M. (1973). Constituents of the higher fungi. Part XII. Identification of involutin as (-)-cis-5-(3,4-dihydroxyphenyl)-3,4-dihydroxy-2-(4-hydroxyphenyl)-cyclopent-2-enone and synthesis of (±)-cis-involutin trimethyl ether from isoxerocomic acid derivatives. *J. Chem. Soc. (London) Perkin Trans. I*, 1529–1537.
- Edwards, R.L., Elsworth, G.C., and Kale, N. (1967). Constituents of higher fungi. Part IV. Involutin, a diphenyl-cyclopenteneone from *Paxillus involutus* (Oeder ex Fries). *J. Chem. Soc. C*, 405–409.
- Forseth, R.R., Amaike, S., Schwenk, D., Affeldt, K.J., Hoffmeister, D., Schroeder, F.C., and Keller, N.P. (2013). Homologous NRPS-like gene clusters mediate redundant small-molecule biosynthesis in *Aspergillus flavus*. *Angew. Chem. Int. Ed. Engl.* 52, 1590–1594.
- Gill, M., and Steglich, W. (1987). Pigments of fungi (Macromycetes). *Fortschr. Chem. Org. Naturst.* 51, 1–317.
- Gruber, G., Kerschensteiner, L., and Steglich, W. (2014). Chromapedic acid, pulvinic acids and acetophenone derivatives from the mushroom *Leccinum chromapes* (Boletales). *Z. Naturforsch.* 69B, 432–438.
- Hermann, R. (1980). Untersuchungen zur Konstitution, Synthese und Biosynthese von Pilzfarbstoffen (Germany: Rheinische Friedrich-Wilhelms-Universität Bonn), doctoral thesis.
- Hoyer, K.M., Mahler, C., and Marahiel, M.A. (2007). The iterative gramicidin S thioesterase catalyzes peptide ligation and cyclization. *Chem. Biol.* 14, 13–22.
- Keszenman-Pereyra, D., Lawrence, S., Twieg, M.E., Price, J., and Turner, G. (2003). The *npgA/cfwA* gene encodes a putative 4'-phosphopantetheinyl transferase which is essential for penicillin biosynthesis in *Aspergillus nidulans*. *Curr. Genet.* 43, 186–190.
- Kohler, A., Kuo, A., Nagy, L.G., Morin, E., Barry, K.W., Buscot, F., Canbäck, B., Choi, C., Cichocki, N., Clum, A., et al. (2015). Convergent losses of decay mechanisms and rapid turnover of symbiosis genes in mycorrhizal mutualists. *Nat. Genet.* 47, 410–415.
- Larrondo, L.F., Gonzalez, B., Cullen, D., and Vicuna, R. (2004). Characterization of a multicopper oxidase gene cluster in *Phanerochaete chrysosporium* and evidence of altered splicing of the *mco* transcripts. *Microbiology* 150, 2775–2783.
- Lindahl, B.D., and Tunlid, A. (2015). Ectomycorrhizal fungi—potential organic matter decomposers, yet not saprotrophs. *New Phytol.* 205, 1443–1447.
- Misiek, M., and Hoffmeister, D. (2008). Processing sites involved in intron splicing of *Armillaria* natural product genes. *Mycol. Res.* 112, 216–224.
- Munde, T., Brand, S., Hidalgo, W., Maddula, R.K., Svatos, A., and Schneider, B. (2013). Biosynthesis of tetraoxygenated phenylphenalenones in *Wachendornia thyrsoiflora*. *Phytochemistry* 91, 165–176.
- Rineau, F., Roth, D., Shah, F., Smits, M., Johansson, T., Canbäck, B., Olsen, P.B., Persson, P., Grell, M.N., Lindquist, E., et al. (2012). The ectomycorrhizal fungus *Paxillus involutus* converts organic matter in plant litter using a trimmed brown-rot mechanism involving Fenton chemistry. *Environ. Microbiol.* 14, 1477–1487.
- Samel, S.A., Wagner, B., Marahiel, M.A., and Essen, L.O. (2006). The thioesterase domain of the fengycin biosynthesis cluster: a structural base for the macrocyclization of a non-ribosomal lipopeptide. *J. Mol. Biol.* 359, 876–889.
- Sanchez, C., Du, L., Edwards, D.J., Toney, M.D., and Shen, B. (2001). Cloning and characterization of a phosphopantetheinyl transferase from *Streptomyces verticillus* ATCC15003, the producer of the hybrid peptide-polyketide anti-tumor drug bleomycin. *Chem. Biol.* 8, 725–738.
- Schneider, P., Weber, M., Rosenberger, K., and Hoffmeister, D. (2007). A one-pot chemoenzymatic synthesis for the universal precursor of antidiabetes and antiviral bis-indolylquinones. *Chem. Biol.* 14, 635–644.
- Schneider, P., Bouhired, S., and Hoffmeister, D. (2008). Characterization of the atromentin biosynthesis genes and enzymes in the homobasidiomycete *Tapinella panuoides*. *Fungal Genet. Biol.* 45, 1487–1496.
- Schwarzer, D., Finking, R., and Marahiel, M.A. (2003). Nonribosomal peptides: from genes to products. *Nat. Prod. Rep.* 20, 275–287.
- Shah, F. (2014). Insights into the Molecular Mechanisms of Litter Decomposition and Assimilation of Nitrogen by Ectomycorrhizal Fungi (Sweden: Lund University), Doctoral thesis. Lund University Publications, ISBN:978-91-7473-938-1.
- Shah, F., Rineau, F., Canbäck, B., Johansson, T., and Tunlid, A. (2013). The molecular components of the extracellular protein-degradation pathways of the ectomycorrhizal fungus *Paxillus involutus*. *New Phytol.* 200, 875–887.
- Stachelhaus, T., Mootz, H.D., and Marahiel, M.A. (1999). The specificity conferring code of adenylation domains in nonribosomal peptide synthetases. *Chem. Biol.* 6, 493–505.
- Steglich, W., Steffan, K., Besl, H., and Bresinsky, A. (1977). Pilzpigmente 29. 2,5-Diarylcylopentan-1,3-dione aus *Chamonixia caespitosa* (Basidiomycetes). *Z. Naturforsch.* 32c, 46–48.
- Trauger, J.W., Kohli, R.M., Mootz, H.D., Marahiel, M.A., and Walsh, C.T. (2000). Peptide cyclization catalysed by the thioesterase domain of tyrocidine synthetase. *Nature* 407, 215–218.
- van Schöll, L., Hoffland, E., and van Breemen, N. (2006). Organic anion exudation by ectomycorrhizal fungi and *Pinus sylvestris* in response to nutrient deficiencies. *New Phytol.* 170, 153–163.
- Wackler, B., Schneider, P., Jacobs, J.M., Pauly, J., Allen, C., Nett, M., and Hoffmeister, D. (2011). Ralfuranone biosynthesis in *Ralstonia solanacearum* suggests functional divergence in the quinone synthetase family of enzymes. *Chem. Biol.* 18, 354–360.
- Wackler, B., Lackner, G., Chooi, Y.H., and Hoffmeister, D. (2012). Characterization of the *Suillus grevillei* quinone synthetase GreA supports a nonribosomal code for aromatic α -keto acids. *ChemBiochem* 13, 1798–1804.
- Wallander, H., and Söderström, B. (1999). *Paxillus*. In *Ectomycorrhizal Fungi: Key Genera in Profile*, J.W.G. Cairney and S.M. Chambers, eds. (Springer-Verlag), pp. 231–252.
- Yeh, H.H., Chiang, Y.M., Entwistle, R., Ahuja, M., Lee, K.H., Bruno, K.S., Wu, T.K., Oakley, B.R., and Wang, C.C. (2012). Molecular genetic analysis reveals that a nonribosomal peptide synthetase-like (NRPS-like) gene in *Aspergillus nidulans* is responsible for microperforanone biosynthesis. *Appl. Microbiol. Biotechnol.* 96, 739–748.
- Zeiler, E., List, A., Alte, F., Gersch, M., Wachtel, R., Poreba, M., Drag, M., Groll, M., and Sieber, S.A. (2013). Structural and functional insights into caseinolytic proteases reveal an unprecedented regulation principle of their catalytic triad. *Proc. Natl. Acad. Sci. USA* 110, 11302–11307.
- Zhou, Z.Y., and Liu, J.K. (2010). Pigments of fungi (Macromycetes). *Nat. Prod. Rep.* 27, 1531–1570.
- Zhu, J., Chen, W., Li, Y.Y., Deng, J.J., Zhu, D.Y., Duan, J., Liu, Y., Shi, G.Y., Xie, C., Wang, H.X., and Shen, Y.M. (2014). Identification and catalytic characterization of a nonribosomal peptide synthetase-like (NRPS-like) enzyme involved in the biosynthesis of echosides from *Streptomyces* sp. LZ35. *Gene* 546, 352–358.

Chemistry & Biology, Volume 22

Supplemental Information

Three Redundant Synthetases Secure

Redox-Active Pigment Production

in the Basidiomycete *Paxillus involutus*

Jana Braesel, Sebastian Götze, Firoz Shah, Daniel Heine, James Tauber, Christian Hertweck, Anders Tunlid, Pierre Stallforth, and Dirk Hoffmeister

Supplemental Information

Three redundant synthetases secure redox-active pigment production in the basidiomycete *Paxillus involutus*

Jana Braesel,¹ Sebastian Götze,² Firoz Shah,³ Daniel Heine,⁴ James Tauber,¹ Christian Hertweck,⁴ Anders Tunlid,³ Pierre Stallforth,² Dirk Hoffmeister^{1,*}

Department Pharmaceutical Microbiology at the Hans Knöll Institute, Friedrich-Schiller-University Jena, Beutenbergstrasse 11a, 07745 Jena, Germany¹;

Junior Group Chemistry of Microbial Communication, Leibniz Institute for Natural Product Research and Infection Biology – Hans Knöll Institute, Beutenbergstrasse 11a, 07745 Jena, Germany²;

Department of Biology, Lund University, Sölvegatan 37, 221 00 Lund, Sweden³;

Department Biomolecular Chemistry, Leibniz Institute for Natural Product Research and Infection Biology - Hans Knöll Institute, Beutenbergstrasse 11a, 07745 Jena, Germany⁴.

#Corresponding author. E-mail address: dirk.hoffmeister@hki-jena.de

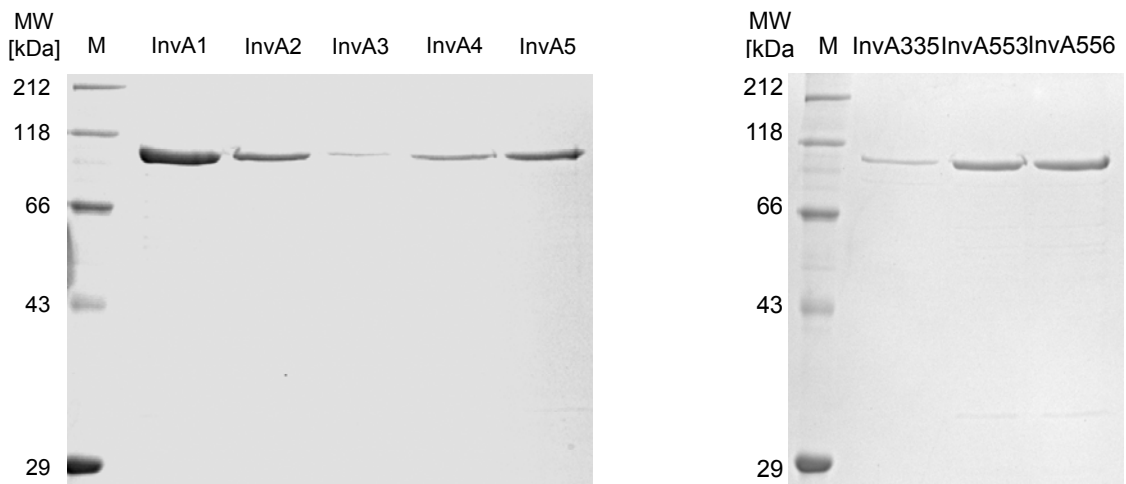
Contents

Figure S1: Enzyme purification and initial determination of substrate specificity	3
Figure S2: High-resolution mass traces of <i>Paxillus involutus</i> metabolites	5
Table S1: Oligonucleotide primers used during this study	7
Table S2: Substrates used for the ATP-[³² P]pyrophosphate exchange assay	8
Supplemental Experimental Procedures	9
Supplemental References	10

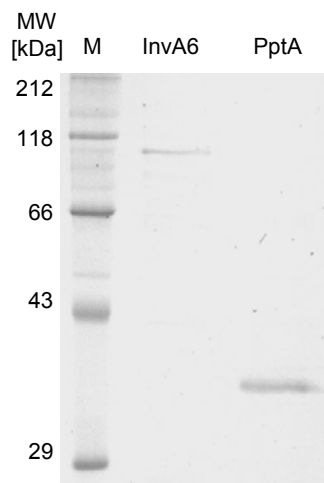
Supplemental Data

Figure S1 (related to Figure 3). I) SDS-polyacrylamide gel of heterologously produced *Paxillus involutus* biosynthetic enzymes after purification on Ni²⁺-NTA and used for the substrate-dependent ATP-[³²P]pyrophosphate exchange assay (Figure 3). Left gel: wild type quinone synthetases, right gel: chimeric quinone synthetases. Below: *P. involutus* 4'-phosphopantetheinyltransferasen and InvA6. M: molecular weight standard. II) Initial determination of substrate specificity of the InvA1-InvA3, and InvA5 adenylation domains, using pools of substrates (Table S2). Error bars indicate standard deviations.

I)



II)



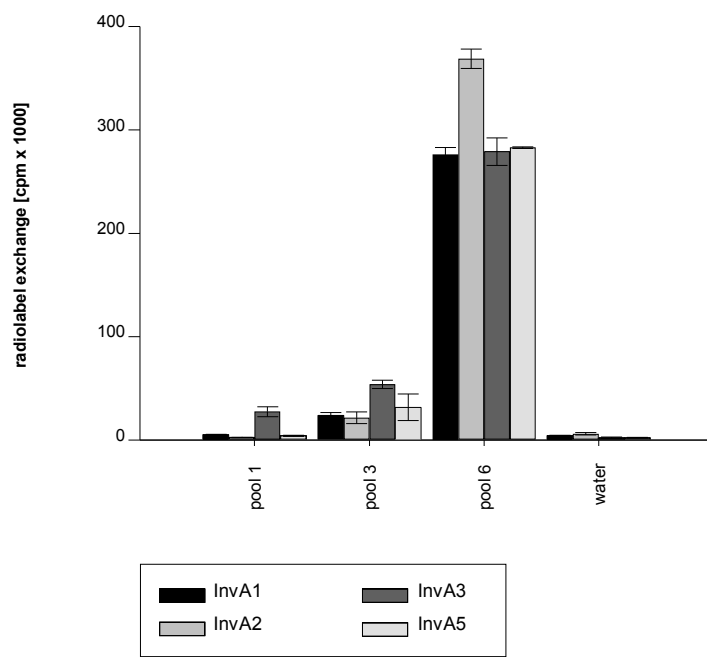
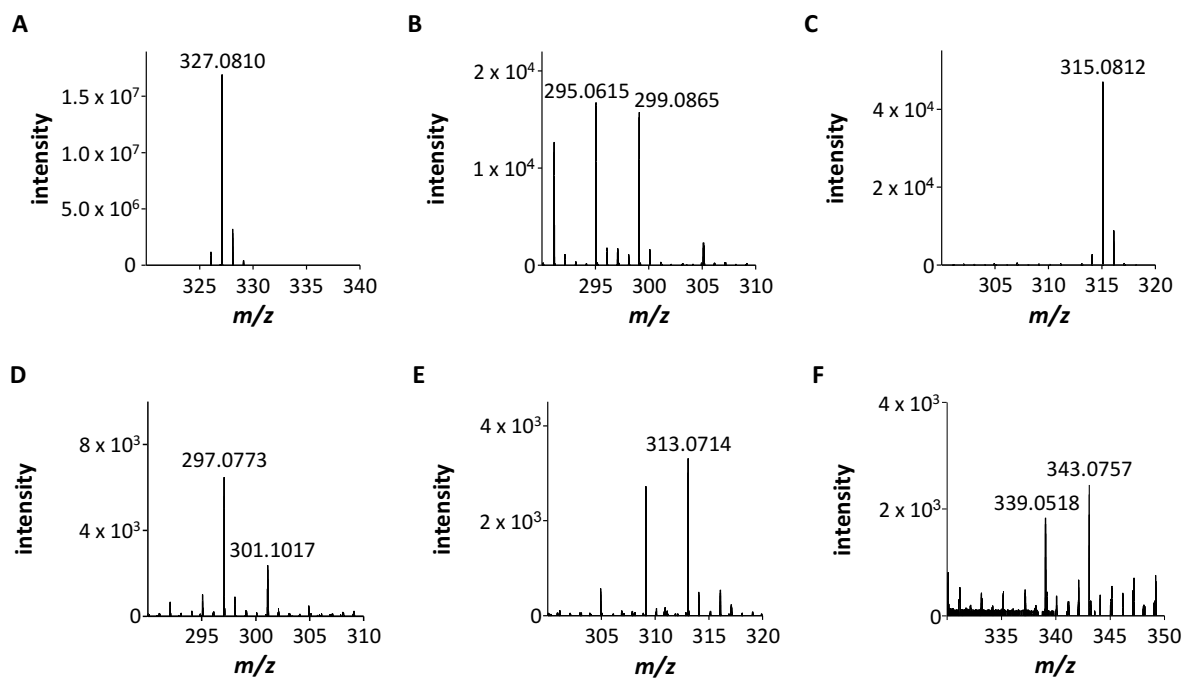


Figure S2 (related to Figure 5).

I) High-resolution mass traces (ESI, negative mode) of metabolites, identified after addition of 3',3'',5',5''-D₄-atromentin to *Paxillus involutus* cultures (see also Figure 5). A: atromentin, B: gyrocyanin, C: gyroporin, D: chamonixin, E: involutin, F: atromentic acid.

II) High-resolution mass traces (ESI, negative mode) of metabolites, identified after feeding unlabeled atromentin to *Paxillus involutus* mycelial homogenate. A: atromentin, B: gyrocyanin, C: gyroporin, D: chamonixin, E: involutin, F: atromentic acid.

I)



II)

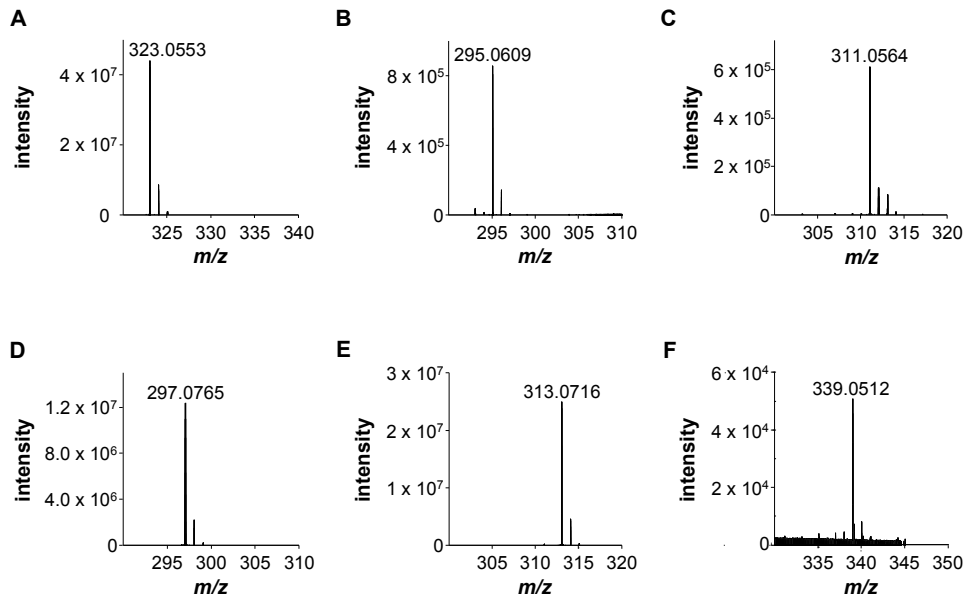


Table S2 (related to Figure 3). Substrates used for the ATP-[³²P]pyrophosphate exchange assay.

All InvA enzymes, except InvA4 and InvA6

L-amino acids: L-Ala, L-His, L-Phe, L-Tyr, L-Trp

α-keto acids: phenylpyruvate, 4-hydroxyphenylpyruvate, indole-3-pyruvate, pyruvate, α-keto glutaric acid

InvA4 and InvA6

pool 1: L-Ala, glycine, L-Leu, L-Ile, L-Val

pool 2: L-Cys, L-Met, L-Pro, L-Ser, L-Thr

pool 3: L-His, L-Phe, L-Tyr, L-Trp

pool 4: L-Asp, L-Asn, L-Glu, L-Gln

pool 5: L-Arg, L-Lys, L-ornithine

pool 6: phenylpyruvate, 4-hydroxyphenylpyruvate, indole-3-pyruvate, pyruvate, α-keto glutaric acid

pool 7: 2-oxobutyric acid, 2-oxovaleric acid, oxalacetic acid, imidazole pyruvate

pool 8: mandelic acid, benzoic acid, *p*-hydroxybenzoic acid, indole-3-acetic acid

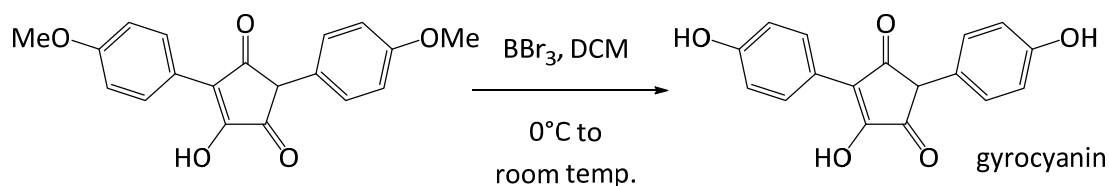
pool 9: phenylglyoxylic acid, phenylacetic acid, cinnamic acid

Supplemental Experimental Procedures

Gene expression and enzyme purification

To produce the enzymes InvA2, InvA4, InvA5, InvA553, InvA556, and PptA heterologously, 20 mL of an overnight culture in LB medium, amended with kanamycin (50 mg/L) or carbenicillin (50 mg/L), were used to inoculate 2 L of the same medium. The cultures were shaken at 37°C at 180 rpm to an optical density (OD₆₀₀) of 0.4 and then incubated at 16°C. Upon reaching an OD₆₀₀ of about 0.6, the expression of *invA2*, *invA4*, *invA5*, *invA553* and *pptA* was induced by adding 0.1% (w/v) L-rhamnose and shaken for further 48 h, before collecting the biomass by centrifugation (4°C, 3,200 g, 20 min). Gene expression of *invA1*, *invA3*, *invA6*, and *invA335* was accomplished in *E. coli* SoluBL transformed with plasmids pJB078, pJB063, pJT026, and pJB074, respectively, to heterologously produce *N*-terminally hexahistidine-tagged proteins. To produce InvA1, InvA3 and InvA335, 40 mL of overnight culture in LB medium, amended with carbenicillin (50 mg/L), were used to inoculate a 0.8 L and a 4 L autoinduction medium culture, respectively, which was shaken at 20°C and 180 rpm for 48 h. The expression was induced by lactose (20 g/L). Production of InvA6 totaled a 2 L LB culture amended with carbenicillin (50 mg/L) initially grown to an OD₆₀₀ = 0.4 at 37°C at 180 rpm and then equilibrated at 15°C for 30 min, induced with 1 mM IPTG (final), and incubated for 48 h until harvest. After centrifugation (4 °C, 3200 g, 20 min) the cells were resuspended in lysis buffer (NaH₂PO₄ 50 mM, NaCl 300 mM, imidazole 5 mM, pH 8.0, and 10% (v/v) glycerol) and disrupted by three pulses (40 s each, at 35% output) by a Branson 450 sonifier. Cell debris was removed by centrifugation (4°C, 14,000 g, 20 min). The proteins were separately purified on Ni²⁺-NTA resin (Macherey&Nagel) by metal-affinity chromatography. The pure enzymes were desalted on PD-10 columns (GE Healthcare) and equilibrated in the respective reaction buffer (see below). The protein concentrations were determined by Bradford's method (Bradford, 1976). The phosphopantetheinyl transferase Svp was produced as described (Schneider et al., 2007).

Synthesis of gyrocyanin



4-Hydroxy-2,5-bis(4-methoxyphenyl)cyclopent-4-ene-1,3-dione (10 mg, 31 μmol) (Besl et al., 1973) was dissolved in anhydrous methylene chloride (8 mL). The yellow solution was cooled to 0°C , and boron tribromide (1 M in methylene chloride, 156 μL , 155 μmol , Sigma Aldrich) was added dropwise while stirring. An immediate color change from yellow to red was observed that subsequently turned dark green to almost black. The solution was warmed to room temperature and stirred for 21 h. The reaction mixture was poured into ice water (20 mL) and was extracted with ethyl acetate (40 mL, HPLC grade, VWR). The organic layer was washed with water (2 x 20 mL) and the solvent was removed under reduced pressure. The residue was dissolved in acetone (1 mL, HPLC grade, VWR) and subjected to size-exclusion chromatography using a Sephadex LH-20 column (30 x 1 cm, GE Healthcare), and HPLC grade methanol as mobile phase. The fractions containing the compound were pooled to yield crude gyrocyanin as a yellow syrup (5 mg). Half of this material was further purified by semi-preparative HPLC (Shimadzu) equipped with a Phenomenex Luna column (Phenyl-Hexyl, 250 x 10 mm, 5 μm particle size) flow rate = 5 mL/min, gradient: 0-1 min: isocratic 10% (v/v) MeCN in water and 0.1% formic acid; 1-20 min: linear gradient 10% to 100% MeCN in water and 0.1% formic acid) to yield gyrocyanin as yellow solid (1 mg, 3 μmol , 20% yield): $t_{\text{R}} = 10.3$ min; $^1\text{H-NMR}$ (500 MHz, d_6 -acetone, Bruker AVANCE III 500): $\delta = 8.22$ (d, $J = 8.8$ Hz, 2H), 7.02 (d, $J = 8.5$ Hz, 2H), 6.92 (d, $J = 8.9$ Hz, 2H), 6.80 (d, $J = 8.5$ Hz, 2H), 4.08 (s, 1H); HR-ESI calcd for $\text{C}_{17}\text{H}_{11}\text{O}_5$ $[\text{M-H}]^-$ 295.0612, found $[\text{M-H}]^-$ 295.0613. HRESI-MS was carried out on a Thermo Accela UPLC-system, coupled to an Exactive mass spectrometer (Thermo Scientific) equipped with an electrospray ion source. Analytical data were in agreement with published data (Besl et al., 1973).

Supplemental References

Bradford, M. (1976). A rapid and sensitive method for the quantitation of microgram quantities of protein utilizing the principle of protein–dye binding. *Anal. Biochem.* *72*, 248-254.

Schneider, P., Weber, M., Rosenberger, K., Hoffmeister, D. (2007). A one-pot chemoenzymatic synthesis for the universal precursor of antidiabetes and antiviral bis-indolylquinones. *Chem. Biol.* *14*, 635-644.

Besl, H., Bresinsky, A., Steglich, W., Zipfel, K. (1973). Pilzpigmente XVII. Über Gyrocyanin, das blauende Prinzip des Kornblumenröhrlings (*Gyroporus cyanescens*) und eine oxidative Ringverengung des Atromentins. *Chem. Ber.* *106*, 3223-3229.

2.2. A Fivefold Parallelized Biosynthetic Process Secures Chlorination of *Armillaria mellea* (Honey Mushroom) Toxins

Wick, J., Heine, D., Lackner, G., Misiek, M., Tauber, J., Jagusch, H., Hertweck, C., and Hoffmeister, D.

Published manuscript (104).

Appl. Environ. Microbiol. (2016) 82: 1196-1204.

Summary and importance

The mushroom *Armillaria mellea* produces many variations of melleolides. These natural products are of interest to chemical ecologists and to medicine because they are phytotoxic and cytotoxic, respectively. A biosynthetic feature of these compounds is regioselective halogenation. This work provided evidence of the genetic and enzymatic basis for halogenation of melleolides, and that this process is done in redundancy (by at least five halogenases).

Contribution to the manuscript

James Tauber contributed to the manuscript by cloning three annotated halogenase genes while supervising a bachelor student. In the context of the entire paper, the other authors worked on: i) identifying potential halogenase genes from the genome; ii) cloning two other similar genes; iii) all enzymatic assays, including all chromatography; iv) phylogenetic analyses; and v) wrote the majority of the manuscript, including figures. James Tauber wrote his respective section for the manuscript as well as reviewed and edited the entire manuscript draft.

A Fivefold Parallelized Biosynthetic Process Secures Chlorination of *Armillaria mellea* (Honey Mushroom) Toxins

Jonas Wick,^a Daniel Heine,^b Gerald Lackner,^c Mathias Misiak,^a James Tauber,^a Hans Jagusch,^a Christian Hertweck,^b Dirk Hoffmeister^a

Department of Pharmaceutical Microbiology, Hans Knöll Institute, Friedrich-Schiller-Universität Jena, Jena, Germany^a; Department of Biomolecular Chemistry, Leibniz Institute for Natural Product Research and Infection Biology-Hans Knöll Institute, Jena, Germany^b; Institute of Microbiology, Swiss Federal Institute of Technology (ETH), Zürich, Switzerland^c

The basidiomycetous tree pathogen *Armillaria mellea* (honey mushroom) produces a large variety of structurally related antibiotically active and phytotoxic natural products, referred to as the melleolides. During their biosynthesis, some members of the melleolide family of compounds undergo monochlorination of the aromatic moiety, whose biochemical and genetic basis was not known previously. This first study on basidiomycete halogenases presents the biochemical *in vitro* characterization of five flavin-dependent *A. mellea* enzymes (ArmH1 to ArmH5) that were heterologously produced in *Escherichia coli*. We demonstrate that all five enzymes transfer a single chlorine atom to the melleolide backbone. A 5-fold, secured biosynthetic step during natural product assembly is unprecedented. Typically, flavin-dependent halogenases are categorized into enzymes acting on free compounds as opposed to those requiring a carrier-protein-bound acceptor substrate. The enzymes characterized in this study clearly turned over free substrates. Phylogenetic clades of halogenases suggest that all fungal enzymes share an ancestor and reflect a clear divergence between ascomycetes and basidiomycetes.

The basidiomycete genus *Armillaria* includes numerous species that are known as notorious butt and root rot agents (1). They are globally distributed as hardwood or conifer pathogens (2) in managed and unmanaged forests and also damage fruit trees and grapes. Therefore, the genus is best known for its economic burden. Despite being serious plant pathogens, *Armillaria* species also play a positive environmental role, as they depolymerize lignocellulose and therefore help maintain the carbon flux in ecosystems.

A remarkable physiological feature of *Armillaria* species is the capacity to produce melleolide natural products (Fig. 1) (3–7). These secondary metabolites feature a unique molecular scaffold composed of an orsellinic acid (2,4-dihydroxy-6-methylbenzoic acid) (Fig. 1) moiety esterified to a tricyclic sesquiterpene (protoilludane) alcohol. The melleolides are intriguing, as they show two distinct structure-activity relationships for their cytotoxic and antifungal bioactivities (8). Phytotoxic activities have also been established (9, 10). Further, the melleolides represent one of the largest fungal natural product families with more than 60 structural variants. This degree of variation stems from a permutational organization of the biosynthesis that combines hydroxylation at various positions of the sesquiterpene, oxidation of the primary alcohol at C-1 to an aldehyde or carboxy group, shift or reduction of the cyclohexene double bond, and methyl ether formation at O-5'. Regioselective chlorination at C-6' also contributes to the structural diversity, reflected by about 25 described chlorinated melleolides.

None of the enzymes that modify the melleolide scaffold has been discovered to date. However, the protoilludene synthase Pro1 (11) and the orsellinic acid synthase ArmB (12) that elaborate the melleolide core structure have been characterized and described. These enzymes and those hypothesized to catalyze the above-mentioned modifications are encoded in a contiguous single-copy cluster of genes (Fig. 2), as is evident from the published genomic sequence of *Armillaria mellea* (13). Intriguingly, the gene cluster does not include any halogenase gene. Covalent attachment of a halogen atom represents a frequently found modifica-

tion of microbial natural products. Currently, more than 4,000 mostly chlorinated or brominated compounds of biological origin are known (14). They include potent bioactive compounds, such as the HSP90 inhibitor radicicol from *Chaetomium chiversii* and *Metacordyceps (Pochonia) chlamydosporia* (15, 16) or the cytotoxic endiayne C-1027 (17) of *Streptomyces globisporus*. Even some clinically used antibiotics and anticancer drugs show halogenation, e.g., the antifungal agent griseofulvin of *Penicillium aethiopicum* (18) and the anticancer drug calicheamicin of *Micromonospora echinospora* subsp. *calichensis* (19), which carry chlorine and iodine atoms, respectively. The gene clusters for the above-mentioned biosyntheses all encode one flavin-dependent halogenase.

Using melleolide F as a model representative of this class of compounds, we provide evidence that five actively transcribed genes outside the *A. mellea* melleolide biosynthesis gene cluster code for functional flavin-dependent halogenases (ArmH1 to ArmH5) that catalyze the transfer of a single chlorine atom to melleolides. This first study on basidiomycete halogenases, therefore, reveals an unprecedented case of a biosynthetic process that is secured by a 5-fold redundancy. *In vitro* characterization using heterologously produced enzymes suggests that these halogenases act on free substrates, i.e., they do not depend on carrier-protein-tethered acceptor molecules.

Received 30 September 2015 Accepted 2 December 2015

Accepted manuscript posted online 11 December 2015

Citation Wick J, Heine D, Lackner G, Misiak M, Tauber J, Jagusch H, Hertweck C, Hoffmeister D. 2016. A fivefold parallelized biosynthetic process secures chlorination of *Armillaria mellea* (honey mushroom) toxins. *Appl Environ Microbiol* 82:1196–1204. doi:10.1128/AEM.03168-15.

Editor: D. Cullen, USDA Forest Products Laboratory

Address correspondence to Dirk Hoffmeister, dirk.hoffmeister@leibniz-hki.de.

Supplemental material for this article may be found at <http://dx.doi.org/10.1128/AEM.03168-15>.

Copyright © 2016, American Society for Microbiology. All Rights Reserved.

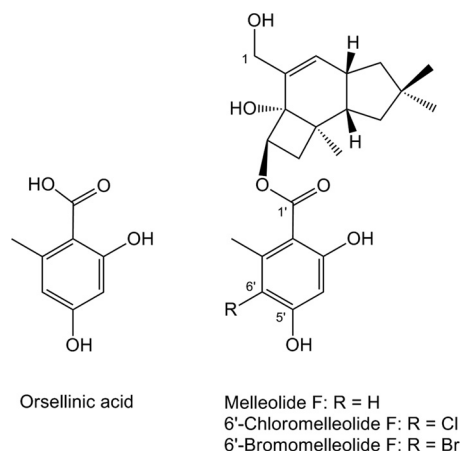


FIG 1 Chemical structures of orsellinic acid and melleolide F and its halogenated derivatives.

MATERIALS AND METHODS

General methods, strains, and chemicals. Chemicals, organic solvents, media, reagents, and antibiotics were purchased from Becton-Dickinson, Roth, Sigma-Aldrich, and VWR, except melleolide F, which was enriched to about 90% purity from *A. mellea* mycelium, following a published procedure (20). Molecular biology methods followed the protocols supplied with the kits, enzymes, and reagents (Fermentas, New England Biolabs, Promega, Thermo, and Zymo Research). *A. mellea* DSM3731 was routinely maintained on malt extract-peptone (MEP) agar, pH 5.6, at 24°C. Liquid cultures were grown in glucose minimal medium (GMM) (21) at 24°C and shaken at 180 rpm for 12 to 14 days in the dark. Stationary cultures were grown in penicillin flasks in 1 liter MEP broth. For bromine and iodine feeding, KCl was replaced by KBr and KI, respectively, in the GMM.

In silico sequence analysis. The published genomic-DNA sequence of *A. mellea* (13) was searched using the protein sequences of the protoiludene cyclase Pro1 (GenBank accession no. [AGR34199](#)), the polyketide synthase (PKS) ArmB (GenBank accession no. [AFL91703](#)), and the halogenase ArmH1 (GenBank accession no. [AEM76785](#)) as queries (11, 12, 22) and using the BLASTP function integrated in the Joint Genome Institute’s Genome Portal (23).

Cloning of *armH1* to *armH5* cDNA. Total RNA was extracted from *A. mellea* DSM3731 mycelium under melleolide-producing conditions. Mycelia were filtered under vacuum, washed with distilled H₂O (dH₂O), and ground by mortar and pestle under liquid nitrogen before total RNA extraction using the SV Total RNA Isolation System (Promega) by following the manufacturer’s spin protocol. First-strand synthesis of *armH1* and

armH2 was accomplished with the oligonucleotide primer cHalR2 (Table 1) and ImProm-II reverse transcriptase, using previously described parameters (24). Using 1 μl of the first-strand synthesis reaction mixture as the template, the *armH1* cDNA was amplified by PCR using *Pfu* polymerase (94°C for 2 min; 40 cycles of 94°C for 40 s, 58°C for 30 s, and 72°C for 4 min; final extension at 72°C for 10 min) and oligonucleotide primers cHalF1 and cHalR1 (Table 1). The PCR product was ligated into pGem-11Zf(-) via EcoRI and BamHI to yield the plasmid pMM1. After sequencing, a correct clone was used as a template for a second PCR under the following conditions: *Pfu* polymerase and primers Hal1-28F and Hal1-28R for 25 cycles (94°C for 40 s, 55°C for 30 s, 72°C for 4 min, and final extension at 72°C for 7 min). The resulting PCR product was ligated into the NdeI and BamHI sites of the vector pET28a, yielding the plasmid pMM21. The *armH2* cDNA was procured as described for *armH1* but using primer Hal2R2 for first-strand synthesis and oligonucleotide primers Hal2F1 and Hal2R1 for cDNA amplification (Table 1). The PCR product was ligated into the NdeI and BamHI sites of pET28a to give pMM13.

For first-strand synthesis of *armH3* to *armH5*, total RNA was primed with oligo(dT)₁₈ primers and reverse transcribed using RevertAid Reverse Transcriptase (Thermo). One microliter of first-strand synthesized *armH3* to *armH5* cDNA was amplified in a Phusion DNA polymerase (NEB) PCR using the recommended master mix from the manufacturer with a final MgCl₂ concentration of 2.0 mM. PCRs for *armH3* to *armH5* were primed with oligonucleotide pairs oJT073/oHJ01, oJT040/oJT041, and oJT042/oJT043, respectively (Table 1), using the following thermal-cycling parameters: initial denaturation at 98°C for 30 s; 30 cycles of 98°C for 10 s, 60°C (*armH3*) or 70°C (*armH4* and *armH5*) for 15 s, and 72°C for 2 min; and a final extension for 5 min at 72°C. Clones of *armH3* to *armH5* were ligated initially to pJET1.2 using the CloneJet PCR cloning kit and subsequently cut and ligated into equally cut pET28b to produce T7 expression plasmids pHJ28 (into NdeI and BamHI sites; *armH3*), pHJ14 (into NdeI and HindIII sites; *armH4*), and pHJ05 (into NdeI and EcoRI sites; *armH5*). The presence of insert integration was verified by DNA sequencing, and all molecular cloning was done in *Escherichia coli* XL-1 Blue, selected by carbenicillin (pJET1.2) or kanamycin (pET28b).

Cloning of the *E. coli* flavine reductase gene *fre*. The flavine reductase gene (*fre*) was amplified by PCR from genomic *E. coli* DNA using *Pfu* polymerase and primers FreN-F and FreN-R (Table 1) (30 cycles of 94°C for 40 s, 57°C for 30 s, and 72°C for 4 min and final extension of 72°C for 5 min). The PCR product was cloned into the NdeI and BglII sites of vector pET15b to yield plasmid pMM14.

Heterologous protein production and purification. For production of ArmH1 to ArmH5, *E. coli* KRX was individually transformed with pMM21 (to express *armH1*), pMM13 (*armH2*), pHJ28 (*armH3*), pHJ14 (*armH4*), or pHJ05 (*armH5*). Each transformed *E. coli* strain was grown in 2× yeast extract-tryptone (YT) medium (supplemented with kanamycin [50 μg/ml]) in Erlenmeyer flasks (10 400-ml flasks) at 37°C and 180 rpm to an optical density at 600 nm (OD₆₀₀) of 0.4. After cooling to 16°C, the

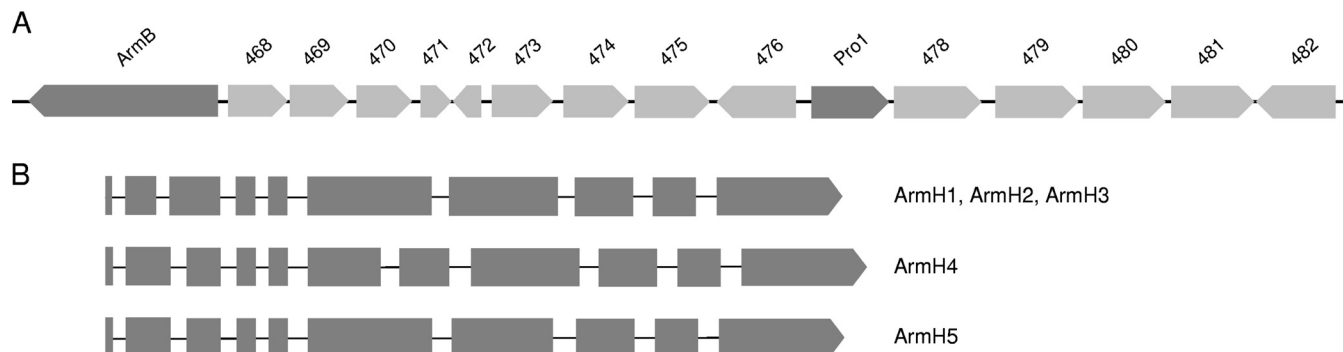


FIG 2 (A) Physical map of the melleolide-biosynthetic gene cluster. The numbers or names of proteins are shown above the respective genes. Introns are not shown. (B) Comparison of the gene structures for halogenases ArmH1 to ArmH5. The lines represent introns.

TABLE 1 Oligonucleotide primers used in this study

Oligonucleotide	Sequence (5' to 3')
cHalF1	CATCGGATCCCATCATGGAAGAAC
cHalR1	CTTGAAATAGAAATTCGGTTTGCC
cHalR2	CACAGCTCTTCATTATAGCCTAC
FreN-F	AGAAAGCATATGACAACCTTA
FreN-R	AGCTTTTTAGATCTCAGATAAATGC
Hal1-28F	ATCCCATATGGAAGAACAAGTG
Hal1-28R	CTCGGATCCGGTTTGCCGCTAAG
Hal2F1	CAGTTCATATGGTTACACAAGTGCC
Hal2R1	CCCTTTGGATCCAGTCTAAAAATCTACG
Hal2R2	AATTCATAACCCCTTTCGTTACAGTC
oJT040	AGCCACCATATGAGCTCACTATTGCC
oJT041	CTACGTAAGCTTAGTGTACGTTTTTCAGCC
oJT042	ATACCTCATATGCCTTCCGAATACGTGC
oJT043	AAAAGAATTCTTAGGCCCTGACCAATCCAAGC
oJT073	TTTTTCATATGGAAGCGCAAGTGCC
oHJ01	AAAAGGATCCCCTAAGCACACACGAG

cells were grown to an OD₆₀₀ of 0.7 and induced with L-rhamnose (0.1% [wt/vol]). After an additional 18 h of shaking at 16°C, the cells were harvested by centrifugation, cooled to 4°C, and lysed by sonication (3 times for 10 s each time). After removal of cell debris by centrifugation, the supernatants were incubated with 2 ml (each) of Ni-nitrilotriacetic acid (NTA) resin for 1 h at 4°C. The resins were transferred onto gravity flow columns and washed with 100 mM phosphate buffer (pH 7.4; 300 mM NaCl) containing increasing imidazole concentrations (10 mM and 20 mM). Elution was performed with 2.5 ml of 400 mM imidazole. The enzymes were rebuffed in 3.5 ml phosphate buffer (100 mM Na₂HPO₄, 100 mM NaCl, pH 7.4) using PD-10 columns (GE Healthcare). For bromination and iodination assays, NaCl was replaced with KBr or KI, respectively. The enzymes were concentrated with a 50-kDa-cutoff Amicon filter (Merck Millipore) and used for subsequent *in vitro* product formation assays. To produce flavin reductase, *E. coli* BL21 transformed with pMM14 was grown in liquid LB medium containing 50 µg/ml carbenicillin at 37°C and 180 rpm to an OD₆₀₀ of 0.5 and then induced with IPTG (isopropyl-β-D-thiogalactopyranoside) (1 mM). Heterologous protein production proceeded overnight at 16°C. Purification of the N-terminally hexahistidine-tagged *E. coli* flavin reductase was carried out as described above for ArmH enzymes.

***In vitro* halogenation assays.** Freshly prepared ArmH enzymes were separately incubated at 25°C overnight in a total volume of 100 µl. The buffer was 100 mM Na₂HPO₄, 100 mM NaCl (or KBr or KI, respectively), pH 7.4. The reaction mixture also contained 2 mM NADH, 10 µM flavin adenine dinucleotide (FAD), 2.4 units *E. coli* flavin reductase (Fre) to supply the respective halogenase with FADH₂, and the acceptor substrate (25 µM melleolide F). Fre activity was determined by following a published procedure (25). Reactions with heat-inactivated enzyme (95°C for 10 min) were run in parallel as negative controls, in particular to exclude nonenzymatic chlorination by hypochlorite that might have formed spontaneously in the assays. To prepare the reaction mixtures for chromatography, they were extracted twice with an equal volume of ethyl acetate plus 1% acetic acid (vol/vol), dried under reduced pressure, and redissolved in 100 µl of methanol.

Liquid chromatography and mass spectrometry. *In vitro* reactions were analyzed on an Agilent 1200 high-performance liquid chromatograph (HPLC) equipped with a Zorbax Eclipse XDB-C₁₈ column (150 by 4.6 mm; 3.5-µm particle size). Solvent A was 0.1% trifluoroacetate in H₂O, and solvent B was acetonitrile. For melleolide analysis, a linear gradient from 50% B to 100% B within 16 min at a flow rate of 0.7 ml/min was applied, followed by a wash step (100% B) for 5 min. Routine mass spectrometry was performed on an Agilent 1260 chromatograph with a Zorbax Eclipse XDB-C₁₈ column (150 by 4.6 mm; 3.5-µm particle size) cou-

pled with an Agilent 6130 mass detector using electrospray ionization in positive and negative modes and applying the gradient described above. Diode array detection was from a λ of 200 to 500 nm, and chromatograms were extracted at a λ of 254 nm. High-resolution electrospray ionization mass spectrometry (HR-ESIMS) was performed on a Thermo Accela liquid chromatograph equipped with a Betasil C₁₈ column (150 by 2.1 mm; 3-µm particle size) and fitted to an Exactive Orbitrap mass spectrometer (ThermoFisher). Solvent A was 0.1% formic acid in H₂O, and solvent B was 0.1% formic acid in acetonitrile. For sample analysis, the column was washed with 95% H₂O for 1 min, followed by a linear gradient (flow rate, 0.2 ml/min) from 5% B to 98% B within 15 min, and held at this relationship for 3 min.

***In silico* sequence and phylogenetic analysis.** To identify exon-intron junctions *in silico*, we used FGENESH (Softberry, Mount Kisco, NY) and Augustus (26) software as described previously (27). Primary sequences of FAD-dependent halogenases were aligned using the MUSCLE algorithm (28) implemented as a plug-in for Geneious 7.1 (Biomatters Ltd., Auckland, New Zealand). The alignment was exported and used to construct a phylogenetic network based on the neighbor net method implemented in the SplitsTree4 program (29). For the construction of a phylogenetic tree, the alignment was exported to MEGA6 (30). Based on a neighbor-joining tree, the optimal model of evolution was determined to be the Le-Gascuel (LG) model (31). A maximum-likelihood (ML) analysis was run using the LG model with 1,000 bootstrap replicates. A FAD-dependent *p*-hydroxybenzoate hydroxylase (PHBH) (Molecular Modeling Database [MMDB] accession no. 57109) from *Pseudomonas fluorescens* was used as the outgroup to root the tree. The GenBank accession numbers of all proteins are compiled in Table S1 in the supplemental material. For phylogenetic analysis, the sequences of the tryptophan halogenases RebH (32), PrnA (33), and PyrH (34) were used, all of them acting on free precursor molecules. We also included SgcC3, involved in halogenation of the enediynes anti-tumor substance C-1027 (17), BhaA from balhimycin biosynthesis (35), and PltA from pyoluteorin biosynthesis (36). All of the last four enzymes have been shown experimentally to depend on carrier-protein-bound intermediates. The halogenase CndH (37) was suggested to interact with a carrier protein, as well, although direct evidence was not provided. AviH from *Streptomyces viridochromogenes* was included, as it chlorinates an orsellinic acid moiety at two positions during avilamycin biosynthesis (38), as well as the halogenase CalO3, which transfers iodine to orsellinic acid (19). Along with the five *A. mellea* halogenases, we included uncharacterized basidiomycete halogenases of *Heterobasidion irregulare* (39) and *Serpula lacrymans* (40) and characterized halogenases from ascomycetes to the phylogenetic analysis. From the latter group of fungi, we added Rdc2 (41) and RadH (16), both involved in radicicol biosynthesis, as well as GsfI of *Penicillium aethiopicum*, which is encoded in the griseofulvin gene cluster (18); PtaM from pestheic acid biosynthesis in *Pestalotiopsis fici* (42); GedL from the geodin pathway in *Aspergillus terreus* (43); and AclH from the aspirochlorine pathway in *Aspergillus oryzae* (44). To root the tree, we used the FAD-dependent PHBH of *P. fluorescens* (45) as the outgroup.

Nucleotide sequence accession numbers. The DNA sequences of *armH3* to *armH5* were deposited in GenBank under the accession numbers KT819179 to KT819181, respectively.

RESULTS

The melleolide gene cluster lacks a halogenase gene. In order to study the genetic basis underlying melleolide biosynthesis, we first searched the genomic sequence of *A. mellea* DSM3731 (13) using the primary sequences of the protoilludene cyclase Pro1 and the polyketide synthase ArmB (11, 12). Notably, the query sequences hit loci that were separated by only nine genes. The result pointed to a clustered arrangement of melleolide biosynthesis genes. This putative gene cluster includes five genes coding for P₄₅₀-dependent monooxygenases (Fig. 2A, proteins 476 and 479 to 482), four NAD⁺-dependent oxidoreductases (proteins 468, 469, 474, and

TABLE 2 Active halogenases/halogenase genes of *A. mellea*

Protein name	Length (aa) ^a	Protein ID ^b	GenBank accession no.	No. of introns in gene	Sequence similarity (%) ^c
ArmH1	522	10956	JF739169	9	
ArmH2	516	2897	JF739170	9	68.3
ArmH3	504	9219	KT819179	9	79.7
ArmH4	533	168	KT819180	10	56.8
ArmH5	523	2211	KT819181	9	49.7

^a aa, amino acids.^b The protein identifier (ID) refers to the *A. mellea* genome project, as provided through the Joint Genome Institute and by Collins et al. (13).^c Percentage of amino acids identical to ArmH1's.

478), one flavin-dependent oxidoreductase (protein 475), and one *O*-methyltransferase (protein 473). The P₄₅₀-dependent enzymes may be involved in protoilludene hydroxylation to elaborate melleolides with multiple alcohol groups, such as melleolide D (3), which carries alcohol functionalities at C-4, C-5, C-10, and C-13. The role of the NAD⁺-dependent enzymes remains unknown. Numerous melleolides, e.g., arnamial (6), show 5'-*O*-methylation of the aromatic moiety. This methylation step may be catalyzed by the methyltransferase encoded in the cluster. Searching for a halogenase, a potential candidate encoded in the cluster is the flavin-dependent oxidoreductase (protein 475). However, it lacks the strongly conserved motif GWXWXXPL (34) of FAD-dependent halogenases and showed homology to glucose-methanol-choline oxidoreductase instead. Thus, we hypothesized that protein 475 does not possess halogenase activity but might represent the dehydrogenase yielding the aldehyde in position 1 of arnamial and other melleolides. In turn, this suggested that the halogenase required for melleolide chlorination is not encoded in the gene cluster.

Identification of halogenase genes in the *A. mellea* genome.

Prior to the release of the *A. mellea* genomic sequence, we identified the sequences of *armH1* and *armH2* (GenBank accession no. JF739169 and JF739170), i.e., two genes coding for putative flavin-dependent halogenases. These two genes are located on a contiguous 71.5-kb portion of the *A. mellea* genome (22) that is not part of the melleolide biosynthesis gene cluster. By searching the genomic sequence, we have now identified three additional putative halogenase genes, here referred to as *armH3*, *armH4*, and *armH5* (GenBank accession no. KT819179 through KT819181), which are located neither within nor near the melleolide gene locus nor close to *armH1* and *armH2*. For all five halogenase genes (*armH1* to *armH5*), cDNA was successfully procured from mycelium, confirming they are actively transcribed genes. Another two gene models encoding putative halogenases were incomplete, with missing portions across the respective genes, which is why we assume misassembled sequence data or pseudogenes.

The reading frames of the genes *armH1*, *armH2*, *armH3*, and *armH5* are disrupted by 9 and that of *armH4* by 10 introns (Fig. 2B) and encode ArmH1 to ArmH5 (Table 2), which possess the canonical halogenase signature sequence (GW[A/V]W[F/L]I) of hydrophobic and aromatic residues.

***In vitro* characterization of *A. mellea* halogenases ArmH1 to ArmH5.** To test if any or all of the five *A. mellea* halogenases function in chlorine transfer during melleolide biosynthesis, we expressed their coding sequences heterologously in *E. coli* KRX so as to produce N-terminally hexahistidine-tagged fusion proteins. The enzymes were purified by metal affinity and anion-exchange

chromatography (Fig. 3) and characterized *in vitro*. Melleolide F (Fig. 1) (46) is a typical representative of the melleolide family of compounds that features a $\Delta^{2,3}$ -protoilludene terpene and an unmodified orsellinic acid moiety. Melleolide F can be procured from mycelial cultures in sufficient quantity and was used as a potential chlorine acceptor substrate in this study.

Product formation was investigated by HPLC and HR-ESIMS. When given free melleolide F as the substrate, product formation could be proven in the chromatograms for all five ArmH enzymes by HPLC analysis. In addition to the melleolide F peak at a retention time (*t_R*) of 10.8 min, formation of a chlorinated product was chromatographically verified at a *t_R* of 11.6 min (Fig. 4A to E). In the high-resolution mass spectra for ArmH1 to ArmH5 reactions, the new peaks corresponded to the mass of 6'-chloromelleolide F (Table 3) and displayed the typical pattern for isotopic abundance of the stable chlorine isotopes ³⁵Cl and ³⁷Cl. Based on the areas under the curve, product formation was most pronounced with ArmH4.

Bromination by ArmH4. We selected ArmH4 as a model to gain insight into the biosynthetic capacities of *A. mellea* halogenases. As it has been established that chlorinases may also catalyze bromination, at least *in vitro* (34), *in vitro* product formation assays were performed as described above but with addition of the potassium salts of iodide or bromide, rather than sodium chlo-

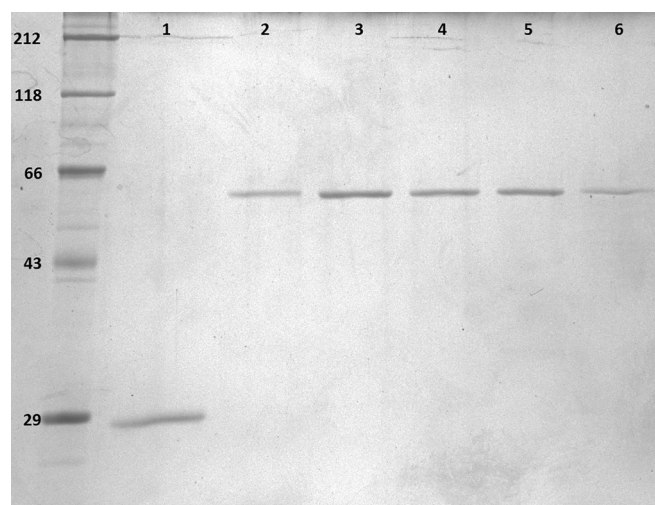


FIG 3 SDS-polyacrylamide gel of heterologously produced and purified *E. coli* flavin reductase (lane 1) and *A. mellea* halogenases ArmH1 to ArmH5 (lanes 2 to 6). Left lane, molecular mass markers; sizes in kilodaltons are indicated.

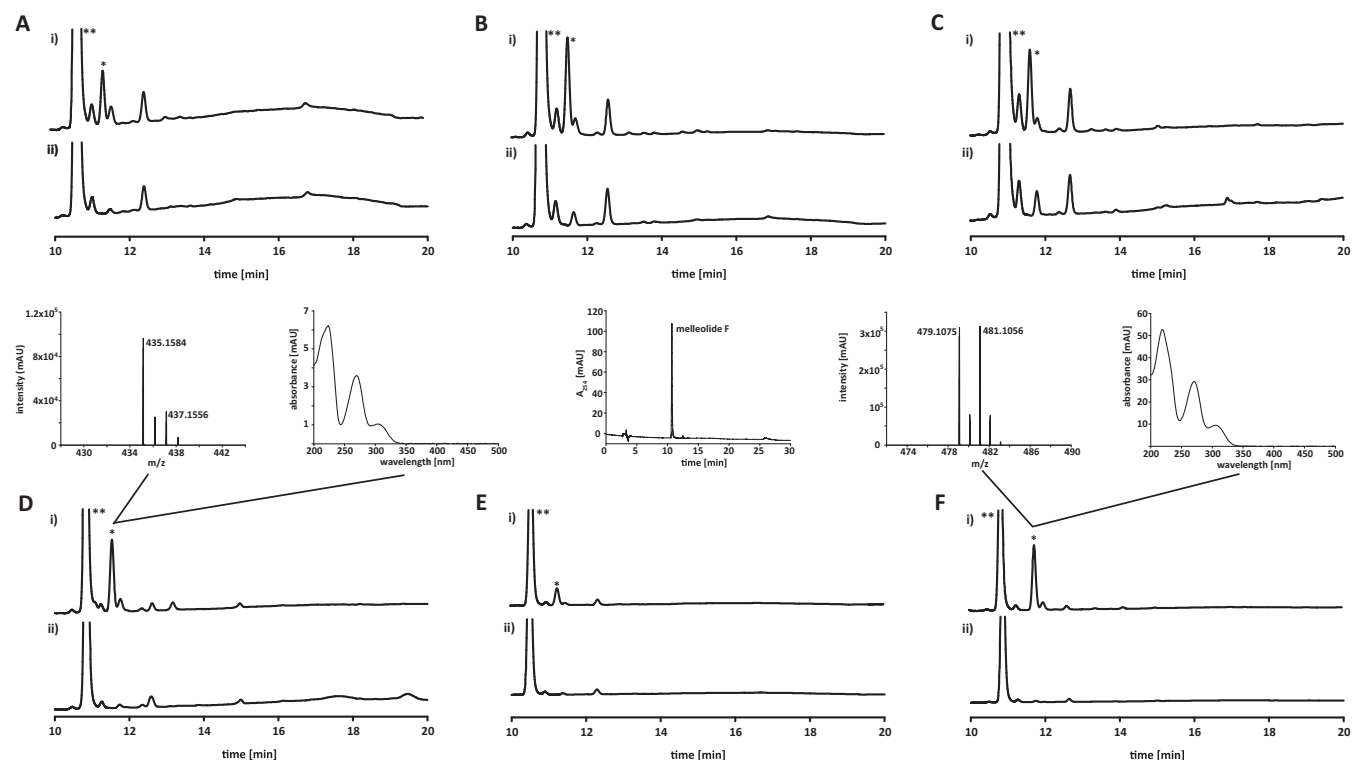


FIG 4 HPLC profiles of ArmH-catalyzed *in vitro* halogenation assays. (A to E) Results for ArmH1 through ArmH5, respectively. Within each panel, chromatogram i shows the enzymatic reaction with melleolide F and chromatogram ii shows the negative control with heat-treated enzyme. (F) ArmH4 reaction with bromide. The single asterisks mark the product peaks, whose absorption values range between 4 and 15 milli-absorbance units (mAU). The double asterisks mark melleolide F. The insets display HR-ESIMS and UV/visible-light (Vis) spectra of the ArmH4-catalyzed chlorinated and brominated products and a chromatogram of the melleolide F substrate.

ride, as the halogen donor substrate for ArmH4. While iodination was not observed, product formation was detected by HPLC and HR-ESIMS when bromide was present (Fig. 4F). Evidence for melleolide bromination came from the masses m/z 479.1075 and 481.1056 (Table 3) and the unique nearly 1:1 abundance ratio of the stable bromine isotopes ^{79}Br and ^{81}Br (Fig. 4F). These results indicated that a single bromine atom was introduced into melleolide F, likely to C-6', as noted above (Fig. 1).

Functional categories are not applicable to fungal halogenases. It has previously been suggested that halogenases can be grouped according to their substrate requirements (37). Group A

TABLE 3 High-resolution mass spectrometry data on *in vitro* chlorinated or -brominated melleolide F, using ArmH1 to ArmH5

Halogenase	m/z [M - H] ⁻	
	Found	Calculated
Chlorination		
ArmH1	435.1581	435.1580 ^a
ArmH2	435.1595	435.1580 ^a
ArmH3	435.1600	435.1580 ^a
ArmH4	435.1584	435.1580 ^a
ArmH5	435.1579	435.1580 ^a
Bromination		
ArmH4	479.1075, 481.1056	479.1069, 481.1049 ^b

^a For $\text{C}_{23}\text{H}_{28}\text{O}_6\text{Cl}$.

^b For $\text{C}_{23}\text{H}_{28}\text{O}_6$ ⁷⁹Br and $\text{C}_{23}\text{H}_{28}\text{O}_6$ ⁸¹Br, respectively.

includes enzymes that act on free substrates, while group B requires carrier-bound substrates for catalytic turnover. The authors differentiate these two groups by a phenylalanine residue (Phe312 in CndH, group B), which is equivalent to a glutamate residue (Glu346 in PrnA) in group A enzymes. According to these categories, all *A. mellea* halogenases would fall into group B of carrier-protein-dependent halogenases, as they show a phenylalanine residue (positions 326, 326, 327, 335, and 326 in ArmH1 to ArmH5, respectively). However, our results clearly prove that all of the above-mentioned halogenases act on free substrates and that the halogen-carbon bond is established as a post-PKS-biosynthetic step. This is in agreement with a previous study on the ascomycetous Rdc2 (41), which was shown to chlorinate a free substrate *in vitro* but has a phenylalanine at position 328. We therefore assume that this signature residue—discovered with bacterial enzymes—is not applicable to differentiate halogenases of basidiomycete origin.

To gain more insight into the evolution of FAD-dependent halogenases, we constructed a phylogenetic network (Fig. 5) and an ML tree (see Fig. S1 in the supplemental material) of experimentally characterized FAD-dependent halogenases and some putative halogenases encoded in genomes of basidiomycetes. The resulting network and tree suggested that fungal halogenases form a monophyletic clade. Thus, our phylogenetic analyses support the notion that categorization into group A or B is not applicable to fungal enzymes. We found that the fungal halogenase tree reflects the phylogenetic split

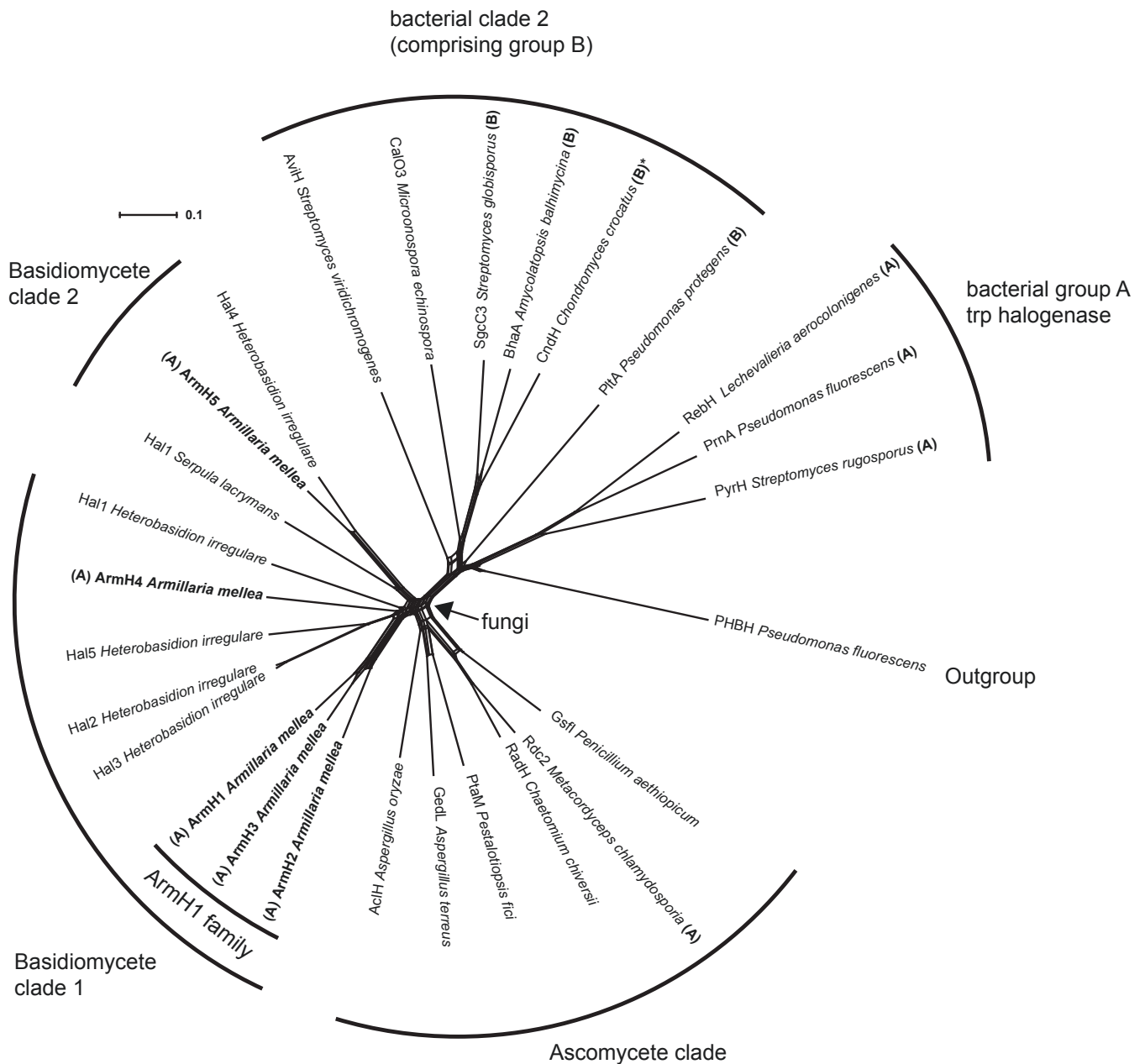


FIG 5 Phylogenetic network of 26 verified and putative halogenases, inferred by the neighbor net method. Fungal halogenases are monophyletic and reflect the phylogenetic split between ascomycetes and basidiomycetes. The functional categories group A (halogenases accepting free substrates) and group B (carrier-protein-bound substrates) are indicated by boldface letters in parentheses. These categories do not strictly correlate with phylogenetic clades. The scale bar indicates the uncorrected pairwise distance. The asterisk indicates a postulated requirement for carrier-protein-bound substrates (37).

between ascomycetes and basidiomycetes. Intriguingly, ArmH1 to ArmH5 are not monophyletic, and only ArmH1 to ArmH3 form a branch of closely related enzymes.

DISCUSSION

Our findings reported here show that halogenases ArmH1 to ArmH5 act on melleolide F, i.e., on free substrates, and that they do not require carrier-protein-tethered intermediates. Cumulatively, we identified these halogenases as melleolide biosynthesis enzymes. We cannot *a priori* exclude the possibility that a position other than C-6' served as an acceptor site for the halogen atom

during catalysis *in vitro*. However, all of the approximately 25 chlorinated melleolides described to date exclusively show 6' chlorination. Thus, a different halogen acceptor position would be inconsistent with all previously established structures.

Mechanistically, different strategies have evolved independently to install halogen atoms onto natural product scaffolds, making use of either the halide anion, hypochlorous acid, or a halogen radical (47, 48). Recently, even a new variant of halogenating enzymes that belongs to the nonheme-iron-dependent halogenases was reported (49). In contrast, our current study focuses on flavin-dependent halogenases, which employ

FAD as a cofactor and use a halide anion and molecular oxygen to produce hypochlorous acid as a halogenating agent. Protein crystallography greatly helped in understanding the structural basis of regioselective formation of the carbon-halogen bond (50–53). *A. mellea* halogenase genes encode the signature motif GW(A/V)W(F/L)I. In the three-dimensional protein structure, these residues line a tunnel inside the enzyme through which the hypochlorous acid is routed from the flavin toward the halogen acceptor substrate binding site (50). Also, the active-site lysine was found in all *A. mellea* halogenases (K77 in ArmH5 and K76 in all the others).

Based on the crystal structure of the chondromycin halogenase CndH (37), it has previously been suggested that flavin-dependent halogenases fall into two functionally dissimilar groups accepting free substrates (group A) or carrier-protein-bound substrates (group B). Although all the halogenases investigated in this study, as well as Rdc2 from *Pochonia chlamydosporia*, seem to accept free substrates, there are not enough data yet to assume that this is a general trait of fungal halogenases. However, rules deduced from bacterial sequences to predict their placement in either functional group are not appropriate for fungal halogenases. Alternatively, categorization of enzymes by activity on free versus enzyme-tethered substrates may not be as critical as previously assumed to draw a demarcation line between groups A and B. The type of substrate (tryptophan versus others) also seems to play a role, which would explain the major split (seen in Fig. S1 in the supplemental material) between bacterial clade 1 and all other halogenases. Therefore, further biochemical studies are necessary to shed more light on this fascinating enzyme family, in particular as members of basidiomycete origin have remained completely uninvestigated, even though aromatic haloorganic natural products are known from these fungi. Besides the melleolides, examples include the alcalinaphenols from *Mycena alcalina* (54) and stephanosporin of *Stephanospora caroticolor* (55). Hence, our work represents the first biochemically and genetically characterized basidiomycete halogenases. Phylogenetically, our work also revealed that ArmH1 to ArmH3 have most likely evolved by gene duplication within the *A. mellea* lineage and that ArmH4 and ArmH5 seem to have distinct phylogenetic histories. However, it is premature to speculate if any functional clusters within the fungal clades can be deduced from the phylogenetic tree. Again, more biochemical studies are warranted to improve functional predictions of putative halogenases unveiled by high-throughput-sequencing projects. In various cases, e.g., for the antibiotic vancomycin and the antitumor agent salinosporamide, increased bioactivity has been attributed to the presence of halogen atoms (47). However, in the case of the melleolides, the physiological reason for introducing a chlorine atom is unclear. Available studies on structure-activity relationships do not support strongly changed bioactivity through chlorination (8, 9, 20). Hence, a role in detoxification of melleolides through halogenation also cannot be assumed, and the reason why *A. mellea* secures chlorination of its toxic natural products to the degree described here remains elusive. Although redundantly encoded pathways are known from both ascomycetes and basidiomycetes (56–58), a 5-fold parallelized biosynthetic step is unprecedented and warrants further investigation of the underlying ecological or environmental reason.

ACKNOWLEDGMENTS

A doctoral fellowship awarded by the Deutsche Bundesstiftung Umwelt (DBU) to M.M. is gratefully acknowledged. Support by the Collaborative Research Center ChemBioSys (SFB 1127/1) to D.H. and J.T. is acknowledged.

We thank Andrea Perner (Leibniz Institute for Natural Product Research and Infection Biology, Hans Knöll Institute, Jena, Germany) for recording high-resolution mass spectra.

REFERENCES

- Baumgartner K, Coetzee MP, Hoffmeister D. 2011. Secrets of the subterranean pathosystem of *Armillaria*. *Mol Plant Pathol* 12:515–534. <http://dx.doi.org/10.1111/j.1364-3703.2010.00693.x>.
- Shaw CG, Kile GA, III. 1991. *Armillaria* root disease. U.S. Department of Agriculture Forest Service handbook no. 691. U.S. Department of Agriculture Forest Service, Washington, DC.
- Arnone A, Cardillo R, Nasini G. 1986. Structures of melleolides B-D, three antibacterial sesquiterpenoids from *Armillaria mellea*. *Phytochemistry* 25:471–474. [http://dx.doi.org/10.1016/S0031-9422\(00\)85503-X](http://dx.doi.org/10.1016/S0031-9422(00)85503-X).
- Bohnert M, Miethbauer S, Dahse HM, Ziemer J, Nett M, Hoffmeister D. 2011. *In vitro* cytotoxicity of melleolide antibiotics: structural and mechanistic aspects. *Bioorg Med Chem Lett* 21:2003–2006. <http://dx.doi.org/10.1016/j.bmcl.2011.02.026>.
- Donnelly D, Sanada S, O'Reilly J, Polonsky J, Prangé T, Pascard CJ. 1982. Isolation and structure (X-ray analysis) of the orsellinate of armillol, a new antibacterial metabolite from *Armillaria mellea*. *J Chem Soc Chem Commun* 1982:135–137.
- Misiek M, Williams J, Schmich K, Hüttel W, Merfort I, Salomon CE, Aldrich CC, Hoffmeister D. 2009. Structure and cytotoxicity of arnamial and related fungal sesquiterpene aryl esters. *J Nat Prod* 72:1888–1891. <http://dx.doi.org/10.1021/np900314p>.
- Yang JS, Chen YW, Feng XZ, Yu DQ, Liang XT. 1984. Chemical constituents of *Armillaria mellea* mycelium I. Isolation and characterization of armillararin and armillaridin. *Planta Med* 50:288–290.
- Bohnert M, Nützmann HW, Schroeckh V, Horn F, Dahse HM, Brakhage AA, Hoffmeister D. 2014. Cytotoxic and antifungal activities of melleolide antibiotics follow dissimilar structure-activity relationships. *Phytochemistry* 105:101–108. <http://dx.doi.org/10.1016/j.phytochem.2014.05.009>.
- Kobori H, Sekiya A, Suzuki T, Choi JH, Hirai H, Kawagishi H. 2015. Bioactive sesquiterpene aryl esters from the culture broth of *Armillaria* sp. *J Nat Prod* 78:163–167. <http://dx.doi.org/10.1021/np500322t>.
- Peipp H, Sonnenbichler J. 1992. Secondary fungal metabolites and their biological activities. II. Occurrence of antibiotic compounds in cultures of *Armillaria ostoyae* growing in the presence of an antagonistic fungus or host plant cells. *Biol Chem Hoppe-Seyler* 373:675–683.
- Engels B, Heinig U, Grothe T, Stadler M, Jennewein S. 2011. Cloning and characterization of an *Armillaria gallica* cDNA encoding protoiludene synthase, which catalyzes the first committed step in the synthesis of antimicrobial melleolides. *J Biol Chem* 286:6871–6878. <http://dx.doi.org/10.1074/jbc.M110.165845>.
- Lackner G, Bohnert M, Wick J, Hoffmeister D. 2013. Assembly of melleolide antibiotics involves a polyketide synthase with cross-coupling activity. *Chem Biol* 20:1101–1106. <http://dx.doi.org/10.1016/j.chembiol.2013.07.009>.
- Collins C, Keane TM, Turner DJ, O'Keeffe G, Fitzpatrick DA, Doyle S. 2013. Genomic and proteomic dissection of the ubiquitous plant pathogen, *Armillaria mellea*: toward a new infection model system. *J Proteome Res* 12:2552–2570. <http://dx.doi.org/10.1021/pr301131t>.
- Chen X, van Pée KH. 2008. Catalytic mechanisms, basic roles, and biotechnological and environmental significance of halogenating enzymes. *Acta Biochim Biophys Sin* 40:183–193. <http://dx.doi.org/10.1111/j.1745-7270.2008.00390.x>.
- Reeves CD, Hu Z, Reid R, Kealey JT. 2008. Genes for the biosynthesis of the fungal polyketides hypothemycin from *Hypomyces subiculosus* and radicicol from *Pochonia chlamydosporia*. *Appl Environ Microbiol* 74:5121–5129. <http://dx.doi.org/10.1128/AEM.00478-08>.
- Wang S, Xu Y, Maine EA, Wijeratne EM, Espinosa-Artiles P, Gunatilaka AA, Molnár I. 2008. Functional characterization of the biosynthesis of radicicol, an Hsp90 inhibitor resorcylic acid lactone from *Chaetomium*

- chiversii*. Chem Biol 15:1328–1338. <http://dx.doi.org/10.1016/j.chembiol.2008.10.006>.
17. Lin S, Van Lanen SG, Shen B. 2007. Regiospecific chlorination of (S)-beta-tyrosyl-S-carrier protein catalyzed by SgcC3 in the biosynthesis of the enediyne antitumor antibiotic C-1027. J Am Chem Soc 129:12432–12438. <http://dx.doi.org/10.1021/ja072311g>.
 18. Chooi YH, Cacho R, Tang Y. 2010. Identification of the viridicatumtoxin and griseofulvin gene clusters from *Penicillium aethiopicum*. Chem Biol 17:483–494. <http://dx.doi.org/10.1016/j.chembiol.2010.03.015>.
 19. Ahlert J, Shepard E, Lomovskaya N, Zazopoulos E, Staffa A, Bachmann BO, Huang K, Fonstein L, Czisny A, Whitwam RE, Farnet CM, Thorson JS. 2002. The calicheamicin gene cluster and its iterative type I enediyne PKS. Science 297:1173–1176. <http://dx.doi.org/10.1126/science.1072105>.
 20. Bohnert M, Scherer O, Wiechmann K, König S, Dahse HM, Hoffmeister D, Werz O. 2014. Melleolides induce rapid cell death in human primary monocytes and cancer cells. Bioorg Med Chem 22:3856–3861. <http://dx.doi.org/10.1016/j.bmc.2014.06.032>.
 21. Shimizu K, Keller NP. 2001. Genetic involvement of a cAMP dependent protein kinase in a G protein signaling pathway regulating morphological and chemical transitions in *Aspergillus nidulans*. Genetics 157:591–600.
 22. Misiek M, Braesel J, Hoffmeister D. 2011. Characterisation of the ArmA adenylation domain implies a more diverse secondary metabolism in the genus *Armillaria*. Fungal Biol 115:775–781. <http://dx.doi.org/10.1016/j.funbio.2011.06.002>.
 23. Nordberg H, Cantor M, Dusheyko S, Hua S, Poliakov A, Shabalov I, Smirnova T, Grigoriev IV, Dubchak I. 2014. The genome portal of the Department of Energy Joint Genome Institute: 2014 updates. Nucleic Acids Res 42:D26–D31. <http://dx.doi.org/10.1093/nar/gkt1069>.
 24. Schneider P, Weber M, Rosenberger K, Hoffmeister D. 2007. A one-pot chemoenzymatic synthesis to the universal precursor of antidiabetic and antiviral bis-indolylquinones. Chem Biol 14:635–644. <http://dx.doi.org/10.1016/j.chembiol.2007.05.005>.
 25. Matsubara T, Ohshiro T, Nishina Y, Izumi Y. 2001. Purification, characterization, and overexpression of flavin reductase involved in dibenzothio-phenone desulfurization by *Rhodococcus erythropolis* D-1. Appl Environ Microbiol 67:1179–1184. <http://dx.doi.org/10.1128/AEM.67.3.1179-1184>.
 26. Stanke M, Morgenstern B. 2005. AUGUSTUS: a Web server for gene prediction in eukaryotes that allows user-defined constraints. Nucleic Acids Res 33:W465–W467. <http://dx.doi.org/10.1093/nar/gki458>.
 27. Misiek M, Hoffmeister D. 2008. Processing sites involved in intron splicing of *Armillaria* natural product genes. Mycol Res 112:216–224. <http://dx.doi.org/10.1016/j.mycres.2007.10.011>.
 28. Edgar RC. 2004. MUSCLE: multiple sequence alignment with high accuracy and high throughput. Nucleic Acids Res 32:1792–1797. <http://dx.doi.org/10.1093/nar/gkh340>.
 29. Huson DH. 1998. SplitsTree: analyzing and visualizing evolutionary data. Bioinformatics 14:68–73. <http://dx.doi.org/10.1093/bioinformatics/14.1.68>.
 30. Tamura K, Stecher G, Peterson D, Filipowski A, Kumar S. 2013. MEGA6: Molecular Evolutionary Genetics Analysis version 6.0. Mol Biol Evol 30:2725–2729. <http://dx.doi.org/10.1093/molbev/mst197>.
 31. Le SQ, Gascuel O. 2008. An improved general amino acid replacement matrix. Mol Biol Evol 25:1307–1320. <http://dx.doi.org/10.1093/molbev/msn067>.
 32. Yeh E, Garneau S, Walsh CT. 2005. Robust *in vitro* activity of RebF and RebH, a two-component reductase/halogenase, generating 7-chlorotryptophan during rebeccamycin biosynthesis. Proc Natl Acad Sci U S A 102:3960–3965. <http://dx.doi.org/10.1073/pnas.0500755102>.
 33. Hammer PE, Hill DS, Lam ST, van Pée KH, Ligon JM. 1997. Four genes from *Pseudomonas fluorescens* that encode the biosynthesis of pyrrolnitrin. Appl Environ Microbiol 63:2147–2154.
 34. Zehner S, Kotszsch A, Bister B, Süßmuth RD, Mendez C, Salas JA, van Pée KH. 2005. A regioselective tryptophan 5-halogenase is involved in pyrroindomycin biosynthesis in *Streptomyces rugosporus* LL-42D005. Chem Biol 12:445–452. <http://dx.doi.org/10.1016/j.chembiol.2005.02.005>.
 35. Puk O, Bischoff D, Kittel C, Pelzer S, Weist S, Stegmann E, Süßmuth RD, Wohlleben W. 2004. Biosynthesis of chloro-beta-hydroxytyrosine, a nonproteinogenic amino acid of the peptidic backbone of glycopeptide antibiotics. J Bacteriol 186:6093–6100. <http://dx.doi.org/10.1128/JB.186.18.6093-6100.2004>.
 36. Dorrestein PC, Yeh E, Garneau-Tsodikova S, Kelleher NL, Walsh CT. 2005. Dichlorination of a pyrrolyl-S-carrier protein by FADH₂-dependent halogenase PltA during pyoluteorin biosynthesis. Proc Natl Acad Sci U S A 102:13843–13848. <http://dx.doi.org/10.1073/pnas.0506964102>.
 37. Buedenbender S, Rachid S, Müller R, Schulz GE. 2009. Structure and action of the myxobacterial chondrochloren halogenase CndH: a new variant of FAD-dependent halogenases. J Mol Biol 385:520–530. <http://dx.doi.org/10.1016/j.jmb.2008.10.057>.
 38. Weitnauer G, Mühlenweg A, Trefzer A, Hoffmeister D, Süßmuth RD, Jung G, Welzel K, Vente A, Girreser U, Bechtold A. 2001. Biosynthesis of the orthosomycin antibiotic avilamycin A: deductions from the molecular analysis of the *avi* biosynthetic gene cluster of *Streptomyces viridochromogenes* Tü57 and production of new antibiotics. Chem Biol 8:569–581. [http://dx.doi.org/10.1016/S1074-5521\(01\)00040-0](http://dx.doi.org/10.1016/S1074-5521(01)00040-0).
 39. Olson A, Aerts A, Asiegbu F, Belbahri L, Bouzid O, Broberg A, Canbäck B, Coutinho PM, Cullen D, Dalman L, Deflorio G, van Diepen LT, Dunand C, Duplessis S, Durling M, Gonthier P, Grimwood J, Fossdal CG, Hansson D, Henrissat B, Hietala A, Himmelstrand K, Hoffmeister D, Högberg N, James TY, Karlsson M, Kohler A, Kües U, Lee YH, Lin YC, Lind M, Lindquist E, Lombard V, Lucas S, Lundén K, Morin E, Murat C, Park J, Raffaello T, Rouzé P, Salamov A, Schmutz J, Solheim H, Ståhlberg J, Véléz H, de Vries RP, Wiebenga A, Woodward S, Yakovlev I, Garbelotto M, Martin F, Grigoriev IV, Stenlid J. 2012. Insight into trade-off between wood decay and parasitism from the genome of a fungal forest pathogen. New Phytol 194:1001–1013. <http://dx.doi.org/10.1111/j.1469-8137.2012.04128.x>.
 40. Eastwood DC, Floudas D, Binder M, Majcherczyk A, Schneider P, Aerts A, Asiegbu FO, Baker SE, Barry K, Bendiksby M, Blumentritt M, Coutinho PM, Cullen D, de Vries RP, Gathman A, Goodell B, Henrissat B, Ihrmark K, Kauserud H, Kohler A, LaButti K, Lapidus A, Lavin JL, Lee YH, Lindquist E, Lilly W, Lucas S, Morin E, Murat C, Oguiza JA, Park J, Pisabarro AG, Riley R, Rosling A, Salamov A, Schmidt O, Schmutz J, Skrede I, Stenlid J, Wiebenga A, Xie X, Kües U, Hibbett DS, Hoffmeister D, Högberg N, Martin F, Grigoriev IV, Watkinson SC. 2011. The plant cell wall-decomposing machinery underlies the functional diversity of forest fungi. Science 333:762–765. <http://dx.doi.org/10.1126/science.1205411>.
 41. Zeng J, Zhan J. 2010. A novel fungal flavin-dependent halogenase for natural product biosynthesis. ChemBioChem 11:2119–2123. <http://dx.doi.org/10.1002/cbic.201000439>.
 42. Xu X, Liu L, Zhang F, Wang W, Li J, Guo L, Che Y, Liu G. 2014. Identification of the first diphenyl ether gene cluster for pesthetic acid biosynthesis in plant endophyte *Pestalotiopsis fici*. ChemBioChem 15:284–292. <http://dx.doi.org/10.1002/cbic.201300626>.
 43. Nielsen MT, Nielsen JB, Anyaogu DC, Holm DK, Nielsen KF, Larsen TO, Mortensen UH. 2013. Heterologous reconstitution of the intact geodin gene cluster in *Aspergillus nidulans* through a simple and versatile PCR based approach. PLoS One 8:e72871. <http://dx.doi.org/10.1371/journal.pone.0072871>.
 44. Chankhamjon P, Boettger-Schmidt D, Scherlach K, Urbansky B, Lackner G, Kalb D, Dahse HM, Hoffmeister D, Hertweck C. 2014. Biosynthesis of the halogenated mycotoxin aspirochlorine in koji mold involves a cryptic amino acid conversion. Angew Chem Int Ed Engl 53:13409–13413. <http://dx.doi.org/10.1002/anie.201407624>.
 45. Schreuder HA, van der Laan JM, Hol WG, Drenth J. 1988. Crystal structure of p-hydroxybenzoate hydroxylase complexed with its reaction product 3,4-dihydroxybenzoate. J Mol Biol 199:637–648. [http://dx.doi.org/10.1016/0022-2836\(88\)90307-5](http://dx.doi.org/10.1016/0022-2836(88)90307-5).
 46. Arnone A, Cardillo R, Di Modugno V, Nasini G. 1988. Isolation and structure elucidation of melleodanols D and E and melleolides E-H, novel sesquiterpenoid aryl esters from *Clitocybe elegans* and *Armillaria mellea*. Gazz Chim Ital 118:517–521.
 47. Neumann CS, Fujimori DG, Walsh CT. 2008. Halogenation strategies in natural product biosynthesis. Chem Biol 15:99–109. <http://dx.doi.org/10.1016/j.chembiol.2008.01.006>.
 48. van Pée KH. 2012. Enzymatic chlorination and bromination. Methods Enzymol 516:237–257. <http://dx.doi.org/10.1016/B978-0-12-394291-3.00004-6>.
 49. Hillwig ML, Liu X. 2014. A new family of iron-dependent halogenases acts on freestanding substrates. Nat Chem Biol 10:921–923. <http://dx.doi.org/10.1038/nchembio.1625>.
 50. Dong C, Flecks S, Unversucht S, Haupt C, van Pée KH, Naismith JH. 2005. Tryptophan 7-halogenase (PrnA) structure suggests a mechanism

- for regioselective chlorination. *Science* 309:2216–2219. <http://dx.doi.org/10.1126/science.1116510>.
51. Bitto E, Huang Y, Bingman CA, Singh S, Thorson JS, Phillips GN, Jr. 2008. The structure of flavin-dependent tryptophan 7-halogenase RebH. *Proteins* 70:289–299.
 52. Zhu X, De Laurentis W, Leang K, Herrmann J, Ihlefeld K, van Pée KH, Naismith JH. 2009. Structural insights into regioselectivity in the enzymatic chlorination of tryptophan. *J Mol Biol* 391:74–85. <http://dx.doi.org/10.1016/j.jmb.2009.06.008>.
 53. Podzelinska K, Latimer R, Bhattacharya A, Vining LC, Zechel DL, Jia Z. 2010. Chloramphenicol biosynthesis: the structure of CmlS, a flavin-dependent halogenase showing a covalent flavin-aspartate bond. *J Mol Biol* 397:316–331. <http://dx.doi.org/10.1016/j.jmb.2010.01.020>.
 54. Peters S, Spiteller P. 2006. Chloro- and bromophenols from cultures of *Mycena alcalina*. *J Nat Prod* 69:1809–1812. <http://dx.doi.org/10.1021/np0603368>.
 55. Lang M, Spiteller P, Hellwig V, Steglich W. 2001. Stephanosporin, a traceless precursor of 2-chloro-4-nitrophenol in the gasteromycete *Stephanospora caroticolor*. *Angew Chem Int Ed Engl* 40:1704–1705. [http://dx.doi.org/10.1002/1521-3773\(20010504\)40:9<1704::AID-ANIE1704>3.0.CO;2-L](http://dx.doi.org/10.1002/1521-3773(20010504)40:9<1704::AID-ANIE1704>3.0.CO;2-L).
 56. Forseth RR, Amaike S, Schwenk D, Affeldt KJ, Hoffmeister D, Schroeder FC, Keller NP. 2013. Homologous NRPS-like gene clusters mediate redundant small-molecule biosynthesis in *Aspergillus flavus*. *Angew Chem Int Ed Engl* 52:1590–1594. <http://dx.doi.org/10.1002/anie.201207456>.
 57. Braesel J, Götze S, Shah F, Heine D, Tauber J, Hertweck C, Tunlid A, Stallforth P, Hoffmeister D. 2015. Three redundant synthetases secure redox-active pigment production in the basidiomycete *Paxillus involutus*. *Chem Biol* 22:1325–1334. <http://dx.doi.org/10.1016/j.chembiol.2015.08.016>.
 58. Throckmorton K, Lim FY, Kontoyiannis DP, Zheng W, Keller NP. 4 August 2015. Redundant synthesis of a conidial polyketide by two distinct secondary metabolite clusters in *Aspergillus fumigatus*. *Environ Microbiol* <http://dx.doi.org/10.1111/1462-2920.13007>.

Supplemental Material

A fivefold parallelized biosynthetic process secures chlorination of *Armillaria mellea* (honey mushroom) toxins

Jonas Wick^a, Daniel Heine^b, Gerald Lackner^c, Mathias Misiek^a, James Tauber^a, Hans Jagusch^a, Christian Hertweck^b, Dirk Hoffmeister^{a,#}

^aDepartment Pharmaceutical Microbiology at the Hans Knöll Institute, Friedrich-Schiller-Universität Jena, Beutenbergstrasse 11a, 07745 Jena, Germany

^bDepartment of Biomolecular Chemistry, Leibniz Institute for Natural Product Research and Infection Biology - Hans Knöll Institute, Beutenbergstraße 11a, 07745 Jena, Germany

^cInstitute of Microbiology, Swiss Federal Institute of Technology (ETH), Vladimir-Prelog-Weg 1-5, 8093 Zürich, Switzerland.

*Corresponding author. Tel.: +49 3641 949851; fax: +49 3641 949852. E-mail address: dirk.hoffmeister@leibniz-hki.de

Running title: *Armillaria mellea* (honey mushroom) halogenases

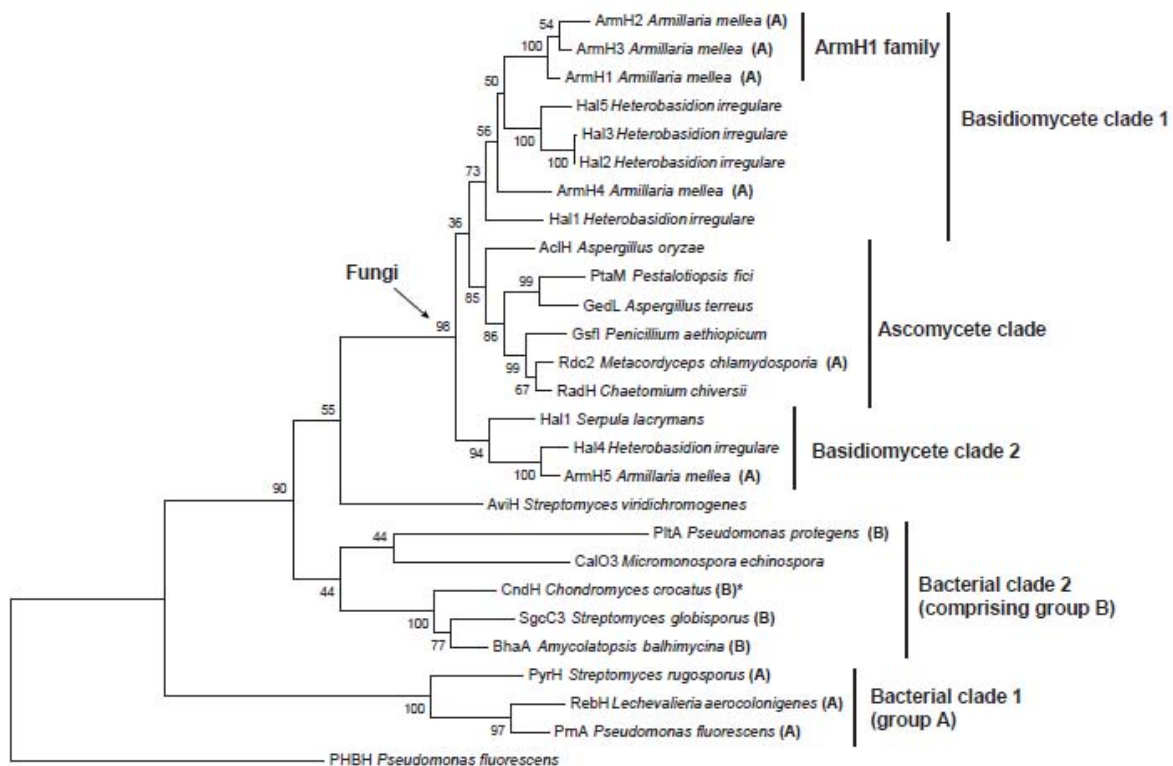


Fig. S1. Phylogenetic tree of 26 verified and putative halogenases inferred by the Maximum Likelihood method based on the LG model [1]. The tree with the highest log likelihood (-10885.8435) is shown. The percentage of trees in which the associated taxa clustered together is shown next to the branches (bootstrap values). The functional categories A (halogenases accepting free substrates) and group B (carrier protein-bound substrates) are indicated by bold letters in parentheses. These categories are not strictly correlated with phylogenetic clades. The *p*-hydroxybenzoate hydroxylase (PHBH) from *Pseudomonas fluorescens* was added as outgroup.

1. **Le SQ, Gascuel O.** 2008. An improved general amino acid replacement matrix. *Mol Biol Evol* **25**:1307-1320.

Table S1: Putative and characterized halogenases used for phylogenetic studies.

Name	Accession	Organism	Sequence Length
SgcC3_Streptomyces_globisporus	AAL06656.1	<i>Streptomyces globisporus</i>	494
RebH_Lechevalieria_aerocolonigenes	Q8KHZ8.1	<i>Lechevalieria aerocolonigenes</i>	530
Rdc2_Metacordyceps_chlamydosporia	ADM86580.1	<i>Metacordyceps chlamydosporia</i>	533
RadH_Chaetomium_chiversii	ACM42402.1	<i>Chaetomium chiversii</i>	520
PyrH_Streptomyces_rugosporus	AU95674.1	<i>Streptomyces rugosporus</i>	511
PtaM_Pestalotiopsis_fici	AGO59046	<i>Pestalotiopsis fici</i>	540
PrnA_Pseudomonas_fluorescens	P95480.1	<i>Pseudomonas fluorescens</i>	538
PltA_Pseudomonas_protegens	AA92059	<i>Pseudomonas protegens</i> Pf-5	449
PHBH_Pseudomonas_fluorescens	1PHH	<i>Pseudomonas fluorescens</i>	394
Hal5_Heterobasidion_irregulare	ETW79545	<i>Heterobasidion irregulare</i> TC 32-1	535
Hal4_Heterobasidion_irregulare	ETW77133	<i>Heterobasidion irregulare</i> TC 32-1	519
Hal3_Heterobasidion_irregulare	ETW76184	<i>Heterobasidion irregulare</i> TC 32-1	524
Hal2_Heterobasidion_irregulare	ETW76158	<i>Heterobasidion irregulare</i> TC 32-1	529
Hal1_Serpula_lacrymans	EGO19147	<i>Serpula lacrymans</i> var. lacrymans S7.9	668
Hal1_Heterobasidion_irregulare	ETW75821	<i>Heterobasidion irregulare</i> TC 32-1	567
Gsfl_Penicillium_aethiopicum	ADI24948	<i>Penicillium aethiopicum</i>	533
GedL_AspERGillus_terreus	XP_001217599	<i>Aspergillus terreus</i> NIH2624	500
CndH_Chondromyces_crocatus	CAQ43074.1	<i>Chondromyces crocatus</i>	512
ChIA_Dictyostelium_discoideum	XP_635556.1	<i>Dictyostelium discoideum</i> _AX4	601
CalO3_Micromonospora_echinospora	AM70353.1	<i>Micromonospora echinospora</i>	420
BhaA_Amycolatopsis_balhimycina	CAA76550	<i>Amycolatopsis balhimycina</i> DSM 5908	491
AviH_Streptomyces_viridichromogenes	AF333038	<i>Streptomyces viridichromogenes</i> Tu57	499
ArmH5_Armillaria_mellea		<i>Armillaria mellea</i> DSM3731	523
ArmH4_Armillaria_mellea		<i>Armillaria mellea</i> DSM3731	533
ArmH3_Armillaria_mellea		<i>Armillaria mellea</i> DSM3731	504
ArmH2_Armillaria_mellea	JF739170	<i>Armillaria mellea</i> DSM3731	516
ArmH1_Armillaria_mellea	JF739169	<i>Armillaria mellea</i> DSM3731	522
AclH_AspERGillus_oryzae	XP_001818590	<i>Aspergillus oryzae</i> RIB40	549

2.3. Bacteria induce pigment formation in the basidiomycete *Serpula lacrymans*

Tauber, J.P., Schroeckh, V., Shelest, E., Brakhage, A.A., and Hoffmeister, D.

Published manuscript (57).

Environmental Microbiology. (2016) 18: 5218–5227.

Summary and importance

There is an increasing interest in biotic interactions, and natural products that may be induced or suppressed in such circumstances. We used the model basidiomycete *Serpula lacrymans*, whose genome contains at least 24 natural product genes, to investigate the regulation of these genes and natural products therefrom during microbial interactions. We found that the atromentin gene cluster was induced and the atromentin-derived pigments accumulated during co-incubation with either *Bacillus subtilis*, *Pseudomonas putida* or *Streptomyces iranensis*. We also found that there exists a common promoter motif in not only two of the three essential atromentin genes in *Serpula lacrymans*, but that this motif extends to twelve other atromentin-producing basidiomycetes. Our work provided the first experimental evidence that a basidiomycete natural product gene cluster was inducible and co-regulated during trans-kingdom co-incubations.

Contribution to the manuscript

James Tauber contributed to the manuscript by designing (with help from others) and executing all wet laboratory work followed by analyses of data. This included microbiological culturing; compound extractions and chromatography; compound isolation and analyses; genetic extractions and qRT-PCR, including designing and verifying primers; and gene cloning, gene over-expression and an enzymatic assay. The other main part of the work, the bioinformatic analyses, as well as additional planning of the work, was done by the other authors. James Tauber helped design and participated in bioinformatic work. James Tauber wrote the majority of the manuscript (main text and supplement), including making three of the four main figures, and all supplemental figures.

Bacteria induce pigment formation in the basidiomycete *Serpula lacrymans*

James P. Tauber,¹ Volker Schroeckh,²
Ekaterina Shelest,³ Axel A. Brakhage^{2,4} and
Dirk Hoffmeister^{1*}

¹Department of Pharmaceutical Microbiology at the Leibniz Institute for Natural Product Research and Infection Biology (HKI), Friedrich Schiller University, Beutenbergstrasse 11a, Jena 07745, Germany.

²Department of Molecular and Applied Microbiology, Leibniz Institute for Natural Product Research and Infection Biology (HKI), Jena, Germany.

³Research Group Systems Biology/Bioinformatics, Leibniz Institute for Natural Product Research and Infection Biology - Hans Knöll Institute, Jena, Germany.

⁴Microbiology and Molecular Biology, Friedrich Schiller University Jena, Germany.

Summary

Basidiomycete fungi are characterized ecologically for their vital functional role in ecosystem carbon recycling and chemically for their capacity to produce a diverse array of small molecules. Chromophoric natural products derived from the quinone precursor atromentin, such as variegatic acid and involutin, have been shown to function in redox cycling. Yet, in the context of an inter-kingdom natural system these pigments are still elusive. Here, we co-cultured the model saprotrophic basidiomycete *Serpula lacrymans* with an ubiquitous terrestrial bacterium, either *Bacillus subtilis*, *Pseudomonas putida*, or *Streptomyces iranensis*. For each, there was induction of the gene cluster encoding a non-ribosomal peptide synthetase-like enzyme (atromentin synthetase) and an aminotransferase which together produce atromentin. Correspondingly, during co-culturing there was an increase in secreted atromentin-derived pigments, *i.e.*, variegatic, xerocomic, isoxerocomic, and atromentic acid. Bioinformatic analyses from 14 quinone synthetase genes, twelve of which are encoded in a cluster, identified a common promoter motif

indicating a general regulatory mechanism for numerous basidiomycetes.

Introduction

Traditionally, natural product research was mainly driven by the search for antimicrobial, cytotoxic, or other bioactive compounds with a goal to develop those compounds into medications to treat human diseases. Prominent examples are the immunosuppressant cyclosporine A, or the antibiotics penicillin and echinocandin (Misieki and Hoffmeister, 2007; Brakhage, 2013). A second focus was placed on identification of metabolites of plant pathogenic fungi and food contaminants such as the aflatoxins and trichothecenes (Keller *et al.*, 2005). In recent years, increasing emphasis was put on elucidating environmental and mechanistic aspects of these complex and often chiral and highly functionalized compounds. In most cases, ascomycete compounds were addressed. Examples include, among numerous others, the T-toxin, a host-selective toxin and high virulence determinant produced by the maize pathogenic fungus *Cochliobolus heterostrophus* race T (Braun *et al.*, 1990; Turgeon and Baker, 2007). Furthermore, the HC-toxin of *Cochliobolus carbonum* was recognized as a histone deacetylase inhibitor (Walton, 2006).

Atromentin is a NRPS-like derived terphenylquinone that serves as a central precursor for numerous basidiomycete natural products (Supporting Information Fig. S1). Nutritionally, atromentin-derived pigments like variegatic acid and the diarylcyclopentenone involutin have been shown to provide redox cycling during Fenton chemistry and thus to represent an essential component to recalcitrant nutritional uptake during lignocellulose breakdown (Eastwood *et al.*, 2011; Braesel *et al.*, 2015; Shah *et al.*, 2015). However, despite their rich secondary metabolite potential, the effect of trans-kingdom co-incubation on encoded non-ribosomal peptide synthetase (NRPS), NRPS-like, polyketide synthase (PKS), and PKS-NRPS hybrid enzymes has not been addressed yet for Basidiomycota.

Therefore, we followed biosynthesis loci of the saprotrophic model brown-rot basidiomycete *Serpula lacrymans* in response to individual co-incubation with a terrestrial, wild-type bacterium. Not only does this basidiomycete's

Received 3 August, 2016; revised 25 September, 2016; accepted 27 September, 2016. *For correspondence. E-mail dirk.hoffmeister@leibniz-hki.de; Tel: +49-3641-949850; Fax: +49-3641-949852.

genome encode numerous secondary metabolite biosynthesis loci, it also represents an ubiquitous economic burden regarding timber degradation (Kausserud *et al.*, 2004; Eastwood *et al.*, 2011). Given that previous co-incubation studies on *Aspergillus* and its interaction with bacteria such as *B. subtilis* (Benoit *et al.*, 2015) or *Streptomyces hygroscopicus* (Schroeckh *et al.*, 2009) showed an altered secondary metabolism response by the fungal partner, we hypothesized that a basidiomycete could also respond under such conditions as part of a natural system. To this end, the model fungus *S. lacrymans* was co-incubated with the terrestrial *Streptomyces iranensis* (Actinobacteria), *Bacillus subtilis* (Firmicutes) or *Pseudomonas putida* (Proteobacteria) bacterium. By monitoring biosynthetic loci in *S. lacrymans* during co-incubations we present genetic and chemical evidence that shows the indiscriminate upregulation of the clustered atromentin biosynthesis genes *NPS3* and *AMT1* (Supporting Information Fig. S1) and increased secretion of atromentin-derived pigments in response to each of the terrestrial bacteria. The *NPS3*-encoded quinone synthetase, as characterized *in vitro* in this work, condenses 4-hydroxyphenylpyruvate symmetrically to atromentin in a process that mechanistically resembles non-ribosomal peptide synthesis. The *AMT1* gene encodes an L-tyrosine:2-oxoglutarate aminotransferase which thus supplies *NPS3* with substrate. Regardless of lifestyle, *S. lacrymans* and other atromentin-producing basidiomycetes share conserved promoter motifs of clustered genes *NPS3* and *AMT1* and thus these pigments may be part of a response mechanism controlled genetically by a generic regulation.

Results

Effect of a bacteria-fungus co-incubation on biosynthesis gene expression

The model fungus *S. lacrymans* was co-incubated with the terrestrial actinomycete *Streptomyces iranensis* (Horn *et al.*, 2014) which belongs phylogenetically to the *S. hygroscopicus* group. To study secondary metabolite regulation of *S. lacrymans* we focused on the genes encoding NRPSs, NRPS-like, PKSs, and PKS-NRPS hybrid enzymes as they assemble the majority of fungal natural products. Except atromentin, the products assembled by these enzymes are not known from *S. lacrymans*, although its genome encodes six PKSs, 15 NRPSs or like enzymes, and two PKS-NRPS hybrids (Eastwood *et al.*, 2011). We re-investigated the annotated genome of *S. lacrymans* S7.9 and included additional unpublished yet annotated natural product genes. For a comprehensive survey on the metabolic response we monitored the following genes for transcriptional changes using qRT-PCR when *S. lacrymans* was co-incubated with *S. iranensis*: *NPS1-NPS4*, *NPS7*, *NPS13-NPS15*, *NPS17* and *NPS18*

(all encoding putative NRPSs, except the NRPS-like quinone synthetase *NPS3*); *NPS5*, *NPS9-NPS12* (encoding putative adenylate-forming reductases, except for characterized *NPS9* and *NPS11*; Brandenburger *et al.*, 2016); *PKS1-PKS6* (encoding putative reducing and non-reducing PKSs); and *NPS6*, *NPS8* and *NPS16* (encoding for putative PKS-NRPS hybrids).

Most of the tested genes had no profound transcriptional changes (less than 12-fold change) during the entire co-incubation period examined (Fig. 1). Interestingly, the quinone synthetase gene *NPS3* was by far the most influenced gene as it was upregulated the entire co-incubation period. Other genes like *NPS1*, which encodes a heptadomain NRPS similar to that for gliotoxin and sirodesmin production (Gardiner *et al.*, 2004; Balibar and Walsh, 2006; Cramer *et al.*, 2006) showed some upregulation (11-fold increase) 7 days after co-incubation, and the PKS-NRPS hybrid gene *NPS8* showed a 12-fold upregulation after 24 h of co-incubation. The respective products are unknown, except for *NPS3* that was proven to catalyze atromentin formation (see below).

Expression of genes in the atromentin locus during co-incubation

The atromentin synthetase gene *NPS3*, now identified as inducible by microbial co-cultivation, encodes a widespread metabolic capacity in basidiomycetes and is shared amongst numerous basidiomycetes independent of lifestyle (see below). The annotated atromentin locus comprises three genes that code for a quinone synthetase (*NPS3* in *S. lacrymans*), an aminotransferase (*AMT1*) and, located between the former two genes, for an alcohol dehydrogenase (*ADH2*; Eastwood *et al.*, 2011). The relative expression of these three genes was monitored by qRT-PCR over time during co-incubation using the same *S. lacrymans* – *S. iranensis* co-culture as above. We additionally investigated two other terrestrial bacteria, *Bacillus subtilis* or *Pseudomonas putida*, in order to represent ubiquitously distributed different phyla of various lifestyles that could potentially encounter a terrestrial, saprotrophic fungus in nature. As a control to exclude unspecific transcriptional activity as consequence of proximity, the adjacent putative glycoside hydrolase gene *GLY1* was included, for which a role in atromentin biosynthesis was not plausible to assume. The co-incubation with each bacterium led to an increase in relative transcription expression levels of *NPS3* and *AMT1* in all co-incubation conditions tested (Fig. 2). Transcription of the *NPS3* gene during co-incubation with either *B. subtilis* or *P. putida* showed an early upregulation (31- and 24-fold after 24 h, respectively) and reached a maximum after 30 h of co-incubation with a 44-fold and 40-fold increase respectively. By day 7, the expression levels had subsided back to those

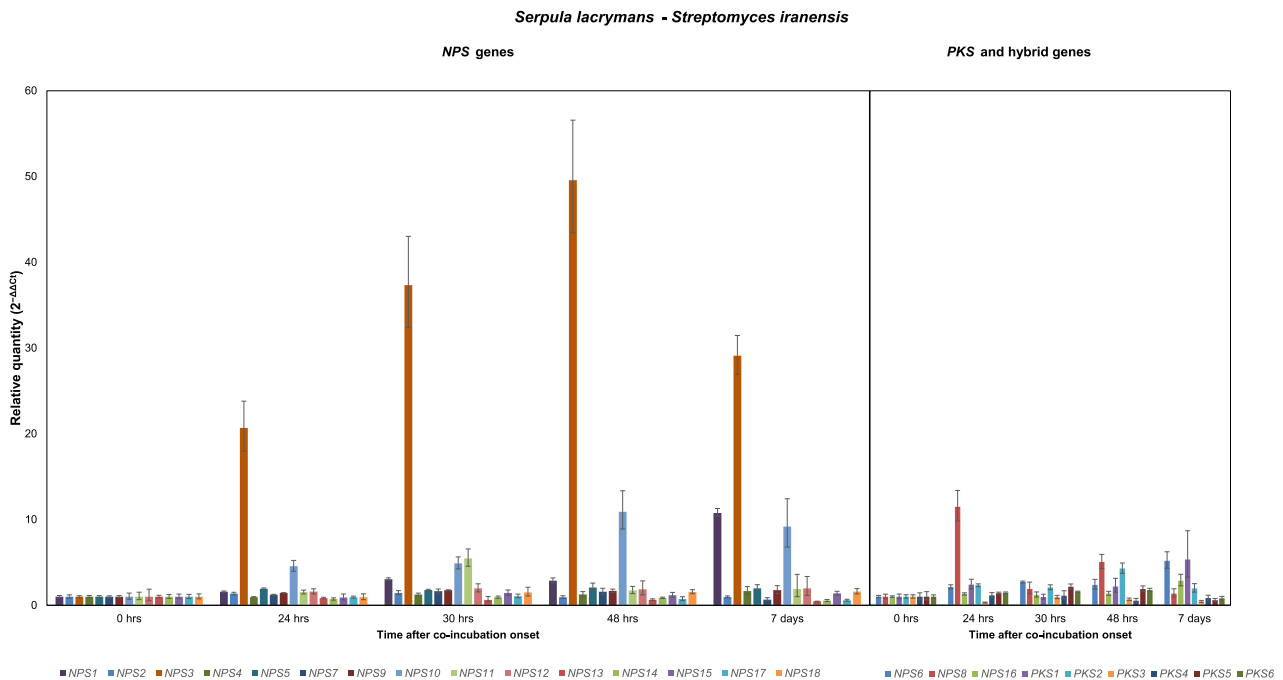


Fig. 1. Relative transcription of *S. lacrymans* natural product genes monitored by qRT-PCR from *S. lacrymans* – *Streptomyces iranensis* co-cultures. The figure shows the linear fold change (error bars indicate standard deviation) of annotated *NPS*, *PKS* and hybrid *PKS-NRPS* genes. The axenic culture of *S. lacrymans* at the onset of co-incubation (time 0) is equal to 1.

observed at the onset of co-incubation, which was the substantial difference compared to *S. iranensis* co-cultures. Co-incubation with *S. iranensis* showed a steady upregulation of *NPS3* peaking at a 49-fold increase 48 h after co-incubation and with prolonged elevated expression (29-fold) even after seven days. In all cases, *AMT1* was correspondingly upregulated alongside *NPS3*. Irrespective of which bacterial organism was present in the co-culture, there was only maximal 4.6-fold change across all samples regarding *ADH2*. Therefore, *NPS3* and *AMT1* are co-expressed while the contribution of *ADH2* still remains unclear.

The adjacent and external control *GLY1* had no significant upregulation as the maximum fold-change, across all samples, was merely 1.7.

Pigment accumulation during co-incubation and NPS3 characterization

Gene expression data from qRT-PCR provided evidence that the atromentin biosynthesis cluster was stimulated when *S. lacrymans* was co-incubated with one of three diverse bacteria. During co-incubation we visually noticed that the white fungal mycelium adjacent to the bacterial

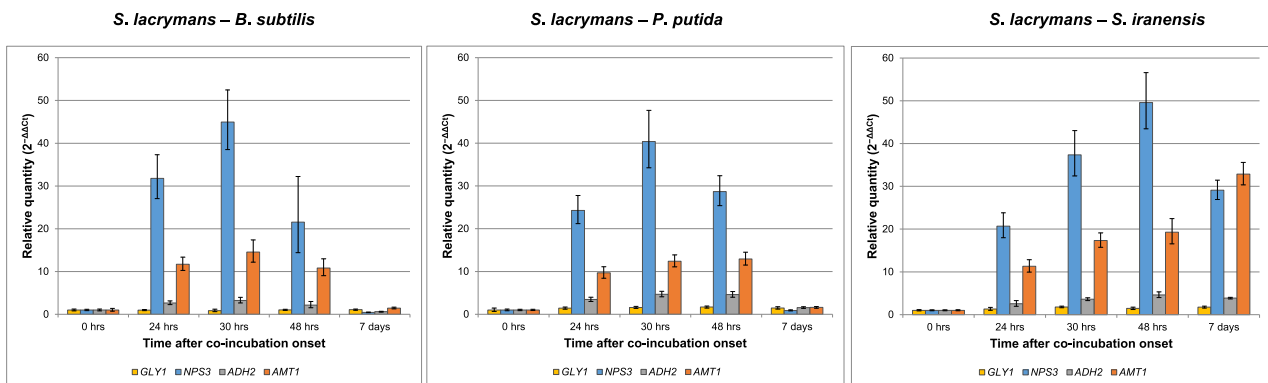


Fig. 2. Relative transcription regulation of clustered atromentin biosynthesis genes (*NPS3*, *AMT1* and *ADH2*) monitored by qRT-PCR from *S. lacrymans* – bacterium co-cultures. An adjacent gene (*GLY1*) was used as negative control. The linear fold change is shown (error bars indicate standard deviation). The axenic culture of *S. lacrymans* at the onset of co-incubation (time 0) is equal to 1.

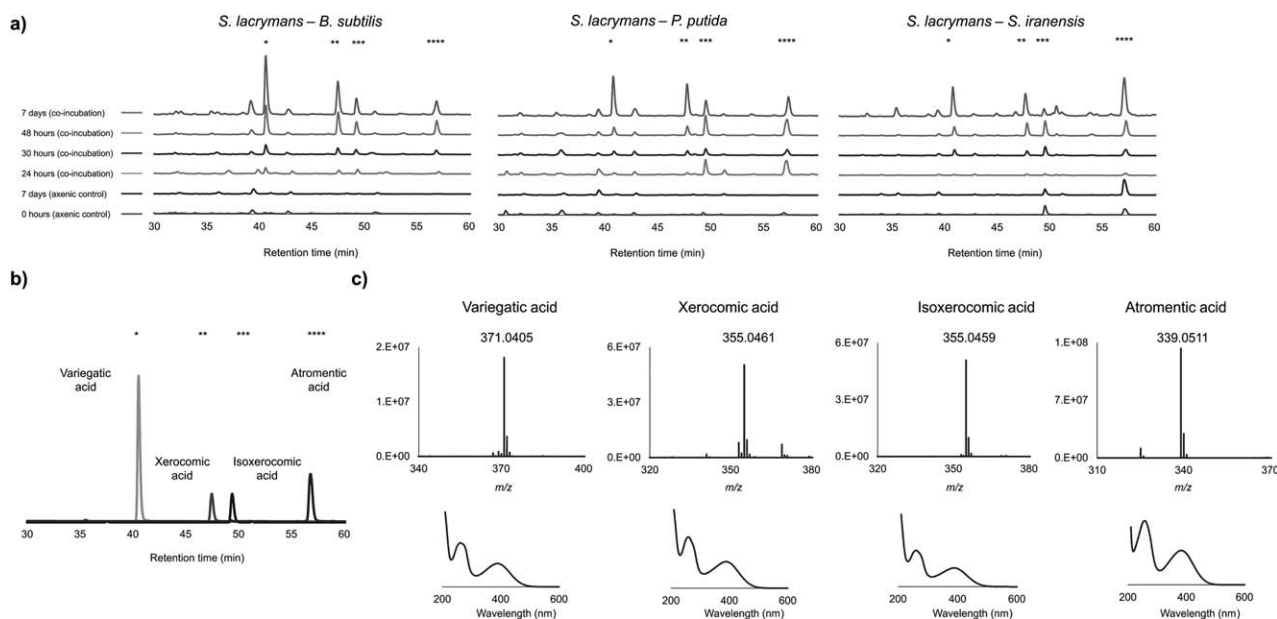


Fig. 3. HPLC analysis of crude extracts from *S. lacrymans* – bacterium co-cultivations. Panel a: chromatograms for co-incubations with *B. subtilis*, *P. putida*, and *S. iranensis*. The absorption units (mAU) for variegatic acid at 7 days after co-incubation were 298 mAU for *B. subtilis*, 201 mAU for *P. putida*, and 150 mAU for *S. iranensis*; panel b: composite chromatograms of authentic standards of variegatic acid (*), xerocomic acid (**), isoxerocomic acid (***), and atromentic acid (****); panel c: high-resolution mass spectra (top) and the respective UV/Vis spectra (bottom) of the authentic standards shown in panel b. All chromatograms were extracted from diode-array data at $\lambda = 254$ nm, and masses were recorded in negative mode.

inocula, the bacterial inocula themselves, and the agar at the point of inoculum started to appear a brilliant yellow color (Supporting Information Fig. S2). We hypothesized that the coloration results from atromentin-derived *S. lacrymans* pigments (Gill and Steglich, 1987). Therefore, the relative amount of secreted atromentin-derived pigments was investigated chromatographically by reversed-phase HPLC as determined by the area under the curve. The pigments of interest differ from each other by the number and position of phenolic hydroxyl groups (Supporting Information Fig. S1) which allows for their facile chromatographic identification by UV/Vis-spectra and electrospray mass spectrometry (ESI-MS), together with comparison to authentic standards and previous literature. Crude extracts from axenic controls and co-cultures were examined for the pigments by HPLC followed by low- and high-resolution LC-MS. Chromatograms extracted at $\lambda = 254$ nm from HPLC runs in addition to LC-MS showed that variegatic, xerocomic, isoxerocomic, and atromentic acid increased in relative concentration over time during co-incubation for each condition (either *B. subtilis*, *P. putida*, or *S. iranensis*), compared to fungal axenic control cultures treated similarly without bacteria (Fig. 3). Retention times were $t_R = 40.5$ min for variegatic acid (371.1 [M-H]⁻) and $t_R = 56.8$ min (339.1 [M-H]⁻) for atromentic acid. The mass for xerocomic acid (355.1 [M-H]⁻) was found in two separate peaks at $t_R = 47.5$ and 49.4

min, indicating that its regioisomer isoxerocomic acid was also produced, which is compatible with previously reported analyses for both compounds from *S. lacrymans* and other Boletales (Gill and Steglich, 1987). All masses were additionally confirmed by high-resolution ESI-MS (Supporting Information Table S1). The central precursor atromentin was detected only in trace amounts by high-resolution mass spectrometry. We found no preferred accumulation between all four pigments so we decided to focus on the relative accumulation of the last tailored pigment from the co-cultures over time focusing on the notable difference seen from qRT-PCR results, *i.e.*, that the atromentin cluster was upregulated for a longer duration with *S. iranensis*. During co-incubation (48 h to 7 days) with *S. iranensis* there was a 212% increase of variegatic acid (versus 105% increase for all pigments) during this time span while with *B. subtilis* and *P. putida* there was a 111% (all: 64%) and 379% increase (all: 89%) of variegatic acid, respectively, compared to no variegatic acid detectable in the axenic controls. It should be stressed that the synthesis route between atromentin production and the final modified pigments remains uncharacterized with regard to genes and enzymes involved. Thus, a definitive correlative conclusion between gene regulation and enzyme turnover warrants further investigation.

Because gene deletion knockout mutants are not possible in *S. lacrymans* to correlatively link the atromentin

cluster to atromentin or atromentin-derived pigments, we then characterized the putative quinone synthetase *in vitro*. *NPS3* was overexpressed in *E. coli* to produce hexahistidine-tagged enzyme which was then purified, subsequently primed *in vitro* as before (Braesel *et al.*, 2015), and its *holo*-form incubated *in vitro* with the substrate 4-hydroxyphenylpyruvate (atromentin precursor) until chromatographic analysis for atromentin production. The quinone synthetase from *S. lacrymans* catalyzed the formation of atromentin from 4-hydroxyphenylpyruvate and thus verified its role in atromentin production (Supporting Information Figs S3–S5, for procedures see Supplemental Methods). Lastly, the isolated pigments were tested for antimicrobial activity by the disk diffusion assay. Each pigment, tested at 1000 µg ml⁻¹, did not significantly inhibit the growth of the tested bacteria and fungi (Supporting Information Table S2).

Atromentin biosynthesis genes share a common promoter motif

An *in silico* approach was additionally taken to complement genetic and chemical work on the atromentin cluster. We assumed that the co-expression of cluster genes is coordinated by common transcription factor(s) (TF), and cluster promoters should thus contain common motifs that serve to bind this shared regulator. This assumption holds true for most clusters and can be used as a distinguishing feature in cluster prediction (Wolf *et al.*, 2015). However, due to the low number of sequences for small clusters, such as the one for atromentin biosynthesis, detection of common patterns is challenging, and in such cases detection can be supported through searching for common binding sites in putative orthologous clusters. A search for quinone synthetase genes (whose products show >80% identity on the amino acid level) with an adjacent annotated aminotransferase gene showed that the cluster genes are conserved and syntenic across multiple genomes, thereby supporting putative orthology of the whole cluster regions (Supporting Information Table S6). Given this degree of conservation, we hypothesized that the regulatory pattern and the underlying sequences are conserved as well. Therefore, we screened for conserved patterns in the sequences of atromentin biosynthesis gene cluster promoters taken from 14 quinone synthetase genes. Together, this search is composed of five *in vitro* characterized quinone (atromentin) synthetases.

To confirm that the motifs are cluster-specific, we applied a discriminative search in cluster promoters against a negative set of promoters of non-cluster and/or non-secondary metabolite genes. The *de novo* motif prediction revealed one motif with high significance (E-value = 1.2e-004). The motif was identified in the promoters of all quinone synthetase and aminotransferase

genes, but absent from those of the alcohol dehydrogenase gene, with one exception (*Suillus decipiens*). The lack of binding sites in the dehydrogenase genes corresponds well with qRT-PCR data since these genes were not profoundly co-regulated under inducing conditions. The strong conservation of the motif within each cluster in promoters of quinone synthetase and aminotransferase genes as well as between putative orthologous cluster regions supports our hypothesis about the conserved mechanisms involved in the regulation of this cluster as a similar transcription factor may bind to these conserved motifs (Fig. 4).

Discussion

We studied the natural product repertoire from the model saprotrophic basidiomycete *S. lacrymans* by focusing on gene transcriptional dynamics of NRPS, PKS, and PKS-NRPS biocatalysts and subsequent product formation when co-cultured with a terrestrial bacterium. We showed that various bacteria induce the NRPS-like atromentin-producing quinone synthetase in *S. lacrymans* and that all four pigment variants increased in relative quantity during co-incubation. Co-cultivations have been recognized as an attractive strategy to investigate natural product biosyntheses as axenic cultures do not reflect natural situations (Schroeckh *et al.*, 2009). This study fills the void in basidiomycete research of natural product induction by transkingdom co-cultures.

Interactions between fungi and bacteria have been studied, e.g., see Wargo and Hogan (2006) and Spraker *et al.* (2016). Previous studies between *Aspergillus* and *Streptomyces* or *B. subtilis* have shown that physical contact occurs during co-incubation (Schroeckh *et al.*, 2009; Benoit *et al.*, 2015). Specifically for *Coprinopsis cinerea*, attachment of *B. subtilis* was noted by utilizing microfluidic co-incubation chambers (Stanley *et al.*, 2014). Intriguingly, intimate contact with *Streptomyces* was required for induction of an otherwise silent polyketide metabolism in *Aspergillus* (Schroeckh *et al.*, 2009). A further epigenetic study showed that the Saga/Ada-mediated histone acetylation was triggered by *Streptomyces* (Nützmann *et al.*, 2011). However, there exists a challenging nature of researching basidiomycetes in comparison to ascomycetes like *Aspergillus*. For instance, the paucity of genetic manipulation protocols, difficult culture protocols or slow growth under laboratory conditions, if at all, (Stadler and Hoffmeister, 2015), favored the prominent use of ascomycetes for research on co-incubation studies over the basidiomycetes (Sillo *et al.*, 2015). As with many other basidiomycetes, genetic manipulation of *S. lacrymans* is not feasible. Still, our work provides insight into basidiomycete-bacterium co-cultivations as we showed that the upregulated quinone synthetase gene does secure

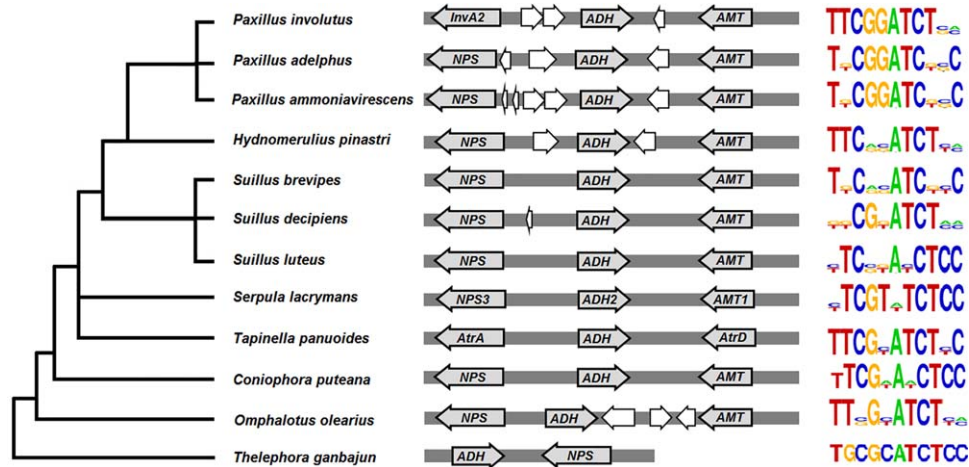


Fig. 4. Conserved promoter motifs of clustered atromentin genes from twelve basidiomycetes. The motifs were found conserved in all quinone synthetase (*NPS*) and aminotransferase (*AMT*) gene promoters, but absent for the alcohol dehydrogenase (*ADH*) with one exception (*Suillus decipiens*). Every logo corresponds to two shared motifs (*NPS* and *AMT*) in each species except for distantly-related *T. ganbajun* where the whole cluster is not conserved and only one motif was found. Of the two examined *NPS*s from *P. involutus*, *InvA2* is shown here because it represents the tightest cluster of genes. The published gene names are given when available. The phylogenetic tree represents a protein cluster-based maximum likelihood tree that has been adapted from the Joint Genome Institutes Mycocosm website (Grigoriev *et al.* 2014, Kuo *et al.*, 2014).

production of atromentin, *i.e.*, the precursor to variegatic acid and related pigments. Basidiomycete chromophoric compounds are nonetheless interesting for their putative ecological roles and warrant investigation. Chromophores, such as ptoporic acid, polyenes and pulvinic-acid types, have been implicated in *in situ* defenses such as insect and animal repellants (Besl and Blumreisinger, 1983; Gill and Steglich, 1987; Spiteller, 2008; Schwenk *et al.*, 2014; Spiteller, 2015), wound-induced mechanisms (Lang *et al.*, 2001; Kindler and Spiteller, 2007; Schwenk *et al.*, 2014), and redox-active compounds for biopolymer breakdown (Eastwood *et al.*, 2011; Shah *et al.*, 2015). All co-incubation cultures tested with taxonomically diverse bacteria led to a response by *S. lacrymans* which already gestures a general response mechanism. To this effect, the tested bacteria presumably have some active or passive inducing agent to which *S. lacrymans* responds, such as a cell wall or membrane component, secreted (lipo-)peptides, or low molecular weight metabolites (Spraker *et al.*, 2016). Co-incubation can lead to a two-way metabolic response of both partners involved and as such a secreted compound may be the eliciting factor (Benoit *et al.*, 2015). This inducing agent(s) may trigger a stress specific response in *S. lacrymans*, but may even be part of a more generic response mechanism. The atromentin-derived pigments were shown here to not have antimicrobial activity and they are also heavily present from a nutritional cue and involved in redox cycling for lignocellulose breakdown (Eastwood *et al.*, 2011; Braesel *et al.*, 2015). Thus, this mechanism may overlap with a nutritional response and as such may be co-regulated alongside

many other cellular processes including stress, nutrition and secondary metabolism. This could be reminiscent of the global fungal regulator LaeA (Bok and Keller, 2004; Bayram *et al.*, 2008; Bok and Keller, 2016) or the complex, nitrogen-dependent regulation of bikaverin from *Fusarium fujikuroi* (Wiemann *et al.*, 2009).

To follow up on a general response notion, we used bioinformatics and searched for common promoter motifs from putative orthologous quinone synthetase loci which do not contain known or conserved transcription factors within the cluster. The *S. lacrymans* atromentin cluster aligns well with syntenic loci of multiple basidiomycetes of various lifestyles. We identified a consensus for both the quinone synthetase and aminotransferase gene that was missing for almost all of the clustered dehydrogenase genes. This supports our qRT-PCR results that the dehydrogenase gene essentially was not co-expressed with the other locus genes. The function of the dehydrogenase nevertheless remains unclear as no reductive or oxidative step is necessary to complete atromentin biosynthesis yet is still very conserved. Our newly presented promoter data indicates the clusters are controlled by a similar transcription factor (*i.e.*, general regulation) for atromentin-producing fungi. This will require further investigation, likely in a genetically malleable organism, to understand transcriptional regulation of natural product loci in Basidiomycota.

Overall, our results indicate that pigment secretion was stimulated by diverse bacteria. Given (i) the wide distribution of atromentin biosynthesis in basidiomycetes and (ii) that bacteria of various phyla induced biosynthesis genes and natural product formation, our findings point to a

possibly widespread pigment response that may open up new avenues of research into the environmental relevance of basidiomycete natural products.

Experimental procedures

Culture conditions

S. lacrymans S7 (Eastwood *et al.*, 2011) was routinely grown on MEP agar (malt extract 30 g l⁻¹, peptone 3 g l⁻¹, agar 18 g l⁻¹, pH 5.6) at room temperature in darkness. For co-culture conditions, *S. lacrymans* was grown as a pre-culture for 13–14 days in a petri plate at room temperature in darkness on synthetic agar based on Modified Melin-Norkrans medium (Marx, 1969) with noted alterations (glucose monohydrate 5 g l⁻¹, 0.1 × Hutner's Trace Elements (Hutner *et al.*, 1950), no malt extract, 1.8% (w/v) agar and pH 5.6 adjusted with NaOH). The agar surface was covered with a sterile 0.45 µm pore cellulose nitrate membrane filter (Sartorius). For *B. subtilis* (Branda *et al.*, 2001) or *P. putida* (ST036147, Jena Microbial Resource Collection JMRC) pre-cultures, two flasks, each with 1 l of LB medium were grown overnight from a 25% (v/v) glycerol stock swab at 30°C and 28°C, respectively, with agitation (180 rpm). For *S. iranensis* (Horn *et al.*, 2014) pre-cultures, eight flasks, each with 400 ml DSMZ M79 medium, were inoculated from 1 ml spore stocks (1.3 × 10⁸ spores ml⁻¹) and incubated for four days at 28°C with agitation (180 rpm). To start a co-incubation culture, biomass from bacterial pre-cultures was pelleted and pooled, washed three times with autoclaved dH₂O, resuspended in phosphate-buffered saline (pH 7.4), and 250 µl were spotted at four different loci evenly spaced across the pre-cultured fungal mycelial bed. Samples were then incubated at room temperature in darkness until harvesting at various time points after the onset of co-incubation. Axenic *S. lacrymans* cultures treated similarly without bacteria were used as control plates. Each experimental condition (fungal-bacterial interaction, time point and control) had four biological replicates. For colony forming unit (CFU) counts of *B. subtilis* and *P. putida*, a dilution series run in duplicates was done. Bacteria were incubated on LB plates (1.8% agar (w/v)) at the respective temperatures. Colonies were counted for plates that had between 25–250 colonies. CFU counts were averaged between all relevant plates and presented as CFU per 250 µl inoculum. For *B. subtilis* each inoculum had 3.8 × 10⁹ CFU and for *P. putida* 1.41 × 10⁸ CFU.

Total RNA extraction and cDNA synthesis

The bacterial inocula were removed from the co-cultured fungal mycelial lawn, the inoculum areas gently blotted with a cotton ball and half of the plate, containing two areas of removed bacterial inoculum, was scraped into a 2 ml Eppendorf tube, shock frozen in liquid nitrogen, and stored at -80°C. Total RNA extraction was carried out using the SV Total RNA Isolation System (Promega) according to the manufacturer's recommended spin protocol (except the on-membrane DNase I step was done at 37°C for 30 min) and the mycelium was disrupted by physical grinding. Total RNA was obtained from each plate independently, quantified and checked for quality with a ScanDrop spectrophotometer (A_{260/280} and A_{260/230} > 2.0). All biological replicates per

condition were then pooled. 4 µg pooled total RNA was used in 20 µl Baseline-Zero™ DNase treatments and incubated at 37°C for 30 min. Then, 11.5 µl of twice-DNase treated total RNA was used in reverse strand syntheses primed with 100 pmol µl⁻¹ d(T)₂₀VN oligonucleotide primer and transcribed using 200 U RevertAid Premium reverse transcriptase (Thermo Scientific) for three hours at 46°C using the manufacturer's recommended master mix. Both steps were done in two separate reactions and pooled. 30 µl of pooled cDNA was treated by alkaline hydrolysis and pink co-precipitant (Bioline) with a 70% (v/v) EtOH wash and lastly resuspended in 30 µl nuclease-free water at 55°C for 10 min. Total RNA was stored at -80°C and cDNA at -20°C.

qRT-PCR

Purified cDNA was diluted 1:10 in nuclease-free water, and 1 µl cDNA (approximately 4–6 ng final concentration) was used in a 20 µl qRT-PCR (quantitative real-time polymerase chain reaction) mixture consisting of 10 µl 2 × MyTaq™ HS Mix (Bioline), 1 µl 20 × EvaGreen (Biotium), 4 pmol each gene-specific qRT-PCR primer (0.4 µl each; Supporting Information Table S3), and 7.2 µl nuclease-free water. Primer efficiency was checked using six 1:10 dilutions of pJET1.2 (CloneJET PCR Cloning Kit) containing the PCR insert as amplified by qRT-PCR primers or containing the full-length gene as amplified by other primers (amplicons were extracted from agarose gel). Reactions were run in triplicate on Applied Biosystems StepOne Real-Time or QuantStudio 3 cyclers. Thermal cycling conditions were: 95°C initial denaturation for 120 s, 40 cycles of 95°C for 5 s and 62°C for 15 s (data acquisition), and a final melt analysis from 60°C to 95°C in 0.3°C sec⁻¹ increments. qRT-PCR data was analyzed using StepOne (version 2.2.3) or Quantstudio Design and Analysis (version 1.2.0) software. Relative quantification was determined by the 2^{-(ΔΔC_t)} equation (Livak and Schmittgen, 2001) using the annotated *S. lacrymans* β-tubulin gene as the endogenous control, which expressed consistently throughout all the treatments and is consistent with other basidiomycete transcript profiling experiments (Wawrzyn *et al.*, 2012; Arfi *et al.*, 2013; Plaza *et al.*, 2014). Pre-cultures of axenic *S. lacrymans* at the onset of co-incubation were used as the reference control and set to a relative quantity = 1. qRT-PCR controls included i) no template (nuclease-free water) mixtures to check for interference and contamination and ii) twice-DNase treated total RNA samples to check for gDNA contamination.

Pigment isolation, chromatography and bioactivity testing

To extract the secreted pigments from the medium and removed bacterial inocula, the agar of four biological replicates was physically macerated, soaked in 500 ml ethyl acetate with 1% (v/v) acetic acid for one hour and then filtered to remove debris. The organic layer was separated after the addition of an equal volume of dH₂O in a separatory funnel and dried under reduced pressure followed by lyophilization. The dry crude extracts were resuspended in 1 ml methanol, and 30 µl were used for chromatography. All samples were first run on an Agilent 1200 integrated system HPLC, equipped with an

Zorbax Eclipse XDB-C₁₈ column (5 µm, 4.6 × 250 mm, fitted with a guard). Solvent A was 0.1% (v/v) trifluoroacetic acid in water and solvent B was acetonitrile. The following gradient was used: 95% A and 5% B held for five minutes, followed by a linear increase to 40% B within 90 min, at a flow of 1 ml min⁻¹. Samples were additionally run on an Agilent LC-MS 1260 build with a 6130 quadrupole MS detector, equipped with the same column and run with the same gradient using electrospray ionization (negative and positive mode). Relative amounts of secreted pigments were measured by calculating the area under the curve using Agilent ChemStation software. UV/Vis spectra were recorded from λ = 210–600 nm and extracted at λ = 254 nm. Spectra and masses were compared to previous work (Gill and Steglich 1987; Eastwood *et al.*, 2011). For bioactivity assays, pigments were isolated by semi-preparative HPLC and identified as above. Antimicrobial bioactivity testing as done by the disk diffusion method is described in the supplement.

In vitro product formation by NPS3 was verified by HPLC on the above instrument equipped with an Eclipse XDB-C₁₈ column (4.6 × 150 mm, 5 µm, fitted with a guard) against an atromentin standard using the following conditions: at a flow rate of 1 ml min⁻¹ using a gradient (with the same solvents as above) of an initial hold at 5% B for 2 min followed by a linear gradient from 5% to 100% B within 18 min. High-resolution mass spectrometry was carried on an Exactive Orbitrap instrument (Thermo) run in the negative and positive mode, and equipped with a Betasil C₁₈ column (Thermo, 2.1 × 150 mm; 3 µm particle size). The flow rate was 0.2 ml min⁻¹. Solvent A was 0.1% (v/v) formic acid in water, solvent B was 0.1% (v/v) formic acid in acetonitrile, and the following gradient was used: an initial hold at 5% B for 1 min, then a linear increase to 98% B within 15 min, followed by a hold at 98% B for 3 min.

Prediction of potential regulatory patterns in natural product gene promoters

Promoter sequences were collected for each gene of the (putative or verified) atromentin clusters from published cosmid libraries of *Tapinella panuoides* and *Suillus grevillei* (Schneider *et al.*, 2008; Wackler *et al.*, 2012). Due to insufficient adjacent sequence data, the latter species was excluded from the cluster alignment. Sequence data from another 11 species was extracted via the JGI MycoCosm portal (Grigoriev *et al.*, 2011; Grigoriev *et al.*, 2014). For analyses from JGI we used *Serpula lacrymans* (Eastwood *et al.*, 2011), *Coniophora puteana* (Floudas *et al.*, 2012), three *Suillus* species (*S. brevipes*, *S. luteus*, *S. decipiens*) (Branco *et al.*, 2015; Kohler *et al.*, 2015), three *Paxillus* species (*P. involutus* (both *InvA2* and *InvA5*), *P. adelphus*, *P. ammoniavirescens*) (Kohler *et al.*, 2015), *Hydnomerulius pinastri* (Kohler *et al.*, 2015), *Omphalotus olearius* VT 653.13 v1.0 (Wawrzyn *et al.*, 2012), and *Thelephora ganbajun*. The promoter region was selected as -1000/+2 bp around the transcription start site as suggested by Wolf *et al.* (2015). The search for common motifs was performed by the MEME software (Bailey and Elkan, 1994) using the discriminative mode against a negative promoter set. The negative training set contained (i) 21 promoters of genes flanking the cluster regions, two up- and two downstream promoters per cluster and (ii) 20 promoters of non-secondary

metabolite genes. All motifs with their respective position, *P*-value, and genes used (clustered and the negative training set) are found in Supporting Information Tables S4–S6. The MEME search was performed with the following parameters: motif length: 8–12 bp; 0 or 1 motifs per sequence; and search for three motifs. The phylogenetic tree in Fig. 4 is based on the fungal Tree of Life, taken from the Joint Genome Institute's MycoCosm portal (Grigoriev *et al.*, 2014), implemented in the Joint Genome Institute's annotation pipeline. Briefly, it utilizes subsets of protein clusters with only one protein in each genome as putative orthologous groups, concatenates proteins of each genome, creates multiple sequence alignment from the concatenation using MAFFT and builds the ML tree using RAXML, see Kuo *et al.*, (2014) for details on the tree building algorithm.

Acknowledgements

This work was supported by the Collaborative Research Center ChemBioSys (grant SFB1127/1; projects B02, B05, INF). We thank Dr. Akos Kovacs (Friedrich-Schiller-University Jena) for supplying bacteria, and Andrea Perner and Christiane Weigel (Leibniz Institute for Natural Product Research and Infection Biology – HKI, Jena) for high-resolution mass spectrometry and antimicrobial assays, respectively. We thank Igor Grigoriev, Alan Kuo, Robert Riley (Joint Genome Institute, Walnut Creek, CA, USA), Hui-Ling Liao and Rytas Vilgalys (Duke University, Durham, NC, USA), Patricia Jargeat (Université Paul Sabatier – Toulouse, France), Francis Martin (INRA, Nancy, France), Joseph Spatafora (Oregon State University, Corvallis, OR, USA), and Pengfei Wang (Yunnan University, Kunming, PR China) for providing access to basidiomycete genomic data.

Conflict of Interest

The authors declare that conflicts of interest do not exist.

References

- Arfi, Y., Levasseur, A., and Record, E. (2013) Differential gene expression in *Pycnoporus coccineus* during interspecific mycelial interactions with different competitors. *Appl Environ Microbiol* **79**: 6626–6636.
- Bailey, T.L., and Elkan, C. (1994) Fitting a mixture model by expectation maximization to discover motifs in biopolymers. *Proceedings of the Second International Conference on Intelligent Systems for Molecular Biology*. AAAI Press, Menlo Park, California, pp. 28–36.
- Balibar, C.J., and Walsh, C.T. (2006) GliP, a multimodular non-ribosomal peptide synthetase in *Aspergillus fumigatus*, makes the diketopiperazine scaffold of gliotoxin. *Biochemistry* **45**: 15029–15038.
- Bayram, O., Krappmann, S., Ni, M., Bok, J.W., Helmstaedt, K., Valerius, O., *et al.* (2008) VeIB/VeA/LaeA complex coordinates light signal with fungal development and secondary metabolism. *Science* **320**: 1504–1506.
- Benoit, I., van den Esker, M.H., Patyshakuliyeva, A., Mattern, D.J., Blei, F., Zhou, M., *et al.* (2015) *Bacillus subtilis* attachment to *Aspergillus niger* hyphae results in mutually altered metabolism. *Environ Microbiol* **17**: 2099–2113.

- Besl, H., and Blumreisinger, M. (1983) *Drosophila melanogaster* suitable for testing the susceptibility of higher fungi to larval feeding. *Z Mykol* **49**: 165–170.
- Bok, J.W., and Keller, N.P. (2004) LaeA, a regulator of secondary metabolism in *Aspergillus* spp. *Eukaryot Cell* **3**: 527–535.
- Bok, J.W., and Keller, N.P. (2016) Insight into fungal secondary metabolism from ten years of LaeA research. In: *The Mycota iii*, 3rd edition. Hoffmeister, D., and Esser K. (eds). Heidelberg: Springer, pp. 21–29.
- Braesel, J., Götz, S., Shah, F., Heine, D., Tauber, J., Hertweck, C., and Hoffmeister, D. (2015) Three redundant synthetases secure redox-active pigment production in the basidiomycete *Paxillus involutus*. *Chem Biol* **22**: 1325–1334.
- Brakhage, A.A. (2013) Regulation of fungal secondary metabolism. *Nat Rev Microbiol* **11**: 21–32.
- Branco, S., Gladieux, P., Ellison, C.E., Kuo, A., LaButti, K., Lipzen, A., et al. (2015) Genetic isolation between two recently diverged populations of a symbiotic fungus. *Mol Ecol* **24**: 2747–2758.
- Branda, S.S., Gonzalez-Pastor, J.E., Ben-Yehuda, S., Losick, R., and Kolter, R. (2001) Fruiting body formation by *Bacillus subtilis*. *Proc Natl Acad Sci USA* **98**: 11621–11626.
- Brandenburger, E., Braga, D., Kombrink, A., Lackner, G., Gressler, J., Künzler, M., Hoffmeister, D. (2016) Multi-genome analysis identifies functional and phylogenetic diversity of basidiomycete adenylate-forming reductases. *Fungal Genet Biol*. <http://dx.doi.org/10.1016/j.fgb.2016.07.008>
- Braun, C.J., Siedow, J.N., and Levings, C.S., 3rd (1990) Fungal toxins bind to the URF13 protein in maize mitochondria and *Escherichia Coli*. *Plant Cell* **2**: 153–161.
- Cramer, R.A., Jr, Gamcsik, M.P., Brooking, R.M., Najvar, L.K., Kirkpatrick, W.R., Patterson, T.F., et al. (2006) Disruption of a nonribosomal peptide synthetase in *Aspergillus fumigatus* eliminates gliotoxin production. *Eukaryot Cell* **5**: 972–980.
- Eastwood, D.C., Floudas, D., Binder, M., Majcherczyk, A., Schneider, P., Aerts, A., et al. (2011) The plant cell wall-decomposing machinery underlies the functional diversity of forest fungi. *Science* **333**: 762–765.
- Floudas, D., Binder, M., Riley, R., Barry, K., Blanchette, R.A., Henrissat, B., et al. (2012) The Paleozoic origin of enzymatic lignin decomposition reconstructed from 31 fungal genomes. *Science* **336**: 1715–1719.
- Gardiner, D.M., Cozijnsen, A.J., Wilson, L.M., Pedras, M.S., and Howlett, B.J. (2004) The sirodesmin biosynthetic gene cluster of the plant pathogenic fungus *Leptosphaeria maculans*. *Mol Microbiol* **53**: 1307–1318.
- Gill, M., and Steglich, W. (1987) Pigments of fungi (Macromycetes). *Prog Chem Org Nat Prod* **51**: 1–317.
- Grigoriev, I.V., Cullen, D., Goodwin, S.B., Hibbett, D., Jeffries, T.W., Kubicek, C.P., et al. (2011) Fueling the future with fungal genomics. *Mycology* **2**: 192–209.
- Grigoriev, I.V., Nikitin, R., Haridas, S., Kuo, A., Ohm, R., Otilar, R., et al. (2014) MycoCosm portal: gearing up for 1000 fungal genomes. *Nucleic Acids Res* **42**: D699–D704.
- Horn, F., Schroeckh, V., Netzker, T., Guthke, R., Brakhage, A.A., and Linde, J. (2014) Draft Genome Sequence of *Streptomyces iranensis*. *Genome Announc* **2**: e00616–e00614.
- Hutner, S.H., Provasoli, L., Schatz, A., and Haskins, C.P. (1950) Some approaches to the study of the role of metals in the metabolism of microorganisms. *Proc Amer Phil Soc* **94**: 152–170.
- Kausserud, H., Hogberg, N., Knudsen, H., Elborne, S.A., and Schumacher, T. (2004) Molecular phylogenetics suggest a North American link between the anthropogenic dry rot fungus *Serpula lacrymans* and its wild relative *S. himantoides*. *Mol Ecol* **13**: 3137–3146.
- Keller, N.P., Turner, G., and Bennett, J.W. (2005) Fungal secondary metabolism - from biochemistry to genomics. *Nat Rev Microbiol* **3**: 937–947.
- Kindler, B.L., and Spiteller, P. (2007) Chemical defense of the crust fungus *Aleurodiscus amorphus* by a tailor-made cyanogenic cyanohydrin ether. *Angew Chem Int Ed* **46**: 8076–8078.
- Kohler, A., Kuo, A., Nagy, L.G., Morin, E., Barry, K.W., Buscot, F., et al. (2015) Convergent losses of decay mechanisms and rapid turnover of symbiosis genes in mycorrhizal mutualists. *Nat Genet* **47**: 410–415.
- Kuo, A., Bushnell, B., and Grigoriev, I.V. (2014) Fungal genomics: Sequencing and annotation. *Adv Bot Res* **70**: 1–53.
- Lang, M., Spiteller, P., Hellwig, V., and Steglich, W. (2001) Stephanosporin, a “Traceless” Precursor of 2-Chloro-4-nitrophenol in the Gasteromycete *Stephanospora caroticolor*. *Angew Chem Int Ed* **40**: 1704–1705.
- Livak, K.J., and Schmittgen, T.D. (2001) Analysis of relative gene expression data using real-time quantitative PCR and the 2(-Delta Delta C(T)) Method. *Methods* **25**: 402–408.
- Marx, D.H. (1969) The influence of ectotrophic mycorrhizal fungi on the resistance of pine roots to pathogenic infections. II. Production, identification, and biological activity of antibiotics produced by *Leucopaxillus cerealis* var. *piceina*. *Phytopathology* **59**: 411–417.
- Misiek, M., and Hoffmeister, D. (2007) Fungal genetics, genomics, and secondary metabolites in pharmaceutical sciences. *Planta Med* **73**: 103–115.
- Nützmans, H.W., Reyes-Dominguez, Y., Scherlach, K., Schroeckh, V., Horn, F., Gacek, A., et al. (2011) Bacteria-induced natural product formation in the fungus *Aspergillus nidulans* requires Saga/Ada-mediated histone acetylation. *Proc Natl Acad Sci USA* **108**: 14282–14287.
- Plaza, D.F., Lin, C.W., van der Velden, N.S., Aebi, M., and Künzler, M. (2014) Comparative transcriptomics of the model mushroom *Coprinopsis cinerea* reveals tissue-specific armories and a conserved circuitry for sexual development. *BMC Genomics* **15**: 492.
- Schneider, P., Bouhired, S., and Hoffmeister, D. (2008) Characterization of the atromentin biosynthesis genes and enzymes in the homobasidiomycete *Tapinella panuoides*. *Fungal Genet Biol* **45**: 1487–1496.
- Schroeckh, V., Scherlach, K., Nützmans, H.W., Shelest, E., Schmidt-Heck, W., Schuemann, J., et al. (2009) Intimate bacterial-fungal interaction triggers biosynthesis of archetypal polyketides in *Aspergillus nidulans*. *Proc Natl Acad Sci USA* **106**: 14558–14563.
- Schwenk, D., Nett, M., Dahse, H.M., Horn, U., Blanchette, R.A., and Hoffmeister, D. (2014) Injury-induced biosynthesis of methyl-branched polyene pigments in a white-rotting basidiomycete. *J Nat Prod* **77**: 2658–2663.
- Shah, F., Schwenk, D., Nicolas, C., Persson, P., Hoffmeister, D., and Tunlid, A. (2015) Involutin Is an Fe³⁺ Reductant

- Secreted by the Ectomycorrhizal Fungus *Paxillus involutus* during Fenton-Based Decomposition of Organic Matter. *Appl Environ Microbiol* **81**: 8427–8433.
- Sillo, F., Zampieri, E., Giordano, L., Lione, G., Colpaert, J.V., Balestrini, R., and Gonthier, P. (2015) Identification of genes differentially expressed during the interaction between the plant symbiont *Suillus luteus* and two plant pathogenic allopatric *Heterobasidion* species. *Mycol Progress* **14**: 106.
- Spiteller, P. (2008) Chemical defence strategies of higher fungi. *Chemistry* **14**: 9100–9110.
- Spiteller, P. (2015) Chemical ecology of fungi. *Nat Prod Rep* **32**: 971–993.
- Spraker, J.E., Sanchez, L.M., Lowe, T.M., Dorrestein, P.C., and Keller, N.P. (2016) *Ralstonia solanacearum* lipopeptide induces chlamyospore development in fungi and facilitates bacterial entry into fungal tissues. *ISME J* (ePub ahead of print, doi: 10.1038/ismej.2016.32.).
- Stadler, M., and Hoffmeister, D. (2015) Fungal natural products - the mushroom perspective. *Front Microbiol* **6**: 127.
- Stanley, C.E., Stockli, M., van Swaay, D., Sabotic, J., Kallio, P.T., Künzler, M., *et al.* (2014) Probing bacterial-fungal interactions at the single cell level. *Integr Biol (Camb)* **6**: 935–945.
- Turgeon, B.G., and Baker, S.E. (2007) Genetic and genomic dissection of the *Cochliobolus heterostrophus* Tox1 locus controlling biosynthesis of the polyketide virulence factor T-toxin. *Adv Genet* **57**: 219–261.
- Wackler, B., Lackner, G., Chooi, Y.H., and Hoffmeister, D. (2012) Characterization of the *Suillus grevillei* quinone synthetase GreA supports a nonribosomal code for aromatic α -keto acids. *Chembiochem* **13**: 1798–1804.
- Walton, J.D. (2006) HC-toxin. *Phytochemistry* **67**: 1406–1413.
- Wargo, M.J., and Hogan, D.A. (2006) Fungal–bacterial interactions: a mixed bag of mingling microbes. *Curr Opin Microbiol* **9**: 359–364.
- Wawrzyn, G.T., Quin, M.B., Choudhary, S., Lopez-Gallego, F., and Schmidt-Dannert, C. (2012) Draft genome of *Omphalotus olearius* provides a predictive framework for sesquiterpenoid natural product biosynthesis in Basidiomycota. *Chem Biol* **19**: 772–783.
- Wiemann, P., Willmann, A., Straeten, M., Kleigrew, K., Beyer, M., Humpf, H., *et al.* (2009) Biosynthesis of the red pigment bikaverin in *Fusarium fujikuroi*: genes, their function and regulation. *Mol Microbiol* **72**: 931–946.
- Wolf, T., Shelest, V., Nath, N., and Shelest, E. (2015) CASSIS and SMIPS promoter-based prediction of secondary metabolite gene clusters in eukaryotic genomes. *Bioinformatics* Dec 9. pii: btv713.

Supporting information

Additional Supporting Information may be found in the online version of this article at the publisher's web-site:

Fig. S1. *S. lacrymans* atromentin cluster and pigment structures.

Fig. S2. Co-incubation plate pictures.

Fig. S3. HPLC profiles of *in vitro* atromentin production.

Fig. S4. HPLC profile of authentic atromentin standard.

Fig. S5. SDS-PAGE gels of NPS3 and PptA.

Table S1. High-resolution mass spectrometry of pigments.

Table S2. Bioactivity assays of pigments.

Table S3. qRT-PCR primers.

Table S4. Quinone synthetase cluster MEME motifs.

Table S5. Negative training set for MEME search

Table S6. Genes used for MEME search

Supporting material for the manuscript

Bacteria induce pigment formation in the basidiomycete *Serpula lacrymans*

James P. Tauber¹, Volker Schroeckh², Ekaterina Shelest³, Axel A. Brakhage^{2,4}, Dirk Hoffmeister^{1*}

¹ Department of Pharmaceutical Microbiology at the Leibniz Institute for Natural Product Research and Infection Biology (HKI), Friedrich Schiller University, Beutenbergstrasse 11a, 07745 Jena, Germany.

² Department of Molecular and Applied Microbiology, Leibniz Institute for Natural Product Research and Infection Biology (HKI), Jena, Germany.

³ Research Group Systems Biology/Bioinformatics, Leibniz Institute for Natural Product Research and Infection Biology - Hans Knöll Institute, Jena, Germany.

⁴ Microbiology and Molecular Biology, Friedrich Schiller University Jena, Germany.

*E-mail: dirk.hoffmeister@leibniz-hki.de, Friedrich Schiller University, Pharmaceutical Microbiology, Beutenbergstrasse 11a, 07745 Jena, Germany.

Table of contents

Figure S1: <i>S. lacrymans</i> atromentin cluster and pigment structures.....	3
Figure S2: Co-incubation plate pictures.....	4
Figure S3: HPLC profiles of <i>in vitro</i> atromentin production.....	5
Figure S4: HPLC profile of authentic atromentin standard.....	6
Figure S5: SDS-PAGE gels of NPS3 and PptA.....	7
Table S1: High-resolution mass spectrometry of pigments.....	8
Table S2: Bioactivity assays of pigments.....	9
Table S3: qRT-PCR primers.....	10
Table S4: Quinone synthetase cluster MEME motifs.....	12
Table S5: Negative training set for MEME search.....	13
Table S6: Genes used for MEME search.....	14
Methods: Characterization of NPS3.....	15
Methods: Antimicrobial bioactivity assays.....	15
References.....	17

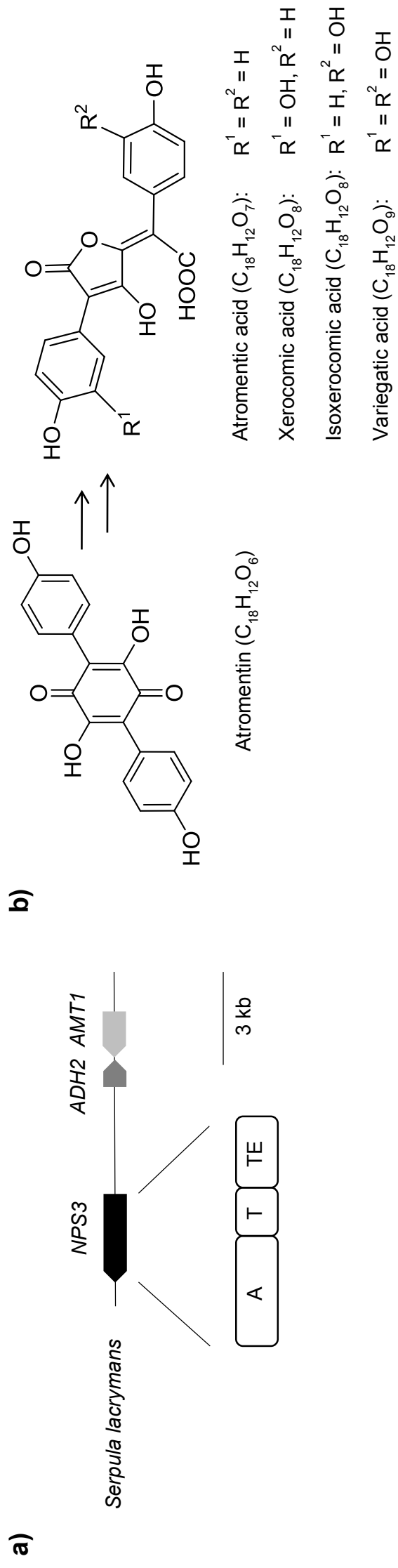


Figure S1: a) The atromentin gene cluster from *S. lacrymans*. Black: quinone (atromentin) synthetase gene (*NPS3*); dark grey: dehydrogenase gene (*ADH2*); light grey: aminotransferase gene (*AMT1*). Arrows indicate genes in their respective transcriptional direction (introns not shown). The domain architecture of the quinone synthetase is indicated below *NPS3*, and the *NPS3* domain order is shown in opposite direction to the transcriptional orientation of the gene. Domain abbreviations: A = adenylation, T = thiolation, TE = thioesterase domain. **b)** Chemical structure of atromentin and its follow-up products atromentic, xerocomic, isoxerocomic and variegatic acid (Gill and Steglich, 1987; Eastwood *et al.*, 2011).

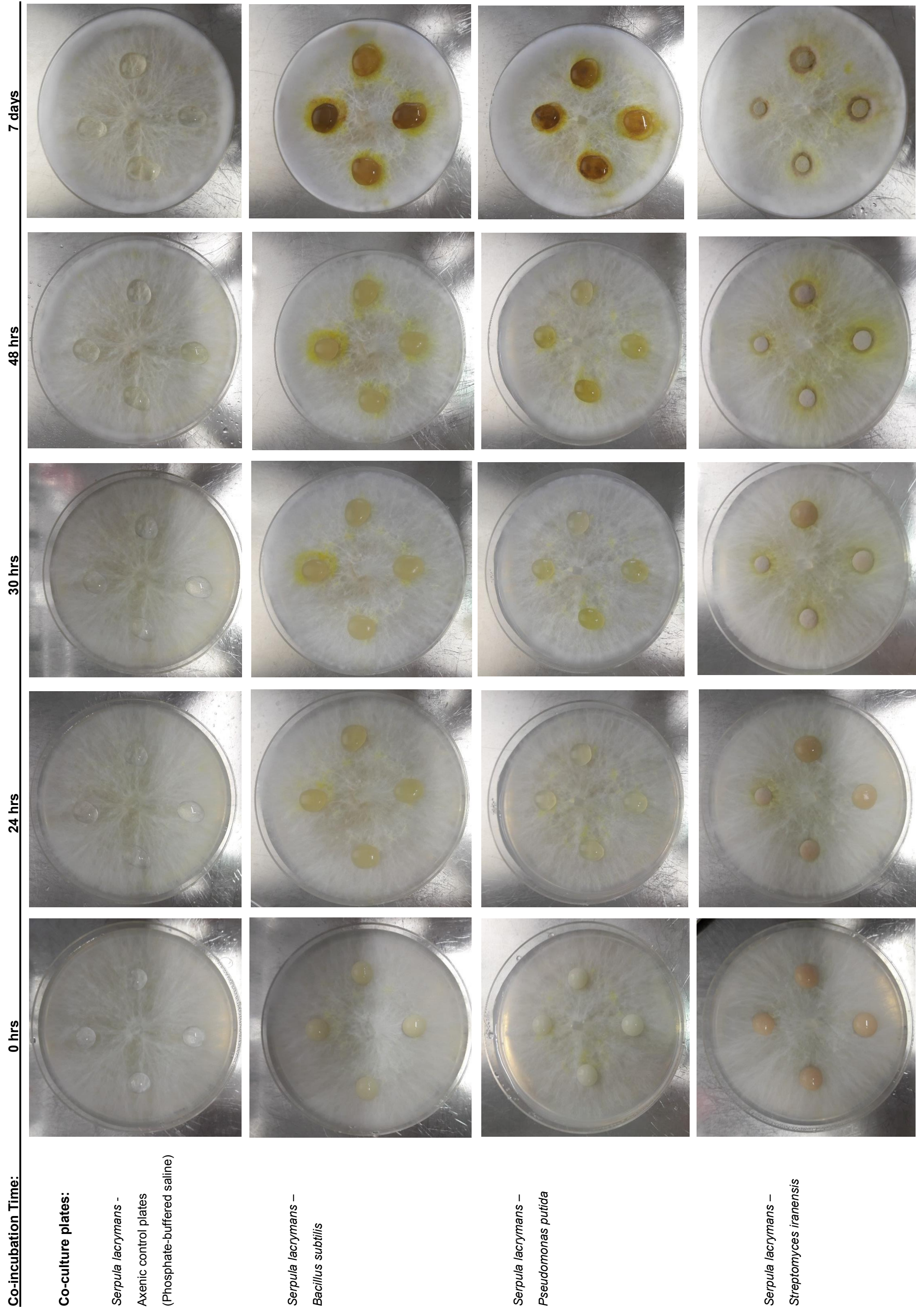


Figure S2: Pictures of *Serpula lacrymans* – bacterium co-cultures taken over time which correspond to time points for qRT-PCR and pigment quantification analyses. Pigmentation was observed around bacterial inocula.

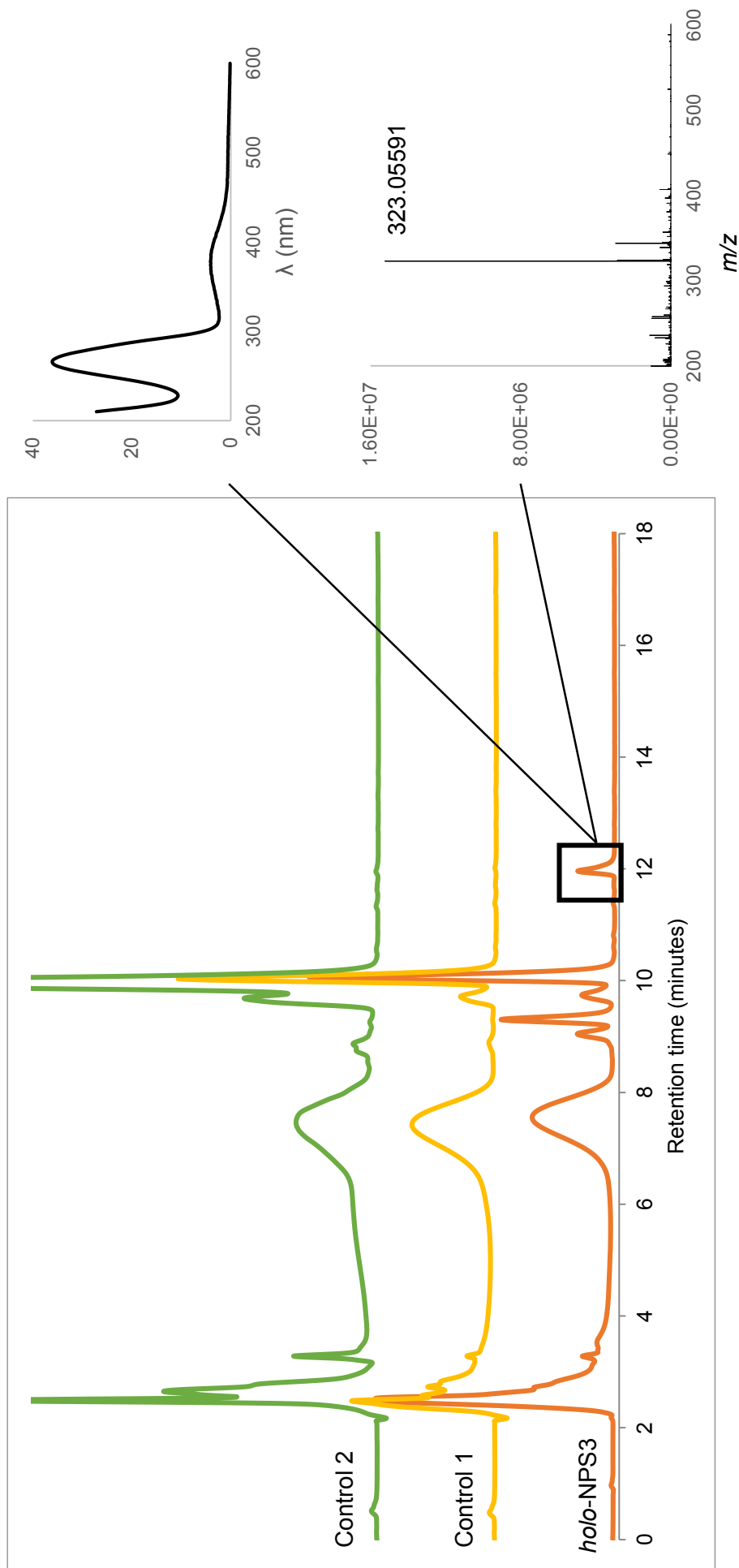


Figure S3: HPLC profiles ($\lambda = 254$ nm) showing *in vitro* atromentin production ($t_R = 11.9$ minutes) when *holo*-NPS3 (quinone synthetase from *S. lacrymans*) was incubated for 24 hours with 4-hydroxyphenylpyruvic acid as substrate. Atromentin was first identified by its characteristic UV/Vis spectrum and then by high-resolution mass spectrometry as shown next to the HPLC profiles. Authentic standards, analyzed similarly, are shown in Figure S4 (below). Controls included 1) heat-denatured NPS3, and 2) a reaction without ATP. The mass $[M-H]^-$ for atromentin from high-resolution mass spectrometry was found in the full reaction and was not observed in the control reactions.

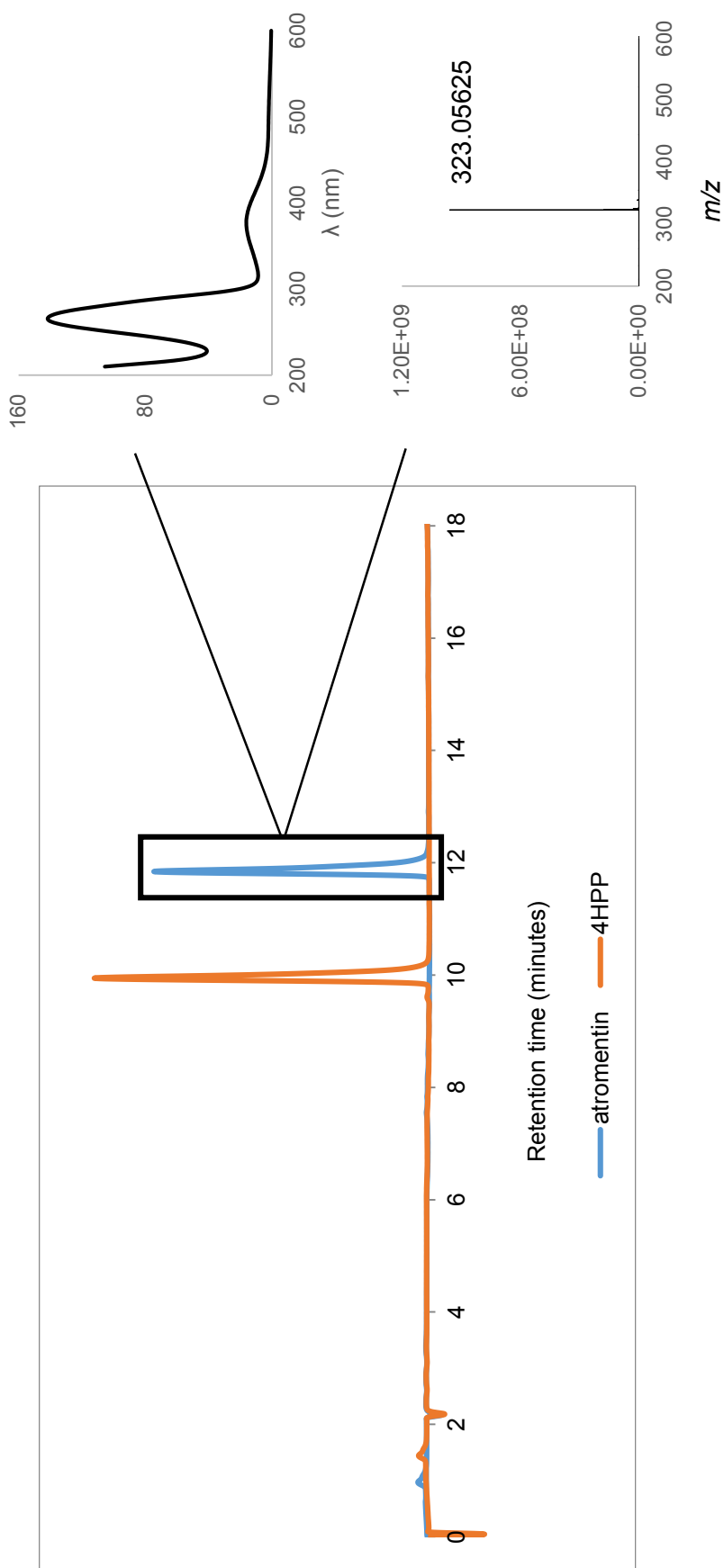


Figure S4: Overlaid HPLC profiles ($\lambda = 254$ nm) showing an authentic atromentin standard ($t_R = 11.9$ minutes) and an authentic 4-hydroxyphenylpyruvic acid (4HPP) standard ($t_R = 10.0$ minutes). The atromentin standard was also analyzed by high-resolution mass spectrometry as shown next to the HPLC profiles.

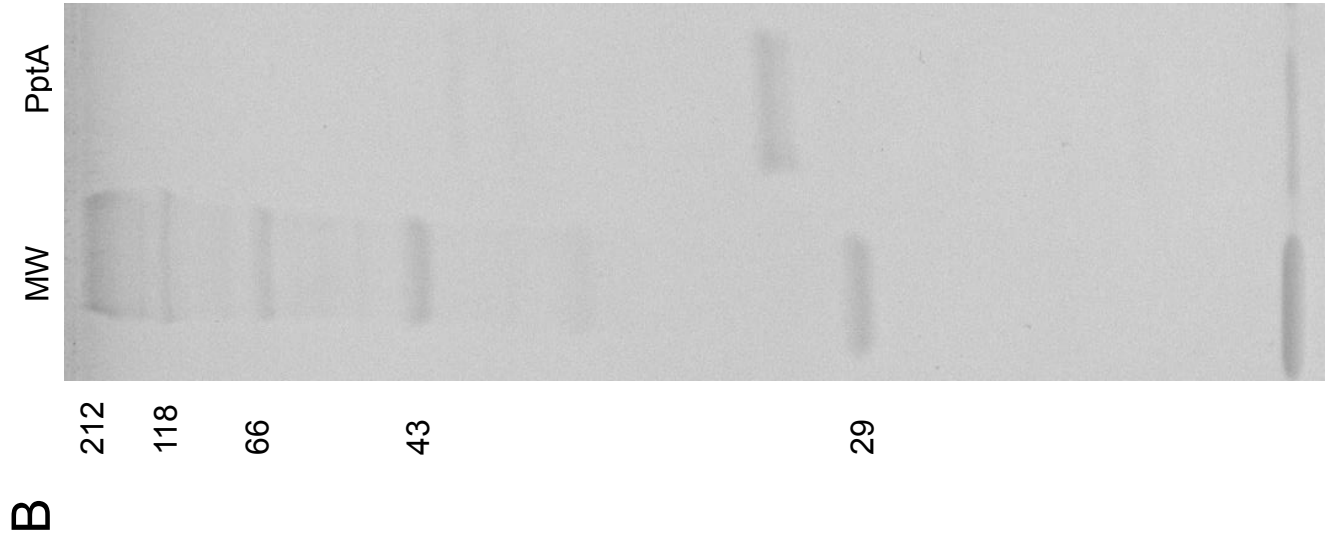
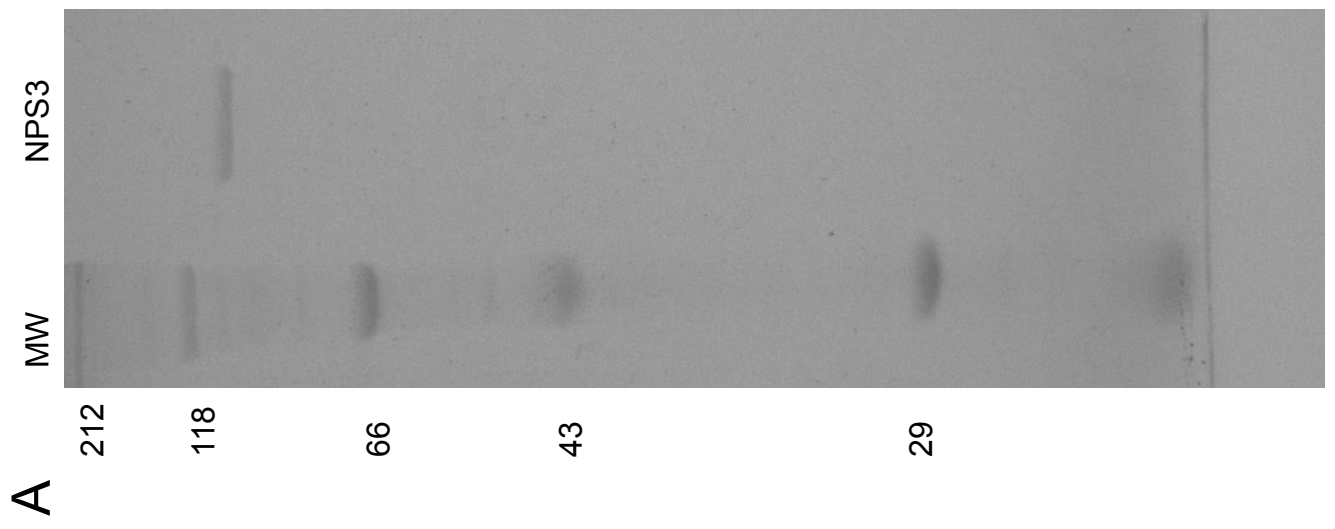


Figure S5: 12% SDS-PAGE gels stained with coomassie blue. A) NPS3 was a 108 kDa hexahistidine - quinone synthetase fusion protein and B) PptA was a 35 kDa hexahistidine - phosphopantetheinyl transferase fusion protein (Laemmli, 1970; Braesel *et al.*, 2015). The molecular weight standard "MW" is shown in kDa (Roti®-Mark Standard).

	Variegatic acid	Xerocomic acid	Isoxerocomic acid	Atromentic acid	Atromentin
S. lacrymans - B. subtilis	371.0403	355.0455	355.0456	339.0506	323.0567
S. lacrymans - P. putida	371.0412	355.0464	355.0465	339.0514	323.0571
S. lacrymans - S. iranensis	371.0403	355.0456	355.0456	339.0505	323.0559
Authentic standard	371.0405	355.0461	355.0459	339.0511	323.0563
Calculated	371.0409	355.0459	355.0459	339.0510	323.0560

Table S1: Masses [m/z, M-H]⁻ of *S. lacrymans* pigments detected by high-resolution electrospray mass spectrometry in co-incubation samples taken after 7 days after co-incubation. All sought pigments were identifiable in each co-culture by UV/Vis and mass spectra. Atromentin was found in trace amounts by high-resolution mass spectrometry.

Compound	Concentration	Organism	<i>Bacillus subtilis</i>	<i>Staphylococcus aureus</i>	<i>Escherichia coli</i>	<i>Pseudomonas aeruginosa</i> (B7)	<i>Pseudomonas aeruginosa</i> (B9)	<i>Staphylococcus aureus</i> (MRSA)	<i>Enterococcus faecalis</i> (VRE)	<i>Mycobacterium vaccae</i>	<i>Sporobolomyces salmonicolor</i>	<i>Candida albicans</i>	<i>Penicillium notatum</i>
Variagatic acid	1000 µg ml ⁻¹	0	0	0	0	0	0	0	0	0	0	0	0
Xerocomic acid	1000 µg ml ⁻¹	0	0	0	0	0	0	0	0	0	0	0	0
Atromentic acid	1000 µg ml ⁻¹	11 ^a	11	0	0	0	10	01 ^d	0	0	0	0	0
Ciprofloxacin	5 µg ml ⁻¹	31	19	24/31 ^b	26	28/36 ^b	0	18 ^c	20 ^b	-	-	-	-
Amphotericin B	10 µg ml ⁻¹	-	-	-	-	-	-	-	-	-	18 ^b	21	18 ^b
Methanol	-	0	0	0	0	0	0	0	0	0	10	0	10

^a some small single colonies; ^b lightly transparent; ^c strong growth on circumference; ^d colony count unclear; MRSA: Methicillin-resistant *Staphylococcus aureus*; VRE: Vancomycin-resistant enterococci

Table S2: Antimicrobial tests by the disk diffusion assay using isolated pigments variagatic, xerocomic, and atromentic acid. Given values are the diameter (mm) of the zone of inhibition.

Gene	JGI Protein ID	Primer sequence (5'-3')	Amplicon (bp)	Primer efficiency (%)
<i>NPS1</i>	417672	ACAGTTGGTGTCTAGGGACG	105	101
		TTGCATGAGAGACGGACTCG		
<i>NPS2</i>	413432	ACAGTCTTGTGCGGAACGTCCG	99	90
		GACATCCTCCACATCATCAGGC		
<i>NPS3</i>	416588	CAGTAGTGCACTCACC	98	98
		CCCGACCCAATTGAGAACATTC		
<i>NPS4</i>	1088337	CATGAGCCCTTCTAGTTCCACG	102	96
		ATGGTTGTGTGCCAGTAGGC		
<i>NPS5</i>	448228	TGCCCGTTCGATATCCTTTGG	101	103
		CACCCATTTGCTACAAGTGC		
<i>NPS6</i>	412786	ACAACCAATATCCCTCCGCC	104	94
		TACACGGTGCCTAGCTTAGG		
<i>NPS7</i>	416428	AAGCTTCAGTCAGGCTACGG	101	95
		TTACCCAAGGTCGTTGGTCCG		
<i>NPS8</i>	417281	GGAGATCGTCTGTACAAGTCCG	100	97
		GTCCTCTAAGCTTGATCTGGCG		
<i>NPS9</i>	450936	TCGGACATCAATGCCATCCC	98	93
		ACATCTGTTGCCAGTACG		
<i>NPS10</i>	448571	CGATAATGACGAACGGTGCC	98	94
		TGATCCCAATCCACCTGTCCG		
<i>NPS11</i>	453044	CCAGTTGCCAAAGGAGTTGTG	98	90
		ATTACTGGAGGAGGCTTCCG		
<i>NPS12</i>	453045	TAGGGGACGCACTGATACGA	100	106
		GCGCTGATTGCCTTCTGTTC		
<i>NPS13</i>	416666	CGCGCTTTACTTGAAGACCC	96	90
		GAACAGCGTGATCGGATTGG		
<i>NPS14</i>	416668	CGCCCAAAGTTTTCGTCTAGC	100	98
		ACAAGTTTGCCGACATCGC		
<i>NPS15</i>	416652	GATTTCCAAGCTGCGACACG	102	92
		GAACAACCTGAGCCATGCCG		
<i>NPS16</i>	1094026	CTTGTGGTGCCCAAAGATCG	97	108
		TGATGCGATAGTCCCAACCG		
<i>NPS17</i>	1093588	ACCTTGCGGGAGTTATTGTCC	102	90
		ACGACATAAGCTGTAGAGCCC		
<i>NPS18</i>	1214913	ACCAGTTGGTGACAGTACGC	103	93
		AAGGTCGGCAAAGACAGTGG		
<i>PKS1</i>	414545	TTCGCGGTTGGATGGATACC	100	98
		AATGCGTCGACCGAGTAAGG		
<i>PKS2</i>	418634	ATGGCAGCCCTGATTGAACC	95	105
		TCGGTGAGATGTTGGAAGGC		
<i>PKS3</i>	443694	TCAAGTTCTGGCATAGGCGG	105	98
		AGGTATGCCGAAAGGGTTGG		
<i>PKS4</i>	411735	TCAAGTAGCAGAGCCCAAGC	103	101
		ACCTGCAGCAATAGAGAGCC		
<i>PKS5</i>	443759	GAAGCCCGTTCATCTTACG	97	110

		TGGGCAAAGGACTTTCCAGG		
<i>PKS6</i>	1095944	TACGGTTCCTTGATGGGCAGG	105	110
		ACGCTGCTATCCGACTTTCC		
<i>AMT1</i>	356993	GCTGTTCCGGACATTGTTGG	96	94
		ATGCAATCTCCCGATGGTGG		
<i>ADH2</i>	471907	TGGGACTTATCGCTCTCTGC	98	94
		CGATAGCATCACGTATGGGC		
<i>GLY1</i>	371376	GCGGTTGATTGTGGTACTGG	98	91
		ACGGTGCAGTTATCGATGGG		
β - tubulin gene	1063468	TACCGAGCTGTCACTGTTCC	96	96
		AGTCAAGTAACGACCGTGCC		

Table S3: qRT-PCR primers used and the respective amplicon length and determined primer efficiency. Primers were created in NCBI Primer-BLAST and ordered HPSF® from Eurofins (Ye *et al.*, 2012).

Basidiomycete	Gene	Position	P -value	Motif
<i>Serpula lacrymans</i>	NPS3	230	1.98e-5	CTC GTAT CTCC
<i>Serpula lacrymans</i>	AMT1	76	2.18e-5	TT CGTTT CTCC
<i>Paxillus involutus</i>	InvA5	922	2.33e-7	TT CGGAT CTCC
<i>Paxillus involutus</i>	InvA2	913	2.32e-7	TT CGGAT CTCC
<i>Paxillus involutus</i>	AMT	162	1.13e-5	TT CGGATCTGA
<i>Paxillus ammoniavirescens</i>	NPS	738	2.33e-7	TT CGGAT CTCC
<i>Paxillus ammoniavirescens</i>	AMT	653	2.87e-5	T CGGAT CGGC
<i>Paxillus adelphus</i>	NPS	486	2.32e-7	TT CGGAT CTCC
<i>Paxillus adelphus</i>	AMT	933	2.87e-5	T CGGAT CGGC
<i>Hydnomerulius pinastris</i>	NPS	906	2.32e-7	TT CGGAT CTCC
<i>Hydnomerulius pinastris</i>	AMT	864	3.20e-5	TT ACATCTTA
<i>Suillus brevipes</i>	NPS	1393	9.29e-7	T CGGAT CTCC
<i>Suillus brevipes</i>	AMT	653	4.39e-5	TT ACAT CGTC
<i>Suillus decipiens</i>	NPS	346	2.18e-5	T CGACAT CTTC
<i>Suillus decipiens</i>	AMT	435	4.81e-5	GTCGTATCTCA
<i>Suillus luteus</i>	NPS	889	1.04e-4	CTCGGAC CTCC
<i>Suillus luteus</i>	AMT	228	7.63e-6	TT CCAT CTCC
<i>Tapinella panuoides</i>	AtrA	886	2.61e-6	TT CGCAT CTTC
<i>Tapinella panuoides</i>	AtrD	986	7.07e-7	TT CGTAT CTCC
<i>Coniophora puteana</i>	NPS	674	1.12e-4	ATCGAAA CTCC
<i>Coniophora puteana</i>	AMT	986	4.76e-7	TT CGTAT CTCC
<i>Omphalotus olearius</i>	NPS	98	2.61e-6	TT CGTAT CTTC
<i>Omphalotus olearius</i>	AMT	534	5.39e-5	TT GGCAT CTCA
<i>Suillus grevillei</i>	GreA	538	1.64e-5	AGCGTAT CTCC
<i>Thelephora ganbajun</i>	NPS	588	3.31e-6	T CGCAT CTCC

Table S4: Promoter motifs extracted from MEME analyses, the coordinate of the motif, and P-value.

Non-secondary metabolite genes (<i>S. lacrymans</i> S7.9, v.2.0):			
Protein ID	Gene name	Gene coordinates	Promoter coordinates
1098786	Chitin synthase	scaffold_6:1287507-1290783 (-)	scaffold_6:1290783-1291783
1206485	Histone H5	scaffold_11:1637330-1638334 (-)	scaffold_11:1638334-1639334
1058563	Electron transfer flavoprotein, alpha subunit	scaffold_6:1195248-1196456 (-)	scaffold_6:1196456-1197456
1165886	Heat shock protein Hsp70	scaffold_5:1045460-1048364 (-)	scaffold_5:1048364-1049364
1192330	Tubulin	scaffold_11:1002406-1004266 (-)	scaffold_11:1004266-1005266
348978	F-actin capping protein, beta subunit	scaffold_7:819546-820861 (-)	scaffold_7:820861-821861
1079209	Actin-crosslinking proteins	scaffold_20:400161-401188 (-)	scaffold_20:401188-402188
1078580	Actin	scaffold_16:735360-738232 (-)	scaffold_16:738232-739232
1052967	MAP kinase	scaffold_2:1584763-1586953 (-)	scaffold_2:1586953-1587953
1054175	Mitochondrial carrier protein	scaffold_4:337246-338895 (-)	scaffold_4:338895-339895
1056717	Subtilisin	scaffold_5:883357-885184 (-)	scaffold_5:885184-886184
1150264	20S proteasome	scaffold_9:1209323-1210408 (-)	scaffold_9:1210408-1211408
374513	Alpha-2-macroglobulin	scaffold_17:301468-304339 (-)	scaffold_17:304339-305339
1214606	Peptidase M50	scaffold_9:232490-235178 (-)	scaffold_9:235178-236178
1081449	3-isopropylmalate dehydratase	scaffold_4:1116202-1118998 (-)	scaffold_4:1118998-1119998
1086809	Citrate synthase	scaffold_12:1340995-1343453 (-)	scaffold_12:1343453-1344453
1151500	DNA repair metallo-beta-lactamase	scaffold_10:754086-755817 (-)	scaffold_10:755817-756817
1148027	DNA repair protein Rad4	scaffold_8:21058-24615 (-)	scaffold_8:24615-25615
1156455	Nucleotide excision repair, TFIIH	scaffold_15:756690-756963 (-)	scaffold_15:756963-757963
1183475	Cryptochrome/DNA photolyase	scaffold_4:2218845-2221349 (-)	scaffold_4:2221349-2222349

Non-cluster genes (2 upstream and 2 downstream the cluster):			
Gene coordinates	Promoter coordinates	Gene coordinates	Promoter coordinates
<i>S. lacrymans</i> S7.9 2.0			
scaffold_9:1431452-1433440	scaffold_9:1430452-1431452	scaffold_82:32162-35933	scaffold_82:31162-32162
scaffold_9:1428731-1429644	scaffold_9:1427731-1428731	scaffold_82:22111-22892	scaffold_82:22892-23892
scaffold_9:1448160-1450403	scaffold_9:1450403-1451403	scaffold_82:61262-66981	scaffold_82:60262-61262
scaffold_9:1446101-1446513	scaffold_9:1446513-1447513	scaffold_82:67691-68856	scaffold_82:66691-67691
<i>S. brevipes</i> v1.0			
scaffold_122:108744-112839	scaffold_122:107744-108744		
scaffold_122:56133-57344	scaffold_122:55133-56133		
scaffold_122:49063-50380	scaffold_122:50380-51380		
scaffold_122:86035-88164	scaffold_122:88164-89164		
scaffold_122:98646-99325	scaffold_122:97646-98646		
<i>P. involutus</i> ATCC 200175 v1.0			
scaffold_4:1403843-1404315	scaffold_4:1404315-1405315		
scaffold_4:1411790-1413998	scaffold_4:1410790-1411790		
scaffold_4:1380124-1380766	scaffold_4:1379124-1380124		
scaffold_4:1377552-1378790	scaffold_4:1376552-1377552		

Table S5: The genes and gene coordinates of the negative training set for the discriminative promoter search.

Basidiomycete	Protein ID		Gene coordinate		ADH	AMT	ADH	AMT
	NPS	ADH	NPS	ADH				
<i>Coniophora puteana</i> v1.0	170203	93972	scaffold_21:47600-51459(-)	scaffold_21:52391-53630(+)	140570	scaffold_21:55211-57220(-)	scaffold_21:55211-57220(-)	
<i>Hydnomerulius pinastri</i> v2.0	94475	94432	scaffold_21:398761-401852(+)	scaffold_21:391733-392908(-)	114625	scaffold_21:386284-388338(+)	scaffold_21:386284-388338(+)	
<i>Omphalotus olearius</i>	7676	7677	scaffold_82:36148-44476(-)	scaffold_82:46163-47346(+)	7681	scaffold_82:54328-56331(-)	scaffold_82:54328-56331(-)	
<i>Paxillus adelphus</i> Ve08.2h10 v2.0	23383	821933	scaffold_222:85273-86334(+)	scaffold_222:76200-77734(-)	821937	scaffold_222:70807-72863(+)	scaffold_222:70807-72863(+)	
<i>Paxillus ammoniavirescens</i> Pou09.2 v1.0	1012486	970378	scaffold_85:67638-70717(+)	scaffold_85:58505-60116(-)	953843	scaffold_85:53336-55097(+)	scaffold_85:53336-55097(+)	
<i>Paxillus involutus</i> ATCC 200175 v1.0	69019	8109	scaffold_4:1399630-1402710(+)	scaffold_4:1390567-1391793-	166727	scaffold_4:1385207-1387249+	scaffold_4:1385207-1387249+	
<i>Serpula lacrymans</i> S7.9 2.0	416588	471907	scaffold_9:1433688-1437022-	scaffold_9:1440388-1441815+	356993	scaffold_9:1441797-1444197-	scaffold_9:1441797-1444197-	
<i>Suillus brevipes</i> v1.0	783497	836870	scaffold_122:66458-69798	scaffold_122:63510-64935(-)	783492	scaffold_122:60330-62635(+)	scaffold_122:60330-62635(+)	
<i>Suillus decipiens</i> EM49 v1.0	1233902	1059129	scaffold_105:118261-121763(-)	scaffold_105:131025-132297(+)	1233904	scaffold_105:133143-135526(-)	scaffold_105:133143-135526(-)	
<i>Suillus grevillei</i>	AFB76152.1, JQ681152.1	-	-	-	-	-	-	
<i>Suillus luteus</i> UH-Slu-Lm8-n1 v2.0	18055	812044	scaffold_30:261590-264729	scaffold_30:254560-256029	812043	scaffold_30:251969-254433	scaffold_30:251969-254433	
<i>Tapinella panuoides</i>	ACH90386.1, EU711405.1	ACH90386.1, EU711405.1	-	-	ACH90387.1, EU711406.1	-	-	
<i>Thelephora gambajun</i> P2 v1.0	3155672	2211506	scaffold_51:28656-31706(-)	scaffold_51:24502-26379 +	-	-	-	

Table S6: Basidiomycetes used for the promoter motif analyses. Genes were extracted from JGI MycoCosm or from cosmid libraries, and shown here are their respective JGI Protein IDs and coordinates.

NPS: quinone synthetase; ADH: alcohol dehydrogenase/zinc binding oxidoreductase; AMT: aminotransferase.

Supplemental Methods

Characterization of NPS3 - *NPS3* of *S. lacrymans* was amplified from cDNA using Phusion DNA polymerase (NEB) with primers 5'-GCTAGCATGGCCCCAGCCCCGAC-3' and 5'-AAGCTTCTAAACTCCACGGGCTTCAAGAC-3' following the manufacturer's instructions by 30 cycles of 98°C for 10 seconds, 69°C for 15 seconds and 72°C for 3 minutes. The amplicon was ligated into pJET1.2 and subsequently into expression vector pRSETb via NheI and HindIII. Accurate amplification was verified by DNA sequencing. Gene overexpression was done in *E. coli* SoluBL for *NPS3* and *E. coli* KRX for *Paxillus involutus pptA* (Braesel *et al.*, 2015) from induction by 500 µM IPTG or 0.1% L-rhamnose (final concentrations), respectively, at OD₆₀₀ 0.7-0.8. After overnight induction at 16°C, the protein was purified from the soluble fraction (taken by discontinuous sonication on ice) on an FPLC instrument (Äkta pure, GE Healthcare) equipped with a HisTrap FF crude (1 ml) column using an imidazole gradient. The eluted protein fraction was checked on a 12% SDS-PAGE gel (Laemmli, 1970; Figure S5). The protein fraction was re-buffered using a PD-10 column and the *in vitro* assay was done similar to previous work (Braesel *et al.*, 2015): *NPS3* was primed using phosphopantetheinyl transferase PptA (0.5 µM each) and 120 µM coenzyme A. Then for atromentin production, the *NPS3*-PptA mixture (0.5 µM each) was incubated in a final 500 µl reaction composed of: 75 mM Tris-HCl buffer (pH 7.4), 5 mM MgCl₂, 125 nM EDTA, 2.5 mM ATP, and 2 mM 4-hydroxyphenylpyruvic acid. The reaction was incubated at 25°C for 24 hours. Two separate reactions per condition were lyophilized, resuspended in 200 µl MeOH, filtered, and 50 µl analyzed by HPLC (see above). Negative controls included a reaction without ATP and one with heat-denatured *NPS3*. The experiments were independently done twice.

Antimicrobial bioactivity assays - Antimicrobial tests by the disk diffusion method for variegatic, xerocomic, and atromentic acid (as used for chromatogram standards) were carried out using Jena Microbial Resource Collection (JMRC) strains *Bacillus subtilis* (6633 B1), *Staphylococcus aureus* (511 B3 and MRSA 134/93 R9), *Escherichia coli* (458 B4), *Pseudomonas aeruginosa* (SG 137 B7 and K799/61 B9), VRE *Enterococcus faecalis* (1528

R10), *Mycobacterium vaccae* (10670 M4), *Sporobolomyces salmonicolor* (549 H4), *Candida albicans* (H8), and *Penicillium notatum* (JP36 P1). Pigments were resuspended in methanol to a testing concentration of 1000 $\mu\text{g ml}^{-1}$ and 50 μl applied. Methanol was used as a negative control and ciprofloxacin (5 $\mu\text{g ml}^{-1}$) and amphotericin B (DMSO/MeOH at 10 $\mu\text{g ml}^{-1}$) as positive controls. Methodology was in accordance with the National Committee for Clinical Laboratory Standards.

References

- Braesel, J., Götze, S., Shah, F., Heine, D., Tauber, J., Hertweck, C., and Hoffmeister, D. (2015) Three Redundant Synthetases Secure Redox-Active Pigment Production in the Basidiomycete *Paxillus involutus*. *Chem Biol* **22**: 1325-1334.
- Eastwood, D.C., Floudas, D., Binder, M., Majcherczyk, A., Schneider, P., Aerts, A., *et al.* (2011) The plant cell wall-decomposing machinery underlies the functional diversity of forest fungi. *Science* **333**: 762-765.
- Gill, M., and Steglich, W. (1987) Pigments of fungi (Macromycetes). *Prog Chem Org Nat Prod* **51**: 1-317.
- Laemmli U. K. (1970) Cleavage of structural protein during the assembly of the head of bacteriophage T4. *Nature* **227**: 680–685.
- Methods for dilution antimicrobial susceptibility tests for bacteria that grow aerobically, Approved Standard, 4th ed.; Clinical and Laboratory Standards Institute: Wayne, PA, 2006; Vol. 26.
- Ye, J., Coulouris, G., Zaretskaya, I., Cutcutache, I., Rozen, S., and Madden, T.L. (2012) Primer-BLAST: a tool to design target-specific primers for polymerase chain reaction. *BMC Bioinformatics* **13**: 134.

2.4. Dissimilar pigment regulation in *Serpula lacrymans* and *Paxillus involutus* during inter-kingdom interactions

Tauber, J.P., Gallegos-Monterrosa, R., Kovács, Á.T., Shelest, E., and Hoffmeister, D.

Accepted. Presented here is the accepted version that required minimal edits.

Microbiology. (2017)

Summary and importance

This work was an extension of our previous work (manuscript, 2.3.). Here, pigmentation in *S. lacrymans* was stimulated by 13 different bacteria and cell-wall damaging enzymes (lytic enzymes and proteases). Conversely, no significant pigmentation by bacteria was observed from the taxonomically related, ectomycorrhiza-forming fungus, *P. involutus*. We found additional lifestyle-dependent promoter motifs preceding atromentin synthetase genes in ectomycorrhiza-forming basidiomycetes. Variegatic acid and its precursor xerocomic acid, but not involutin, inhibited swarming and biofilm formation of *Bacillus subtilis* but did not kill *B. subtilis*. This work provided new bioactivities of microbial-induced, community-influencing basidiomycete natural products. The conserved motifs further highlighted conserved genetic regulation of a basidiomycete natural product gene cluster that will assist in

future studies to determine global regulators, signaling pathways and associated transcription factors of basidiomycetes.

Contribution to the manuscript

James Tauber contributed to the manuscript by designing (with the help of others) and executing most wet laboratory work followed by analyses of data. This included microbiological culturing; compound extractions and chromatography; compound isolation and analyses; and genetic extractions and qRT-PCR. The other main part of the work, the bioinformatic analyses and biofilm/swarming assays, as well as additional planning of the work, was done by the other authors. James Tauber helped design and participated in bioinformatic work. James Tauber wrote the majority of the manuscript (main text and supplement), including making three-and-a-half of the five main figures, and five of the eight supplemental figures.

Dissimilar pigment regulation in *Serpula lacrymans* and *Paxillus involutus* during inter-kingdom interactions

James P. Tauber,¹ Ramses Gallegos-Monterrosa,² Ákos T. Kovács,^{2,3} Ekaterina Shelest^{4†} and Dirk Hoffmeister^{1,*}

Abstract

Production of basidiomycete atromentin-derived pigments like variegatic acid (pulvinic acid-type) and involutin (diarylcylopentenone) from the brown-rotter *Serpula lacrymans* and the ectomycorrhiza-forming *Paxillus involutus*, respectively, is induced by complex nutrition, and in the case of *S. lacrymans*, bacteria. Pigmentation in *S. lacrymans* was stimulated by 13 different bacteria and cell-wall-damaging enzymes (lytic enzymes and proteases), but not by lysozyme or mechanical damage. The use of protease inhibitors with *Bacillus subtilis* or heat-killed bacteria during co-culturing with *S. lacrymans* significantly reduced pigmentation indicating that enzymatic hyphal damage and/or released peptides, rather than mechanical injury, was the major cause of systemic pigment induction. Conversely, no significant pigmentation by bacteria was observed from *P. involutus*. We found additional putative transcriptional composite elements of atromentin synthetase genes in *P. involutus* and other ectomycorrhiza-forming species that were absent from *S. lacrymans* and other brown-rotters. Variegatic and its precursor xerocomic acid, but not involutin, in return inhibited swarming and colony biofilm spreading of *Bacillus subtilis*, but did not kill *B. subtilis*. We suggest that dissimilar pigment regulation by fungal lifestyle was a consequence of pigment bioactivity and additional promoter motifs. The focus on basidiomycete natural product gene induction and regulation will assist in future studies to determine global regulators, signalling pathways and associated transcription factors of basidiomycetes.

INTRODUCTION

Basidiomycetes play a critical role in element cycling and lignocellulose disintegration, yet they have also entered the spotlight for their unprecedented capacity to make an array of natural products. These small and often highly functionalized molecules may serve local or global processes (e.g. defence or carbon cycling, respectively). The terphenylquinone atromentin is a widespread pigment and precursor to numerous compounds depending on the cleavage of the benzoquinone ring and subsequent various modifications (Fig. 1; [1, 2]). Atromentin-derived compounds, variegatic acid from *Serpula lacrymans* and involutin from *Paxillus involutus*, were inducible under nutritional cues, and *in vitro* evidence identified them as Fe³⁺-reductants in Fenton chemistry for lignocellulose degradation, thus highlighting their involvement in carbon cycling [3, 4]. The brown-rotter *S. lacrymans* and the ectomycorrhiza-forming *P. involutus*

are taxonomically related (*Boletales*), but live different lifestyles. The former is recognized as an economic burden because it degrades timber whereas *P. involutus* is an important symbiont that promotes tree health by nutrient exchange [5–7].

We previously reported that the enzymes involved in the production of atromentin are encoded within a cluster that is widely orthologous in basidiomycetes, and the promoters of the two essential genes (encoding an atromentin/quinone synthetase and aminotransferase) have a conserved genetic promoter motif [8–10]. Additionally, three fungal–bacterial co-incubations led to gene cluster induction and subsequent pigment accumulation in the model *S. lacrymans* [9]. Here, using both *S. lacrymans* and *P. involutus*, we expanded our understanding of atromentin-derived pigments and its regulation during co-incubation with bacteria. We questioned (i) how universal pigment induction was in *S. lacrymans*

Received 16 August 2017; Accepted 16 November 2017

Author affiliations: ¹Department of Pharmaceutical Microbiology at the Hans Knöll Institute, Friedrich-Schiller-University, Winzerlaer Str. 2, 07745 Jena, Germany; ²Terrestrial Biofilms Group, Institute of Microbiology, Friedrich Schiller University, Neugasse 23, 07743 Jena, Germany; ³Bacterial Interactions and Evolution Group, Department of Biotechnology and Biomedicine, Technical University of Denmark, Anker Engelunds Vej, 2800 Kgs. Lyngby, Denmark; ⁴Research Group Systems Biology/Bioinformatics, Leibniz Institute for Natural Product Research and Infection Biology - Hans Knöll Institute, Beutenbergstr. 11a, 07745 Jena, Germany.

***Correspondence:** Dirk Hoffmeister, dirk.hoffmeister@leibniz-hki.de or dirk.hoffmeister@hki-jena.de

Keywords: basidiomycetes; natural products; biofilms; promoters; transcriptional regulation.

Abbreviations: HPLC, high performance liquid chromatography; MEP, malt extract peptone; MEME, Multiple Em for Motif Elicitation.

†Present address: German Centre for Integrative Biodiversity Research (iDiv), Deutscher Platz 5e, 04103 Leipzig, Germany.

Supplementary material is available with the online version of this article.

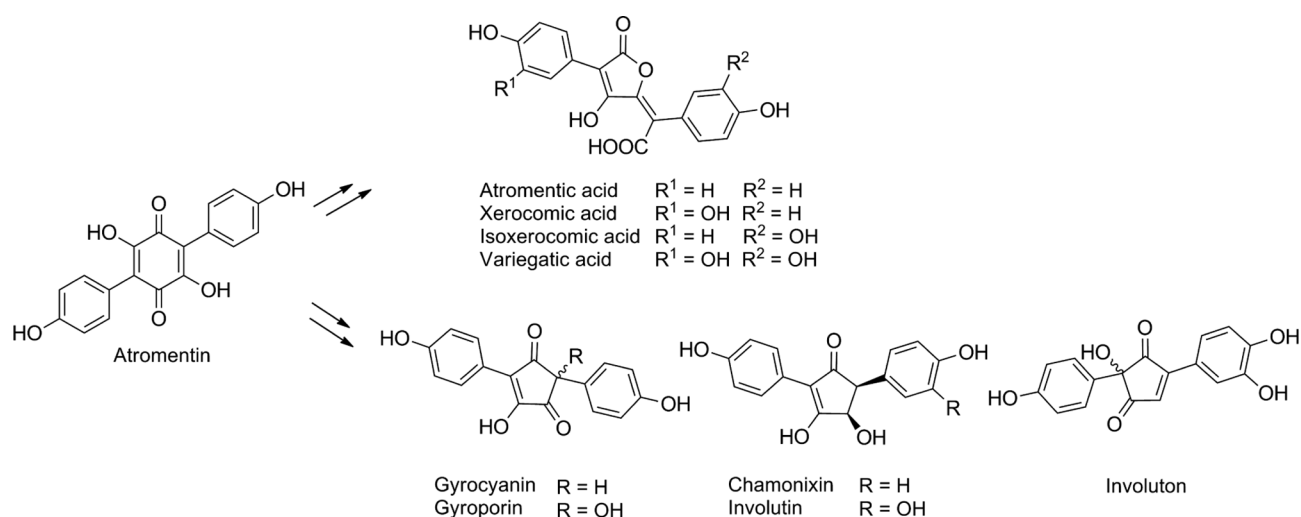


Fig. 1. Chemical structures of atromentin and congener pigments.

and whether related fungal species that follow a different lifestyle would be similarly stimulated; (ii) what the underlying eliciting factor was; and (iii) what local function the pigments might have during co-incubation. We show that although pigmentation by bacteria appeared ubiquitous in *S. lacrymans*, this was not the case in *P. involutus*, and that certain pigments from *S. lacrymans* impacted biofilm spreading and swarming motility.

METHODS

Organisms and growth conditions

For *Serpula lacrymans* S7.9 [3] co-incubations, we followed a published protocol with some modifications [9]. A synthetic medium agar plug containing *S. lacrymans* mycelium was inoculated atop a fresh synthetic agar plate (KH_2PO_4 500 mg l^{-1} , NH_4Cl 200 mg l^{-1} , $MgSO_4 \times 7 H_2O$ 150 mg l^{-1} , $CaCl_2 \times 2 H_2O$ 50 mg l^{-1} , $NaCl$ 25 mg l^{-1} , $FeCl_3 \times 6 H_2O$ 12 mg l^{-1} , Thiamin 1 mg l^{-1} , D-glucose monohydrate 5 g l^{-1} , 1.8% w/v agar, pH 5.6 by NaOH) and grown axenically for 13–14 days at ambient temperature. For all bacteria except *B. subtilis* to be inoculated atop the fungus, an overnight culture from a 25% glycerol stock was grown in LB (tryptone 10 g l^{-1} , yeast extract 5 g l^{-1} , $NaCl$ 5 g l^{-1}) or German Collection of Microorganisms and Cell Culture M79-Medium 426 (D-glucose monohydrate 10 g l^{-1} , bacto peptone 10 g l^{-1} , casamino acids 2 g l^{-1} , yeast extract 2 g l^{-1} , $NaCl$ 6 g l^{-1} , pH 7.8) with agitation at 28 °C. The culture was pelleted, washed three times with autoclaved water in 50 ml tubes and resuspended in water to make a 200-fold concentrate from the initial culture. Two 500 μ l and two 250 μ l droplets were then added atop a fungal mycelial bed which started the co-incubation. *B. subtilis* 3610 was grown in LB with agitation at 37 °C and concentrated 100-fold. For *B. subtilis*, rinsed and suspended bacteria were split and

tested under three conditions: (i) as is, with ca. 3.8×10^9 c.f.u. per 250 μ l droplet; (ii) autoclaved; or (iii) incubated with one EDTA-free protease inhibitor cocktail tablet (Sigmafast, Sigma) before being introduced to the fungus. Separately, enzymatic damage to the fungus was performed. Here, two 500 μ l droplets (50 mg ml^{-1} solution in PBS) of lysing enzymes from *Trichoderma harzianum* (Sigma), proteases (from *Streptomyces griseus*, Sigma), or lysozyme from chicken egg white (Sigma) were inoculated atop the fungal mycelial bed. As controls, mechanical damage to the mycelia was carried out by scalpel wounding, and all cultures were run alongside water or PBS droplet controls. Co-cultures, enzymatic assay cultures or controls were run at ambient temperature in darkness in duplicates and repeated twice. Co-cultures were extracted after 7 days, *B. subtilis*-related co-cultures after 2 days, and enzymatic assays after 3 days. *O. olearius* [11] co-cultures with *B. subtilis* or *P. putida* were executed the same as for *S. lacrymans*, except cultures were extracted after 3 days of growth. Co-cultures of *Suillus bovinus* JMRC: SF013586 with *B. subtilis* were also performed as described for *S. lacrymans*, but using an 11-day-old axenic culture prior to adding *Bacillus*.

P. involutus ATCC 200175 [6] was grown at ambient temperature in darkness. For *P. involutus* co-culturing, conditions I–III (below) were tested, each based on established growth methodologies utilizing glass beads submerged in liquid media whereby the fungus remained stationary within the same petri dish, and liquid media can be exchanged [12–14].

Condition I: the fungus was grown axenically on 15 ml synthetic broth for 14 days. Then, 150 μ l pre-rinsed bacteria listed in Table 1 was spotted atop the mycelia (similar to above with *S. lacrymans*' co-culturing), and co-incubated for 3 days until extraction.

Table 1. Bacteria used in co-incubation experiments with *S. lacrymans* and *P. involutus*

Bacteria were obtained from previous works or the Jena Microbial Resource Collection.

Bacterium	Taxonomy	Strain/reference
<i>Bacillus subtilis</i> 3610*	Bacilli	[9]
<i>Lysinibacillus fusiformis</i> M5	Bacilli	[28]
<i>Streptomyces iranensis</i> *	Actinobacteria	[9]
<i>Arthrobacter</i> spp.	Actinobacteria	[59]
<i>Micrococcus luteus</i>	Micrococcales	[59]
<i>Acetobacter pasteurianus</i> subsp. <i>pasteurianus</i>	Alphaproteobacteria	ATCC 9433
<i>Sphingomonas</i> spp.	Alphaproteobacteria	ST027129
<i>Methylobacterium mesophilicum</i>	Alphaproteobacteria	ATCC 29983
<i>Pseudomonas putida</i> *	Gammaproteobacteria	[9]
<i>Escherichia coli</i> XL1-Blue	Gammaproteobacteria	Stratagene
<i>Pseudomonas tolaasii</i>	Gammaproteobacteria	[60]
<i>Pseudomonas fluorescens</i>	Gammaproteobacteria	[59]
<i>Acinetobacter</i> spp.	Gammaproteobacteria	[59]

*Indicated initial bacteria tested that set the basis for testing various other strains [9].

Condition II: the fungus was axenically grown for 9 days on 15 ml synthetic broth, whereby the broth was then discarded and the petri was replaced with fresh synthetic media. Then, 3 days later, soil-isolated bacteria, each set to an $OD_{600}=1.8$ by water from pelleted and rinsed bacterial pre-cultures, were inoculated (1 ml each or 1 ml from equally pre-mixed consortia) into the media and atop of the fungus. The co-culture was terminated after 7 days.

Condition III: an agar plug containing mycelium (mycelium facing aially) was placed atop glass beads submerged in 15 ml synthetic broth and the fungus grown for 9 days. Then, the broth was removed, the mycelia and beads washed with autoclaved dH_2O , and 15 ml synthetic broth without inorganic nitrogen was added. After 24 h, the broth was discarded from the N-starved fungal mycelia, and then introduced to 15 ml MEP (malt extract peptone medium; malt extract 30 g l^{-1} , soytone 3 g l^{-1}) amended with D-glucose monohydrate (5 g l^{-1}). The day before the onset of co-culturing, soil-isolated *Bacilli* (isolation described later) were grown overnight at 37°C with agitation (180 r.p.m.) in 400 ml LB and used as a seed culture in fresh LB, which was then grown to an $OD_{600}=0.20-0.25$. Then, 0.2 ml of bacteria suspension was added to the fungal MEP culture. For the bacterial consortia, 0.2 ml of each bacterium was added. As a negative control, 0.6 ml of blank LB was added to axenic fungal cultures. After 7 days, the conditioned broth was extracted for chromatography (below).

Soil samples for quantification and isolation

Soil was collected from directly underneath *P. involutus* mushrooms. 16S and 28S rDNA was amplified from the soil samples after gDNA nucleic acid extraction (cetyltrimethylammonium bromide and phenol:chloroform:isoamyl alcohol methodology), using taxonomic-specific or universal primers for bacteria, fungi, or archaea (detailed in Table S1

and Fig. S3; available in the online version of this article). Isolation of spore-forming bacteria from soil samples was performed by suspending 1 g wet soil samples in 10 ml PBS, incubating at 80°C for 15 min, creating a 1:10 dilution series using PBS, spreading $100\text{ }\mu\text{l}$ of the suspension onto MEP or synthetic agar, and incubating at 28°C or ambient temperature for up to 2 weeks until colony growth was observed. Bacteria were re-streaked until single colonies were isolated and chosen by distinct colony morphology. Colonies were grown in liquid LB or M79, and their 16S rDNA was sequenced using 27F and 1492R universal primers (Table S1, [15, 16]). Soil isolates were deposited at the Jena Microbial Resource Collection (Table S2).

Sequence collection and motif search

Sequence data were downloaded from the JGI MycoCosm portal [17]. A list of the 23 atromentin-producing species is provided in Fig. 4 [2, 3, 6, 11, 18, 19]. Promoter sequences of *Tapinella panuoides* and *Suillus grevillei* were collected from a cosmid library [2, 9, 10]. The promoter region was selected as $-1000/+2\text{ bp}$ around the transcription start site [20]. *De novo* motif prediction was performed by the MEME (Multiple Em for Motif Elicitation) software [21, 22]. The negative promoter set used for discriminative mode had been established and reapplied here [9]. In short, it contained 41 promoters including (i) promoters of genes flanking cluster regions, and (ii) promoters of non-secondary metabolite genes. The parameters for the MEME search were: motif length: 8–12 bp; and 0 or 1 motifs per sequence. Analyses were grouped as follows: (i) 23 fungi in total; (ii) ‘larger *Paxillus*’ and ‘*Serpula*’ groups; and (iii) within the ‘*Paxillaceae*.’ The generic name *NPS* was used for annotated or characterized atromentin/quinone synthetases, *ADH* for alcohol dehydrogenases/oxidoreductases, and *AMT* for aminotransferases.

Sequence alignment and phylogeny reconstruction

Alignments were performed in MUSCLE with standard parameters [23, 24]. The phylogenetic trees were built by PhyML v3.0.1 [25], and statistical branch supports were computed with a Bayes likelihood-based method. The best evolutionary model for the ML analysis was selected by the Smart Model Selection (SMS) in PhyML [26], and the best substitution models according to the selection criterion AIC (Akaike information criterion) were HKY85 for nucleotide sequences and Le-Gascuel for proteins. The architectures of the promoter and protein ML trees were compared by tanglegrams that were performed by the EPoS framework for phylogenetic analysis [27].

Pigment isolation and chromatographic analyses

For *S. lacrymans*, *S. bovinus* and *O. leariius* co-cultures, the plates including the inocula and mycelia (two plates made one biological replicate) were soaked in 200 ml ethyl acetate, which was amended to a final volume of 400 ml using dH₂O and glacial acetic acid (1 % v/v), and incubated with intermittent shaking for 1 h. The organic phase was removed, and dried under reduced pressure, followed by lyophilization [9]. For *P. involutus* co-cultures, the conditioned broth (two plates made one biological replicate) was extracted vigorously with twice volume ethyl acetate amended with 1 % (v/v) glacial acetic acid with intermittent shaking or in a rotator, and dried as above.

High performance liquid chromatography (HPLC) analyses followed a published protocol [9]. Authentic standards were isolated from the axenic, aged secretomes of either *S. lacrymans* S7.9 (variegatic, xerocomic, isoxerocomic and atromentic acids; xerocomorubin and variegatorubin), or *P. involutus* (involutin, gyroporin and chamonixin) by semi-preparative HPLC as performed before with some modifications [1, 8, 9], and purity was verified by analytical HPLC. Statistical significance from three biological replicates was determined by one-way ANOVA with a post-hoc Tukey honest significant difference test using the peak area under the curve of known pigments.

Bioactivity assays

We used a described assay to assess the effect that different pigments have on biofilm development and wrinkle formation of *B. subtilis* 3610 [28]. To assess the effect that different compounds have on swarming motility of *B. subtilis* 3610 we used 90 mm diameter LB plates with 0.7 % (w/v) agar that were prepared and dried as described [29]. The antibiotic activity of different compounds was assessed via OD₅₉₀ kinetics of liquid cultures of *B. subtilis* 3610 (final concentration of 0.25 mg ml⁻¹). All bright-field and fluorescence images of colonies were obtained with an Axio Zoom V16 stereomicroscope (Zeiss, Germany) [29]. More details are found in the supplement.

RESULTS AND DISCUSSION

Cell-wall-damaging enzymes induced pigmentation in *S. lacrymans*

We used our established *S. lacrymans*-bacterium co-incubation system to screen for additional organisms or mechanisms that could also induce pigmentation as examined by HPLC [9]. We analysed pigmentation intensity by focusing on the signals (area under the curve) for the main pulvinic acid-type pigments (variegatic, xerocomic, isoxerocomic and atromentic acids; Fig. 1; [1]). Additionally, other variants of pulvinic acid-type pigments were detected. We also identified oxidized variants of variegatic acid and isoxerocomic acid, which are formed from the production of a second lactone ring from the carboxylic acid to produce variegatorubin and xerocomorubin, respectively.

In total, a set of 13 different bacteria were tested (Table 1), all of which induced pigmentation after 72 h when the fungus was grown on non-inducing media. As a control, cultures were compared to axenic fungal cultures that were exposed to water droplets *in lieu* of bacteria. Accumulation of pulvinic acid-type pigments from co-culturing was observed in all cases by HPLC (Fig. S1). As an exemplar co-incubation, *S. lacrymans* – *Sphingomonas* sp. showed intense pigmentation (Fig. 2a). As different bacteria were able to induce pigmentation, we then considered that a common inducing mechanism may be shared amongst many bacteria. Numerous bacteria release degrading enzymes, such as general proteases or oxidoreductases and hydrolases (reviewed in [30, 31]). Thus, we hypothesized that hyphal damage may represent such a common factor. We tested this hypothesis and exposed *S. lacrymans* to fungal cell-wall-lysing enzymes (containing β -glucanase, cellulase, protease and chitinase activity) or general proteases. Pulvinic acid-type pigments were observed in the chromatograms for both instances (Fig. 2b). For controls, we tested lysozyme that does not target fungal cell-walls, and mechanical damage by scalpel. Mechanical damage was shown to induce the biosynthesis of polyene defence compounds in a stercaceous mushroom [32]. Various other controls that did not result in pigmentation were run in parallel (excessive inorganic nitrogen, water or PBS). Based on the enzymatic assays we hypothesized that an eliciting factor from the bacterial partner, like a protease, was secreted which damaged the fungal cell-wall. For example, proteases are involved in mycoparasitism [33]. Therefore, we grew the fungus in the presence of pre-rinsed and water-resuspended *B. subtilis* NCIB 3610 (hereafter 3610) amended with a protease/metalloprotease inhibitor cocktail, in addition to testing heat-killed *B. subtilis*. The inhibition of proteases or introduction of dead bacteria showed a significantly reduced fungal pigment response compared to the alive *B. subtilis* 3610 co-incubation ($*P < 0.01$; Fig. 2c). Nevertheless, the amended or heat-killed *B. subtilis* caused slight pigmentation. We cannot exclude that the protease inhibitor cocktail would fail to abolish all protease activity (for example, *B. subtilis* 168, the derivative of 3610, is known to produce eight different

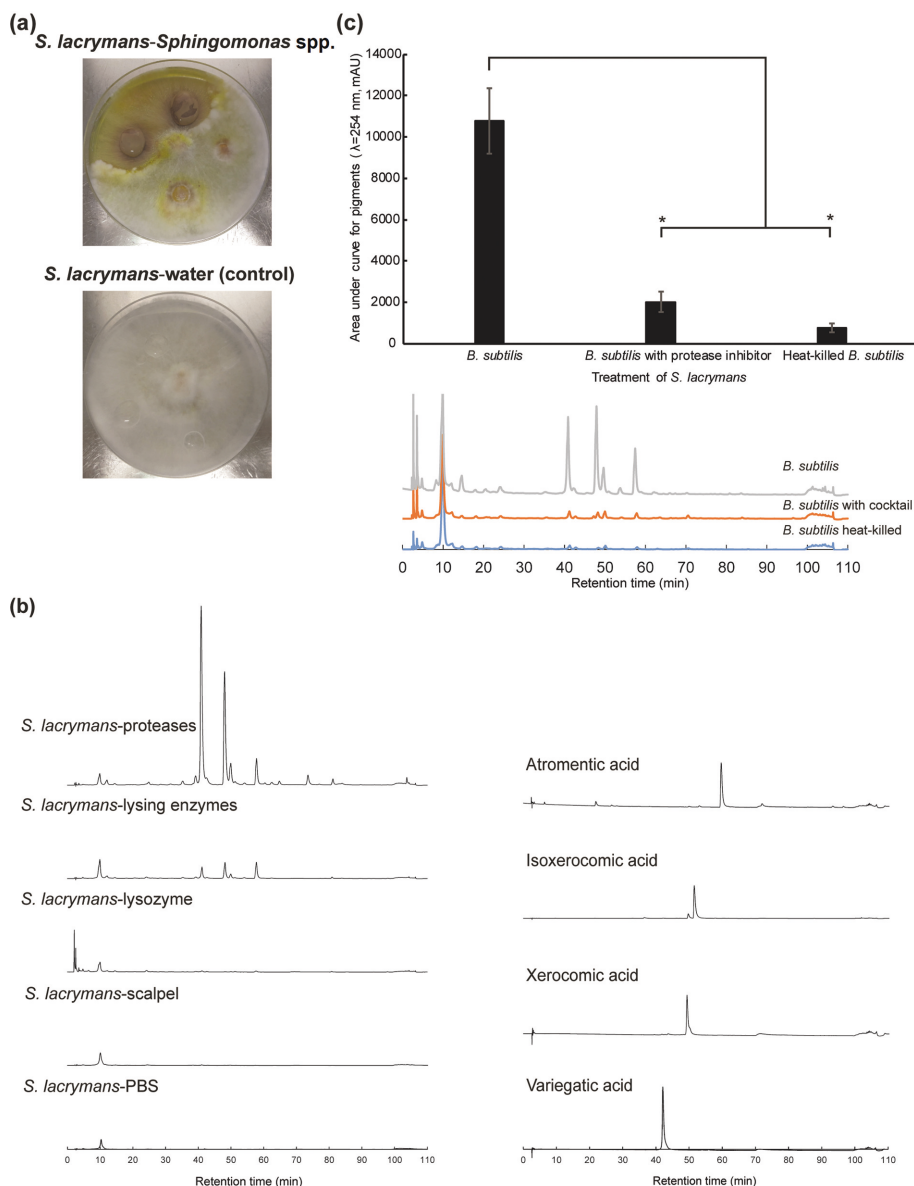


Fig. 2. (a) Representative example of strong pigment induction of *S. lacrymans* by *Sphingomonas* spp. The two 500 μ l inocula had a greater observed effect than the 250 μ l inocula. (b) Representative chromatograms ($\lambda=254$ nm) of enzymatic assays that show pigment induction by proteases and lysing enzymes, but not in the controls. Chromatograms are proportionally scaled. Further, chromatograms of authentic standards are shown: variegatic acid ($t_R=42.1$ min), xerocomic acid ($t_R=49.2$ min), isoxerocomic acid ($t_R=51.4$ min) and atromentic acid ($t_R=59.5$ min). (c) Cumulative compound titres (as assessed by the signal area under the curve at $\lambda=254$ nm) of the four main pigments (variegatic, xerocomic, isoxerocomic and atromentic acid) showing statistical difference ($*P<0.01$) between *S. lacrymans* co-incubated with alive *B. subtilis*, and *B. subtilis* amended with a protease inhibitor cocktail or heat-killed *B. subtilis*. The arithmetic mean and standard error from three biological replicates are shown, as well as representative chromatograms of each condition.

proteases [34–36]). Released peptides or cell-wall components from the fungus itself or exo-proteins due to the action of proteases or lysing enzymes may trigger pigmentation, and would draw comparisons that organic, but not inorganic, nitrogen also induced pigmentation [3]. Nor could we eliminate the idea that the fungus may be stimulated by other bacterial factors, such as secreted peptides, secreted low molecular weight compounds, competition for

nutrition, or intimate physical contact [37, 38]. Degrading exo-enzymes from bacteria such as proteases, lysing enzymes or oxidases that harm the fungus may be a direct consequence of the co-incubation or merely the bacterium modifying the environment to, for example, secure food. This remains to be studied by focusing on the bacterial partner's response during co-incubation using proteomics and/or transcriptomics. Due to the lack of genetic tractability of

basidiomycetes, the global transcriptomic response of the fungal partner is of additional interest which will help deduce whether bacterium-induced pigmentation correlates with cell-wall repair, stress-related or nitrogen metabolism genes, or whether these responses are independent. Our bacteria-induced pigmentation was also applicable for another atromentin-producing, wood-rotting basidiomycete, *Omphalotus olearius*, whereby significant brown pigmentation occurred after the introduction of either *B. subtilis* 3610 or *P. putida*. The pigment was verified to be atromentin by HPLC (Fig. S2). All in all, our results showed that pigment induction was triggered, although not definitively correlated, by an enzymatic degradation of the fungal cell-wall.

Co-culturing with *P. involutus* did not cause pigmentation

To expand our *Serpula*-based study on natural product induction through inter-kingdom co-incubation, we tested if a similar pigmentation response was also valid for atromentin-producing *Boletales* that follow a symbiotic lifestyle. We chose the model ectomycorrhizal fungus *Paxillus involutus*, and focused on the most abundantly secreted pigment under known media-inducing conditions, involutin [4]. The route to biosynthesize involutin via atromentin is redundantly secured by three atromentin synthetase genes [8, 39], which are constitutively expressed at low levels even in non-pigment inducing media (the same with *S. lacrymans*), and overly expressed in high organic nitrogen-containing media [8]. Other atromentin-derived pigments (gyroporin, chamomixin, involuton and atromentic acid) from *P. involutus* are generally produced in insignificant amounts under laboratory conditions [8].

For our co-culturing work with *P. involutus*, we grew the fungus on non-pigment-inducing media [4], and tested a diverse set of bacteria pairwise against *P. involutus* that were used for *S. lacrymans* (most species from Table 1). The bacteria did not cause significant pigmentation when examining involutin titres by HPLC (condition I; Fig. 3a). We also co-incubated *P. involutus* with *B. subtilis* 3610 as performed with *S. lacrymans* by using alive *B. subtilis*, and for control heat-killed *B. subtilis*, and *B. subtilis* incubated with a protease inhibitor. We presumed that the conditions used before may have an opposite effect. Here, we found no significant change in accumulation of involutin between all these conditions (Fig. S4).

We presumed that if ‘outside, antagonistic’ bacteria did not induce pigmentation, then perhaps community-associated bacteria may do so. Such species interactions can be quite specific (discussed below), and thus we wanted to perform a community-guided approach. We first monitored the soil directly underneath a troop of growing *P. involutus* mushrooms at two time points by qRT-PCR using 16S or 28S rDNA (Fig. S3). The isolation of bacteria pertaining to *Actinobacteria* and *Firmicutes* was led by the verification of their highest 16S copy numbers at both measured time points. After isolation by morphology, the following soil-derived

bacteria were identified by 16S rDNA sequencing and used for further co-incubation work: *Bacillus aryabhatai*, *Bacillus subtilis* subsp. *subtilis*, *Bacillus subtilis* subsp. *inaquosorum* and *Micromonospora aurantiaca* (Table S2). The bacteria we isolated were deposited in the Jena Microbial Resource Collection.

From the soil-guided approach, we tested the bacteria with *P. involutus* using two further conditions involving multi-partner interactions that may resemble the soil community around fungal hyphae. For condition II, we continued testing *P. involutus* on non-inducing synthetic media. We used pairwise and consortia co-incubations of soil isolates. Similar to the previous results, we observed no accumulation of involutin when compared to the axenic fungal control (Fig. 3b). We then co-incubated the fungus with different consortia of *Bacilli* soil-isolates in a rich medium (malt extract-peptone) that supported both strong growth of bacteria and was also a rich source of organic nitrogen that is known to stimulate the secretion of involutin (condition III; [4]). The multi-partner cultures were carried out with the fungus co-incubated with either one (pairwise), two (tripartite) or three (consortia) different soil-isolated *Bacilli*. We found that the control (i.e. axenic *P. involutus*) had increased involutin titres when compared to the fungus grown on non-inducing medium which was consistent with previous work [4]; concurrently, no signals for the other pigments were found. We looked for even the slightest variations in pigment accumulation. Each co-culture in condition III showed no statistical difference in involutin accumulation when compared to the control, and the only statistical difference was determined to be between pairwise *B. aryabhatai* and two tripartite co-cultures ($*P < 0.01$; Fig. 3c). Representative chromatograms in all cases are shown in Fig. S4. Another ectomycorrhizal-forming basidiomycete, *Suillus bovinus*, that produces atromentin-derived metabolites [1] was also tested for bacteria-induced pigmentation. Here, no pigmentation after the introduction of bacteria was observed (Fig. S5).

One hypothesis that may support the more passive response of ectomycorrhizal fungi is that saprophytes associate with less bacteria than ectomycorrhizae [40], i.e. fungal lifestyle dictates the surrounding community structure, which may indicate that saprophytes are more competitive. In support of this, mycorrhizae generally support (or at least allow for) the formation of biofilms on their hyphae [41]. Hence our results, at least with respect to pigmentation, follow suit. Conversely, such microbial communities can be very specific and biotic interactions can have very specific outcomes. Examples have shown that the mushroom’s identity shapes its specific bacterial community [42]; fungal–bacterial and bacterial–bacterial interactions and consequences therefrom (antagonistic, growth promoting or neutral) can be quite species-specific [43, 44]; a dissimilar fungal response by the exact same ‘mycorrhiza helper’ strain was possible [45]; a ‘mycorrhiza helper’ strain possesses both the capacity to promote and suppress fungal growth [46]; and the presence

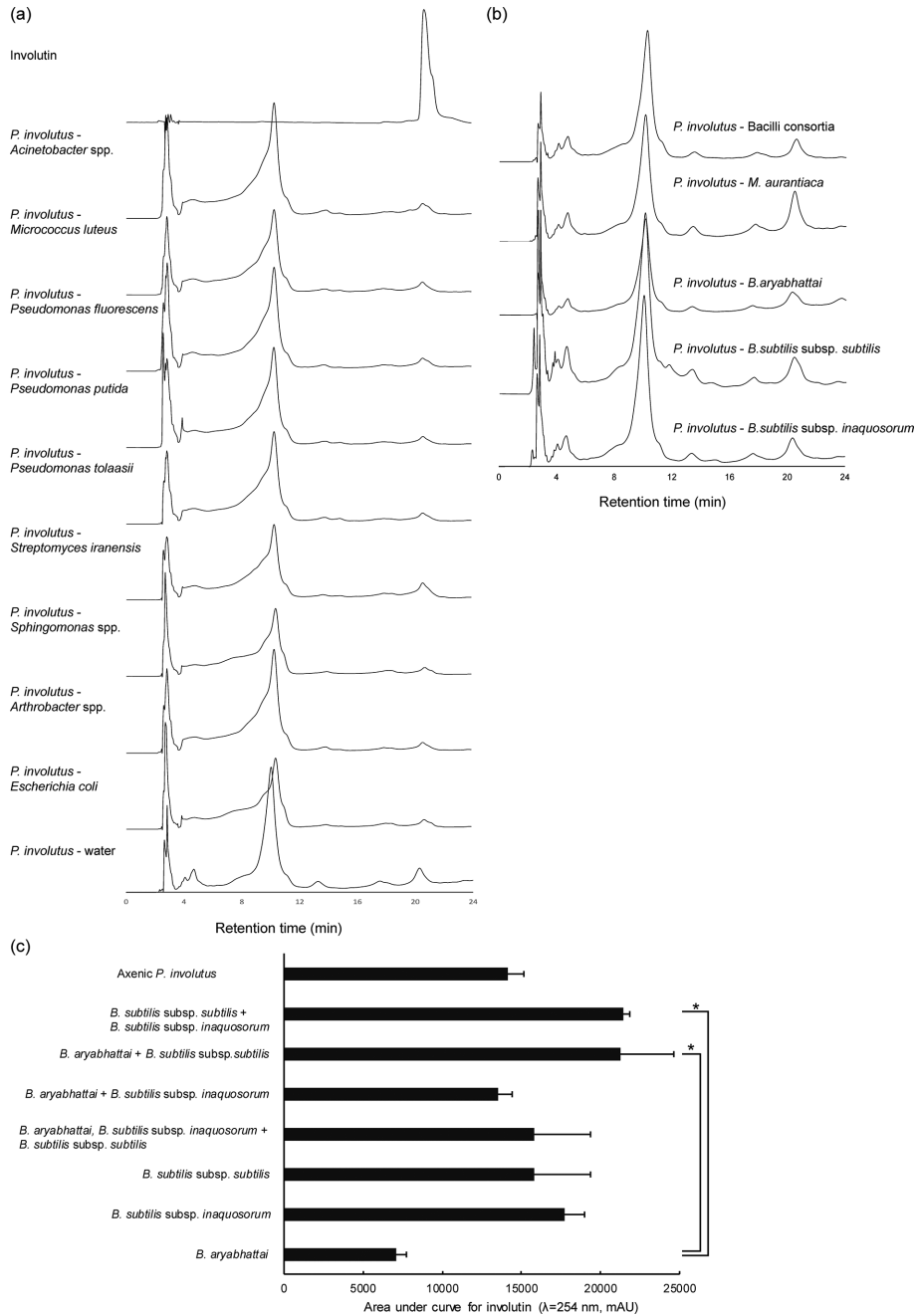


Fig. 3. (a, b) Representative HPLC chromatograms ($\lambda=254$ nm) of *P. involutus* co-cultures. Chromatograms are proportionally scaled. (a) Testing growth condition I using various bacteria from Table 1 whereby no substantial accumulation of involutin was observed. Spectroscopic data for involutin is shown in Fig. S6. Co-cultures with *B. subtilis* 3610 and other growth manipulations of *B. subtilis* are shown in Fig. S4. (b) Testing growth condition II using various soil-isolates. Again, no substantial accumulation of involutin was observed. (c) Mushroom soil-isolates, *Bacillus aryabhatai*, *B. subtilis* subsp. *inaquosorum*, *B. subtilis* subsp. *subtilis*, were both individually co-incubated with *P. involutus* as well as in various consortia in organic nitrogen-rich medium (condition III). The arithmetic mean of involutin titres (HPLC, $\lambda=254$ nm) from three biological replicates and standard error are shown. Statistical significance was observed between pairwise *B. aryabhatai* and two tripartite co-cultures ($*P<0.01$), but no statistical significance was observed between the control (axenic *P. involutus*) and the remaining samples. Representative chromatograms are shown in Fig. S4.

of the symbiotic plant partner affects the secretion of fungal bioactive compounds [47]. Thus, we cannot definitively exclude that other bacteria could have stimulated

pigmentation in *P. involutus*. Similarly, there may have been other fungal responses that were missed because we only looked for pigmentation in order to draw comparisons with

S. lacrymans. Still, the conditions that induced and altered pigmentation in *S. lacrymans* and *O. olearius* do not parallel the observations from *P. involutus* and *S. bovinus*. The dissimilar pigment response was further investigated bioinformatically and biochemically to help explain the discrepancy.

Dissimilar genetic regulation of atromentin synthetase genes

Our initial observation between orthologous atromentin biosynthetic gene clusters of 12 basidiomycetes was a common promoter motif shared in the clustered atromentin synthetase (*NPS*) and aminotransferase genes (*AMT*) [9]. We now expanded our search to a total of 23 atromentin-producing basidiomycetes [17]. Applying MEME software [21, 22] to discover ungapped motifs in upstream sequences of the clustered genes to the new, extended set of fungi genomes, we again observed the aforementioned core promoter motif, termed motif 1, for *NPS* and *AMT* which was absent for most clustered alcohol dehydrogenase genes (Fig. 4a; Table S3). In addition, we not only found remarkable conservation of the atromentin clusters and respective promoter motifs, but also of the whole orthologous *NPS* promoter regions, suggesting that promoters co-evolved with their respective genes (Fig. 4b; combined tree: Fig. S7). The high degree of conservation gave rise to our initial hypothesis that multiple basidiomycetes would have a similar pigmentation response to bacteria.

As only *S. lacrymans*, but not *P. involutus*, was stimulated for pigment production by bacteria, we re-inspected the upstream regions of the atromentin clusters to look for variations in transcriptional regulatory elements. Aiming at the differences between ectomycorrhizal and non-mycorrhizal/brown-rot fungi, we confronted these two groups using representative species. For a more focused search, we used subgroups from the larger groups as shown in Fig. 4(a). Within the ectomycorrhizal group, the first subgroup was termed the 'larger *Paxillus* group', denoted with *, and therein also '*Paxillaceae*', denoted with **. From the non-mycorrhizal/brown-rot group, the subgroup was termed the '*Serpula* group', denoted with *.

As mentioned, promoter sequences followed the same evolutionary paths as their cognate genes. A MEME search for promoters of all 23 species confirmed that there were no further motifs other than the core motif 1 between species within the 'larger *Paxillus* group' and '*Serpula* group'. The promoters of the '*Paxillaceae* group' were highly conserved and this conservation was unusually high for fungal promoters [on average ~80 % similarity with up to 100 % coverage (Table 2)]. *Hydnomerulius pinastri* had the least amount of coverage when compared to the other species, likely due to divergence within the *Paxillaceae*. The overall conservation of the promoter sequences suggested the possible occurrence of other motifs shared within. To find the motifs that were specific to either group, we ran a discriminative MEME search confronting the 'larger *Paxillus*' and '*Serpula*' groups. No significant motifs were predicted for the '*Serpula* group', possibly because of higher phylogenetic divergence

within the group [6, 39]. Promoters of the 'larger *Paxillus* group', in contrast, showed several interesting features that were not present in the '*Serpula* group'. First, we found highly conserved palindromic sequences around the core motif 1 of the *NPS* in *Paxillaceae*, and in two *Suillus* spp. (*S. brevipes* and *S. luteus*), as shown underlined in Fig. 4(a). Interestingly, a separate search thereafter showed the observed palindromic sequence in *Pisolithus microcarpus* (family: *Sclerodermataceae*). Secondly, we found two further statistically significant motifs (motif 2: consensus DYRSD-CABSBBB, *E-value* 1.3e-004; and motif 3: consensus YGAR-YCRRNBM, *E-value* 1.2e-003) in the promoters of the 'ectomycorrhizal group' that were absent in *S. lacrymans* and other representatives of non-mycorrhizal/brown-rot fungi (Fig. 4a: motifs 2 and 3). Motif 2 seemed as prevalent as motif 1 for all examined ectomycorrhiza fungi, even in the distantly related *Thelephora ganbajun*. With one exception, *Hydnomerulius pinastri*, a brown-rotter that is monophyletic within the ectomycorrhizal '*Paxillaceae* group', contained the additional observed motifs. The motif search results and their respective position to the 'start' site and *P-values* are listed in Table S3.

To summarize, we found significant differences in the promoter structure of *NPS* in *S. lacrymans* and *P. involutus*, with the latter possessing a highly conserved pattern of three motifs. Even though the core motif 1 was present in the majority of the atromentin-producing fungi and thus the transcription factor in question could recognize each binding site similarly, the fact that there exists a palindromic sequence around the core motif as well as a co-occurrence of two additional motifs (possible composite elements) for *P. involutus* indicated that there may be a different regulatory mechanism, e.g. involving homodimer-binding and co-transcription factors. Many species considered to be ectomycorrhiza-forming also share brown-rot mechanisms, and many of the species in question formed a paraphyletic group [39]. It is possible that the additional genetic regulation involved in the biosynthesis of atromentin was the result of a divergence in lifestyle from brown-rot to symbiosis, especially with the formation of the *Paxillaceae* clade. We question how and why the distantly related *T. ganbajun* has the same motifs, the inconsistencies in the promoter regions between *S. luteus*, *S. brevipes* and the remaining *Suillus* spp., and which (co-)transcription factors are supposedly widely shared.

For basidiomycetes there is a scarcity of sustenance on regulatory mechanisms regarding natural products. For example, *in vitro* combined with *in vivo* evidence for basidiomycete transcription factors in natural product regulation is mostly undescribed. As a rare example, a putative transcriptional gene in *Ustilago maydis* was identified [48]. Deletion of said gene caused constitutive production of a siderophore under suppressed conditions, and the gene was speculated to encode for a zinc factor-like transcription factor. The three largest families of fungal transcription factors are 'C₆ Zn cluster', 'C₂H₂ Zn finger' and 'HD-like' [49]. The

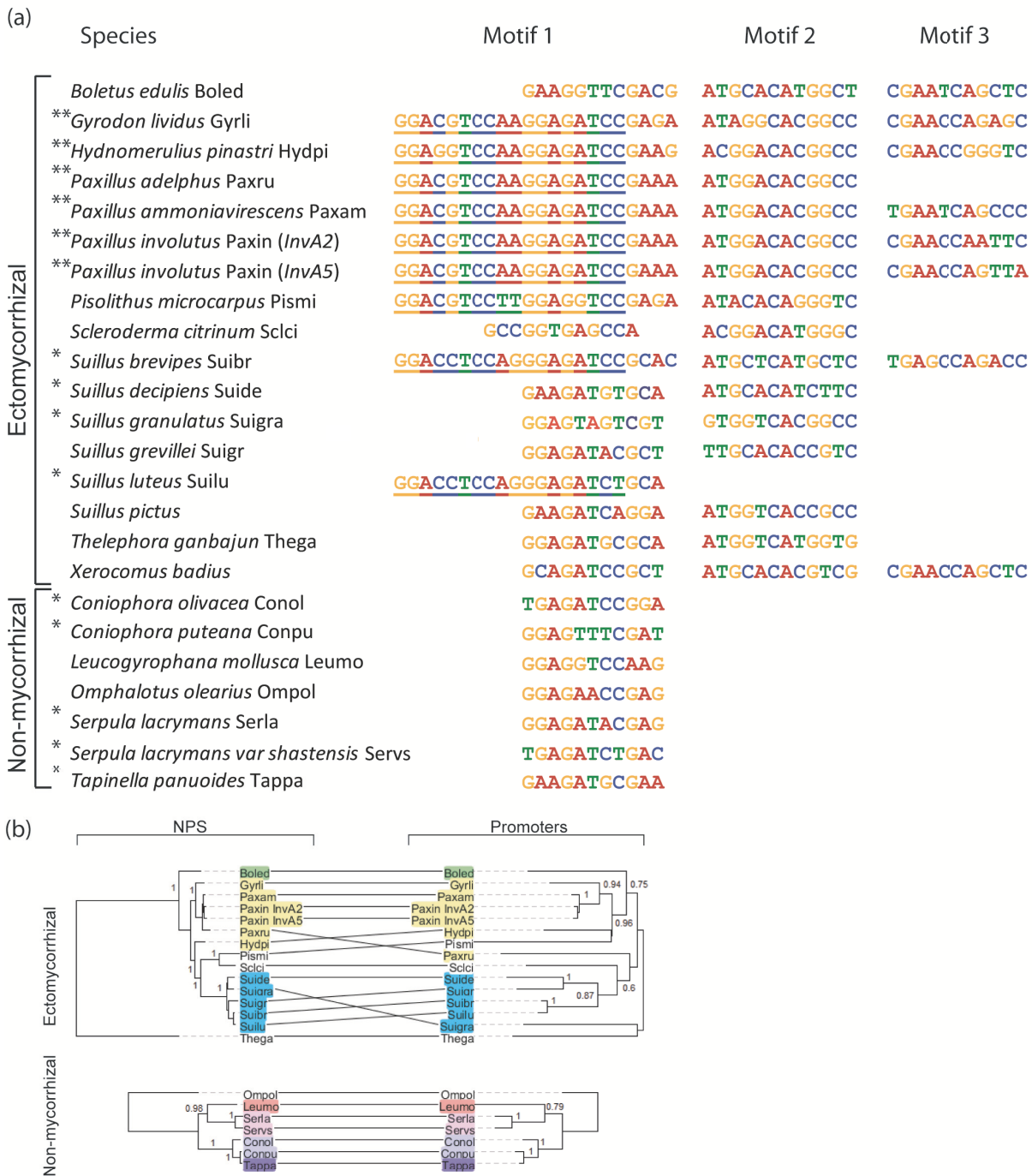


Fig. 4. *In silico* analyses of the upstream regions of annotated or characterized atromentin synthetase genes (*NPSs*) from various atromentin-producing basidiomycetes. Annotated genomes were accessed via the JGI MycoCosm portal, except for *T. panuoides* and *S. grevillei*. (a) A total of 23 atromentin-producing basidiomycetes, including abbreviation of species' names used in the tanglegram (below), that are grouped into ectomycorrhizal fungi and non-mycorrhizal/brown-rot fungi, and then further subgrouped. Within the ectomycorrhizal group, the first subgroup was termed the 'larger *Paxillus* group' (*), and therein '*Paxillaceae*' (**). Within the non-mycorrhizal/brown-rot group, the '*Serpula* group' (*). Motif 1 was shared by all fungi, whereas motifs 2 and 3 were only found in the ectomycorrhizal fungi group and in the brown-rotter *Hydnomerulius pinastri*. The palindromic sequence around motif 1, shared mostly in '*Paxillaceae*', is underlined. All motifs with their respective position to the 'start' and *P*-value are listed in Table S3. For *P. involutus*, two

atromentin synthetases (*InvA2* and *InvA5*) were used. (b) A tanglegram comparing trees' architectures that represent congruent evolutionary histories of the promoter region (nucleotide) and respective NPS (amino acids). The trees were built separately for the 'Paxillaceae' and 'Serpula' groups, and rooted by *T. ganbajun* and *O. olearius*, respectively. Only NPSs that were part of gene clusters were used for the tree reconstruction.

Zn cluster family has progressively increased its distribution in the genomes from chytrids, to zygomycetes, basidiomycetes, and finally to ascomycetes (where it has the largest distribution), and is considered the most common family of transcription factors that regulate fungal gene clusters [49–51]. While we can get an idea of what families of transcription factors are associated with different fungal groups, their associated motifs are rarely experimentally verified for basidiomycetes (e.g. reviewed for *U. maydis* [52]). We preliminarily searched our motif 1 from the ectomycorrhizal group against a motif database (JASPAR CORE (2016) fungi) in the tool TomTom [21]. Top hits were motifs associated with the Zn coordinating class of transcription factors, but no definitive conclusions could be made from such a search. With this knowledge though, it may not be overly zealous to presume that the transcription factor in question that regulates atromentin biosynthesis may fall into this class. Similarly, to our knowledge, there is no *in vivo* evidence describing a global regulator like LaeA in basidiomycetes, although, for example, Velvet domain-containing protein homologues that would associate with LaeA were noted in *Coprinopsis cinerea* as well as in most of the fungal kingdom [53–55]. Compounding our research for regulatory elements of the atromentin gene cluster was the fact that the gene cluster has no adjacent annotated regulatory genes. Therefore, we relied on motif searches for a first insight into possible regulatory mechanisms of the atromentin gene cluster. In conclusion, our approach suggested, although not yet experimentally proven, that additional regulatory requirements are involved in atromentin regulation for ectomycorrhizal fungi.

Bioactivity of pulvinic acid-type pigments

We investigated the bioactivity of the pigments to determine if the pigment response may have a specific role during co-

incubation. We chose our model *S. lacrymans* – *B. subtilis* co-incubation system as a model for further investigation. We first tested whether a growing colony of *B. subtilis* 3610 exposed to compounds freely diffusing from a filter disc would show phenotypic changes, mainly focusing on the formation of wrinkled colony biofilms [28, 56]. When *B. subtilis* was exposed to methanol as a control, atromentic acid, involutin, or atromentin, *B. subtilis* developed wrinkled colony biofilms that showed an opaque surface (i.e. no effect). However, upon exposure to variegatic or xerocommic acid, colonies developed flat or only slightly wrinkled colonies that showed decreased expansion on the agar plates (Fig. 5a). We first assumed that these effects might have been due to antimicrobial activity of the tested compounds. Therefore, we monitored the growth of *B. subtilis* in liquid cultures exposed to each pigment. After 18 h of incubation, we did not observe growth differences between cultures exposed to methanol (2.5 % v/v) or the pigments (0.25 mg ml⁻¹) (Fig. 5b). This was congruent with our previous results that the pulvinic acid-type pigments do not inhibit microbial growth [9].

Next, we examined the ability of variegatic and xerocommic acid to affect the motility behaviour of *B. subtilis*. Biofilm colonies of *B. subtilis* exposed to these compounds showed decreased colony expansion. We therefore monitored the swarming motility of *B. subtilis* colonies as they swarm across an agar plate whereby they would be challenged with an area infused with variegatic or xerocommic acid [29]. *B. subtilis* showed constant motility and swarming over an area infused with methanol (control) at a similar rate as on areas distant from the methanol deposition spot. In contrast, swarming colonies of *B. subtilis* showed a delay in motility when exposed to variegatic or xerocommic acid (20 µg; Figs 5c, d, S8). Upon reaching the compound

Table 2. The promoter regions (–1000/+2 bp) of the five species from Paxillaceae showing the percentage of region similarity (% identity)

For *P. involutus*, two characterized NPSs were included. The grey shades show the percentage of coverage. Corresponding JGI protein IDs are listed in Table S3.

% identity	<i>P. involutus</i> (<i>InvA2</i>)	<i>P. involutus</i> (<i>InvA5</i>)	<i>Paxillus</i> <i>ammoniaevirescens</i>	<i>Paxillus</i> <i>adelphus</i>	<i>Hydnomerulius</i> <i>pinastri</i>	<i>Gyrodon</i> <i>lividus</i>	
<i>P. involutus</i> (<i>InvA2</i>)	–	87 %	87 %	84 %	72 %	74 %	
<i>P. involutus</i> (<i>InvA5</i>)	87 %	–	85 %	83 %	82 %	72 %	90–100 %
<i>Paxillus</i> <i>ammoniaevirescens</i>	87 %	85 %	–	83 %	92 %	73 %	70–90 %
<i>Paxillus</i> <i>adelphus</i>	84 %	83 %	83 %	–	80 %	72 %	50–70 %
<i>Hydnomerulius</i> <i>pinastri</i>	72 %	82 %	92 %	81 %	–	77 %	30–50 %
<i>Gyrodon</i> <i>lividus</i>	74 %	72 %	73 %	72 %	76 %	–	<30 %

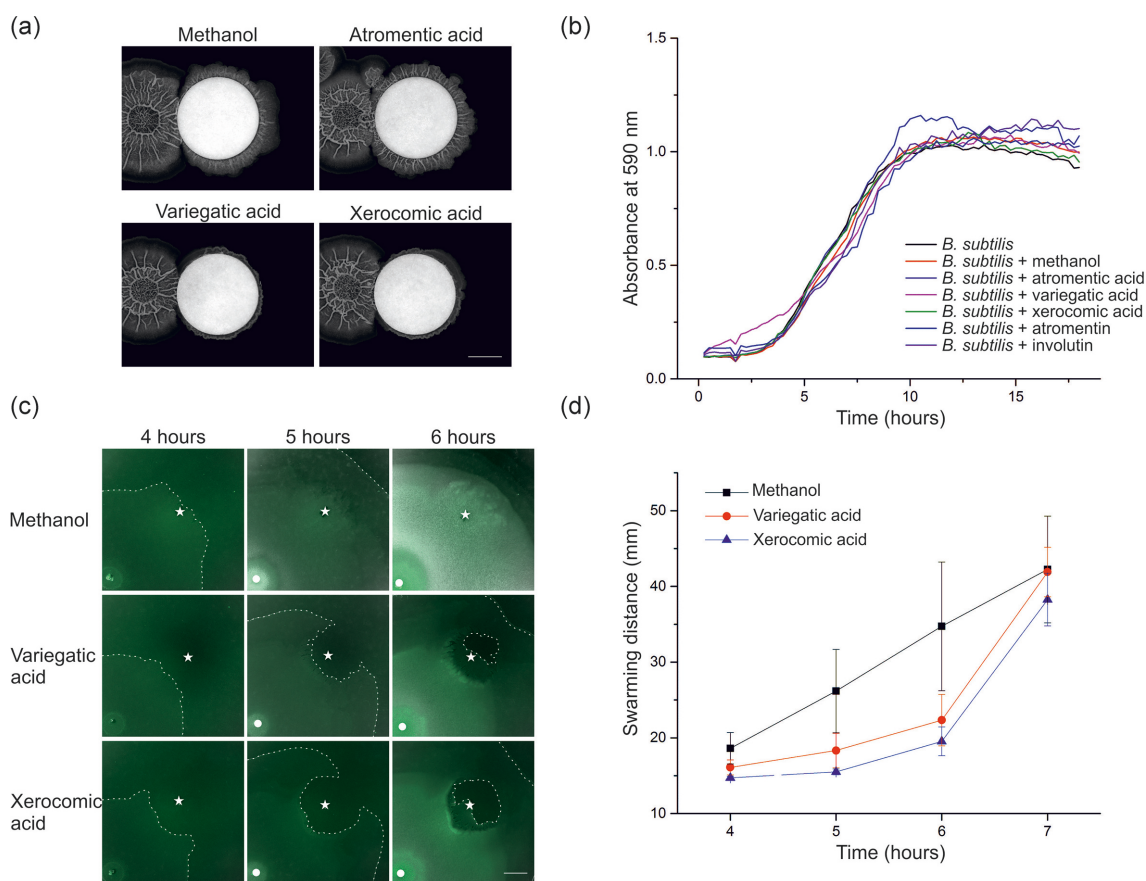


Fig. 5. Effect of diverse compounds on swarming colony expansion and spread of biofilm formation of *B. subtilis* 3610. (a) Effect of the pigments on colony biofilm development of *B. subtilis* 3610. Bright-field images of colonies are shown after 72 h of incubation. The scale bar represents 5 mm. (b) No antibiotic activity by the pigments was observed when accessed by OD₅₉₀ kinetics of liquid cultures of *B. subtilis* 3610. (c) Delay in swarming colony expansion caused by variiegatic and xerocomic acid. Composite and artificially marked images of green fluorescence and bright-field are shown. White circles mark the bacterial inoculation spot. White stars mark the deposition spot for tested compounds. Dashed white lines mark the edge of the expanding colonies. The scale bar represents 5 mm. The figure without markings is shown as Fig. S8. (d) Colony expansion after 4, 5, 6 and 7 h on 0.7 % LB agar when exposed to methanol, variiegatic acid or xerocomic acid. Each data point represents the average of five independent colonies. Error bars represent sd.

deposition spot (~4 h of incubation), the front of the swarming colony showed a delay in growth atop of the natural product-infused area, while *B. subtilis* continued to grow around the deposition area. After 7 h of incubation, the colony covered the natural product-infused area and continued to swarm, covering similar distances over the agar plate as colonies challenged with methanol.

Taken together, these results suggested that variiegatic acid and xerocomic acid affected biofilm colony morphology of *B. subtilis* not as a consequence of antimicrobial activity, but rather by inhibiting the ability of the colonies to expand upon surfaces. It remains to be determined whether this nontoxic effect is because bacteria are able to extrude polyphenols and thus are resistant to these compounds [57], or the fungus is simply modulating the bacterium in its favour. Although *B. subtilis* utilizes different molecules for quorum sensing, compared to Gram-

negative bacteria, we speculate that basidiomycetes have resources to modulate bacterial communications, given the example of lactonases from *Coprinopsis cinerea* that can cleave quorum sensing *N*-acyl-homoserine lactones [58]. Here, pulvinic acid-type pigments would be responsible for such influences. Alternatively, the significant reduction in pigmentation due to protease inhibition could be that external proteases are involved in swarming motility of *B. subtilis* [34]. The inhibition of proteases could have severely limited swarming and biofilm spreading of *B. subtilis* and thus *S. lacrymans* may not have required such a strong response to modulate *B. subtilis*. Conversely and noted beforehand, lack of released peptides from proteases may be the cause. Future research is warranted to study the influence of said compounds on the other bacteria tested in our co-incubations and whether or not the pigments have overlapping functional roles.

Conclusions

Although the atromentin biosynthetic gene cluster appeared well conserved in basidiomycetes, our work revealed dissimilar, lifestyle-dependent pigment stimulation. We suggest that this phenomenon, at least in part, can be explained by the bioactivity of these pigments and by additional putative composite elements of the atromentin synthetase gene promoters. Hence, our results set the stage for further research to understand basidiomycete natural product regulation.

Funding information

This work was supported by the Collaborative Research Center ChemBioSys (SFB1127/1). R.G.-M. was supported with a doctoral fellowship by the Consejo Nacional de Ciencia y Tecnología and the German Academic Exchange Service.

Acknowledgements

We thank the following members of the Friedrich Schiller University and of the Leibniz Institute for Natural Product Research and Infection Biology - Hans-Knöll-Institute: Andrea Perner (high-resolution mass spectrometry); Julia Gressler (sample preparation); Felix Blej (chromatography); Professor Axel Brakhage (providing access to qRT-PCR instrument); Ron Hermenau and Evgeni Bratovanov (bacterial strains); and Jana Braesel (authentic compounds). We also thank Igor Grigoriev, Alan Kuo and Robert Riley (Joint Genome Institute, Walnut Creek, CA, USA); Hui-Ling Liao and Rytas Vilgalys (Duke University, Durham, NC, USA); Francis Martin (INRA, Nancy, France); Raul Castanera (Universidad Pública de Navarra, Pamplona, Spain); and In-Geol Choi (Korea University, Seoul, Korea) for providing access to basidiomycete genomic data.

Conflicts of interest

The authors declare that there are no conflicts of interest.

References

- Gill M, Steglich W. Pigments of fungi (Macromycetes). *Prog Chem Org Nat Prod* 1987;51:1–317.
- Wackler B, Lackner G, Chooi YH, Hoffmeister D. Characterization of the *Suillus grevillei* quinone synthetase GreA supports a nonribosomal code for aromatic α -keto acids. *ChemBiochem* 2012;13:1798–1804.
- Eastwood DC, Floudas D, Binder M, Majcherczyk A, Schneider P et al. The plant cell wall-decomposing machinery underlies the functional diversity of forest fungi. *Science* 2011;333:762–765.
- Shah F, Schwenk D, Nicolás C, Persson P, Hoffmeister D et al. Involutin is an Fe³⁺ reductant secreted by the ectomycorrhizal fungus *Paxillus involutus* during Fenton-based decomposition of organic matter. *Appl Environ Microbiol* 2015;81:8427–8433.
- Kausarud H, Svegård IB, Saetre GP, Knudsen H, Stensrud Ø et al. Asian origin and rapid global spread of the destructive dry rot fungus *Serpula lacrymans*. *Mol Ecol* 2007;16:3350–3360.
- Kohler A, Kuo A, Nagy LG, Morin E, Barry KW et al. Convergent losses of decay mechanisms and rapid turnover of symbiosis genes in mycorrhizal mutualists. *Nat Genet* 2015;47:410–415.
- Pellitier PT, Zak DR. Ectomycorrhizal fungi and the enzymatic liberation of nitrogen from soil organic matter: why evolutionary history matters. *New Phytol* 2017; doi: 10.1111/nph.14598.
- Braesel J, Götze S, Shah F, Heine D, Tauber J et al. Three redundant synthetases secure redox-active pigment production in the basidiomycete *Paxillus involutus*. *Chem Biol* 2015;22:1325–1334.
- Tauber JP, Schroeckh V, Shelest E, Brakhage AA, Hoffmeister D. Bacteria induce pigment formation in the basidiomycete *Serpula lacrymans*. *Environ Microbiol* 2016;18:5218–5227.
- Schneider P, Bouhired S, Hoffmeister D. Characterization of the atromentin biosynthesis genes and enzymes in the homobasidiomycete *Tapinella panuoides*. *Fungal Genet Biol* 2008;45:1487–1496.
- Wawrzyn GT, Quin MB, Choudhary S, López-Gallego F, Schmidt-Dannert C. Draft genome of *Omphalotus olearius* provides a predictive framework for sesquiterpenoid natural product biosynthesis in Basidiomycota. *Chem Biol* 2012;19:772–783.
- Rineau F, Roth D, Shah F, Smits M, Johansson T et al. The ectomycorrhizal fungus *Paxillus involutus* converts organic matter in plant litter using a trimmed brown-rot mechanism involving Fenton chemistry. *Environ Microbiol* 2012;14:1477–1487.
- van Schöll L, Hoffland E, van Breemen N. Organic anion exudation by ectomycorrhizal fungi and *Pinus sylvestris* in response to nutrient deficiencies. *New Phytol* 2006;170:153–163.
- Essig A, Hofmann D, Münch D, Gayathri S, Künzler M et al. Copsin, a novel peptide-based fungal antibiotic interfering with the peptidoglycan synthesis. *J Biol Chem* 2014;289:34953–34964.
- Turner S, Pryer KM, Miao VP, Palmer JD. Investigating deep phylogenetic relationships among cyanobacteria and plastids by small subunit rRNA sequence analysis. *J Eukaryot Microbiol* 1999;46:327–338.
- Lane DJ. *16S/23S rRNA Sequencing*. New York, NY: John Wiley and Sons; 1991.
- Grigoriev IV, Nikitin R, Haridas S, Kuo A, Ohm R et al. MycoCosm portal: gearing up for 1000 fungal genomes. *Nucleic Acids Res* 2014;42:D699–D704.
- Branco S, Gladieux P, Ellison CE, Kuo A, Labutti K et al. Genetic isolation between two recently diverged populations of a symbiotic fungus. *Mol Ecol* 2015;24:2747–2758.
- Floudas D, Binder M, Riley R, Barry K, Blanchette RA et al. The paleozoic origin of enzymatic lignin decomposition reconstructed from 31 fungal genomes. *Science* 2012;336:1715–1719.
- Wolf T, Shelest V, Nath N, Shelest E. CASSIS and SMIPS: promoter-based prediction of secondary metabolite gene clusters in eukaryotic genomes. *Bioinformatics* 2016;32:1138–1143.
- Bailey TL, Boden M, Buske FA, Frith M, Grant CE et al. MEME SUITE: tools for motif discovery and searching. *Nucleic Acids Res* 2009;37:W202–W208.
- Bailey TL, Elkan C. Fitting a mixture model by expectation maximization to discover motifs in biopolymers. *Proc Int Conf Intell Syst Mol Biol* 1994;2:28–36.
- Edgar RC. MUSCLE: multiple sequence alignment with high accuracy and high throughput. *Nucleic Acids Res* 2004;32:1792–1797.
- Dereeper A, Guignon V, Blanc G, Audic S, Buffet S et al. Phylogeny.fr: robust phylogenetic analysis for the non-specialist. *Nucleic Acids Res* 2008;36:W465–W469.
- Guindon S, Dufayard JF, Lefort V, Anisimova M, Hordijk W et al. New algorithms and methods to estimate maximum-likelihood phylogenies: assessing the performance of PhyML 3.0. *Syst Biol* 2010;59:307–321.
- Lefort V, Longueville JE, Gascuel O. SMS: Smart Model Selection in PhyML. *Mol Biol Evol* 2017;34:2422–2424.
- Griebel T, Brinkmeyer M, Böcker S. EPOs: a modular software framework for phylogenetic analysis. *Bioinformatics* 2008;24:2399–2400.
- Gallegos-Monterrosa R, Kankel S, Götze S, Barnett R, Stallforth P et al. *Lysinibacillus fusiformis* M5 Induces Increased Complexity in *Bacillus subtilis* 168 Colony Biofilms via Hypoxanthine. *J Bacteriol* 2017;199:e00204-17.
- Hölscher T, Dragoš A, Gallegos-Monterrosa R, Martin M, Mhatre E et al. Monitoring spatial segregation in surface colonizing microbial populations. *J Vis Exp* 2016;116. doi:10.3791/54752.
- Karigar CS, Rao SS. Role of microbial enzymes in the bioremediation of pollutants: a review. *Enzyme Res* 2011;2011:1–11.
- Mäntsälä P, Zalkin H. Extracellular and membrane-bound proteases from *Bacillus subtilis*. *J Bacteriol* 1980;141:493–501.
- Schwenk D, Nett M, Dahse HM, Horn U, Blanchette RA et al. Injury-induced biosynthesis of methyl-branched polyene pigments in a white-rotting basidiomycete. *J Nat Prod* 2014;77:2658–2663.

33. Gruber S, Seidl-Seiboth V. Self versus non-self: fungal cell wall degradation in *Trichoderma*. *Microbiology* 2012;158:26–34.
34. Connelly MB, Young GM, Sloma A. Extracellular proteolytic activity plays a central role in swarming motility in *Bacillus subtilis*. *J Bacteriol* 2004;186:4159–4167.
35. Krishnappa L, Dreisbach A, Otto A, Goosens VJ, Cranenburgh RM et al. Extracytoplasmic proteases determining the cleavage and release of secreted proteins, lipoproteins, and membrane proteins in *Bacillus subtilis*. *J Proteome Res* 2013;12:4101–4110.
36. Westers L, Westers H, Zanen G, Antelmann H, Hecker M et al. Genetic or chemical protease inhibition causes significant changes in the *Bacillus subtilis* exoproteome. *Proteomics* 2008;8:2704–2713.
37. Benoit I, van den Esker MH, Patyshakuliyeva A, Mattern DJ, Blei F et al. *Bacillus subtilis* attachment to *Aspergillus niger* hyphae results in mutually altered metabolism. *Environ Microbiol* 2015;17:2099–2113.
38. Netzker T, Fischer J, Weber J, Mattern DJ, König CC et al. Microbial communication leading to the activation of silent fungal secondary metabolite gene clusters. *Front Microbiol* 2015;6:299.
39. Shah F, Nicolás C, Bentzer J, Ellström M, Smits M et al. Ectomycorrhizal fungi decompose soil organic matter using oxidative mechanisms adapted from saprotrophic ancestors. *New Phytol* 2016;209:1705–1719.
40. de Carvalho MP, Türck P, Abraham WR. Secondary metabolites control the associated bacterial communities of saprophytic basidiomycotina fungi. *Microbes Environ* 2015;30:196–198.
41. Guennoc CM, Rose C, Labbe J, Deveau A. Bacterial biofilm formation on soil fungi: a widespread ability under controls. *bioRxiv* 2017:130740.
42. Pent M, Pöldmaa K, Bahram M. Bacterial communities in boreal forest mushrooms are shaped both by soil parameters and host identity. *Front Microbiol* 2017;8:836.
43. Bontemps C, Toussaint M, Revol PV, Hotel L, Jeanbille M et al. Taxonomic and functional diversity of *Streptomyces* in a forest soil. *FEMS Microbiol Lett* 2013;342:157–167.
44. Schrey SD, Erkenbrack E, Früh E, Fengler S, Hommel K et al. Production of fungal and bacterial growth modulating secondary metabolites is widespread among mycorrhiza-associated streptomycetes. *BMC Microbiol* 2012;12:164.
45. Schrey SD, Schellhammer M, Ecke M, Hampp R, Tarkka MT. Mycorrhiza helper bacterium *Streptomyces* Ach 505 induces differential gene expression in the ectomycorrhizal fungus *Amanita muscaria*. *New Phytol* 2005;168:205–216.
46. Riedlinger J, Schrey SD, Tarkka MT, Hampp R, Kapur M et al. Auxofuran, a novel metabolite that stimulates the growth of fly agaric, is produced by the mycorrhiza helper bacterium *Streptomyces* strain Ach 505. *Appl Environ Microbiol* 2006;72:3550–3557.
47. Duchesne LUCC, Peterson RL, Ellis BE. Pine root exudate stimulates the synthesis of antifungal compounds by the ectomycorrhizal fungus *Paxillus involutus*. *New Phytol* 1988;108:471–476.
48. Voisard C, Wang J, Mcevoy JL, Xu P, Leong SA. urbs1, a gene regulating siderophore biosynthesis in *Ustilago maydis*, encodes a protein similar to the erythroid transcription factor GATA-1. *Mol Cell Biol* 1993;13:7091–7100.
49. Shelest E. Transcription Factors in Fungi: TFome Dynamics, Three Major Families, and Dual-Specificity TFs. *Front Genet* 2017;8:53.
50. Yin W, Keller NP. Transcriptional regulatory elements in fungal secondary metabolism. *J Microbiol* 2011;49:329–339.
51. Todd RB, Zhou M, Ohm RA, Leeggangers HA, Visser L et al. Prevalence of transcription factors in ascomycete and basidiomycete fungi. *BMC Genomics* 2014;15:214.
52. Basse CW, Farfving JW. Promoters and their regulation in *Ustilago maydis* and other phytopathogenic fungi. *FEMS Microbiol Lett* 2006;254:208–216.
53. Plaza DF, Lin CW, van der Velden NS, Aebi M, Künzler M. Comparative transcriptomics of the model mushroom *Coprinopsis cinerea* reveals tissue-specific armories and a conserved circuitry for sexual development. *BMC Genomics* 2014;15:492.
54. Bayram O, Braus GH. Coordination of secondary metabolism and development in fungi: the velvet family of regulatory proteins. *FEMS Microbiol Rev* 2012;36:1–24.
55. Brakhage AA. Regulation of fungal secondary metabolism. *Nat Rev Microbiol* 2013;11:21–32.
56. Branda SS, González-Pastor JE, Ben-Yehuda S, Losick R, Kolter R. Fruiting body formation by *Bacillus subtilis*. *Proc Natl Acad Sci USA* 2001;98:11621–11626.
57. Tegos G, Stermitz FR, Lomovskaya O, Lewis K. Multidrug pump inhibitors uncover remarkable activity of plant antimicrobials. *Antimicrob Agents Chemother* 2002;46:3133–3141.
58. Stöckli M, Lin CW, Sieber R, Plaza DF, Ohm RA et al. *Coprinopsis cinerea* intracellular lactonases hydrolyze quorum sensing molecules of Gram-negative bacteria. *Fungal Genet Biol* 2017;102:49–62.
59. Wagner K, Gallegos-Monterrosa R, Sammer D, Kovacs AT, Krause K et al. The ectomycorrhizospheric habitat: Norway spruce and *Tricholoma vaccinum* shape their environment. Submitted for publication.
60. Scherlach K, Lackner G, Graupner K, Pidot S, Bretschneider T et al. Biosynthesis and mass spectrometric imaging of tolaasin, the virulence factor of brown blotch mushroom disease. *Chembiochem* 2013;14:2439–2443.

Edited by: S. Pöggeler and V. J. Cid

Five reasons to publish your next article with a Microbiology Society journal

1. The Microbiology Society is a not-for-profit organization.
2. We offer fast and rigorous peer review – average time to first decision is 4–6 weeks.
3. Our journals have a global readership with subscriptions held in research institutions around the world.
4. 80% of our authors rate our submission process as 'excellent' or 'very good'.
5. Your article will be published on an interactive journal platform with advanced metrics.

Find out more and submit your article at microbiologyresearch.org.

1 **Supplementary materials**

2

3 **Dissimilar pigment regulation in *Serpula lacrymans* and *Paxillus involutus***
4 **during inter-kingdom interactions**

5

6 James P. Tauber,¹ Ramses Gallegos-Monterrosa,² Ákos T. Kovács,^{2,3} Ekaterina
7 Shelest,⁴ Dirk Hoffmeister¹

8

9 ¹Department of Pharmaceutical Microbiology at the Hans Knöll Institute, Friedrich
10 Schiller University, Winzerlaer Str. 2, 07745 Jena, Germany

11 ²Terrestrial Biofilms Group, Institute of Microbiology, Friedrich Schiller University,
12 Neugasse 23, 07743 Jena, Germany

13 ³Bacterial Interactions and Evolution Group, Department of Biotechnology and
14 Biomedicine, Technical University of Denmark, Anker Engelunds Vej, 2800 Kgs.
15 Lyngby, Denmark

16 ⁴Research Group Systems Biology/Bioinformatics, Leibniz Institute for Natural
17 Product Research and Infection Biology - Hans Knöll Institute, Beutenbergstr. 11a,
18 07745 Jena, Germany

19

20

21

22

23	Table of contents	
24	Supplementary methods	3
25	Figure S1. Representative chromatograms for <i>S. lacrymans</i>	12
26	Figure S2. Representative chromatograms for <i>O. olearius</i>	14
27	Figure S3. qRT-PCR results from soil	15
28	Figure S4. Representative chromatograms for <i>P. involutus</i>	16
29	Figure S5. Representative chromatograms for <i>S. bovinus</i>	18
30	Figure S6. Spectroscopic data of authentic standards	19
31	Figure S7. Combined tree	20
32	Figure S8. Unmarked images from Fig. 5(c)	21
33	Table S1. Primers	22
34	Table S2. Identification of soil isolates	24
35	Table S3. MEME motifs	25
36	References	27
37		
38		
39		
40		
41		
42		

43 **Supplementary methods**

44 **Weather conditions from soil time points.** The troop of *P. involutus* mushrooms
45 was determined by morphological characteristics and by sequencing of qRT-PCR
46 amplicons of partially amplified 28S-rDNA from the gDNA nucleic acid extractions.
47 Sequences were searched in BLAST [1]. The mushrooms were found adjacent to a
48 birch tree in Jena, Germany. Time point one (October 21, 2016) had a high of 8 °C,
49 low of 3 °C, and 2 mm precipitation. Time point two was one week afterwards
50 (October 28, 2016), and had a high of 11 °C, low of 7 °C, and 0 mm precipitation.

51 **Soil collection and DNA extraction and purification.** Soil 0-10 cm in depth directly
52 under an immediately removed *P. involutus* mushroom cap and stem was collected
53 into sterile 50 ml centrifuge tubes, and stored at -20 °C. Three biological replicates
54 were taken from time point one and four from time point two, which included newly
55 developed mushrooms, compared to time point one. After homogenizing the soil of
56 each sample, an aliquot of each replicate per time point was pooled together,
57 lyophilized and then weighed ("dry soil"). Two 0.5 g dry-weight soil sub-samples from
58 each time point were added to a plastic screwcap tube that contained a similar weight
59 of glass beads (\varnothing 0.25-0.50 mm). Then, 1 ml extraction buffer was added (2.5 %
60 CTAB, 0.5 M NaCl, 240 mM K_2HPO_4 , 20 mM EDTA, pH = 8.0 by NaOH; modified
61 from [2]). The samples were incubated at 65°C for 30 min. The samples were bead-
62 beaten using a Fastprep-24 (MP) for 20 s at 5.5 m s^{-1} , and then chilled on ice. This
63 procedure was repeated. Then, 500 μl phenol:chloroform: isoamyl alcohol (PCI,
64 25:24:1) was added. At this point, an internal standard was spiked into the sample
65 (see below). The samples were bead-beaten again similarly, and centrifuged ($14,000$
66 $\times g$, 2 min). The supernatant was removed, and the soil samples were treated again
67 twice with 500 μl PCI and shaken as above. The aqueous phase was aspirated, and

68 the organic phase back-extracted with 500 μl extraction buffer. The aqueous phases
69 were subjected to 1 ml chloroform to remove residual phenol. All aqueous phases
70 were then pooled, including technical replicates. A 500 μl aliquot was mixed with 500
71 μl of precipitant buffer without the pink coloration (SureClean Plus, Bioline), and the
72 manufacture's protocol was followed except the centrifugation and incubation steps
73 were doubled and two 70 % ethanol wash steps were included. The pellet was
74 suspended in 50 μl nuclease-free water at 55 $^{\circ}\text{C}$ for 10 min, and quantity and quality
75 were then measured spectroscopically (ScanDrop, AnalytikJena) in triplicate. Each
76 sample was normalized to about 45 $\text{ng } \mu\text{l}^{-1}$, using nuclease-free water, and stored at
77 -20 $^{\circ}\text{C}$ until qRT-PCR. All materials and reagents were used fresh from the
78 manufacturer, washed with ethanol, autoclaved and/or exposed to ultraviolet light for
79 60 min prior to use. When possible, preparation was done in a biological safety
80 cabinet.

81 **qRT-PCR on DNA extracted from soil.** For soil samples, qRT-PCR was carried out
82 using MyTaq™ HS Mix (Bioline). Gene quantification was monitored by EvaGreen
83 (Biotium)-labeled PCR fragments. Reactions were run on a QuantStudio 3 cycler
84 (ThermoFischer) in triplicate using this cycling condition: initial denaturation at 95 $^{\circ}\text{C}$
85 for 5 min, and then 40 cycles of 95 $^{\circ}\text{C}$ for 30 s, specific annealing temperature for 45
86 s, 72 $^{\circ}\text{C}$ for 60 s, and 81 $^{\circ}\text{C}$ for 5 s for data acquisition (ramping 1.6 $^{\circ}\text{C } \text{s}^{-1}$). A final
87 melt analysis was done starting at 60 $^{\circ}\text{C}$ for 60 s followed by a step-and-hold
88 increase to 95 $^{\circ}\text{C}$ in increments of 0.1 $^{\circ}\text{C}$ every two seconds. The PCR mixture
89 consisted of 10 μl 2 \times MyTaq HS Mix (Bioline), 1 μl 20 \times EvaGreen (in water;
90 Biotium), 4 pmol each qRT-PCR primer (0.4 μl each), 7.2 μl nuclease-free water, and
91 1 μl template of community gDNA (2.25 ng final). Primers used were either universal
92 or taxon-specific, and all were already validated for qPCR in previous publications

93 (Table S1). Negative controls for each primer set were done in a reaction without
94 template which showed in some cases primer dimer formation (that was absent from
95 experimental samples) and thus we chose to measure fluorescence at 81 °C.

96 Standard curves were made using a 1:10 dilution series of a recombinant plasmid
97 containing one representative rDNA copy as obtained by amplification from each
98 primer set. qRT-PCR quantitation, as standardized to copy numbers (16S or 28S
99 rDNA gene copies), was analyzed using Quantstudio Design and Analysis (version
100 1.4.0) and Excel (Microsoft). Primer efficiency was also determined (Table S1).

101 Three considerations were made for nucleic acid isolated from soil: i) Inhibition by soil
102 contaminants; ii) sample variation; and iii) sequence of amplicons produced. For
103 considerations i) and ii), a dilution series using previously described PCR efficiency
104 methodology was done [3]. pJT086 (pJET1.2-*NPS1*) containing the amplicon of
105 *NPS1* as amplified by published *NPS1*-specific primers was isolated using a plasmid
106 miniprep kit (Zymo), and 2 µl was spiked into the soil during extraction to provide an
107 internal standard. Both the *NPS1* gene and the respective fungus, *S. lacrymans*,
108 were presumed to be absent from the soil. After nucleic acid isolation, a dilution
109 series (1:10) of each soil sample was run using *NPS1* specific primers. The two
110 samples were compared by linear regression using the C_T from the dilution series of
111 each time point and input into GraphPad software's online QuickCalcs tool. The
112 coefficient of variance was calculated by $((C_T \text{ standard deviation at 95 \% confidence}) / (C_T \text{ mean}) \times 100)$ at each dilution series, and compared between both
113 time points. Sequencing was prepared as below, and revealed specificity and some
114 mismatching as expected.

116 We determined to reject any qRT-PCR threshold cycle (C_T) above 30 because the
117 highest coefficient of variance was observed at $C_T > 30$. Compared to the internal

118 standard extracted without any potential influence of soil contaminants, the PCR
119 efficiency of *NPS1* as determined by a dilution series ($C_T < 30$) differed and indicated
120 the presence of some inhibition as expected (pure standard: 101 % where $R^2 =$
121 0.999; soil time point one: 111 % where $R^2 = 0.999$; and soil time point two: 125 %
122 where $R^2 = 0.999$). The linear regression between soil samples using the C_T values
123 of *NPS1* had a goodness of fit where R^2 was 0.9997 (P value < 0.0001). Therefore,
124 we concluded that both nucleic acid extractions from each time point were
125 comparable at $C_T < 30$.

126 **Plasmid preparation for sequencing.** qRT-PCR reactions per taxon-specific or
127 universal amplification were pooled if there was amplification in the qRT-PCR
128 reactions, and 2 μ l of PCR product ligated to pJET1.2 after a blunting step using the
129 pJET1.2 CloneJet kit (Thermo). Then, chemically-competent *E. coli* XL1-Blue cells
130 were transformed with 10 μ l of ligation mixture. Transformants were plated onto LB
131 agar-carbenicillin (50 μ g ml^{-1}). Five colonies per plate were picked, inoculated into 5
132 ml LB-carbenicillin (50 μ g ml^{-1}) and grown overnight. Plasmids were isolated using a
133 modified alkaline lysis and alcohol precipitation [4, 5]. Correct cloning was confirmed
134 by DNA-sequencing. Sequences were submitted online in EzBioCloud [6]. For the
135 internal standard of *NPS1*, the insert was cross checked using NCBI's nucleotide
136 BLAST search engine [1]. Plasmids used as template to create qRT-PCR standard
137 curves were additionally purified using a DNA concentrator kit (Zymo), and copy
138 number quantified from an $A_{260/280}$ reading using a ScanDrop instrument
139 (AnalytikJena).

140 **Isolation of spore-forming bacteria.** Spore-forming, non-fastidious bacteria were
141 isolated from the soil. 1 g of mixed soil was mixed well with 10 ml PBS, and
142 incubated at 80 °C for 15 min. A 1:10 dilution series was made using PBS, and 100

143 μ l was plated on MEP or synthetic agar plates. After three days of incubation at 28 °C
144 for MEP plates or weeks for synthetic agar plates, phenotypically different single
145 colonies were selected for further processing. Single colonies were inoculated into
146 50-100 ml DSMZ M79-Medium 426 or LB and incubated with agitation (140 rpm) at
147 28 °C to dense cultures. An aliquot was used to make a 25 % glycerol stock to be
148 used for co-incubation work, and 1-2 ml was used to extract gDNA for 16S rDNA
149 sequencing using the fungi protocol from the Animal and Fungi DNA preparation kit
150 (Jena Bioscience). 16S rDNA was amplified from universal primers 27F and 1492R
151 (Table S1) using 1.25 U Dreamtaq DNA polymerase (Thermo) in the following
152 reaction mixture and cycling conditions: 50 mM MgCl₂, 2.5 μ l 10 \times green DreamTaq
153 buffer, 0.5 μ l dNTPs (10 mM each), 20 pmol each primer (2 μ l), and 2 μ l of gDNA; an
154 initial hold at 95 °C for 5 min, cycling 40 times of 95 °C for 30 s, 55 °C for 45 s, 72 °C
155 for 90 s, and then a final extension at 72 °C for 10 min [7, 8]. Amplicons were run in a
156 1 % agarose gel, excised, purified using a Zymoclean™ Gel DNA recovery kit and
157 sequenced. For identified bacteria see Table S2.

158 **Natural product isolation.** Pigments were isolated from *S. lacrymans* S7 or *P.*
159 *involutus* by semi-preparative HPLC on an Agilent 1200 series integrated system with
160 diode array detection and equipped with column #1 (Zorbax RX-C₁₈, 9.4 x 250 mm, 5
161 μ m particle size), or column #2 (Zorbax XDB-C₁₈, 4.6 x 150 mm, 5 μ m particle size).
162 Either column was fitted with a guard and held at 25 °C. All pigments have been
163 previously described and were determined by their characteristic UV-Vis spectra and
164 high-resolution electrospray ionized masses recorded in the negative mode [9-18].

165 **Pulvinic acid-type pigments.** *S. lacrymans* S7.9 [19] was grown from MEP agar
166 plugs containing mycelia in a volume of 1 l synthetic medium broth within a 3 l glass
167 penicillin flask for up to four months at ambient temperature in darkness without

168 agitation. The conditioned culture broth was separated from the biomass by Büchner
169 filtration and then liquid-liquid extracted with ethyl acetate amended with either acetic
170 acid (1 % v/v) or 6 N HCl until there was a visual shift in pigmentation from the
171 aqueous to organic phase [17]. The organic phase was dried under reduced
172 pressure. The remaining water was removed by lyophilization. The crude extract was
173 suspended in methanol and subjected to semi-preparative HPLC using column #1
174 with the following gradient at 2 ml min⁻¹ (solvent A: methanol, solvent B: 0.1 %
175 trifluoroacetic acid (TFA, v/v) in water): initial hold at 10 % A for 2 min followed by a
176 linear increase to 100 % A over 28 min. Compounds were dried as above. If
177 necessary, compounds were submitted again with column #2 using the following
178 gradient at 1 ml min⁻¹ (solvent A: acetonitrile, solvent B: 0.1 % TFA (v/v) in water):
179 initial hold for 2 min at 5 % A, then a linear increase to 65 % A over 17 min.

180 **Diarylcyclopentenone pigments.** *Paxillus involutus* ATCC 200175 [20] was grown
181 on synthetic agar plates, macerated by a scalpel, and inoculated in a volume of 100
182 ml of synthetic broth within 500 ml Erlenmeyer Flasks and grown up to four to six
183 months at ambient temperature in darkness without agitation; as the culture aged the
184 broth pigmented. The conditioned culture broth was separated from the biomass by
185 Büchner filtration, and the broth was then incubated with Amberlite XAD-16N resin
186 overnight at room temperature with agitation. The broth was decanted and the
187 pigments were exhaustively eluted using methanol which was then dried under
188 vacuum. The crude extract was pre-fractionated using a methanol: water step
189 gradient (25 % increments) in a Waters Sep-Pak C₁₈ 35 cc 10 g column, and
190 pigments were isolated from the first solid-phase extraction fractionation using the
191 same RP-HPLC procedure above.

192 **Pigment analyses.** For co-cultures, enzymatic assays and controls from *S.*
193 *lacrymans*, the dried crude extract was resuspended in 1 ml methanol and 30 μ l was
194 run on an Agilent 1200 instrument equipped with a Zorbax Eclipse XDB-C₁₈ column
195 (4.6 \times 250 mm, 5 μ m particle size, fitted with a guard, held at 25°C) and the following
196 gradient at 1 ml min⁻¹ with solvent acetonitrile (B) and 0.1 % TFA-amended (v/v)-
197 water: initial hold of 5 % B for 5 min followed by two linear increases (to 40 % B over
198 90 min, then to 100 % over 5 min) and a final isocratic hold for 2 min [3]. For *P.*
199 *involutus* co-cultures and controls, crude extracts from ethyl acetate extractions were
200 carried using the same protocol for *S. lacrymans*, except 100 μ l (condition I), 50 μ l
201 (condition II), or 70 μ l (condition III) was injected, and some sets of runs were
202 programmed to stop early to only investigate the pigment involutin. *O. olearius* co-
203 incubations were extracted and run exactly as done for *S. lacrymans*, except on an
204 Agilent 1260 build. In all cases, chromatograms were monitored and extracted at
205 λ =254 nm with reference at λ =600 nm, except for variegatorubin and xerocomorubin
206 which were at λ =500 nm (absorbance recorded 190-600 nm in all cases). High
207 resolution mass spectrometry was run exactly as before [3].

208 **Colony biofilm assay.** We used a described colony biofilm assay to assess the
209 effect that different compounds have on biofilm development and wrinkle formation of
210 *B. subtilis* NCIB 3610 [21]. 50 μ l of the tested compound (1 mg ml⁻¹) solutions were
211 deposited on the center of 12 mm-diameter cotton discs that were placed on 90 mm-
212 diameter 2 \times SG agar plates. These plates were dried for a minimum of 20 min
213 before deposition of the compounds by keeping them completely open in a laminar
214 flow sterile bench. 2 μ l of an overnight culture of the *B. subtilis* NCIB 3610 were then
215 inoculated at 5 mm from the edge of the cotton discs [22]. The plates were incubated
216 at 30°C for a total of 72 hours. Every 24 hours the cotton discs were reimpregnated

217 with 25 μ l of the corresponding compounds. All compounds were tested as 1 mg ml⁻¹
218 methanol solutions. After the incubation period, the plates were used for
219 stereomicroscopy imaging without further treatment.

220 **Swarming motility assay.** To assess the effect that different compounds have on
221 swarming motility of *B. subtilis* we used 90 mm-diameter LB plates with 0.7 % agar
222 prepared and dried as described [23]. 2 μ l of an overnight culture of *B. subtilis* TB34
223 (DK1042 *amyE:P_{hyperspank}-gfp*) adjusted to OD₆₀₀=0.2 were inoculated on the plates,
224 and 10 μ l of the compound dissolved in methanol (2 mg ml⁻¹) were deposited at 2 cm
225 from the bacterial inoculation spot [24]. The plates were further dried for 10 min by
226 keeping them completely open in a laminar flow sterile bench. Afterwards, the plates
227 were incubated at 37°C for 7 hours. Swarming expansion of the colonies was
228 monitored via stereomicroscopy after 4, 5, 6, and 7 h of incubation. All swarming
229 distance measurements were made using Zen 2012 blue edition software (Zeiss,
230 Germany). This was done by tracing a line between the bacterial inoculation spot and
231 the compound deposition spot, and measuring the distance from the inoculation spot
232 to the colony edge closest to the deposition spot along said line.

233 **Antibiotic activity assay.** The antibiotic activity of different compounds was
234 assessed via OD₅₉₀ kinetics of liquid cultures of *B. subtilis* 3610. For this, a fresh
235 culture of *B. subtilis* 3610 with OD₅₉₀=0.6 was diluted to a 1:10 ratio with LB liquid
236 medium. 10 μ l of this dilution were used to inoculate a 96-well microplate with LB
237 liquid medium. The tested compounds dissolved in methanol or pure methanol as a
238 control were added to these wells (final volume 200 μ l). The microplate was
239 incubated at 30°C with shaking, and OD₅₉₀ was measured every 15 min for 18 hours
240 using a microplate reader (Infinite 200 PRO, Tecan, Switzerland) to assess growth of

241 *B. subtilis*. Final concentrations were methanol at 2.5 % or the pigments at 0.25 mg
242 ml⁻¹.

243 **Stereomicroscopy.** All bright-field and fluorescence images of colonies were
244 obtained with an Axio Zoom V16 stereomicroscope (Zeiss, Germany) equipped with
245 a Zeiss CL 9000 LED light source, a PlanApo Z 0.5× objective, HE 38 eGFP filter set
246 (excitation at 470/40 nm and emission at 525/50 nm), and an AxioCam MRm
247 monochrome camera. Images were obtained with exposure times of 20 ms for bright-
248 field, and 10 s for green fluorescence when needed [23].

249

250

251

252

253

254

255

256

257

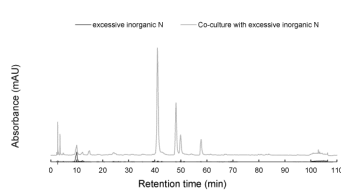
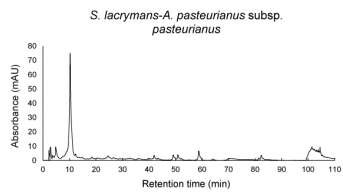
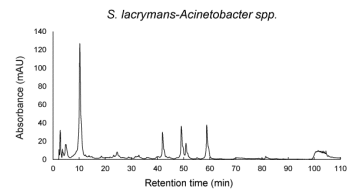
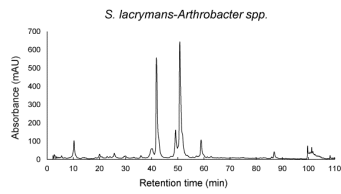
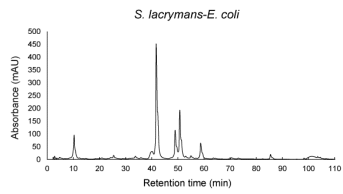
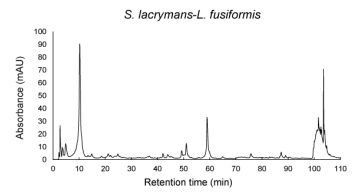
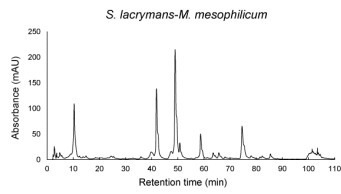
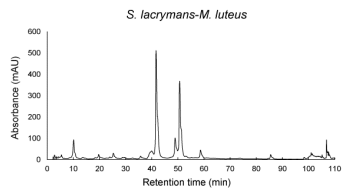
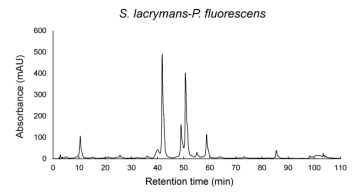
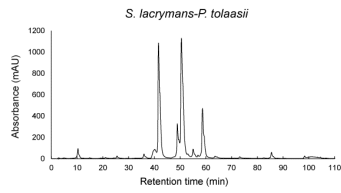
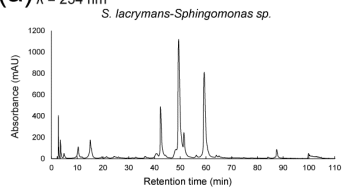
258

259

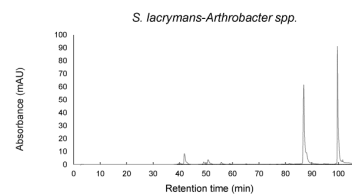
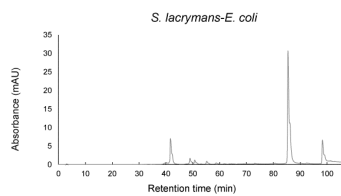
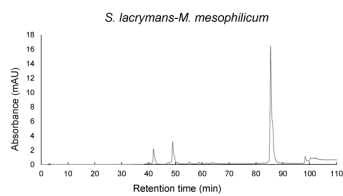
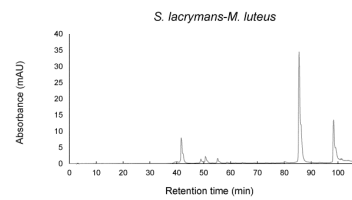
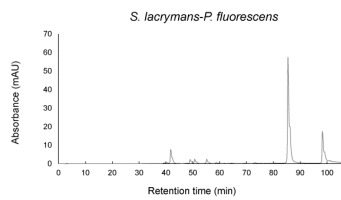
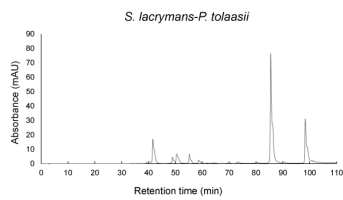
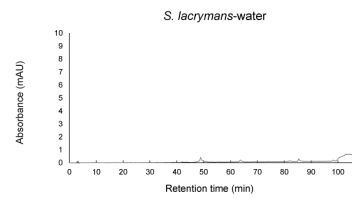
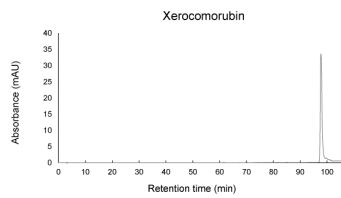
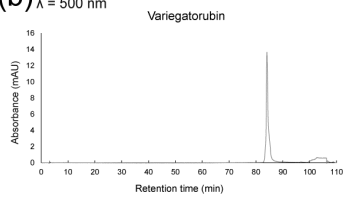
260

261

(a) $\lambda = 254 \text{ nm}$



(b) $\lambda = 500 \text{ nm}$



262

263

264

265 **Fig. S1.** Representative chromatograms for co-cultures and controls of *S. lacrymans*
266 (one biological replicate for each condition is shown) used for analyses of pigments.
267 Authentic standards (shown in the main text) of pigments isolated from aged axenic
268 *S. lacrymans* cultures extracted at $\lambda=254$ nm: Variegatic acid ($t_R = 42.1$ min),
269 xerocomic acid ($t_R = 49.2$ min), isoxerocomic acid ($t_R = 51.4$ min), and atromentic
270 acid ($t_R = 59.5$ min); and extracted at $\lambda=500$ nm: variegatorubin ($t_R = 87.0$ min), and
271 xerocomorubin ($t_R = 97.7$ min). **(a)** Co-cultures of *S. lacrymans* with various bacteria
272 inoculated as droplets atop the fungus after grown on synthetic medium. **(b)** In some
273 co-cultures from (a), two pulvinic acid-type pigment variants (variegatorubin and
274 xerocomorubin) were observed.

275

276

277

278

279

280

281

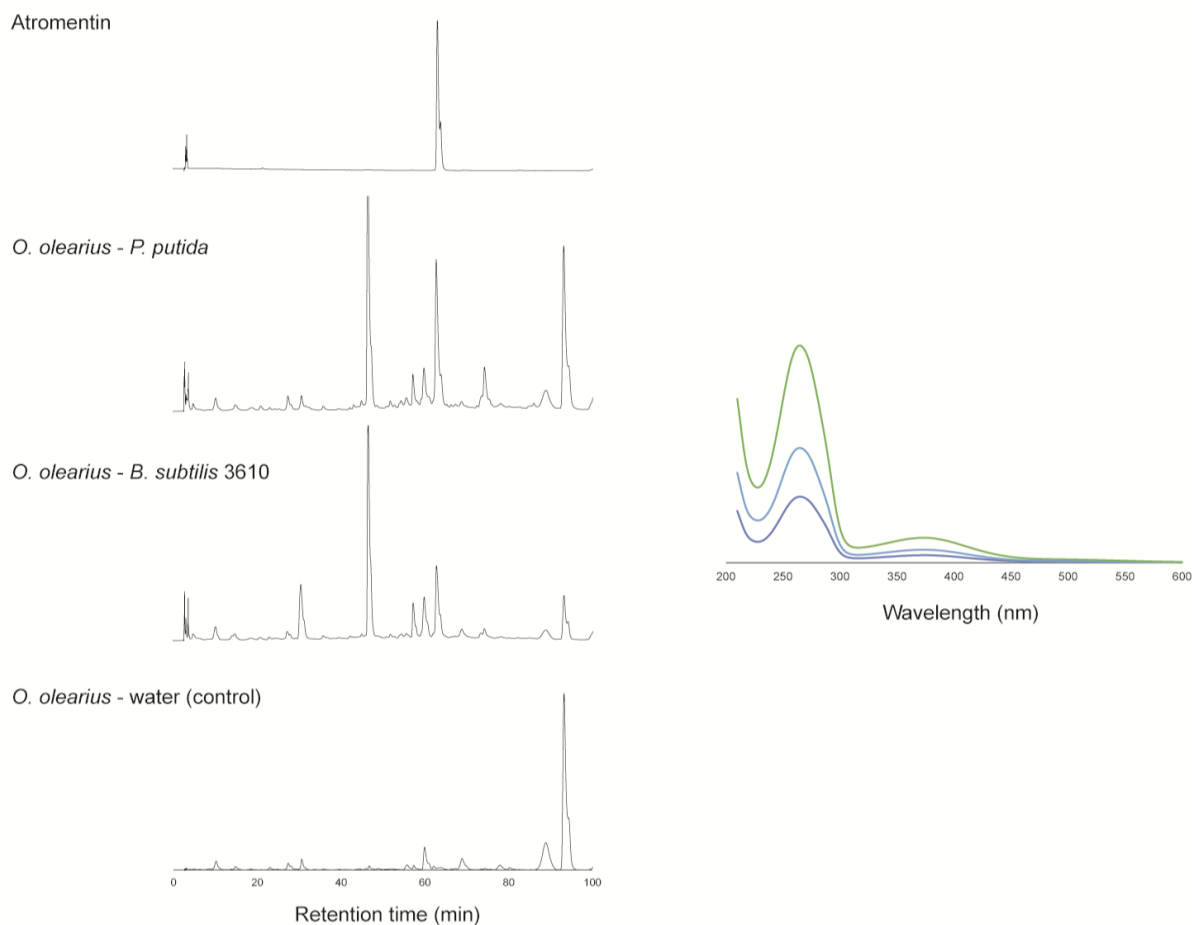
282

283

284

285

286



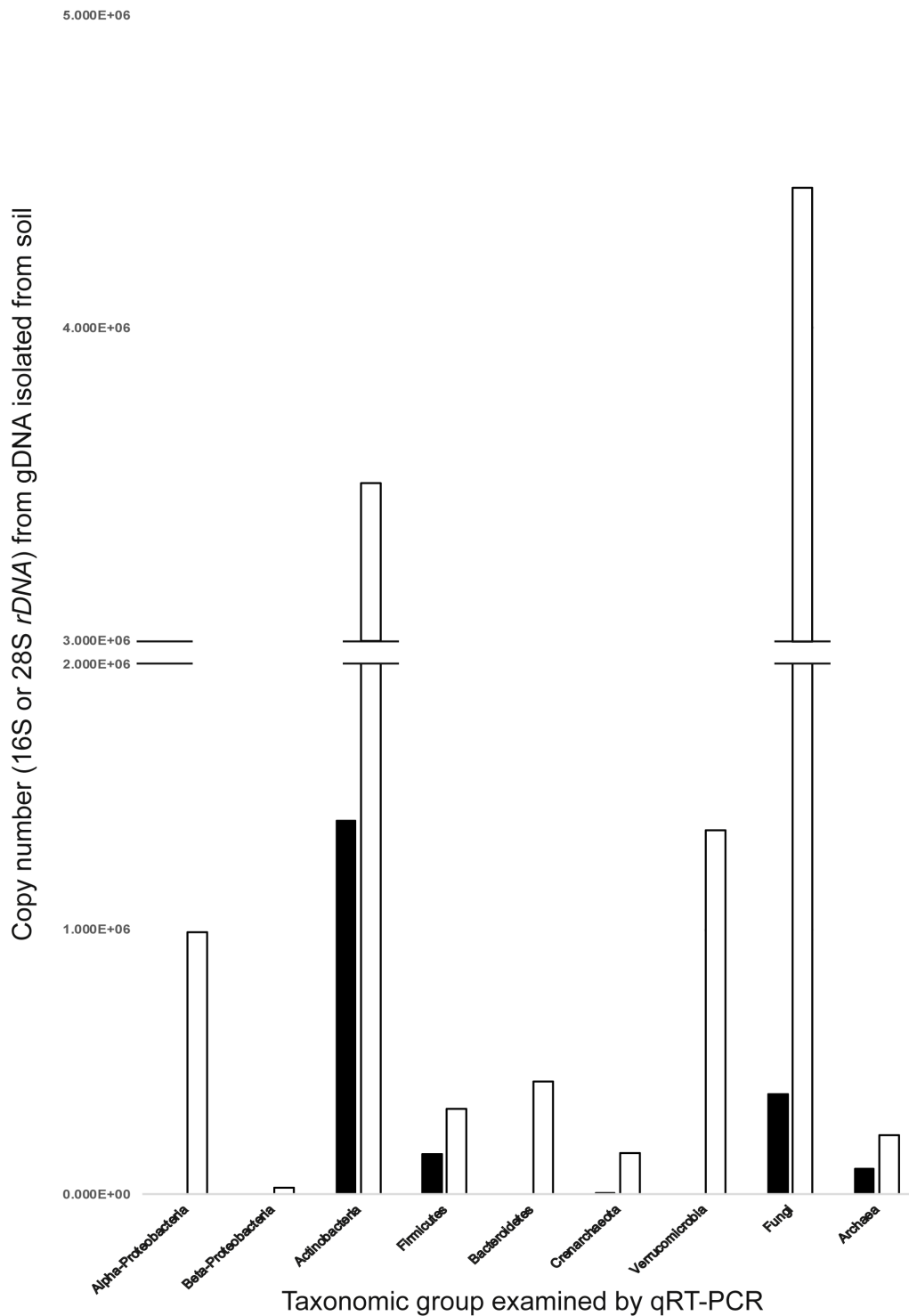
287

288

289 **Fig. S2.** Representative chromatograms at $\lambda=254$ nm of *Omphalotus olearius* co-
 290 cultures (one biological replicate for each condition is shown) used for analyses of
 291 pigments (run on an Agilent 1260 build). Overlaying UV-Vis spectra of atromentin
 292 signals from both co-cultures and the authentic standard are shown, and the
 293 authentic standard of atromentin was provided from earlier work [25], and confirmed
 294 previously by NMR and high-resolution mass spectrometry. Atromentin and other
 295 pigments have been isolated from *Omphalotus olearius* [26].

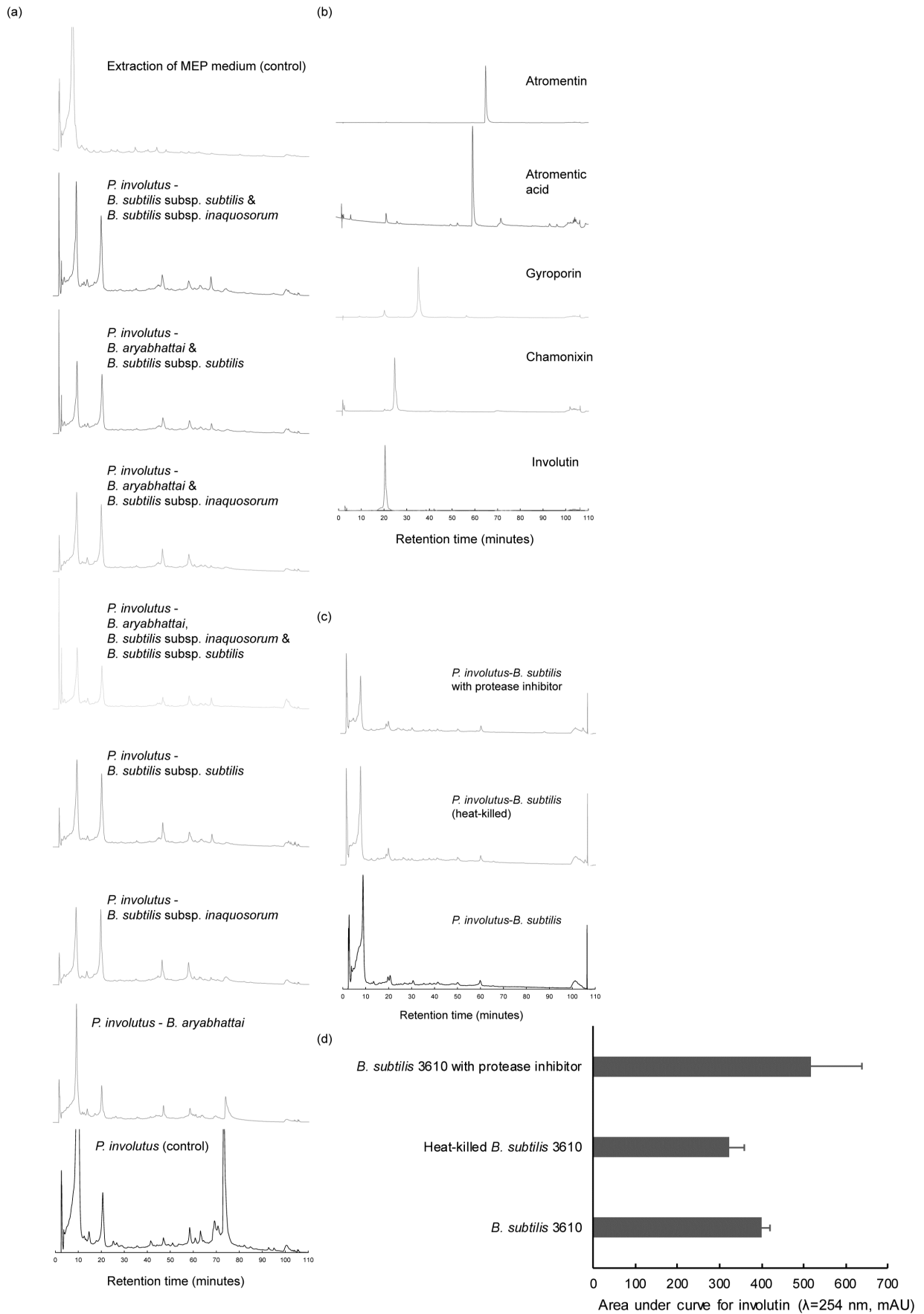
296

297



298

299 **Fig. S3.** qRT-PCR results of the abundance of organism as given in copy number
 300 (16S or 28S rDNA) found in the soil associated with *P. involutus* at both time point
 301 one (black) and time point two (white). Primers are given in Table S1. α -
 302 *Proteobacteria*, β -*Proteobacteria*, and *Bacteroidetes* were present only at time point
 303 two which corresponded with newly grown mushrooms.



305 **Fig. S4.** Representative chromatograms extracted at $\lambda=254$ nm (one biological
306 replicate for each condition is shown) of *P. involutus* co-culture ethyl acetate
307 extractions used for analyses of pigments (run on an Agilent 1200 build). The
308 chromatograms are proportionally scaled. **(a)** Co-cultures from condition III (bacilli
309 consortia with *P. involutus* in MEP medium). **(b)** Authentic standards of pigments
310 isolated from aged axenic *P. involutus* cultures: involutin ($t_R = 20.4$ min), chamonixin
311 ($t_R = 25.4$ min), gyroporin ($t_R = 35.8$ min), atromentic acid ($t_R = 59.5$ min), and
312 atromentin ($t_R = 65.2$ min). **(c)** Co-cultures from condition I (bacilli treated differently
313 and co-incubated with *P. involutus* in synthetic medium). **(d)** Involutin titer analyses
314 from (c). *B. subtilis* 3610, heat-killed *B. subtilis* 3610, and *B. subtilis* 3610 amended
315 with a protease inhibitor cocktail were tested with *P. involutus* in non-inducing
316 synthetic medium and there were no statistically significant differences between the
317 conditions.

318

319

320

321

322

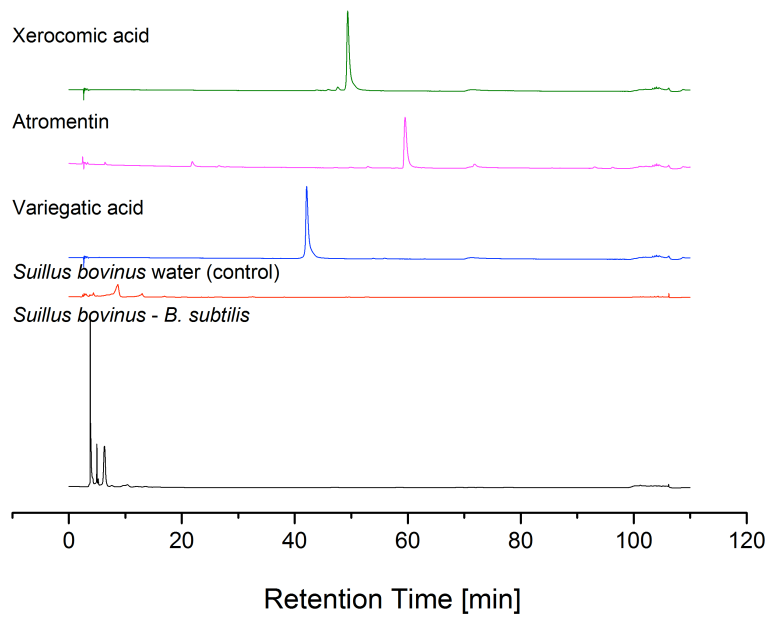
323

324

325

326

327



328

329 **Fig. S5.** Chromatograms extracted at $\lambda=254$ nm (one biological replicate for each
 330 condition is shown) used for analyses of pigments from *Suillus bovinus* – *Bacillus*
 331 *subtilis* 3610 co-culture ethyl acetate extractions. Chromatograms of standard
 332 compounds are shown above.

333

334

335

336

337

338

339

340

341

342

343

344
345
346
347
348
349
350
351
352
353
354
355
356
357
358
359
360
361
362
363
364
365
366
367
368

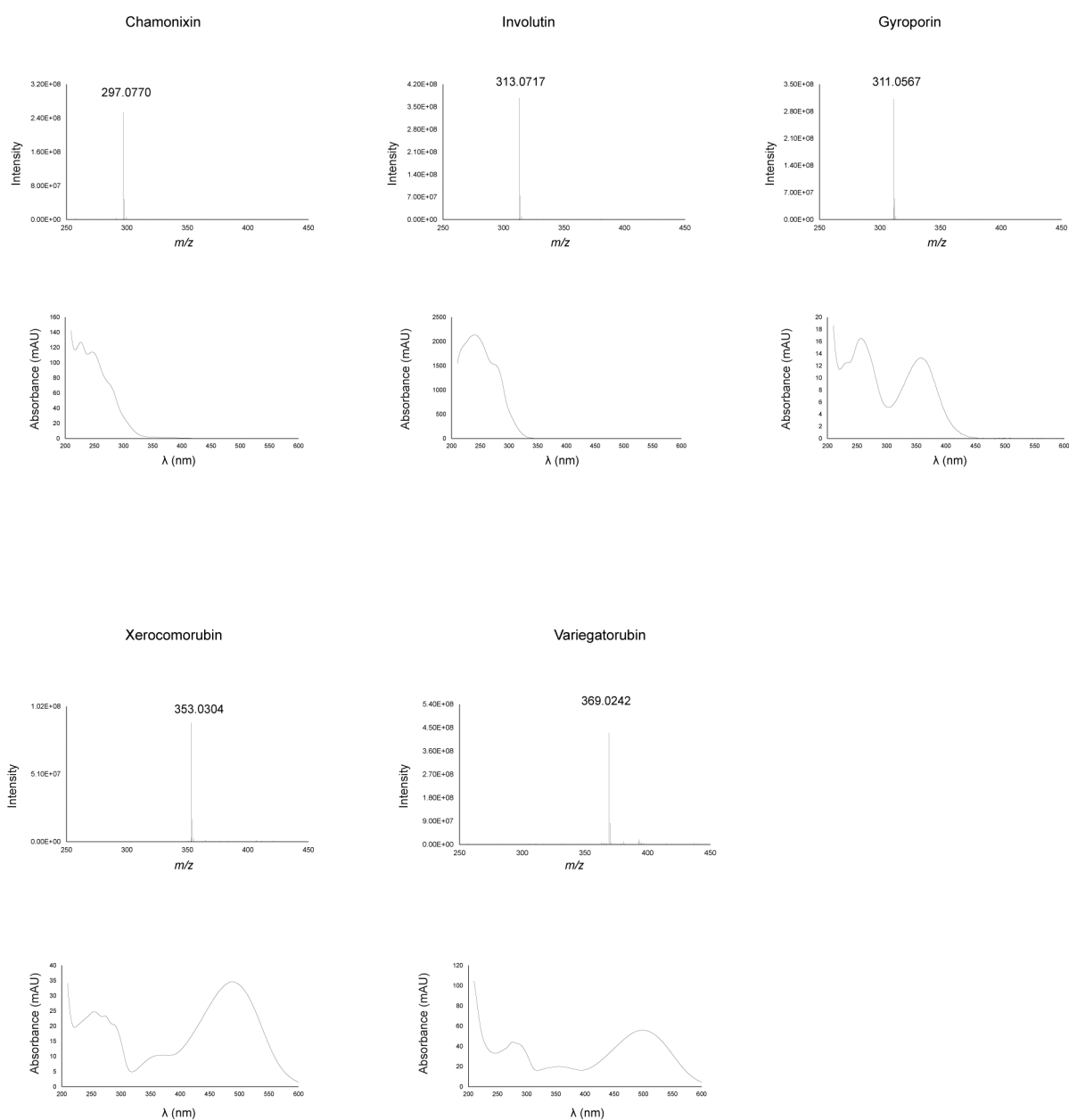
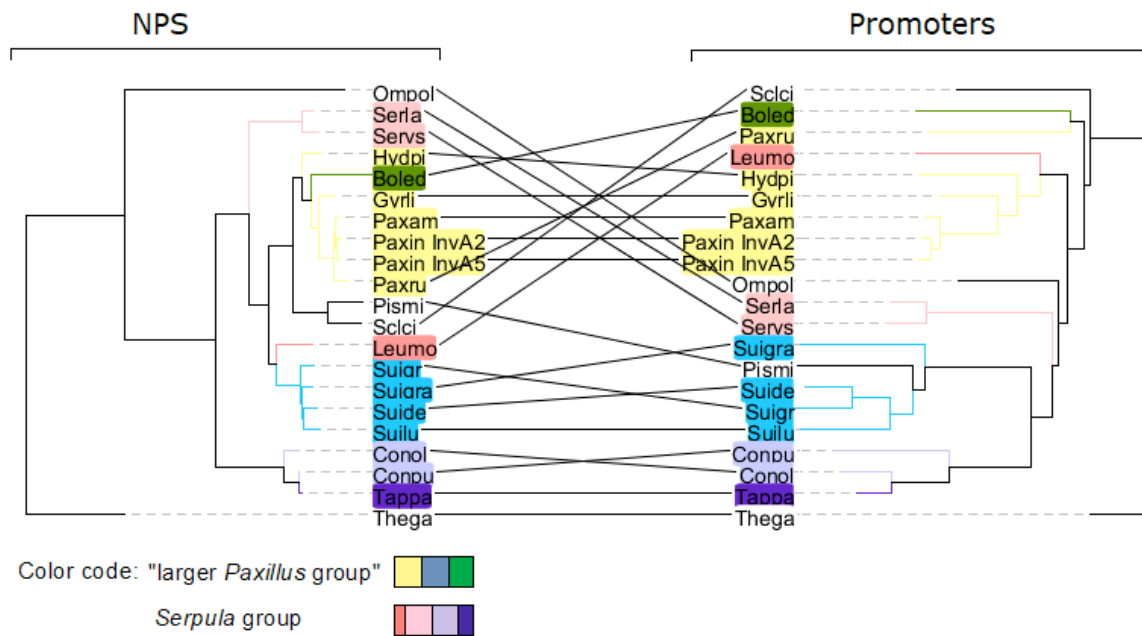


Fig. S6. Monoisotopic masses $[M-H]^-$ and UV/Vis spectra of authentic standards that were isolated for this study. Other standards (variegatic acid, xerocomic acid, isoxerocomic acid, atromentic acid, and atromentin) were isolated in our previous works [3, 25]. Ionized masses were recorded in the negative mode.



369

370 **Fig. S7.** Comparison of NPS (left) and promoter (right) trees' architectures. The
 371 combined trees include both "*Paxillaceae*" and "*Serpula*" groups (rooted by *T.*
 372 *ganbajun*). In spite of some differences in the overall tree architectures, the main
 373 groupings in promoter and NPS trees correspond to each other.

374

375

376

377

378

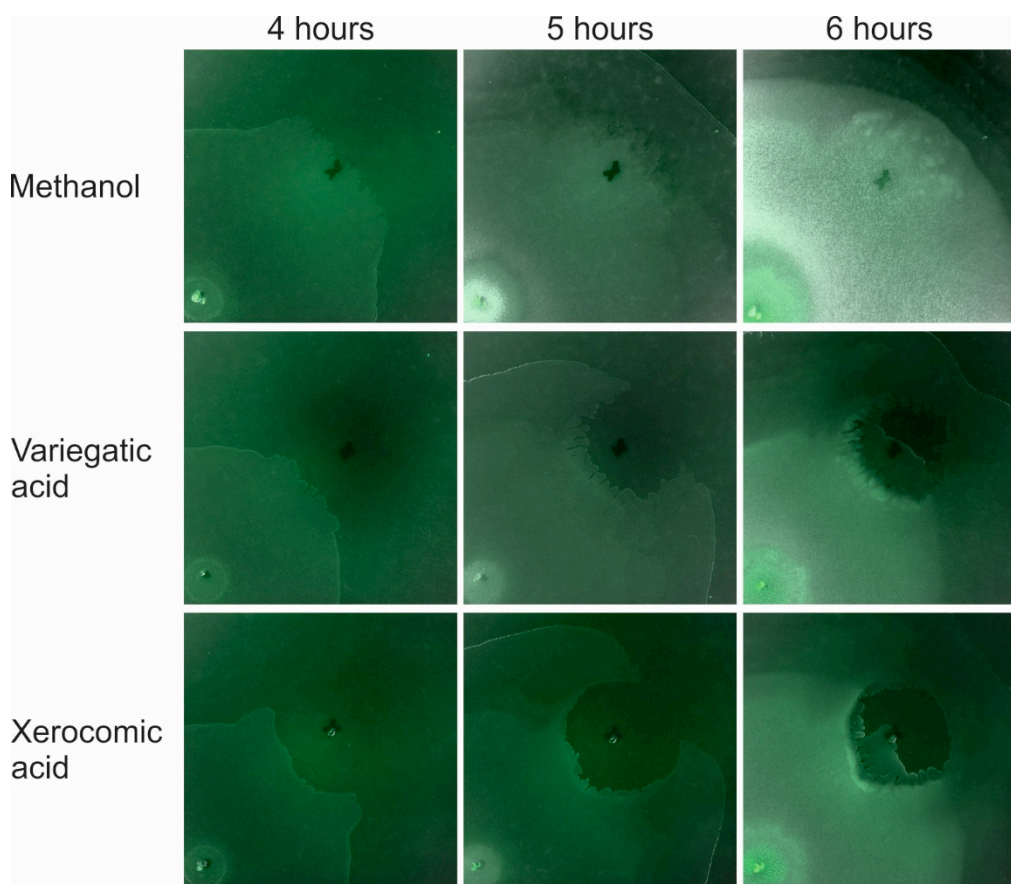
379

380

381

382

383



384

385 **Fig. S8.** Unmarked images from Fig. 5(c).

386

387

388

389

390

391

392

Target phylum	Oligonucleotide	Sequence (5'→3')	Amplicon length in bp (approximate)	Annealing temperature (°C)	Reference	Primer Efficiency (%) and R ²
<i>Actinobacteria</i>	Actino243F	CGCGGCCTATCAGCTTGTTG	275	60	[27, 28]	90.75%; 1.000
	Eub518R	ATTACCGCGGCTGCTGG				
α - <i>Proteobacteria</i>	Eub338F	ACTCTACGGGAGGCAGCAG	347	53 (54)	[7, 28]	85.91%; 0.988
	Alf685	TCTACGRATTTCACCYCTAC				
β - <i>Proteobacteria</i>	Eub338	ACTCTACGGGAGGCAGCAG	360	60	[28-30]	94.115%; 0.998
	Bet680	TCACTGCTACACGYG				
<i>Crenarchaeota</i>	Cren771F	ACGGTGAGGGATGAAAGCT	186	54	[28, 31]	100.762%; 0.990
	Cren957R	CGGCGTTGACTCCAATTG				
<i>Verrucomicrobia</i>	Ver53F	TGGCGGCGTGGWTAAGA	465	60	[28, 32]	92.903%; 1.000
	Eub518R	ATTACCGCGGCTGCTGG				
<i>Firmicutes</i>	Lgc353	GCAGTAGGGAATCTTCCG	180	60	[30, 33]	95.852%; 1.000
	Eub518R	ATTACCGCGGCTGCTGG				
<i>Bacteroidetes</i>	Cfb319	GTA CTGAGACACGGACCA	220	65	[30, 34]	93.157%; 0.998
	Eub518R	ATTACCGCGGCTGCTGG				
Eukarya (Fungi)	NL1f	ATATCAATAAGCGGAGGAAAAG	250	57	[35-37]	91.111%; 0.997
	LS2r	ATCCCAACAACCTGACTC				
Archaea	A915-for	AGG AAT TGG CGG GGG AGC AC	273	60	[38]	94.874%; 1.000
	Arc 1059r	GCC ATG CAC CWC CTC T				
Universal (bacteria)	27F	AGAGTTTGATCCTGGCTCAG	1465	55	[7, 8]	
	1492R	GGTTACCTTGTACGACTT				

Table S1. Previously published primers used in this study to amplify 16S or 28S rDNA extracted from soil samples associated with *P. involutus*, and also universal bacterial primers to identify soil isolates.

Hit taxon name	Strain; Accession	Similarity %	Completeness	Hit taxonomy	JMRC strain code
<i>Bacillus aryabhatai</i>	B8W22(T); EF114313	99.86	95.30%	Bacteria;Firmicutes;Bacilli	ST036349- T2_4
<i>Bacillus subtilis</i> subsp. <i>subtilis</i>	NCIB 3610(T); ABQL01000001	99.86	95.30%	Bacteria;Firmicutes;Bacilli	ST036350- T2_5
<i>Bacillus subtilis</i> subsp. <i>inaquosorum</i>	KCTC 13429(T); AMXN010000021	99.93	95.60%	Bacteria;Firmicutes;Bacilli	ST036351- T1_2
<i>Micromonospora aurantiaca</i>	ATCC 27029(T); CP002162	100	96.20%	Bacteria;Actinobacteria;Actinobacteria_c	ST036352- T1_4

Table S2. Bacteria isolated from the soil underneath *P. involutus* mushrooms and their identification. 16S rDNA was amplified from gDNA and sequenced using 27F and 1492R primers, and submitted to the EzBioCloud database for identification [6-8]. Soil isolates were deposited at the Jena Microbial Resource Collection (JMRC).

Species name	Abbr.	JGI protein ID	NPS			AMT			NPS			NPS						
			Motif 1	Start	p-value	Motif 1	Start	p-value	Motif 3	Start	p-value	Motif 2	Start	p-value				
<i>Boletus edulis</i> v1.0	Boled	856878	GAA GGTTC GACG	925	5.23e-4													
<i>Gyrodan lividus</i> BX v1.0	Gyrl	712553	GACG TCC AA G CA TCC GACA	899	5.1e-10	GTA CA TCT GAA	780	8.98e-6	C AA T CA GCTC	376	3.93e-6	AT G CA CA T GGCT	723	1.68e-5				
<i>Hydnorullus pinastri</i> v2.0	Hydpl	94475	GAG GTCC AA G CA TCC GAAG	895	1.5e-9	TAA GA TCT GAA	864	3.20e-5	C AA CC GG CTC	413	1.70e-5	AT G CA CA C GGCC	663	3.40e-5				
<i>Paxillus adalphus</i> Ve08.2h10 v2.0	Paxru	23383	GACG TCC AA G CA TCC CAAA	475	5.1e-10	CC GA TCC GCA	933	2.87e-5				AT G CA CA C GGCC	222	5.58e-8				
<i>Paxillus ammoniavirescens</i> Pou09.2 v1.0	Paxam	1012486	GACG TCC AA G CA TCC CAAA	727	5.1e-10	CC GA TCC GCA	653	2.87e-5	T CA T CA CCCC	668	1.46e-5	AT G CA CA C GGCC	469	5.58e-8				
<i>Paxillus involutus</i> ATCC 200175 v1.0	Paxin (InvA1)	69019	GACG TCC AA G CA TCC CAAA	902	5.1e-10	TCA GA TCC GAA	161	4.09e-6	C AA CC AA TTC	404	5.13e-6	AT G CA CA C GGCC	649	5.58e-8				
<i>Pisolithus microcarpus</i> 441 v1.0	Pismi (InvA5)	77684	GACG TCC AA G CA TCC CAAA	912	5.1e-10				C AA CC AA TTA	399	1.14e-5	AT G CA CA C GGCC	640	5.58e-8				
<i>Pisolithus microcarpus</i> 441 v1.0	Pismi	598581	GACG TCC TT G CA GGTCC GAGA	985	2.1e-10							AT A CA CA GG GTC	206	6.02e-5				
<i>Scleroderma citrinum</i> Fouq A v1.0	Sclici	1214465	CC GGT GAG CC CA	896	8.31e-4							AC GG CA T GGCC	236	2.14e-5				
<i>Suillus brevipes</i> Sb2 v2.0	Suibr	783497	GACC TCC AG G CA TCC GCAC	1383	2.08e-9	GAC GA TCT GAA	653	4.39e-5	T CA CC AG ACC	128	1.98e-5	AT G CA CA T GCTC	1003	5.04e-5				
<i>Suillus decipiens</i> EM49 v1.0	Suidec	1233902	CAA GA TCT CC CA	346	2.18e-5	TCA GA TAC GAC	434	1.97e-6				AT G CA CA T CTTC	345	3.68e-5				
<i>Suillus granulatus</i> EM37 v1.0	Suigra	377806457	GCA TA CTC CT	254	8.88e-5	GCA GT CCC AG	203	3.4e-05				GT GG T CA CGCC	556	8.54e-6				
<i>Suillus grevillei</i>	Suigr	AFB76152.1	GCA TA CGCT	538	1.64e-5							TT CA CA CC GTC	869	3.68e-5				
<i>Suillus luteus</i> UH-Slu-Lm8-n1 v2.0	Suillu	1832788	GACC TCC AG G CA TCC GCA	889	5.96e-9	GGA TA GAA	228	7.63e-6										
<i>Suillus pictus</i> EM44 v1.0	Suipic	1400428	CAA GA TCC AG CA	420	7.78e-4	TCA GA TAC GAC	469	1.97e-6				AT G CA CA CC GCC	665	7.91e-7				
<i>Thelephora ganbajun</i> P2 v1.0	Thega	3155672	GCA TA CGCA	588	3.31e-6							AT G CA CA T GGTG	464	5.18e-6				
<i>Xerocomus badius</i> 84.06 v1.0	Xerba	1510657	CA GA TCC CT	792	5.73e-4				C AA CC AG CTC	916	2.27e-7	AT G CA CA C TCCG	644	1.44e-5				
<i>Coniophora olivacea</i> MUCL 20566 v1.0	Conol	826590	TCA GA TCC GA	29	4.68e-6	TCA GA TCC GA	7	3.42e-6										
<i>Coniophora puteana</i> v1.0	Conpu	170203	GCA TT CC AT	674	1.12e-4	GCA GA TAC GAA	985	6.53e-7										
<i>Leucogyrophana mollusca</i>	Leumo	1020208	GCA GGT CC AA G	874	3.50e-7	GCT GA TCC GA	789	7.52e-6										
<i>Omphalotus olearius</i>	Ompol	7676	GCA GA CC AG	1299	5.10e-6	TCA GA TCC AA	534	5.39e-5										
<i>Serpula lacrymans</i> S7.9 v2.0	Serla	416588	GCA GA TAC AG	229	1.07e-6	GGA AA AC GA	76	2.18e-5										
<i>Serpula lacrymans</i> var shastensis SH421-2 v1.0	Serls	39620	TCA GA TCC AC	779	6.30e-6	GCA AA TAC GA	353	6.30e-6										
<i>Tapinella panuoides</i>	Tappa	ACH90386.1	CAA GA TCC GA	886	2.61e-6	GCA GA TAC GA	986	7.07e-7										

Table S3. Tabularized 23 atromentin-producing basidiomycetes, including abbreviation of species' names, used for MEME motif searches and phylogenetic work. Annotated genomes were accessed via the JGI MycoCosm portal, except for *T. panuoides* and *S. grevillei* [19, 20, 39-45]. The bolded line separates the ectomycorrhizal fungi (top) from the non-mycorrhizal/brown rot fungi (bottom). Please note that *Hydnomerulius pinastri* is a brown rotter that is part of the *Paxillaceae*. All motifs are listed with their respective position to the start site ("Start"), and *p-value*. The palindromic sequence around motif 1 is underlined. For *P. involutus*, two atromentin synthetases (*InvA2* and *InvA5*) were used [25]. *NPS* = atromentin/quinone synthetase gene; *AMT* = aminotransferase gene. Note that motif 1 shown here is the reverse complement from the same motif from our previous work [3].

References

1. **Altschul SF, Gish W, Miller W, Myers EW, Lipman DJ.** Basic local alignment search tool. *J Mol Biol* 1990;215:403-410.
2. **Barnard RL, Osborne CA, Firestone MK.** Responses of soil bacterial and fungal communities to extreme desiccation and rewetting. *ISME J* 2013;7:2229-2241.
3. **Tauber JP, Schroeckh V, Shelest E, Brakhage AA, Hoffmeister D.** Bacteria induce pigment formation in the basidiomycete *Serpula lacrymans*. *Environ Microbiol* 2016;18:5218-5227.
4. **Birnboim HC.** A rapid alkaline extraction method for the isolation of plasmid DNA. *Methods Enzymol* 1983;100:243-255.
5. **Birnboim HC, Doly J.** A rapid alkaline extraction procedure for screening recombinant plasmid DNA. *Nucleic Acids Res* 1979;7:1513-1523.
6. **Yoon SH, Ha SM, Kwon S, Lim J, Kim Y et al.** Introducing EzBioCloud: a taxonomically united database of 16S rRNA gene sequences and whole-genome assemblies. *Int J Syst Evol Microbiol* 2017;67:1613-1617.
7. **Lane DJ.** *16S/23S rRNA sequencing*. New York, NY: John Wiley and Sons; 1991.
8. **Turner S, Pryer KM, Miao VP, Palmer JD.** Investigating deep phylogenetic relationships among cyanobacteria and plastids by small subunit rRNA sequence analysis. *J Eukaryot Microbiol* 1999;46:327-338.
9. **Edwards RL, Gill M.** Constituents of the Higher Fungi Part XII. *JCS Perkin Transactions* 1973;15:1529-1537.
10. **Holzapfel M, Kilpert C, Steglich W.** Fungal Pigments. 60. Leucomentins, Colorless Precursors of Atromentin from the Mushroom *Paxillus atrotomentosus*. *Liebigs Ann Chem* 1989;8:797-801.

11. **Gruber G.** *Isolierung und Strukturaufklärung von chemotaxonomisch relevanten Sekundärmetaboliten aus höheren Pilzen, insbesondere aus der Ordnung der Boletales.* Ludwig-Maximilians-Universität München; 2002.
12. **Edwards RL, Eisworthy GC, Kale N.** Constituents of the Higher Fungi. Part IV.* Involutin, a Diphenyl-cyclopenteneone from *Paxillus involutus* (Oeder ex Fries) *JCS Perkin Transactions* 1967;15:405-409.
13. **Besl H, Bresinsky A, Kilpert C, Marschner W, Schmidt HM et al.** Isolation and Synthesis of Methyl Bovinate, an Unusual Pulvinic Acid Derivative from *Suillus bovinus* (Basidiomycetes). *Z Naturforsch* 2008;39:887-893.
14. **Steglich W, Besl H, Zipfel K.** Festlegung der Struktur von Pulvinsäuren mit Hilfe der NMR-Spektroskopie. *Z Naturforsch* 1974;29b:96-98.
15. **Gill M.** Pigments of fungi (Macromycetes). *Nat Prod Rep* 1994;11:67-90.
16. **Feling R, Polborn K, Steglich W, Mühlbacher J, Bringmann G.** The absolute configuration of the mushroom metabolites involutin and chamonixin. *Tetrahedron* 2001;57:7857–7863.
17. **Davoli P, Weber RW.** Simple method for reversed-phase high-performance liquid chromatographic analysis of fungal pigments in fruit-bodies of Boletales (Fungi). *J Chromatogr A* 2002;964:129-135.
18. **Steglich W, Furtner W, Prox A.** New pulvinic acid derivatives from *Xerocomus chrysenteron* (Bull. ex St. Amans) Quel. and studies on the question of the occurrence of anthraquinone pigments in *boletaceae*. *Z Naturforsch B* 1968;23:1044-1050.
19. **Eastwood DC, Floudas D, Binder M, Majcherczyk A, Schneider P et al.** The plant cell wall-decomposing machinery underlies the functional diversity of forest fungi. *Science* 2011;333:762-765.

20. **Kohler A, Kuo A, Nagy LG, Morin E, Barry KW et al.** Convergent losses of decay mechanisms and rapid turnover of symbiosis genes in mycorrhizal mutualists. *Nat Genet* 2015;47:410-415.
21. **Gallegos-Monterrosa R, Kankel S, Götze S, Barnett R, Stallforth P et al.** *Lysinibacillus fusiformis* M5 induces increased complexity in *Bacillus subtilis* 168 colony biofilms via hypoxanthine. *J Bacteriol* 2017;199 (doi: 10.1128/JB.00204-17).
22. **Branda SS, Gonzalez-Pastor JE, Ben-Yehuda S, Losick R, Kolter R.** Fruiting body formation by *Bacillus subtilis*. *Proc Natl Acad Sci U S A* 2001;98:11621-11626.
23. **Hölscher T, Dragos A, Gallegos-Monterrosa R, Martin M, Mhatre E et al.** Monitoring Spatial Segregation in Surface Colonizing Microbial Populations. *J Vis Exp* 2016;116 (doi: 10.3791/54752).
24. **Seccareccia I, Kovacs AT, Gallegos-Monterrosa R, Nett M.** Unraveling the predator-prey relationship of *Cupriavidus necator* and *Bacillus subtilis*. *Microbiol Res* 2016;192:231-238.
25. **Braesel J, Götze S, Shah F, Heine D, Tauber J et al.** Three redundant synthetases secure redox-active pigment production in the basidiomycete *Paxillus involutus*. *Chem Biol* 2015;22:1325-1334.
26. **Gill M, Steglich W.** Pigments of fungi (Macromycetes). *Prog Chem Org Nat Prod* 1987;51:1-317.
27. **Stach JE, Maldonado LA, Ward AC, Goodfellow M, Bull AT.** New primers for the class Actinobacteria: application to marine and terrestrial environments. *Environ Microbiol* 2003;5:828-841.
28. **Sheik CS, Beasley WH, Elshahed MS, Zhou X, Luo Y et al.** Effect of warming and drought on grassland microbial communities. *ISME J* 2011;5:1692-1700.

29. **Overmann J, Coolen MJ, Tuschak C.** Specific detection of different phylogenetic groups of chemocline bacteria based on PCR and denaturing gradient gel electrophoresis of 16S rRNA gene fragments. *Arch Microbiol* 1999;172:83-94.
30. **Fierer N, Jackson JA, Vilgalys R, Jackson RB.** Assessment of soil microbial community structure by use of taxon-specific quantitative PCR assays. *Appl Environ Microbiol* 2005;71:4117-4120.
31. **Ochsenreiter T, Selezi D, Quaiser A, Bonch-Osmolovskaya L, Schleper C.** Diversity and abundance of Crenarchaeota in terrestrial habitats studied by 16S RNA surveys and real time PCR. *Environ Microbiol* 2003;5:787-797.
32. **Stevenson BS, Eichorst SA, Wertz JT, Schmidt TM, Breznak JA.** New strategies for cultivation and detection of previously uncultured microbes. *Appl Environ Microbiol* 2004;70:4748-4755.
33. **Meier H, Amann R, Ludwig W, Schleifer KH.** Specific oligonucleotide probes for in situ detection of a major group of gram-positive bacteria with low DNA G + C content. *Syst Appl Microbiol* 1999;22:186-196.
34. **Manz W, Amann R, Ludwig W, Vancanneyt M, Schleifer KH.** Application of a suite of 16S rRNA-specific oligonucleotide probes designed to investigate bacteria of the phylum cytophaga-flavobacter-bacteroides in the natural environment. *Microbiology* 1996;142:1097-1106.
35. **Cocolin L, Manzano M, Aggio D, Cantoni C, Comi G.** A novel polymerase chain reaction (PCR) - denaturing gradient gel electrophoresis (DGGE) for the identification of *Micrococcaceae* strains involved in meat fermentations. Its application to naturally fermented Italian sausages. *Meat Sci* 2001;58:59-64.
36. **Bates ST, Garcia-Pichel F.** A culture-independent study of free-living fungi in biological soil crusts of the Colorado Plateau: their diversity and relative contribution to microbial biomass. *Environ Microbiol* 2009;11:56-67.

37. **O' Donnell K.** *Fusarium and its near relatives*. Wallingford: CAB International; 1993.
38. **Yu Y, Lee C, Kim J, Hwang S.** Group-specific primer and probe sets to detect methanogenic communities using quantitative real-time polymerase chain reaction. *Biotechnol Bioeng* 2005;89:670-679.
39. **Grigoriev IV, Cullen D, Goodwin SB, Hibbett DS, Jeffries TW et al.** Fueling the future with fungal genomics. *Mycology* 2011;2:192-209.
40. **Grigoriev IV, Nikitin R, Haridas S, Kuo A, Ohm R et al.** MycoCosm portal: gearing up for 1000 fungal genomes. *Nucleic Acids Res* 2014;42:D699-704.
41. **Schneider P, Bouhired S, Hoffmeister D.** Characterization of the atromentin biosynthesis genes and enzymes in the homobasidiomycete *Tapinella panuoides*. *Fungal Genet Biol* 2008;45:1487-1496.
42. **Wackler B, Lackner G, Chooi YH, Hoffmeister D.** Characterization of the *Suillus grevillei* quinone synthetase GreA supports a nonribosomal code for aromatic alpha-keto acids. *Chembiochem* 2012;13:1798-1804.
43. **Floudas D, Binder M, Riley R, Barry K, Blanchette RA et al.** The Paleozoic origin of enzymatic lignin decomposition reconstructed from 31 fungal genomes. *Science* 2012;336:1715-1719.
44. **Wawrzyn GT, Quin MB, Choudhary S, Lopez-Gallego F, Schmidt-Dannert C.** Draft genome of *Omphalotus olearius* provides a predictive framework for sesquiterpenoid natural product biosynthesis in Basidiomycota. *Chem Biol* 2012;19:772-783.
45. **Branco S, Gladieux P, Ellison CE, Kuo A, LaButti K et al.** Genetic isolation between two recently diverged populations of a symbiotic fungus. *Mol Ecol* 2015;24:2747-2758.

2.5. Analysis of basidiomycete pigments *in situ* by Raman spectroscopy

Tauber, J.P., Matthäus, C., Lenz, C., Hoffmeister, D., and Popp, J.

Publication has been prepared for submission. Authors have reviewed the draft.

Summary and importance

Given the increasing interest in natural products during microbial interactions, we repurposed a platform to non-invasively investigate these compounds during basidiomycete - basidiomycete and basidiomycete - bacteria interactions. This was done by applying Raman spectroscopy coupled to a microscope. Here, we could quickly, non-destructively and on a hyphal scale resolution monitor the pigment response of basidiomycetes during co-incubation. Raman spectra of induced compounds obtained *in situ* were matched to a library of measured authentic standards, thus eliminating the need for exhaustive extractions and chromatography for every sample. Notably, the pigmentation response of *S. lacrymans* during co-incubation was monitored (extension of manuscripts, 2.3. and 2.4.). Additionally, described here are three putatively new polyene or polyene-like pigments whose structural class was supported by Raman spectra and/or MS² data. Overall, our application of Raman spectroscopy to study natural products during microbial interactions will help facilitate further work to understand the role, regulation, and localization of basidiomycete natural products during competition.

Contribution to the manuscript

James Tauber contributed to the manuscript by designing (with the help of others) and executing most wet laboratory work. James Tauber cultured organisms, measured and analyzed Raman data with C.M., and wrote the majority of the manuscript (main text), including assembling the five main text figures with spectra input from the other authors. Tandem MS analyses as well as additional planning of the work was done by the other authors.

1 **Analysis of basidiomycete pigments *in situ* by Raman spectroscopy**

2

3 James P. Tauber¹, Christian Matthäus^{2,3}, Claudius Lenz¹, Dirk Hoffmeister^{1*}, Jürgen
4 Popp^{2,3*}

5

6 ¹ Department of Pharmaceutical Microbiology at the Hans Knöll Institute, Friedrich
7 Schiller University, Winzerlaer Str.2, 07745 Jena, Germany

8 ² Leibniz Institute of Photonic Technology, Albert-Einstein-Str. 9, 07745 Jena,
9 Germany

10 ³ Institute of Physical Chemistry and Abbe Center of Photonics, Friedrich-Schiller-
11 University, Helmholtzweg 4, 07743 Jena, Germany

12

13 *E-mail: Dirk.Hoffmeister@hki-jena.de

14 *E-Mail: Juergen.Popp@leibniz-ipht.de

15

16 **Running title:** Pigment identification by Raman spectroscopy

17 **Keywords:** Raman spectroscopy, basidiomycetes, natural products, pigments, multi-
18 partner interactions

19

20

21

22

23 **Abstract**

24 Basidiomycetes, *i.e.*, mushroom-type fungi, are known to produce pigments in
25 response to environmental impacts. As anti-oxidants with a high level of unsaturation,
26 these compounds can neutralize highly oxidative species. In the event of close
27 contact with other microbes, the enzymatically controlled pigment production is
28 triggered and pigment secretion is generated at the interaction zone. The
29 identification and analysis of these pigments is important to understand the defense
30 mechanism of fungi, which is essential to counteract an uncontrolled spread of
31 harmful species. Usually, a detailed analysis of the pigments is time consuming as it
32 depends on laborious sample preparation and isolation procedures. Further, the
33 applied protocols often influence the chemical integrity of the compound of interest. A
34 possibility to non-invasively investigate the pigmentation is Raman micro-
35 spectroscopy. The methodology has the potential to analyze the chemical
36 composition of the sample spatially resolved at the interaction zone. After the
37 acquisition of a representative spectroscopic library, the pigment production by
38 basidiomycetes was monitored during their response to different fungi and bacteria.
39 The presented results describe a very efficient, non-invasive way of pigment analysis
40 which can be applied with minimal sample preparation.

41

42

43

44

45

46

47 **Introduction**

48 The basidiomycetes, *i.e.*, mushroom-type fungi, are recognized for their essential role
49 in lignocellulose disintegration and as tree symbionts. Therefore, they are critical for
50 global carbon cycling and to maintain forest ecosystems. To exert their ecological
51 role, basidiomycetes have the capacity to produce diverse natural products ^{1, 2}.
52 Historically, research into these natural products has primarily been driven by drug
53 development, crop plant protection purposes, or biopolymer degradation ³. More
54 recently, increasing emphasis has been put on their ecological role in natural
55 systems, such as chemical mediators during competition or cooperation between
56 multiple organisms ⁴.

57 Typically, natural products are made via the terpene or polyketide metabolism, or
58 they derive from amino acids that may be oligomerized into more complex structures.
59 Following suit, generally multi-modular and iteratively-acting enzymes catalyze these
60 compounds, namely terpene synthases, polyketides synthases (PKSs) or non-
61 ribosomal peptide synthetases (NRPSs), respectively. Furthermore, it is a hallmark
62 feature of natural products that they are often highly modified and functionalized ¹. Of
63 particular note, many natural products feature chromophores ⁵ and some have been
64 recognized as inducible by co-cultures ⁶ or by physical injury ⁷; to protect from UV
65 light during symbiosis ⁸; to deter insects ⁹; and as iron-reductants during
66 lignocellulose breakdown ¹⁰, reviewed in ¹¹⁻¹³. Therefore, pigments from higher fungi
67 serve local and global processes, e.g., defense, and carbon cycling, respectively.

68 Among the amino acid-derived pigments, polyporic acid (**1**, Figure 1) is the simplest
69 terphenylquinone. Other very common mushroom pigments are pulvinic acid-type
70 compounds like atromentic acid (**2**), xerocomic acid (**3**), and variegatic acid (**4**, Figure
71 1), along with xerocomorubin (**5**) and variegatorubin (**6**, Figure 1). They all derive

72 from atromentin (**7**), an L-tyrosine-derived terphenylquinone, that is produced by an
73 NRPS-like dedicated synthetase and represents the central precursor also to
74 diarylcyclopentenone, and pyrandione pigments, e.g., involutin (**8**), gyroporin (**9**), and
75 the grevillins (**10-12**, Figure 1). Conversely, non-carotenoid polyenes or
76 anthraquinones are derived from formal acetate units, and their biosynthesis is
77 catalyzed by polyketide synthases ^{7, 14}.

78 The techniques used to study the aforementioned pigments were inherently
79 destructive, *i.e.*, liquid chromatography required solvent-based extraction and MALDI-
80 TOF required drying and fixation of biological material. Thus, the pigments in
81 question needed to be removed from their producers. An alternative to studying
82 chemical compounds from biological systems is Raman vibrational spectroscopy.
83 This technique can fingerprint compounds based on Stokes scattering, and has been
84 applied to bacteria, plants, fungi (mainly lichens), algae, and cyanobacteria ¹⁵. The
85 coupling of Raman spectroscopy with conventional microscopy has become a
86 popular methodology to investigate biological samples on the micrometer scale. As
87 the technique is based on the intrinsic vibrational properties of the molecules of the
88 samples, it can be used for characterization and identification with no or minimal
89 sample preparation. Over the past years, it has become a widely used and well-
90 established method for the characterization of various microorganisms ¹⁶⁻²¹. Studies
91 focusing on microbial pigments have exhaustively excluded basidiomycetes.
92 However, given the overwhelming diversity of pigments produced by this ecologically
93 important group of fungi ⁵, its absence from Raman studies warranted further
94 investigation. One relevant Raman-based example involving a basidiomycete was
95 the study of indigo pigmentation from *Schizophyllum commune* co-cultures, although

96 this analysis was coupled to a destructive technique (liquid extraction surface
97 analysis)²².

98 Here we identified basidiomycete pigments *in situ* from multi-partner cultures (fungi-
99 fungi and fungi-bacteria) by Raman spectroscopy that was appended with a
100 microscope. Using this technique, we non-invasively, quickly and on a hyphal-scale
101 resolution identified pigments without destruction of the organisms being monitored.
102 We first created a spectral library of authentic standards which showed distinguishing
103 features based on the structural class of the pigment. We then obtained hyphal-scale
104 *in situ* spectra from co-cultures, and matched these spectra to the defined library. As
105 a proof of concept, we also applied Raman spectroscopy to fruiting bodies of
106 *Laetiporus sulphureus*, *i.e.*, the chicken-of-the-woods fungus that produces the
107 polyene laetiporic acid²³, and putatively assigned unknown natural products from the
108 basidiomycetes *Paxillus involutus* (roll-rim mushroom) and *Coniophora puteana* (wet
109 rot fungus). As there is increasing interest to study natural products as part of natural
110 systems, *e.g.*, during inter-organismal competition or cooperation, our work provides
111 a basis for advantageously studying compounds during multi-partner co-cultures.
112 This is the first study to highlight the diversity of basidiomycete pigments via Raman
113 spectroscopy, and applying the references *in situ* for rapid identification.

114

115 **Materials and Methods**

116 **Growth conditions for Raman spectroscopy.** Basidiomycetes were grown on MEP
117 agar (malt extract 30 g l⁻¹, peptone 3 g l⁻¹, agar 18 g l⁻¹, pH 5.6) and/or synthetic agar
118 medium based on Modified Melin-Norkrans medium⁶. Agar plugs containing
119 mycelium were inoculated onto the MEP agar, and, depending on growth speed,
120 basidiomycetes were either plated before one another or simultaneously in opposite

121 ends of the 90 ø mm petri dish. Co-cultures of only fungi were grown on MEP, and
122 incubated at ambient temperature without exposure to light. The *Serpula lacrymans*
123 S7.9²⁴ - bacterium co-incubation system was set up exactly as previously described
124 ⁶. Specific for *Streptomyces coelicolor* A3(2), 1 ml spore stock (1×10^6 spores ml⁻¹)
125 was inoculated into 400 ml M79-Medium 426 (D-glucose monohydrate 10 g l⁻¹, bacto
126 peptone 10 g l⁻¹, casamino acids 2 g l⁻¹, yeast extract 2 g l⁻¹, NaCl 6 g l⁻¹, pH 7.8)
127 broth and incubated at 28°C with agitation (140 rpm) for 72 hours, washed three
128 times with dH₂O, and suspended in phosphate-buffered saline (pH 7.4) to be
129 inoculated atop of *S. lacrymans*. For other co-cultures, 250 µl of *Streptomyces*
130 *iranensis* (grown in M79-Medium 426 as referenced ⁶) was streaked on half the
131 circumference of a synthetic agar plate that had a pre-culture of *Fomitiporia*
132 *mediterranea* or *Hapalopilus rutilans*. Cultures were independently repeated twice. All
133 organisms tested are listed in Table 1.

134

135 **Natural product isolation and chromatography**

136 When available, authentic standards were used: i) pulvinic acid-type family
137 (variegatic, xerocomic, atromentic acids; variegatorubin, and xerocomorubin) from *S.*
138 *lacrymans* ⁶; ii) polyenes 18-methyl-19-oxoicosaenoic acid and 20-methyl-21-
139 oxodocosanoic acid from fungus BY1 ⁷; iii) atromentin, gyroporin and involutin
140 from *P. involutus* ^{25, 26}; and hypholomine B from *F. mediterranea*. β-carotene (>97%
141 purity) was purchased from Sigma. Authentic standards of grevillins, bisnoryangonin,
142 and polyporic acid were kindly provided by Professor Wolfgang Steglich (Ludwig-
143 Maximilians-Universität Munich, Germany) ²⁷.

144 Additional pigments were isolated by reverse-phase high performance liquid
145 chromatography (RP-HPLC) on an Agilent 1200 integrated system equipped with

146 either column 1 (Agilent Eclipse XDB C₁₈, 5 μm, 9.4 x 250 mm), column 2 (Agilent
147 Zorbax RX-C₁₈, 5 μm, 9.4 x 250 mm), or column 3 (Phenomenex Luna-C₁₈, 10μm,
148 21.2 x 250 mm), each fitted with a guard and held at 25°C. Runs were monitored at
149 wavelengths between 210-600 nm by a diode-array detector, and compounds
150 isolated by a signal-based integrated fraction collector. Solvents were A (0.1% (v/v)
151 trifluoroacetic acid in water) with solvent B (acetonitrile). Gradient 1 was a linear
152 increase from 5% to 100% B within 28 min, at a flow of 2 ml min⁻¹; gradient 2
153 included an initial hold at 40% for 7 min, then linear increase to 100% B within 8 min,
154 at a flow of 20 ml min⁻¹; gradient 3 began at 18% B, held for 2 min, followed by a
155 linear increase to 100% B within 13 min, at a flow of 3 ml min⁻¹.

156 *C. puteana* was grown on synthetic agar plates, and after the mycelia pigmented over
157 one month of growth, the agar and mycelia were well macerated using a scalpel and
158 inoculated in 300-500 ml synthetic broth within a 3 l glass penicillin flask which were
159 grown for up to 3-6 months. The biomass was removed from the conditioned broth
160 using a Büchner funnel, and the pigments were solubilized by the addition of
161 methanol until the mycelia appeared white. The supernatant was removed by
162 filtration, dried under reduced pressure, lyophilized, and suspended in methanol.
163 Pigments were isolated with column 2 and gradient 1. For *P. involutus*, the
164 unassigned polyenes were initially isolated as before using XAD-16N resin
165 (Amberlite, Sigma), as described²⁶. The crude extract was further purified by
166 preparative (column 3, gradient 2) and subsequent semi-preparative HPLC (column
167 1, gradient 3). Specific for the putative polyenes, UV absorbance was monitored at
168 λ=410 nm for *P. involutus* or 430 nm for *C. puteana* (reference wavelength 600 nm).
169 High-resolution (tandem) mass spectrometry runs were either done as before⁶, or
170 similar to another protocol²⁸.

171 **Raman spectroscopy**

172 Raman spectra were acquired using a WITec (Ulm, Germany) CRM Alpha-300Rplus
173 confocal Raman microscope. Excitation at 785 nm (ca. 10 mW at the sample) was
174 provided by a cw diode laser (Toptica Photonics, Gräfelingen, Germany). The
175 exciting laser radiation was coupled into a Zeiss microscope through a wavelength-
176 specific single mode optical fibre. The incident laser beam was collimated via an
177 achromatic lens and passes a band pass filter, before it is focused onto the sample
178 through the microscope objective. A Zeiss EC Epiplan-Apochromat 50x/NA=0.95 HD
179 DIC objective was used in most of the studies reported here. In the event of focusing
180 problems, a 10x/0.2 NA objective was used). The sample was located on a piezo-
181 electrically driven microscope scanning stage with an x,y resolution of ca. 3 nm and a
182 repeatability of ± 5 nm, and z resolution of ca. 0.3 nm and ± 2 nm repeatability.

183 Raman backscattered radiation was collected through the microscope objective and
184 passed through a holographic edge filter to block Rayleigh scattering and reflected
185 laser light before being focused into a multimode optical fiber. The 50 μm -diameter
186 single-mode input fiber and the 100 μm -diameter multi-mode output fiber provided
187 the optical apertures for the confocal measurement. The light emerging from the
188 output optical fiber was dispersed by a 300/mm or 600/mm grating, blazed at 800 nm.
189 The light was finally detected by a back-illuminated deep-depletion 1024 x 128 pixel
190 charge-coupled device (CCD) camera, operating at -68°C . The spatial resolution of
191 the acquired spectra was about 0.5 μm . Spectra were collected with a dwell time of
192 1-5 s. Spectra of the authentic standard samples were acquired on reusable CaF_2
193 windows in order to avoid background signals generated by common glass slides.
194 All files were opened in WITec Project 2.10 software, and imported into the OPUS
195 software package from Bruker and subjected to a background correction.

196

197 **Bioactivity tests**

198 Antimicrobial tests by the disk diffusion method for isolated pigments were carried out
199 exactly as before using bacteria and fungi strains from the Jena Microbial Resource
200 Collection (JMRC) ⁶. Pigments were suspended in methanol to a concentration of 1
201 mg ml⁻¹ of which 50 µl were applied in 9 mm holes. Methanol was used as a negative
202 control, and ciprofloxacin (5 µg ml⁻¹) and amphotericin B (DMSO/methanol at 10 µg
203 ml⁻¹) as positive controls.

204

205 **Results**

206 The presented Raman spectra are single point spectra obtained under the described
207 conditions. The most indicative spectral region of organic molecules of biological
208 origin lies in the spectral region between 1800 and 500 cm⁻¹, often referred to as the
209 fingerprint region, because of its very distinct nature that can be used for
210 identification. Almost all molecular functionalities exhibit spectral features within that
211 region, as either stretching or bending modes. CH, NH and OH stretching vibrations
212 are observed between 3750 and 2800 cm⁻¹. However, the associated band positions
213 and shapes are usually less specific and therefore not shown here. The spectral
214 region between 2800 and 1800 cm⁻¹ is normally void of any spectral information.
215 Within the fingerprint region, the most pronounced Raman bands can be readily
216 assigned to the stretching of the C=C conjugated double bonds, which are typical for
217 the pigments investigated here. The bands associated with the C=C stretches were
218 observed between about 1625 and 1525 cm⁻¹. Generally, the longer the conjugation
219 the lower the band shift associated with the stretching vibration. In the case of very

220 extended conjugation, as in the case of the polyenes, a second similarly intense
221 Raman band is observed around 1130 to 1150 cm^{-1} . Both bands are associated with
222 the anti-symmetric and symmetric variations of the vibrations, respectively. All other
223 Raman bands can be assigned to the individual fragments of the particular
224 compounds, as in this study there were often phenyl moieties and their residues or
225 functionalities. Typically, their intensities are less pronounced, but contribute
226 nonetheless to the overall appearance of the spectrum and are therefore of analytical
227 relevance.

228

229 **Spectra library from *in vitro* and *in vivo* measurements**

230 **Terphenylquinones and derivatives**

231 Compound **1**, the simplest fungal terphenylquinone examined, showed a
232 distinguishable band associated with the C=C stretching vibration at 1624 cm^{-1}
233 (Figure 1). All pulvinic acid-type pigments (**2-4**), as well as **5** and **6** had distinguishing
234 signals at 1603, 1607, 1595, 1589, and 1602 cm^{-1} , respectively. Pigments **2**, **3**, and **4**
235 showed two moderately pronounced bands at 1280 and 1381 cm^{-1} that were absent
236 from compounds with a benzofuran moiety, **5** and **6**. Vice-versa, **5** and **6** showed
237 bands at 1101 and 1255 cm^{-1} (Figure 1). Compound **7**, the central terphenylquinone
238 precursor to the pulvinic acids ²⁹ and the diarylcyclopentenones ²⁵, had a
239 distinguishable band at 1625 cm^{-1} . Diarylcyclopentenones **8** and **9** showed
240 distinguishable bands at 1611 and 1604 cm^{-1} , respectively (Figure 1). Pyrandiones
241 **10-12**, but not **7**, had a distinguishable band of 1551 cm^{-1} , which was a major band
242 shift from the other similar pigments, and with a shouldering effect observed for **10**
243 and **12** at 1592 cm^{-1} (Figure 1).

244 **Aliphatic pigments featuring conjugated double bonds**

245 The non-terpenoid polyenes, (3Z,5E,7E,9E,11E,13Z,15E,17E)-18-methyl-19-
246 oxoicosa-3,5,7,9,11,13,15,17-octaenoic acid (**13**, Figure 2) and
247 (3E,5Z,7E,9E,11E,13E,15Z,17E,19E)-20-methyl-21-oxodocosa
248 3,5,7,9,11,13,15,17,19-nonaenoic acid (**14**) from the stereaceous fungus BY1 are
249 produced by the same highly-reducing PKS, the polyene synthase PPS1, and only
250 when the mycelia is physically wounded¹⁴. We measured **13** and **14** by Raman
251 spectroscopy, and three distinctive bands were observed at 997, 1140/1147 and
252 1533 cm⁻¹ (Figure 2). Among **13** and **14**, the latter showed a band shift from 1140 to
253 1147 cm⁻¹ and a shouldering signal around 1536 cm⁻¹ when compared to **13**, due to
254 the chain extension of two carbons. β -carotene, a conjugated terpene branched-
255 chain compound, was measured and compared to those obtained from **13** and **14**, in
256 order to provide reference Raman spectra for aliphatic pigments featuring conjugated
257 double bonds. The Raman spectrum of β -carotene also exhibits three distinguishing
258 bands at 1004, 1151 and 1517 cm⁻¹, thus confirming the aliphatic nature of these
259 polyenes³⁰.

260 We expanded our measurements to the fruiting body of *Laetiporus sulphureus*.
261 Various non-carotenoid polyene pigments, termed laetiporic acids, were described
262 from this species, which are the vibrant colors seen on *Laetiporus* fruiting bodies²³,
263 ³¹. Consistent with this, Raman spectra obtained from the mushroom, both from the
264 'orange' and 'yellow' hymenia, revealed spectral patterns characteristic of polyenes
265 (1130 and 1522 cm⁻¹; (Figure 2)).

266

267 **Styrylpyrone pigments**

268 Bisnoryangonin (**15**) is a simple monomeric styrylpyrone that represents an entire
269 class of pigments produced by numerous wood-inhabiting mushrooms. Specifically,
270 its derivative hispidin attracted attention because it is a precursor of the fungal
271 luciferin that mediates bioluminescence³².

272 Pure **15** showed distinguishable bands at 1168, 1536, 1599, 1640 cm⁻¹ (Figure 2).
273 Hypholomine B (**16**), a dimeric styrylpyrone, showed a band pattern at 1117, 1159,
274 1300, 1546, 1595, 1629 cm⁻¹(Figure 2). A summary of all prominent Raman bands
275 observed for each compound class is presented in Table 2.

276

277 ***In situ* spectra from co-cultures**

278 Basidiomycetes that produce the aforementioned pigments were studied in multi-
279 partner co-cultures, and pigment induction at the interaction zones was monitored by
280 Raman spectroscopy. In all cases, Raman spectra were also obtained from axenic
281 basidiomycete cultures as controls, and the pigmented mycelia provided similar
282 spectra to those obtained from the authentic standards. These spectra are aligned
283 with those obtained from the co-cultures.

284

285 **Fungal co-cultures**

286 Since wood- and root-rotting basidiomycetes are immobile, wood habitat-sharing
287 organisms, and given that natural compounds are often highly functionalized as
288 defense molecules, it is presumable that two or three fungi could co-exist, and
289 interactions between them could induce a pigment defense response. Here we
290 sought to investigate such interactions non-invasively by Raman spectroscopy.

291 We initially set up dual co-incubations of fungi: i) fungus BY1 - *Armillaria mellea*, ii)
292 fungus BY1 - *Omphalotus subilludens*, and iii) *Serpula lacrymans* - fungus BY1. As
293 representative examples, we show spectra obtained from the dual-cultures *S.*
294 *lacrymans* - fungus BY1 and fungus BY1 - *A. mellea*. We identified each fungus'
295 respective pigments via Raman spectroscopy at the fungal interaction zones (Figure
296 3). We then made the culture more complex in a tripartite co-culture with BY1, *H.*
297 *rutilans*, and *S. lacrymans*, each producing a different class of pigments. Generally,
298 excessive pigmentation was observed only at the interaction zone; however, aged *S.*
299 *lacrymans* will pigment over time when grown on a complex medium²⁴, and fungus
300 BY1 will also pigment during inoculation where the mycelial has been wounded by
301 scalpel⁷. As in the cases above with dual co-cultures, Raman measurements of the
302 tri-partite culture at an interaction zones identified pigments easily and rapidly (Figure
303 3).

304 **Fungus-bacterium co-cultures**

305 As co-inhabiting fungi are to be expected, so is the possibility of fungi with bacteria.
306 We used our *S. lacrymans* co-incubation system for which we have shown that
307 various bacteria induce the atromentin gene cluster in *S. lacrymans* (*i.e.*, the genetic
308 basis for atromentin biosynthesis), and subsequent accumulation of atromentin-
309 derived pulvinic acid-type pigments⁶. The pigments produced during co-incubation
310 were previously identified as **2**, **3**, and **4**. To bypass such lengthy preparation and
311 chromatography runs as done before, we turned to Raman spectroscopy, and
312 monitored co-cultures of *S. lacrymans* with either *Streptomyces iranensis*, *Bacillus*
313 *subtilis* NCIB 3610, *Pseudomonas putida*, *Arthrobacter* spp., or *Streptomyces*
314 *coelicolor* A3(2). The Raman spectra obtained of the mycelia adjacent to the bacterial

315 inocula showed the formation of these pigments, although not at a resolution able to
316 individually identify the varying degree of hydroxylation (Figure 4).

317 We also tested co-incubation plates of *F. mediterranea* or *H. rutilans* grown at a
318 distance from *S. iranensis*. In these plates, we observed earlier pigmentation of the
319 fungus in co-incubation plates than when the fungus was grown axenically. Their
320 pigments (**16** and **1**, respectively) were confirmed rapidly by Raman spectroscopy
321 (Figure 4). Specific for *F. mediterranea*, heightened pigmentation appeared at
322 mycelia closest to the bacterial inoculum. Lastly, **16** from *F. mediterranea* and **1** from
323 *H. rutilans* were tested for antibacterial and antifungal activity by the disk diffusion
324 method, from which only the latter showed relative bioactivity that was compatible
325 with described data ^{33, 34}.

326

327 **Identification of new natural products**

328 Low titers or unavailability of sufficient material may prevent research into new fungal
329 compounds. To validate the concept, we sought to apply our Raman-based approach
330 to unknown compounds that were identified from the secretome of *P. involutus* or
331 mycelium of *C. puteana* during purification of other pigments and Raman
332 measurement of pigmented mycelia, respectively. The compounds were isolated by
333 RP-HPLC and initially assigned by their UV-Vis spectra obtained by a diode array
334 detector (Figure 5A, 5B). The UV-Vis spectra with absorbance in the approximate
335 340-460 nm range were similar to other compounds featuring extended conjugated
336 double bond systems, including piptoporic acid ³⁵, laetiporic acid ²³, carotenoids, and
337 polyenes **13** and **14** ⁷. The assignment to this class of natural products was further
338 supported by Raman spectroscopy, which yielded spectra similar to **13** and **14** as
339 well as to β -carotene (Figure 2). From *P. involutus*, the two compounds isolated were

340 termed putative “Pax polyene 1” and “Pax polyene 2”, and high-resolution mass
341 spectrometry revealed ionized masses of m/z 471.2489 [M-H]⁻ and 485.2643 [M-H]⁻
342 (calculated for C₂₆H₃₅O₆N₂ m/z 471.2495 and for C₂₇H₃₇O₆N₂ 485.2651, respectively).
343 The Raman spectra obtained for “Pax polyene 2” showed a band shift of the
344 asymmetric C=C stretching mode from 1530 to 1525 cm⁻¹ and a shouldering effect of
345 the band 1533 cm⁻¹ compared to the band from “Pax polyene 1”. Efforts to elucidate
346 the structures of these polyenes from *P. involutus* by NMR spectroscopy were
347 prevented by their low abundance; extensive preparative work yielded less than 100
348 µg of putative “Pax polyene 2” out of 10 l of liquid cultures of *P. involutus*. Analyzing
349 MS²-spectra alongside with the high resolution mass spectrometry isotope pattern of
350 [M-H]⁻ and making use of the software SIRIUS³⁶ corroborated the assumed sum
351 formula of “Pax polyene 2” (Figure 5C). The MS² spectrum showed characteristic
352 neutral losses of MeOH ([M-32]⁻), and CO₂ ([M-44]⁻), indicating methoxy and carboxy
353 functions, respectively. Neutral loss of [M-129]⁻ as well as the fragment m/z 130
354 pointed at the existence of a C₆H₁₃NO₂ moiety in both putative polyenes,
355 speculatively (iso-)leucine. Additional losses of C₃H₂O₃ (often observed with malonyl
356 groups) and C₇H₉NO₂ gave rise to the well abundant fragment ion m/z 185,
357 corresponding to [C₁₃H₁₃O]⁻. This observation implied that out of the 10.5 double
358 bond equivalents of [M-H]⁻, 7.5 remained in this very fragment, leading to the
359 assumption that the respective part of the molecule had a high degree of conjugation
360 as one would expect for a polyene structure.

361 *C. puteana* is known for producing **4**²⁹ (Figure 1). The rationale to isolate a new
362 compound from its yellowed mycelia arose from Raman measurements. The *in situ*
363 spectrum of the unknown compound featured a characteristic band pattern
364 suggestive of a conjugated hydrocarbon chain, rather than **4** or another pulvinic acid

365 (Figure 2). The compound was isolated and putatively assigned as above and termed
366 “Con polyene.” The molecular mass was m/z 329.2324 [M-H]⁻ (calculated for
367 C₁₈H₃₃O₅ m/z 329.2327).

368

369 **Discussion**

370 Studying multi-partner interactions provides new insight into chemical ecology and
371 the natural products that mediate chemical communication or competition¹. In our
372 previous work, induction of bioactive pigments in basidiomycetes by other fungi or
373 bacteria appeared ubiquitous which incited further interests into this phenomenon.
374 This prompted us to search for advanced techniques to facilitate studies thereof. The
375 number of accessible basidiomycete genomes increases exponentially³⁷. While this
376 is a positive development, usually the number of genetically identified natural product
377 pathways exceeds the number of known compounds from the same species.
378 Consequently most natural products still remain “dark matter”³⁸. Raman
379 spectroscopy was useful in compound identification on agar plates and on isolated
380 mushrooms. Given the advancements of portable Raman spectrometers, one could
381 envisage applying Raman spectroscopy to analyze fungi in an even more natural
382 context, as only very minor amounts are required and spatial resolution is
383 unparalleled. In our case, Raman assisted in the assignment of three new
384 compounds, and even facilitated in the initial discovery phase for a natural product. In
385 this particular case, *C. puteana* was known to produce **4**, *i.e.*, a yellow pigment which
386 we presumed to be the compound that was causing the mycelia to be pigmented. In
387 fact, obtained Raman spectra suggested an as-of-yet undescribed putative polyene.
388 For *P. involutus*, we also isolated two putative polyenes that were supported by its
389 spectral characteristics. To our knowledge, there is no literature describing such

390 compounds from these fungi. Polyenes are notoriously difficult in studying as
391 structure prediction by the PKS enzymatic module is not possible¹⁴ and the
392 compounds photoisomerize upon exposure to light.

393 A main benefit of applying Raman spectroscopy, when additionally coupled to a
394 microscope, is the non-destructive nature of the measurements. Alternatively, Matrix
395 Assisted Laser Desorption/Ionization-time of flight-mass spectrometry (MALDI-TOF-
396 MS) would have been a solution to avoid exhaustive solvent extractions and lengthy
397 liquid chromatography runs, yet obtain spectra at a precise locus, as was done
398 recently for the wound-induced polyenes from fungus BY1¹⁴. However, whereas we
399 could immediately measure and re-measure over time without any preparation or
400 destruction, in addition to focusing at an even finer resolution (*i.e.*, at a micrometer,
401 hyphal scale), MALDI-TOF MS would have been more laborious with less resolution.
402 Raman spectroscopy was even applicable for measurement on fruiting bodies as
403 also done previously with MALDI imaging of the button mushroom³⁹. That said,
404 MALDI-TOF is superior as this technique allows for total ionization of the sample
405 which can facilitate discovery of novel compounds³⁹. Also, MALDI-TOF is a possible
406 alternative to measure compounds that only produce fluorescence in Raman.
407 Generally, the concurrent generation of a fluorescence background by exciting the
408 Raman signal with a visible laser is one of the major drawbacks of the technique and
409 can be a limiting factor for certain applications especially under field conditions. The
410 problem can be avoided to a great extent by using NIR excitation ($\lambda=785$ nm), and by
411 applying long illumination times prior to the measurement to efficiently photo-bleach
412 the sample. However, for routine usage, non-visible excitation at, for example,
413 $\lambda=1064$ nm may be a better solution¹⁵. All together, we showed that Raman
414 spectroscopy was nonetheless an advantageous technique to studying biological

415 systems, and future investigations may couple MALDI-TOF and Raman spectroscopy
416 to combine spatial and temporal monitoring of biological phenomena, and to combine
417 advantageous aspects of both methods.

418 Overall, the role of basidiomycete pigments during confrontation with other diverse
419 organisms warrants further work, and can be accelerated with non-invasive
420 spectroscopic techniques.

421

422 **Acknowledgments**

423 We thank Nico Ueberschaar (Friedrich Schiller University Jena) for high-resolution
424 mass spectrometry runs, and Andrea Perner and Christiane Weigel (both Hans Knöll
425 Institute, Jena) for high-resolution mass spectrometry runs and antimicrobial assays,
426 respectively. We thank Professor Wolfgang Steglich (Ludwig-Maximilians-University
427 Munich), Jana Braesel and Daniel Braga (Hans Knöll Institute, Jena) for providing
428 authentic standards. This work was supported by the Collaborative Research Center
429 ChemBioSys (grant SFB1127/1), and C.L. acknowledges a doctoral fellowship by the
430 International Leibniz Research School for Microbial Interactions.

431

432 **Conflict of interest**

433 The authors declare that conflicts of interest do not exist.

434 **References**

435 [1] C. Schmidt-Dannert *Curr Opin Chem Biol.* **2016**, *31*, 40-49.

436 [2] G. Lackner, M. Misiek, J. Braesel, D. Hoffmeister *Fungal Genet Biol.* **2012**, *49*,
437 996-1003.

- 438 [3] I. V. Grigoriev, D. Cullen, S. B. Goodwin, D. S. Hibbett, T. W. Jeffries, C. Kubicek,
439 J. K. Magnuson, F. Martin, J. W. Spatafora, A. Tsang, S. E. Baker *Mycology*. **2011**, 2,
440 192-209.
- 441 [4] A. A. Brakhage, V. Schroeckh *Fungal Genetics and Biology*. **2011**, 48, 15-22.
- 442 [5] Z. Y. Zhou, J. K. Liu *Nat Prod Rep*. **2010**, 27, 1531-1570.
- 443 [6] J. P. Tauber, V. Schroeckh, E. Shelest, A. A. Brakhage, D. Hoffmeister *Environ*
444 *Microbiol*. **2016**, 18, 5218-5227.
- 445 [7] D. Schwenk, M. Nett, H. M. Dahse, U. Horn, R. A. Blanchette, D. Hoffmeister *J*
446 *Nat Prod*. **2014**, 77, 2658-2663.
- 447 [8] F. Lohezic-Le Devehat, B. Legouin, C. Couteau, J. Boustie, L. Coiffard *J*
448 *Photochem Photobiol B*. **2013**, 120, 17-28.
- 449 [9] H. Besl, C. H. Krump, M. Schefcsik *Zeitschrift für Mykologie*. **1987**, 53, 273-282.
- 450 [10] F. Shah, D. Schwenk, C. Nicolas, P. Persson, D. Hoffmeister, A. Tunlid *Appl*
451 *Environ Microbiol*. **2015**, 81, 8427-8433.
- 452 [11] P. Spiteller *Chemistry*. **2008**, 14, 9100-9110.
- 453 [12] P. Spiteller *Nat Prod Rep*. **2015**, 32, 971-993.
- 454 [13] H. Halbwachs, J. Simmel, C. Bassler *Fungal Biology Reviews*. **2016**, 30, 36-61.
- 455 [14] P. Brandt, M. Garcia-Altare, M. Nett, C. Hertweck, D. Hoffmeister *Angew Chem*
456 *Int Ed*. **2017**, 56, 5937-5941.
- 457 [15] J. Jehlicka, H. G. Edwards, A. Oren *Appl Environ Microbiol*. **2014**, 80, 3286-
458 3295.
- 459 [16] J. P. Harrison, D. Berry *Front Microbiol*. **2017**, 8, 675.
- 460 [17] B. Lorenz, C. Wichmann, S. Stockel, P. Rosch, J. Popp *Trends Microbiol*. **2017**,
461 25, 413-424.
- 462 [18] W. E. Huang, M. Li, R. M. Jarvis, R. Goodacre, S. A. Banwart *Adv Appl*
463 *Microbiol*. **2010**, 70, 153-186.

- 464 [19] A. Silge, E. Abdou, K. Schneider, S. Meisel, T. Bocklitz, H. Lu-Walther, R.
465 Heintzmann, P. Rösch, J. Popp *Cell Microbiol.* **2015**, *17*, 832-842.
- 466 [20] B. Kumar, B. Kampe, P. Rösch, J. Popp *Analyst.* **2015**, *140*, 4584-4593.
- 467 [21] K. Grosser, L. Zedler, M. Schmitt, B. Dietzek, J. Popp, G. Pohnert *Biofouling.*
468 **2012**, *28*, 687-696.
- 469 [22] R. C. Menezes, M. Kai, K. Krause, C. Matthäus, A. Svatos, J. Popp, E. Kothe
470 *Anal Bioanal Chem.* **2015**, *407*, 2273-2282.
- 471 [23] P. Davoli, A. Mucci, L. Schenetti, R. W. Weber *Phytochemistry.* **2005**, *66*, 817-
472 823.
- 473 [24] D. C. Eastwood, D. Floudas, M. Binder, A. Majcherczyk, P. Schneider, A. Aerts,
474 F. O. Asiegbu, S. E. Baker, K. Barry, M. Bendixby, M. Blumentritt, P. M. Coutinho,
475 D. Cullen, R. P. de Vries, A. Gathman, B. Goodell, B. Henrissat, K. Ihrmark, H.
476 Kauserud, A. Kohler, K. LaButti, A. Lapidus, J. L. Lavin, Y. H. Lee, E. Lindquist, W.
477 Lilly, S. Lucas, E. Morin, C. Murat, J. A. Oguiza, J. Park, A. G. Pisabarro, R. Riley, A.
478 Rosling, A. Salamov, O. Schmidt, J. Schmutz, I. Skrede, J. Stenlid, A. Wiebenga, X.
479 Xie, U. Kües, D. S. Hibbett, D. Hoffmeister, N. Högberg, F. Martin, I. V. Grigoriev, S.
480 C. Watkinson *Science.* **2011**, *333*, 762-765.
- 481 [25] J. Braesel, S. Götze, F. Shah, D. Heine, J. Tauber, C. Hertweck, A. Tunlid, P.
482 Stallforth, D. Hoffmeister *Chem Biol.* **2015**, *22*, 1325-1334.
- 483 [26] J. Tauber, R. Gallegos-Monterrosa, A. Kovacs, E. Shelest, D. Hoffmeister
484 *Microbiology.* **2017**, accepted.
- 485 [27] M. Gill *Nat Prod Rep.* **1994**, *11*, 67-90.
- 486 [28] J. F. Mori, N. Ueberschaar, S. Lu, R. E. Cooper, G. Pohnert, K. Kusel *ISME J.*
487 **2017**, *11*, 1075-1086.
- 488 [29] M. Gill, W. Steglich *Prog Chem Org Nat Prod.* **1987**, *51*, 1-317.

- 489 [30] I. V. Ermakov, M. Sharifzadeh, M. Ermakova, W. Gellermann *J Biomed Opt.*
490 **2005**, *10*, 064028.
- 491 [31] R. W. S. Weber, A. Mucci, P. Davoli *Tetrahedron Letters.* **2004**, *45*, 1075-1078.
- 492 [32] K. V. Purtov, V. N. Petushkov, M. S. Baranov, K. S. Mineev, N. S. Rodionova, Z.
493 M. Kaskova, A. S. Tsarkova, A. I. Petunin, V. S. Bondar, E. K. Rodicheva, S. E.
494 Medvedeva, Y. Oba, Y. Oba, A. S. Arseniev, S. Lukyanov, J. I. Gitelson, I. V.
495 Yampolsky *Angew Chem Int Ed.* **2015**, *54*, 8124-8128.
- 496 [33] D. Brewer, W. S. Maass, A. Taylor *Can J Microbiol.* **1977**, *23*, 845-851.
- 497 [34] D. Brewer, W. C. Jen, G. A. Jones, A. Taylor *Can J Microbiol.* **1984**, *30*, 1068-
498 1072.
- 499 [35] M. Gill in Polyolefinic 18-methyl-19-oxoicosenoic acid pigments from the fungus
500 *Piptoporus australiensis* (Wakefield) Cunningham Vol. 13 (Ed.^Eds.: Editor), City,
501 **1982**.
- 502 [36] S. Bocker, M. C. Letzel, Z. Liptak, A. Pervukhin *Bioinformatics.* **2009**, *25*, 218-
503 224.
- 504 [37] I. V. Grigoriev, R. Nikitin, S. Haridas, A. Kuo, R. Ohm, R. Otilar, R. Riley, A.
505 Salamov, X. Zhao, F. Korzeniewski, T. Smirnova, H. Nordberg, I. Dubchak, I.
506 Shabalov *Nucleic Acids Res.* **2014**, *42*, D699-704.
- 507 [38] T. Wakimoto *Chem Rec.* **2017**.
- 508 [39] K. Graupner, K. Scherlach, T. Bretschneider, G. Lackner, M. Roth, H. Gross, C.
509 Hertweck *Angew Chem Int Ed.* **2012**, *51*, 13173-13177.
- 510 [40] S. D. Bentley, K. F. Chater, A. M. Cerdeno-Tarraga, G. L. Challis, N. R.
511 Thomson, K. D. James, D. E. Harris, M. A. Quail, H. Kieser, D. Harper, A. Bateman,
512 S. Brown, G. Chandra, C. W. Chen, M. Collins, A. Cronin, A. Fraser, A. Goble, J.
513 Hidalgo, T. Hornsby, S. Howarth, C. H. Huang, T. Kieser, L. Larke, L. Murphy, K.
514 Oliver, S. O'Neil, E. Rabinowitsch, M. A. Rajandream, K. Rutherford, S. Rutter, K.

515 Seeger, D. Saunders, S. Sharp, R. Squares, S. Squares, K. Taylor, T. Warren, A.
516 Wietzorrek, J. Woodward, B. G. Barrell, J. Parkhill, D. A. Hopwood *Nature*. **2002**,
517 *417*, 141-147.

518 [41] A. Kohler, A. Kuo, L. G. Nagy, E. Morin, K. W. Barry, F. Buscot, B. Cănbăck, C.
519 Choi, N. Cichocki, A. Clum, J. Colpaert, A. Copeland, M. D. Costa, J. Dore, D.
520 Floudas, G. Gay, M. Girlanda, B. Henrissat, S. Herrmann, J. Hess, N. Hogberg, T.
521 Johansson, H. R. Khouja, K. LaButti, U. Lahrmann, A. Levasseur, E. A. Lindquist, A.
522 Lipzen, R. Marmeisse, E. Martino, C. Murat, C. Y. Ngan, U. Nehls, J. M. Plett, A.
523 Pringle, R. A. Ohm, S. Perotto, M. Peter, R. Riley, F. Rineau, J. Ruytinx, A. Salamov,
524 F. Shah, H. Sun, M. Tarkka, A. Tritt, C. Veneault-Fourrey, A. Zuccaro, A. Tunlid, I. V.
525 Grigoriev, D. S. Hibbett, F. Martin *Nat Genet*. **2015**, *47*, 410-415.

526 [42] S. S. Branda, J. E. Gonzalez-Pastor, S. Ben-Yehuda, R. Losick, R. Kolter *Proc*
527 *Natl Acad Sci U S A*. **2001**, *98*, 11621-11626.

528 [43] M. Misiek, J. Williams, K. Schmich, W. Huttel, I. Merfort, C. E. Salomon, C. C.
529 Aldrich, D. Hoffmeister *J Nat Prod*. **2009**, *72*, 1888-1891.

530 [44] F. Horn, V. Schroeckh, T. Netzker, R. Guthke, A. A. Brakhage, J. Linde *Genome*
531 *Announc*. **2014**, *2*.

532 [45] K. Wagner, R. Gallegos-Monterrosa, D. Sammer, Á. T. Kovács, K. Krause, E.
533 Kothe *Submitted for publication*.

534 [46] D. Floudas, M. Binder, R. Riley, K. Barry, R. A. Blanchette, B. Henrissat, A. T.
535 Martinez, R. Otilar, J. W. Spatafora, J. S. Yadav, A. Aerts, I. Benoit, A. Boyd, A.
536 Carlson, A. Copeland, P. M. Coutinho, R. P. de Vries, P. Ferreira, K. Findley, B.
537 Foster, J. Gaskell, D. Glotzer, P. Gorecki, J. Heitman, C. Hesse, C. Hori, K. Igarashi,
538 J. A. Jurgens, N. Kallen, P. Kersten, A. Kohler, U. Kues, T. K. Kumar, A. Kuo, K.
539 LaButti, L. F. Larrondo, E. Lindquist, A. Ling, V. Lombard, S. Lucas, T. Lundell, R.
540 Martin, D. J. McLaughlin, I. Morgenstern, E. Morin, C. Murat, L. G. Nagy, M. Nolan,

541 R. A. Ohm, A. Patyshakuliyeva, A. Rokas, F. J. Ruiz-Duenas, G. Sabat, A. Salamov,
542 M. Samejima, J. Schmutz, J. C. Slot, F. St John, J. Stenlid, H. Sun, S. Sun, K. Syed,
543 A. Tsang, A. Wiebenga, D. Young, A. Pisabarro, D. C. Eastwood, F. Martin, D.
544 Cullen, I. V. Grigoriev, D. S. Hibbett *Science*. **2012**, 336, 1715-1719.

545

546 **Figure legends**

547 **Figure 1:** Raman spectra obtained from authentic standards of terphenylquinone-
548 derived pigments with their structures. *H. rutilans* produced polyporic acid (**1**). *S.*
549 *lacrymans* produced the pulvinic acid-type pigments atromentic acid (**2**), xerocomic
550 acid (**3**), variegatic acid (**4**), xerocomorubin (**5**), and variegatorubin (**6**). *P. involutus*
551 produced atromentin (**7**), involutin (**8**), and gyroporin (**9**). *Suillus* sp. produced
552 grevillins A (**10**), B (**11**), and C (**12**).

553 **Figure 2:** Raman spectra obtained from authentic standards of polyene-based,
554 putative polyene, and styrylpyrone pigments with their structures, if available. Fungus
555 BY1 produced two polyenes, 18-methyl-19-oxoicosaoctaenoic acid (**13**) and 20-
556 methyl-21-oxodocosanonaenoic acid (**14**). Putative polyenes from *P. involutus* (“Pax
557 polyene 1” and “Pax polyene 2”) were isolated and measured. A putative polyene
558 from *C. puteana* (con polyene) was also isolated. Shown here is an additional Raman
559 spectrum obtained *in situ* from the pigmented mycelium. The putative polyenes were
560 measured with 600 grooves. A Raman spectrum from a fruiting body of *L. sulphureus*
561 was obtained, which also showed the typical spectral features of polyenes. Raman
562 spectra of bisnoryangonin (**15**) and hypholomine B (**16**), the latter produced by *F.*
563 *mediterranea*, are also provided.

564 **Figure 3:** Raman spectra obtained *in situ* from fungal co-cultures, and compared to
565 reference spectra of authentic standards and fungal cultures to confirm pigment

566 identity. Individual colored dots per species mark the inoculum point of the fungus,
567 and arrows show from where Raman spectra were obtained. At the interaction zone
568 from each co-culture, known pigments from each fungus were identified: **13** from
569 BY1, **1** from *H. rutilans* and **4** from *S. lacrymans*. Three co-cultures were monitored at
570 their interaction zones: the dual fungal culture BY1 and *S. lacrymans*; the dual fungal
571 culture BY1 and *A. mellea*; and the tri-culture of BY1, *H. rutilans*, and *S. lacrymans*.

572 **Figure 4:** Raman spectra obtained *in situ* from basidiomycete-bacterium co-cultures.
573 *S. lacrymans* – *Arthrobacter* sp. is shown as a representative example for co-
574 cultures. Note the yellow pigmentation around the bacterial inocula (pink). *In situ*-
575 obtained spectra were compared to that of **4** to confirm its presence. Mycelia
576 measured outside of this area provided a negative control. *F. mediterranea* was
577 grown as a pre-culture (17 days), and *S. iranensis* was then streaked on the edge of
578 the plate. Shown are pictures 3 days after the onset of co-incubation, and Raman
579 spectra obtained *in situ* that confirmed the increased production of **16**. Lastly, *H.*
580 *rutilans* was grown as a pre-culture (17 days), and *S. iranensis* was streaked on the
581 edge of the plate. Shown are pictures 3 days after the onset of co-incubation, and
582 Raman spectra that confirmed pigment **1**.

583 **Figure 5:** Additional spectroscopic data supporting the putative polyenes. For *P.*
584 *involutus*, composite RP-HPLC chromatograms ($\lambda=410$ nm) of isolated compounds
585 with their respective UV-Vis spectrum and ionized masses obtained by high
586 resolution mass spectrometry. For *C. puteana*, a RP-HPLC chromatogram ($\lambda=450$
587 nm) of the isolated compound with its respective UV-Vis spectrum and ionized
588 masses. Structures were putatively assigned by their UV-Vis spectra and Raman
589 spectra (Figure 2). For “Pax polyene 2”, tandem MS data that supports its chemical
590 structure.

591

592

Basidiomycete	Reference	Bacterium	Reference
<i>Serpula lacrymans</i> S7.9	24	<i>Streptomyces coelicolor</i> A3(2)	40
<i>Paxillus involutus</i> ATCC200175	41	<i>Bacillus subtilis</i> NCIB3610	42
<i>Armillaria mellea</i> DSM3731	43	<i>Pseudomonas putida</i>	ST036147
<i>Omphalotus subilludens</i>	CBS660.85	<i>Streptomyces iranensis</i>	44
<i>Coniophora puteana</i>	46	<i>Arthrobacter</i> sp.	45
<i>Hapalopilus rutilans</i>	CBS490.95	<i>Acinetobacter</i> spp.	45
<i>Fomitiporia mediterranea</i>	46		

593

594 **Table 1:** Organisms used in this work. References are given as publications or strain
595 collection number from the respective strain collection.

596

597

598

Compound class	Most prominent observed bands
Terphenylquinone-derived	1589-1625 (for grevillins only: 1551)
Pulvinic acid-type	1589-1601
Terphenyl benzoquinone	1625
Diarylcyclopentenone	1606-1613
Grevillin	1551
Conjugated hydrocarbon chain	1142-1152, 1511-1536
Polyene	1142, 1533
β -Carotene	1152, 1511
Styrylpyrone	1164, 1537-1635
Monomer	1164, 1537-1635 (1537, 1601 ⁺ , 1635 ⁺)
Dimer	1164, 1550-1629 (1550, 1595 ⁺ , 1629 ⁺)

599

600 **Table 2:** Summary of the most prominent Raman spectral bands that were used to
601 categorize the pigments. Specific pigments were sub-grouped under each main
602 category, and the wavenumbers provided for the main groups were based on
603 summarized data from the subgroups. Values are given in relative band positions,
604 (cm^{-1}). Only compounds that have been structurally elucidated were included.

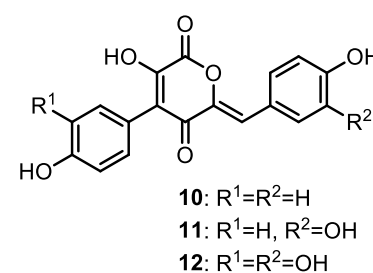
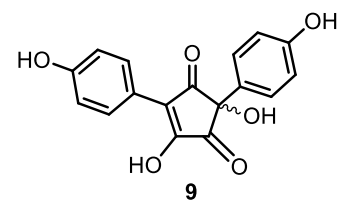
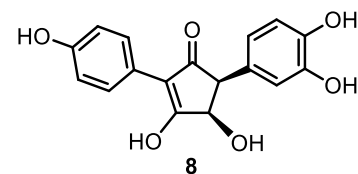
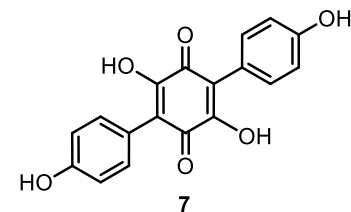
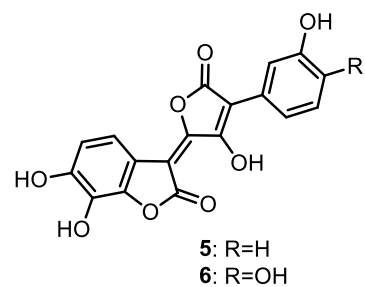
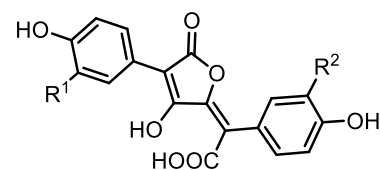
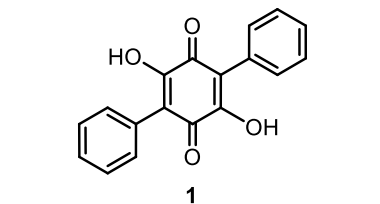
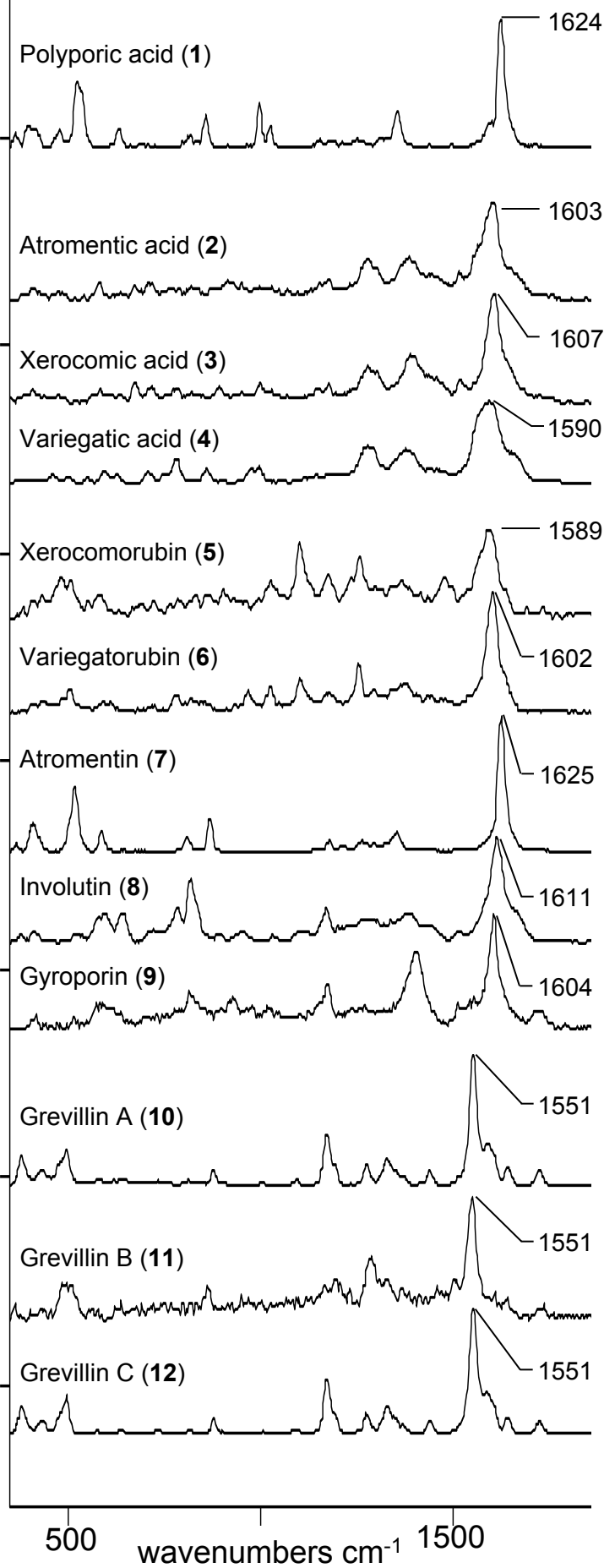
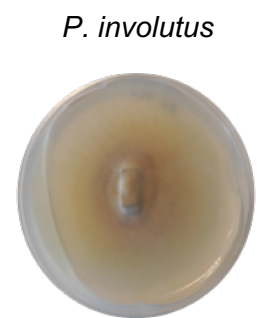
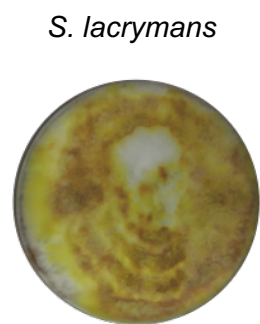
605 ⁺Shouldering effect of band.

606

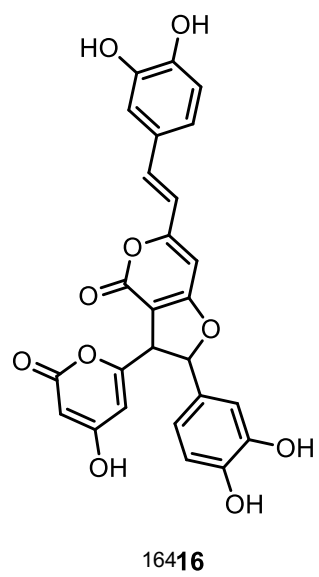
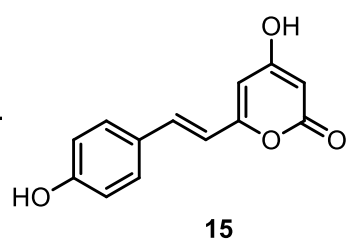
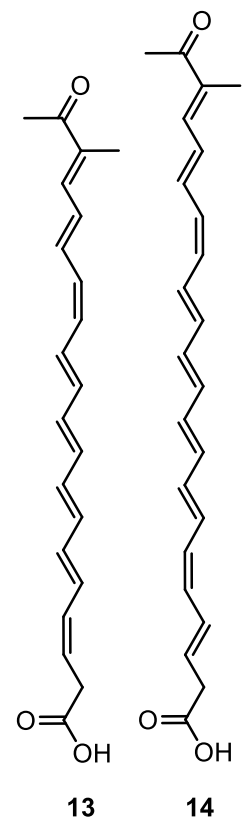
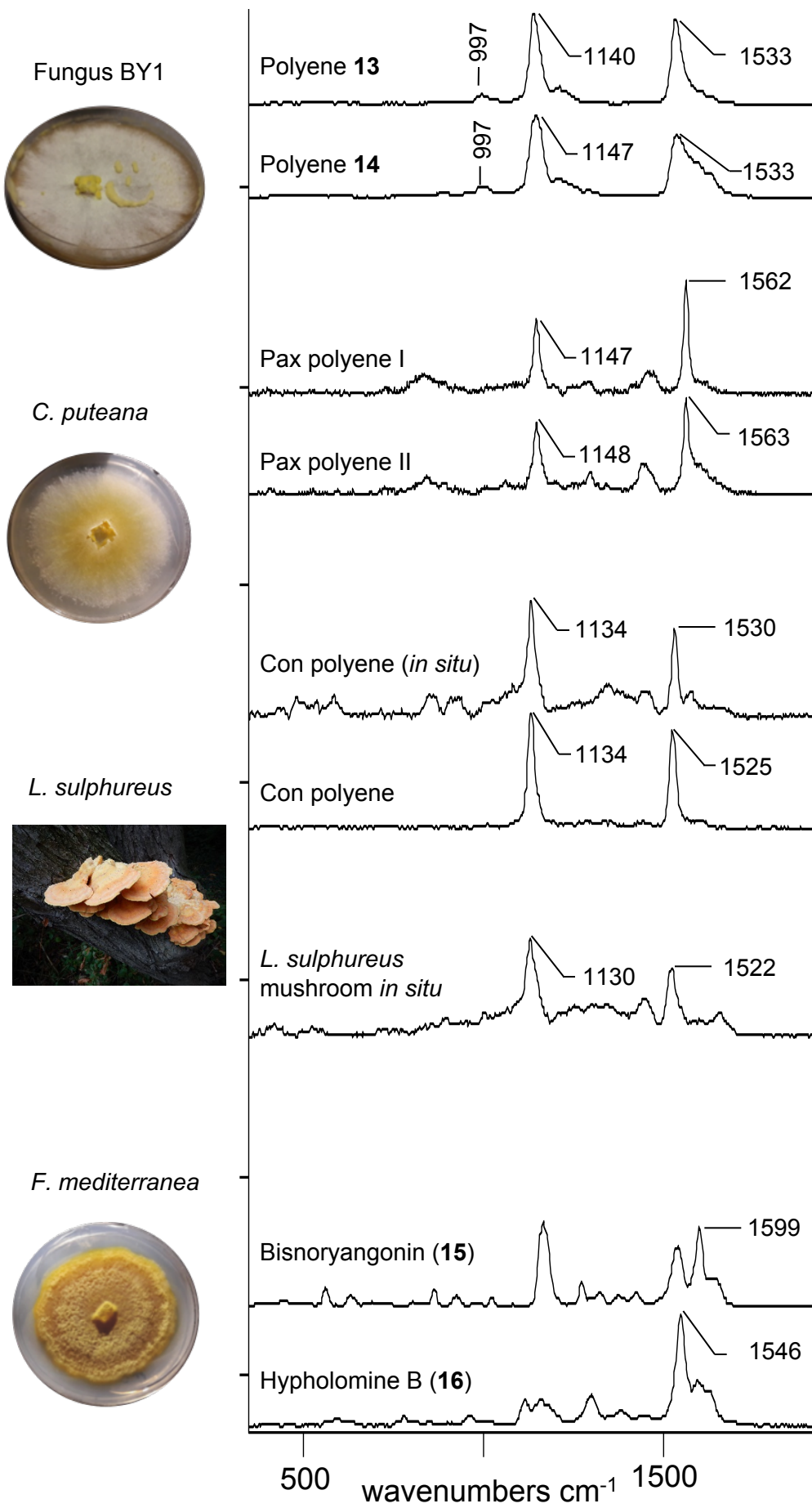
607

608

Terphenylquinones and derivatives

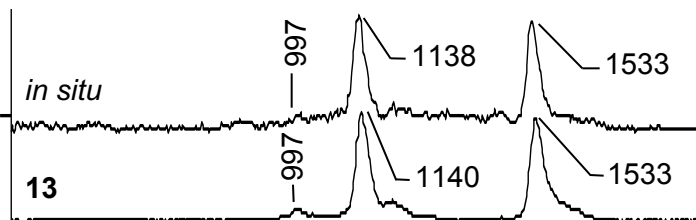
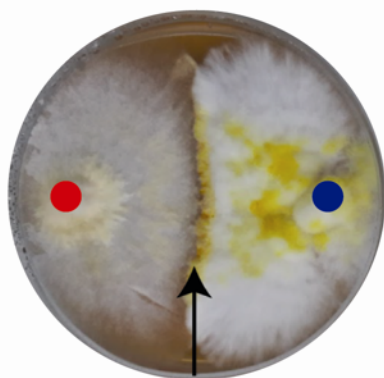


Aliphatic and styrylpyrone pigments

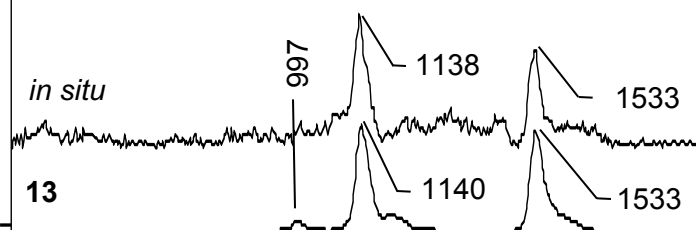
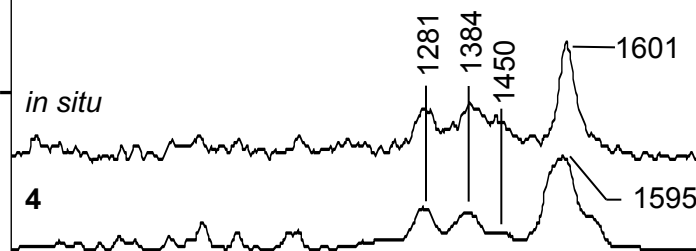
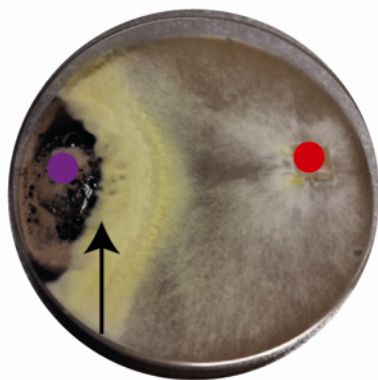


Co-cultures of basidiomycetes

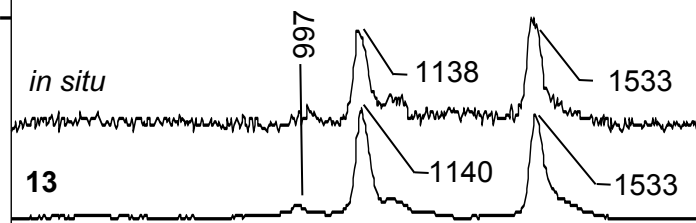
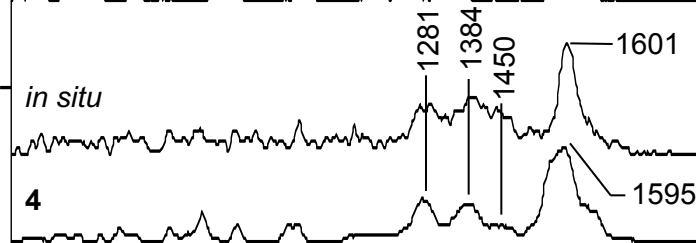
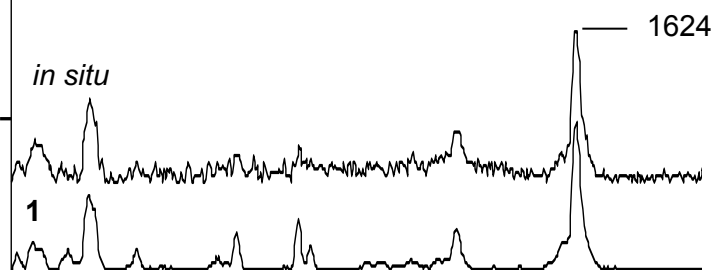
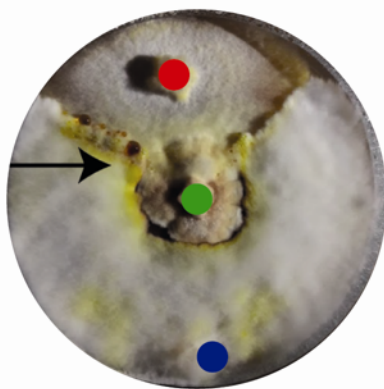
BY1 – *S. lacrymans*



BY1 – *A. mellea*



BY1 – *H. rutilans* – *S. lacrymans*



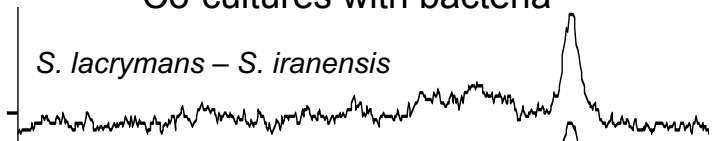
500 wavenumbers cm^{-1} 1500

Co-cultures with bacteria

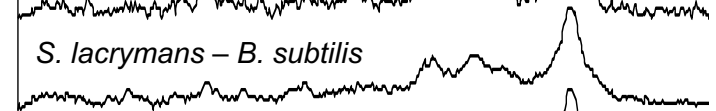
S. lacrymans – *Arthrobacter* sp.



S. lacrymans – *S. iranensis*



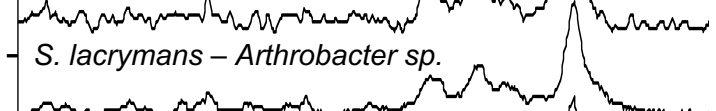
S. lacrymans – *B. subtilis*



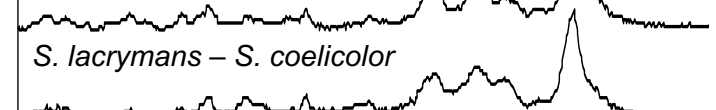
S. lacrymans – *P. putida*



S. lacrymans – *Arthrobacter* sp.



S. lacrymans – *S. coelicolor*



S. lac. unpigmented area



4



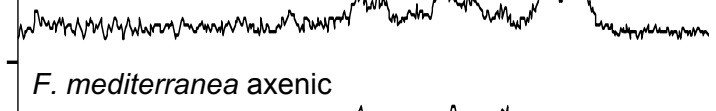
F. mediterranea axenic



F. mediterranea – *S. iranensis*



F. mediterranea axenic



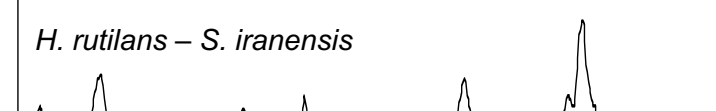
H. rutilans axenic



H. rutilans – *S. iranensis*



H. rutilans axenic



H. rutilans – *S. iranensis*

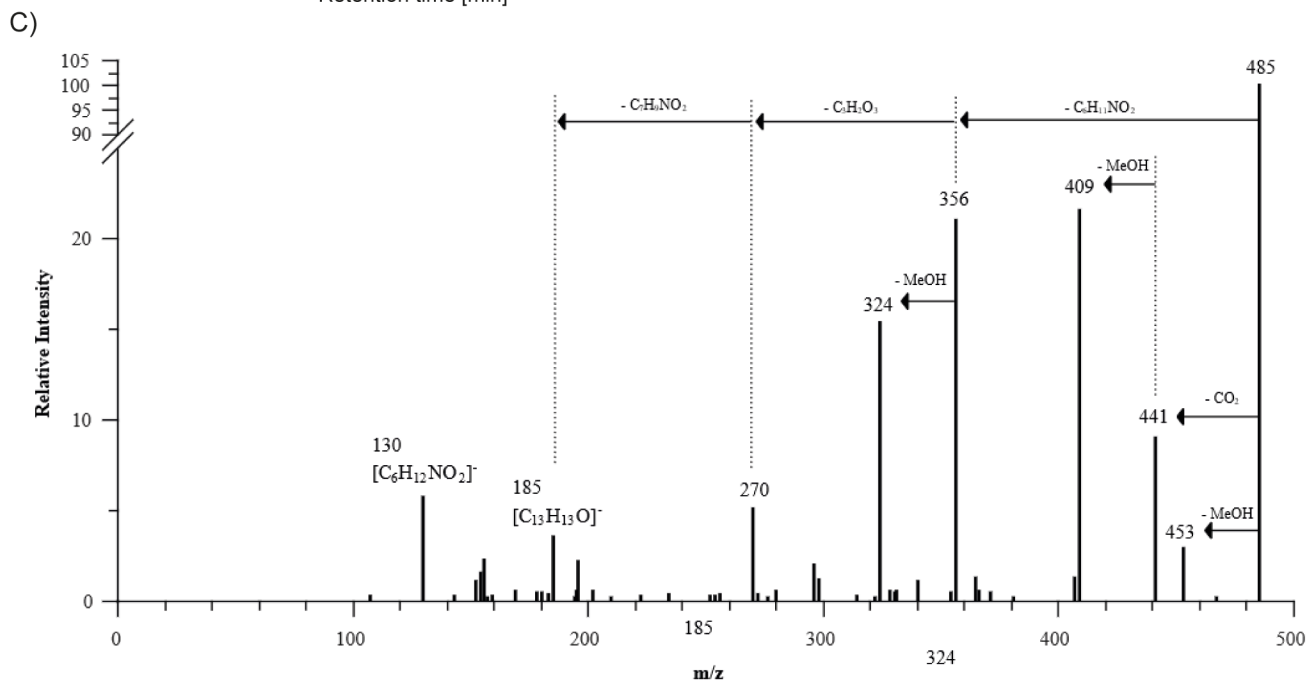
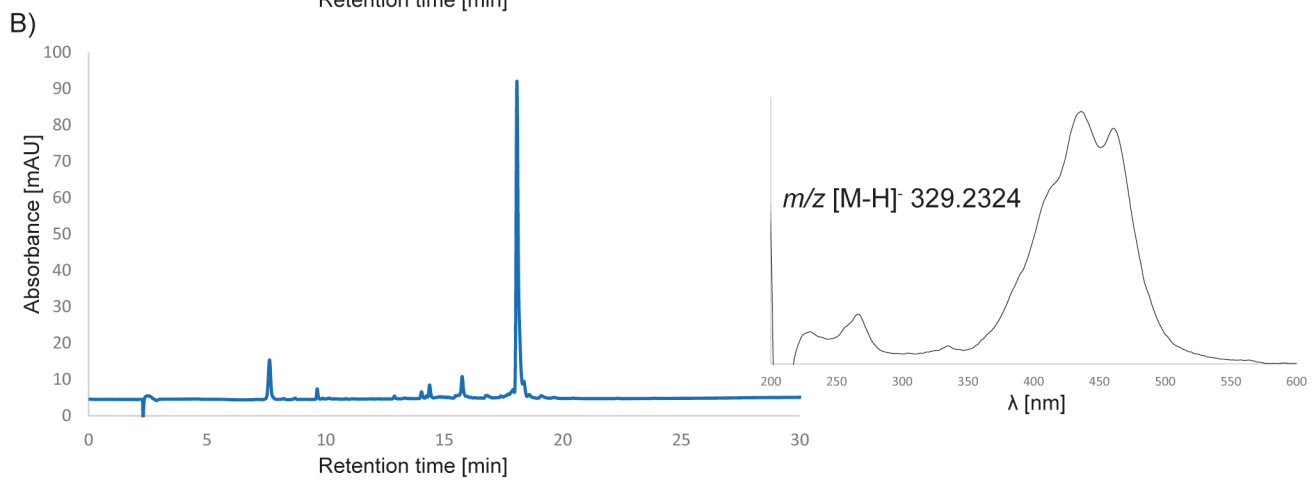
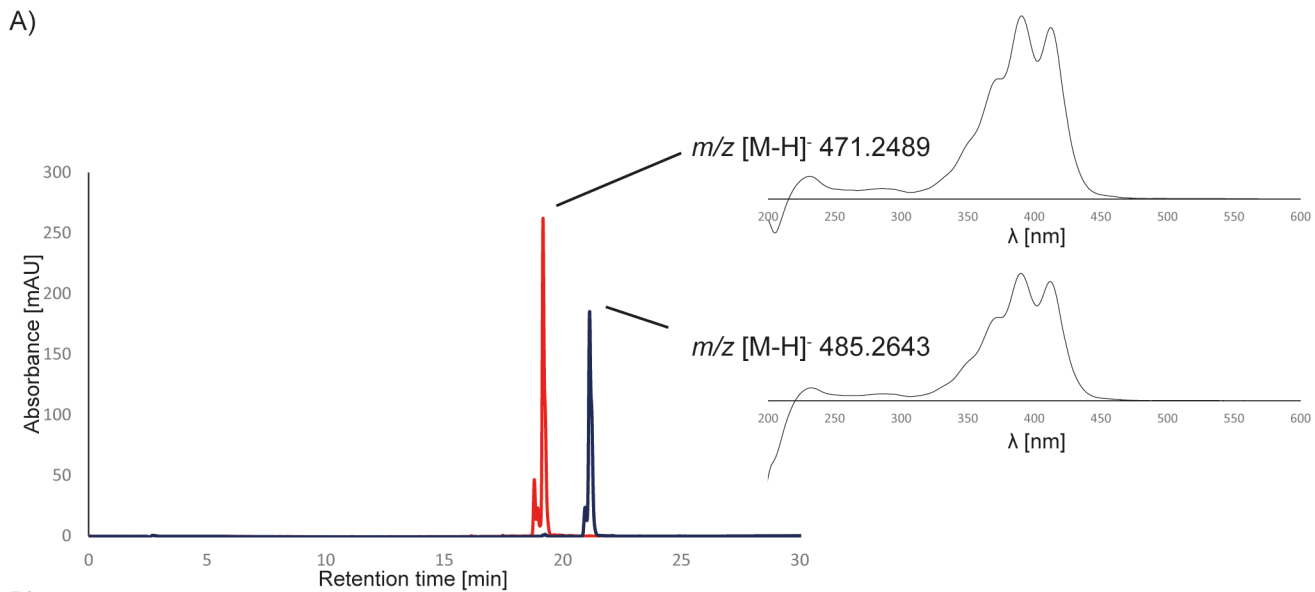


1



500 wavenumbers cm^{-1} 1500

166



3. Unpublished results

3.1. RNA-sequencing of *Serpula lacrymans* – *Bacillus subtilis*

Previous work on the transcriptional regulation of natural product genes in *Serpula lacrymans* showed an up-regulation of the atromentin synthetase gene as well as some other natural product genes during co-incubation with bacteria (manuscript, 2.3.). Although qRT-PCR provided high resolution of gene expression levels, a drawback of the method was that only selective genes were monitored. The next step in the investigation of these co-cultures was to understand more regulatory processes of the basidiomycete. A global snapshot of messenger RNA expression levels represents a general regulatory status of an organism, as these levels generally represent protein levels that control many biological processes (*i.e.*, part of the “central dogma” theory). These global processes that can be examined include primary metabolism (e.g., TCA cycle), secondary metabolism (e.g., natural product production), active or suppressed transporters for ions or metabolites, and repair- or stress-related processes (e.g. DNA repair or chaperones; (105)). Therefore, we chose RNA-sequencing (RNA-seq) of the model co-culture *S. lacrymans* – *B. subtilis* to expand on our initial qRT-PCR results.

3.1.1. Methods

Co-cultures were set up exactly as before (57). Total RNA isolation was done like before with the same kit, except the volumes for the kit reagents were doubled up

until the final wash steps. Total RNA was eluted from the spin column using 100 µl nuclease-free water. Total RNA samples were checked spectroscopically by ScanDrop (Analytik Jena). Replicates that had good values ($A_{260/280}$ and $A_{260/230} > 2.0$) were pooled (two to four samples per pool; three biological replicates for each condition: axenic *S. lacrymans* at time zero, and *S. lacrymans* - *B. subtilis* at co-incubation time 30 hours). 10 µg was used in a second DNase treatment using Baseline-Zero™ DNase (Epicentre) in a five-fold master mix reaction. After 20 minutes at 37°C, the samples were purified using the NucleoSpin® RNA Clean-up kit (Macherey-Nagel) following the manufacturer's instructions. 1 µl was then used to check for integrity using capillary electrophoresis by QIAxcel (Qiagen), following the manufacturer's protocol. Briefly, 1 µl was mixed with 1 µl of denature buffer and denatured at 70°C for 2 minutes, followed by dilution using dilution buffer to a final volume of 10 µl. Samples were run in the machine using the total RNA "CM-RNA" program with default settings. The instrument and reagents were kindly provided by Prof. Dr. Axel Brakhage and Dr. Volker Schroeckh (HKI). The RNA integrity numbers (RIS) for each sample were: axenic sample 1 ("A1"): 6.5; axenic sample 2 ("A2"): 6.9; axenic sample 3 ("A3"): 6.4; co-culture sample 1 ("B1"): 6.7; co-culture sample 2 ("B2"): 6.7; and co-culture sample 3 ("B3"): 7.2. Samples were shipped on dry ice to Microsynth, Switzerland for library preparation, sequencing and preliminary analyses.

After sample quality control, the strand specific Illumina TruSeq RNA library preparation kit v2 with polyA enrichment was used to construct libraries from total RNA. Subsequent sequencing was done using the Illumina NextSeq 500 platform (2x 75bp, high output v2 kit). The produced reads which passed Illumina's chastity filter were subject to de-multiplexing and trimming of Illumina adaptor residuals using Illumina's real-time analysis software (no further refinement or selection). Quality of the reads in fastq format was checked with the software FastQC (version 0.11.5).

The mapping software bowtie2 (version 2.2.6) with very sensitive local pre-setting was used to map the reads to the reference genome (*Serpula lacrymans* S7.9 v2.0, available via the JGI MycoCosm portal). To count the uniquely mapped reads to annotated genes, the software htseq-count (HTSeq version 0.6.0) was used. Normalization of the raw counts and differential gene expression analysis were carried out with help of the software package DESeq2 (version 1.6.3). Only filtered analyses were used. Significance was determined by an adjusted p value (padj) less than 0.05.

3.1.2. Results

Sample	#Reads	#Bases	Mean Read Length	Mean Q20%	Mean Q30%	Mean Q	#Masked
A1_R1	51581276	3839390537	75	96.05	93.93	34	51560
A1_R2	51581276	3844264274	75	93.93	91.43	34	159
A2_R1	54662013	4067024409	75	95.97	93.82	34	80100
A2_R2	54662013	4074188356	75	90.12	86.52	33	224
A3_R1	57494792	4277690692	74	96.16	94.07	34	39716
A3_R2	57494792	4282171590	74	93.76	91.23	34	100
B1_R1	52536342	3900063375	74	95.89	93.7	34	114736
B1_R2	52536342	3909508709	74	93.66	91.12	34	256
B2_R1	50999643	3795804419	74	96.02	93.87	34	29843
B2_R2	50999643	3799371169	74	93.15	90.42	34	49
B3_R1	60976554	4538498888	74	96.1	93.99	34	43120

B3_R2	60976554	4543412600	75	94.14	91.69	34	67
-------	----------	------------	----	-------	-------	----	----

Table 3-1: Presented here is an overview of the quality of RNA-sequencing for each condition (A and B) that were run in replicates (R). For next-generation sequencing, a Phred Quality Score (Q) above 30 represents high quality sequences.

Sample	Total reads	Mapped reads to genome	Unmapped reads to genome	Ambiguous reads
A1	47781528	41385263 (86.614%)	6166887 (12.906%)	229378 (0.480%)
A2	48354148	41348596 (85.512%)	6806720 (14.077%)	198832 (0.411%)
A3	53865093	46992721 (87.242%)	6616298 (12.283%)	256074 (0.475%)
B1	48263670	41612140 (86.218%)	6440676 (13.345%)	210854 (0.437%)
B2	47867075	41700936 (87.118%)	5933425 (12.396%)	232714 (0.486%)
B3	57351842	49999476 (87.180%)	7072246 (12.331%)	280120 (0.488%)

Table 3-2: Presented here is an overview of RNA-sequencing reads and mapping to the reference genome (*Serpula lacrymans* S7.9 2.0 from JGI's MycoCosm portal). In

all cases, the conditions (A and B) had greater than 85% mapped reads to the reference genome, thus providing good coverage. Averaged total reads were about 50 million.

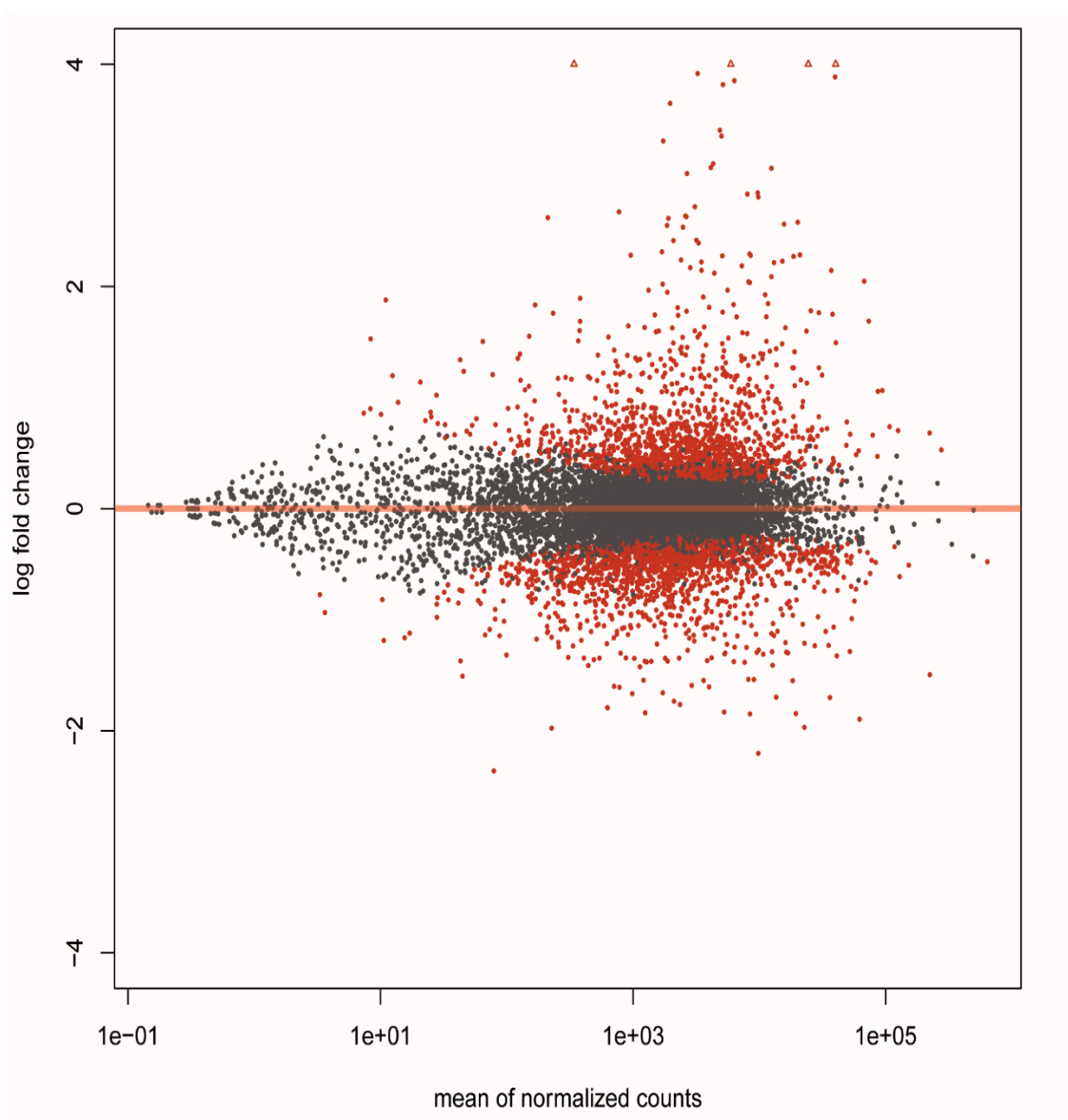


Figure 3-1: A MA plot showing genes (dots) that are either insignificantly (grey) or significantly (red; $p_{adj} < 0.05$) differentially expressed between the *S. lacrymans* – *B. subtilis* co-culture and *S. lacrymans* axenic culture. For each gene, the dot on the x-axis represents the mean of normalized counts from three biological replicates, and y-axis is the log2 fold change. Namely, higher expressed genes slide to the right, and up-regulated genes slide up. A triangle represents a value greater than what is represented on the y-axis. The horizontal line representing zero indicates equal expression levels between samples.

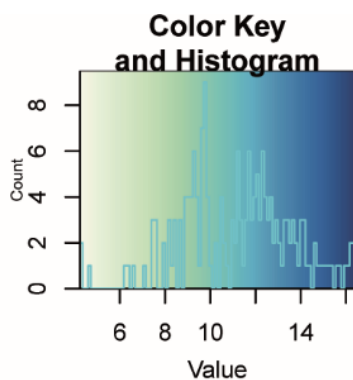
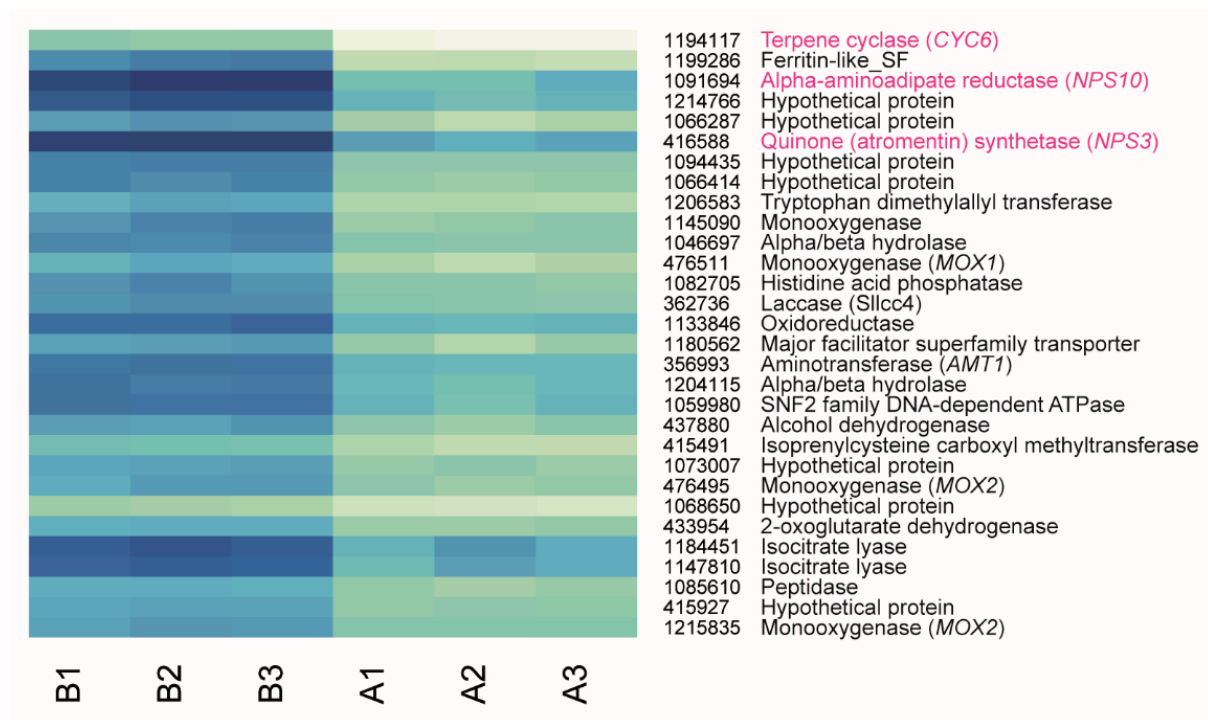
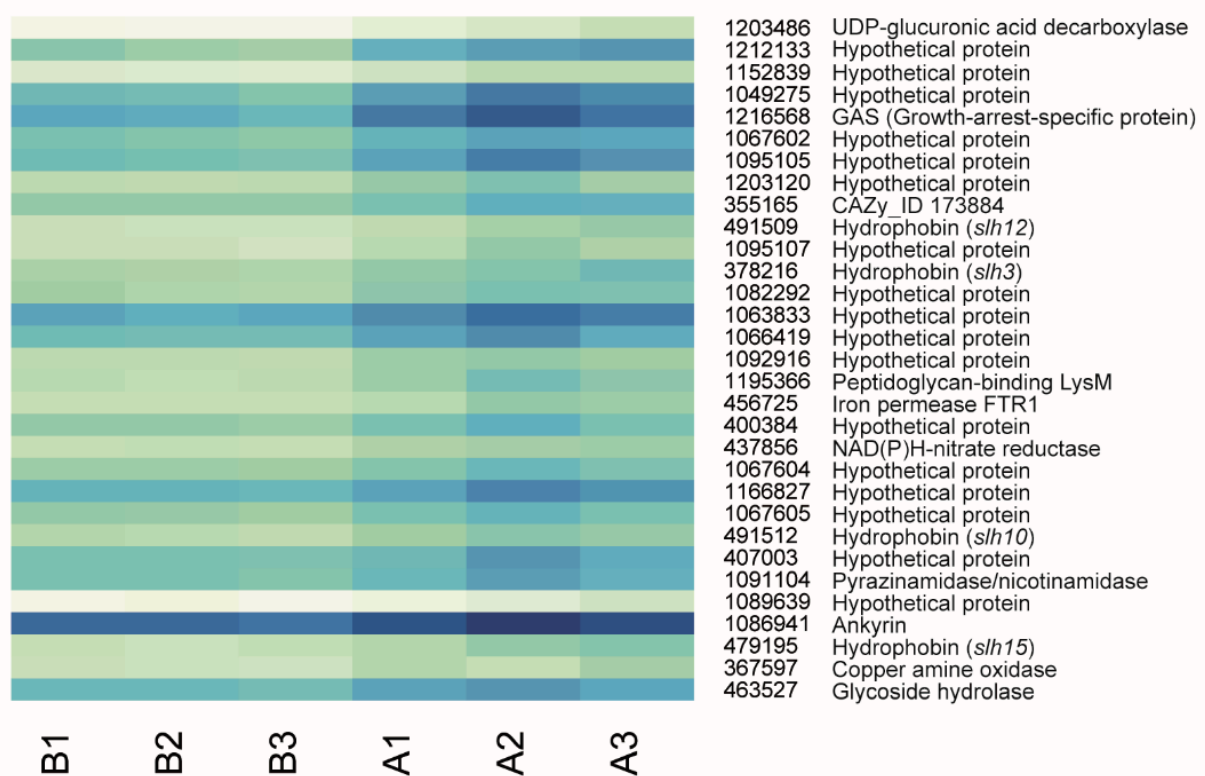


Figure 3-2: A heatmap of the top 30 most significantly up-regulated genes from *S. lacrymans* – *B. subtilis* co-cultures (samples “B”) compared to axenic *S. lacrymans* cultures at the onset of co-incubation (samples “A”). Each sample number represents a biological replicate derived from pooled technical replicates. The color scheme represents expression values for the genes: light green represents the lowest expression, dark blue represents the highest, and with transiting colors for varying expression in between. All genes are uncharacterized except for *NPS3*, which encodes for the atromentin synthetase. Three up-regulated natural product genes are highlighted. Gene transcript IDs and annotations are from JGI’s MycoCosm portal for *Serpula lacrymans* S7.9 2.0.



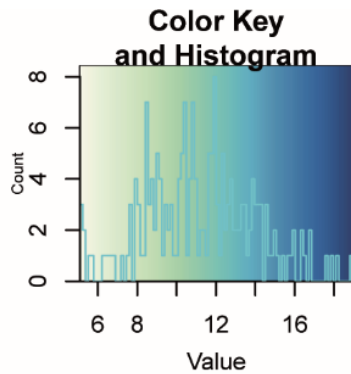


Figure 3-3: A heatmap of the top 30 most significantly down-regulated genes from *S. lacrymans* – *B. subtilis* co-cultures (samples “B”) compared to axenic *S. lacrymans* cultures at the onset of co-incubation (samples “A”). Each sample number represents a biological replicate derived from pooled technical replicates. The color scheme represents expression values for the genes: light green represents the lowest expression, dark blue represents the highest, and with transiting colors for varying expression in between. All genes are uncharacterized. Gene transcript IDs and annotations are from JGI’s MycoCosm portal for *Serpula lacrymans* S7.9 2.0.

In the search for putative transcription factor genes (*i.e.*, regulatory proteins that would potentially bind to the conserved promoter motif(s) of the atromentin synthetase gene), manually filtering up- and down-regulated genes using $\text{padj} < 0.05$ produced 1,180 significantly up-regulated genes and 1,100 significantly down-regulated genes. A further refinement with more stringency for up-regulated genes (\log_2 fold change > 2.0) revealed 53 “very” significantly up-regulated genes during co-incubation. Relaxing the stringency (\log_2 fold change > 1.5) added 46 up-regulated genes. Three up-regulated annotated transcription factors were as follows: Transcript ID: 1059175, “FOG: Zinc-finger (Zinc finger, C2H2-type),” \log_2 : 2.022, padj : 1.29E-16; Transcript ID: 1103782, “Fungal transcriptional regulatory protein

Fungal Zn(2)-Cys(6) binuclear cluster domain,” log2: 1.76, padj: 1.11E-11; Transcript ID: 1059569, “FOG: Zn-finger: Fungal transcriptional regulatory protein Fungal Zinc finger, C2H2-like,” log2: 1.57, padj: 1.57E-21.

Significantly up- and down-regulated genes determined by RNA-seq need to be validated by qRT-PCR before any conclusions.

3.2. Spectroscopic (MALDI-TOF-MS & MS²) analyses of pigments

The work presented here showed that the pulvinic acid-type pigments inhibited swarming and biofilm formation of *Bacillus subtilis* (manuscript, 2.4.). Although this bioactivity was observed, the mechanism of action by which the pigments conferred their bioactivity remained unknown. Because the pigments did not actually kill the bacterium but rather slowed it down in a sense, we sought other mechanisms than those epitomized for antibiotics (*i.e.*, interruption of cell wall biosynthesis, nucleic acid metabolism, protein synthesis or membrane disruption). Further experiments were done to get a first glimpse at potential reasons for the bioactivity and to help assist in further studies. This was done by MALDI-TOF-MS (Matrix-assisted laser desorption/ionization mass spectrometry), a laser-based mass spectrometric technique that ionizes the sample all at once (106), and by tandem mass spectrometry (MS²).

3.2.1. Methods

MALDI-TOF-MS analyses of pigment binding to *B. subtilis*

B. subtilis NCIB 3610 was grown overnight in 50-100 ml LB from a 25% glycerol stock, and the next day the cells were pelleted by centrifugation (12,000 x g). The cells were washed three times with autoclaved dH₂O and suspended in 400 µl dH₂O, which was then split four ways (100 µl each) into new 1.5 ml centrifuge tubes. 10 µg of each compound (10 µl of 1 mg ml⁻¹ concentration in methanol) or 10 µl of methanol (control) was incubated with the cells at ambient temperature overnight. The next day, the cells were washed ten times with dH₂O by centrifugation, and the pellet was then lyophilized.

Samples were suspended in 5 to 10 µL dH₂O, then 2 µL was spotted on stainless steel targets and allowed to dry in the dark at room temperature. Then, spots were rinsed with TFA 2% for 5 seconds to remove salts, dried, and then 1 µL of matrix (α -Cyano-4-hydroxycinnamic (HCCA; Sigma Aldrich) in acetonitrile) was added. The samples were then dried at room temperature and protected from light. Samples were measured in an UltrafleXtreme MALDI TOF/TOF mass spectrometer with a smartbeam-II™ laser of 1000 Hz (Bruker Daltonics). It was operated in the negative reflector mode on fully manual mode using flexControl software v.3.0. The analysis of single MS was performed with 30% laser intensity (laser type 3), accumulating 1000 shots by taking 250 random shots at every raster position. Acquisition method was calibrated externally using Peptide Calibration Standard II (Bruker Daltonics) containing Bradykinin1-7, Angiotensin II, Angiotensin I, Substance P, Bombesin, ACTH clip1-17, ACTH clip18-39 and Somatostatin 28. Spectra were internally

calibrating with the $[M-H]^-$ and $[2M-H]^-$ of HCCA. Recording of pigments was done in reflector negative mode with a mass accuracy ± 0.6 Da. This was done in collaboration with Dr. María García-Altareo Pérez (HKI).

Orbitrap MS² analyses of pigments

Orbitrap measurements were done as described in the prepared publication from section 2.5. This was done in collaboration with Dr. Nico Ueberschaar (FSU).

3.2.2. Results

After incubation of *B. subtilis* with each pulvinic acid-type pigment (variegatic, xerocomic or atromentic acid), the pigment was detectable by MALDI-TOF-MS in all cases. This showed that the pigments were binding to the bacterium, or that the bacterium was retaining the pigments. MS² analyses and schematics by Dr. Nico Ueberschaar (FSU) revealed a fingerprint for these pigments. Here, $M-CO-(CO_2)_2$, which was a complete decomposition of the tetronic acid system, was shared by variegatic, xerocomic, and atromentic acids. MS² fingerprinting of the pigments will help in future experiments when investigating how the pigments interact with the bacterium.

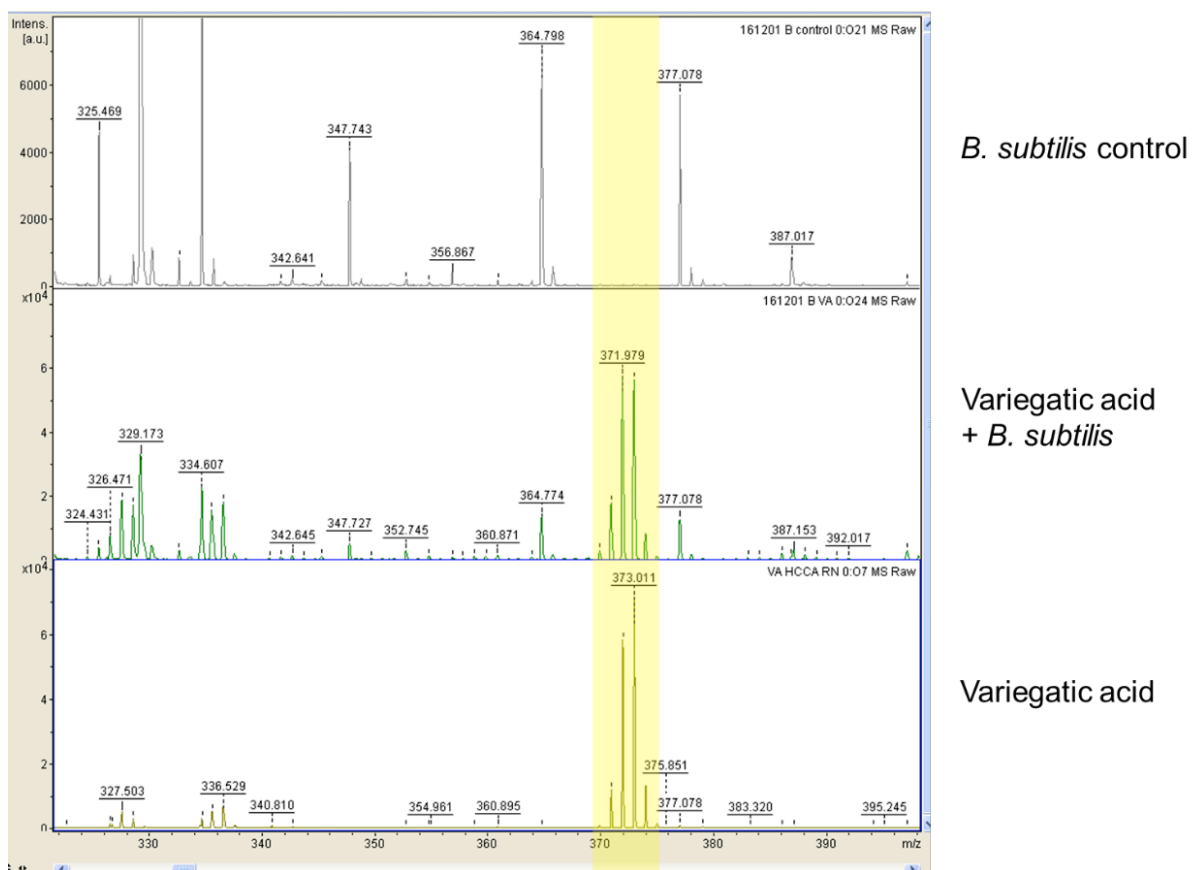


Figure 3-4: MALDI-TOF-MS analysis of *B. subtilis* incubated with 10 µg variegatic acid (experimental sample) or methanol (control) and only variegatic acid (reference). The ionized masses for variegatic acid were identified in the experimental sample and reference but absent in the control.

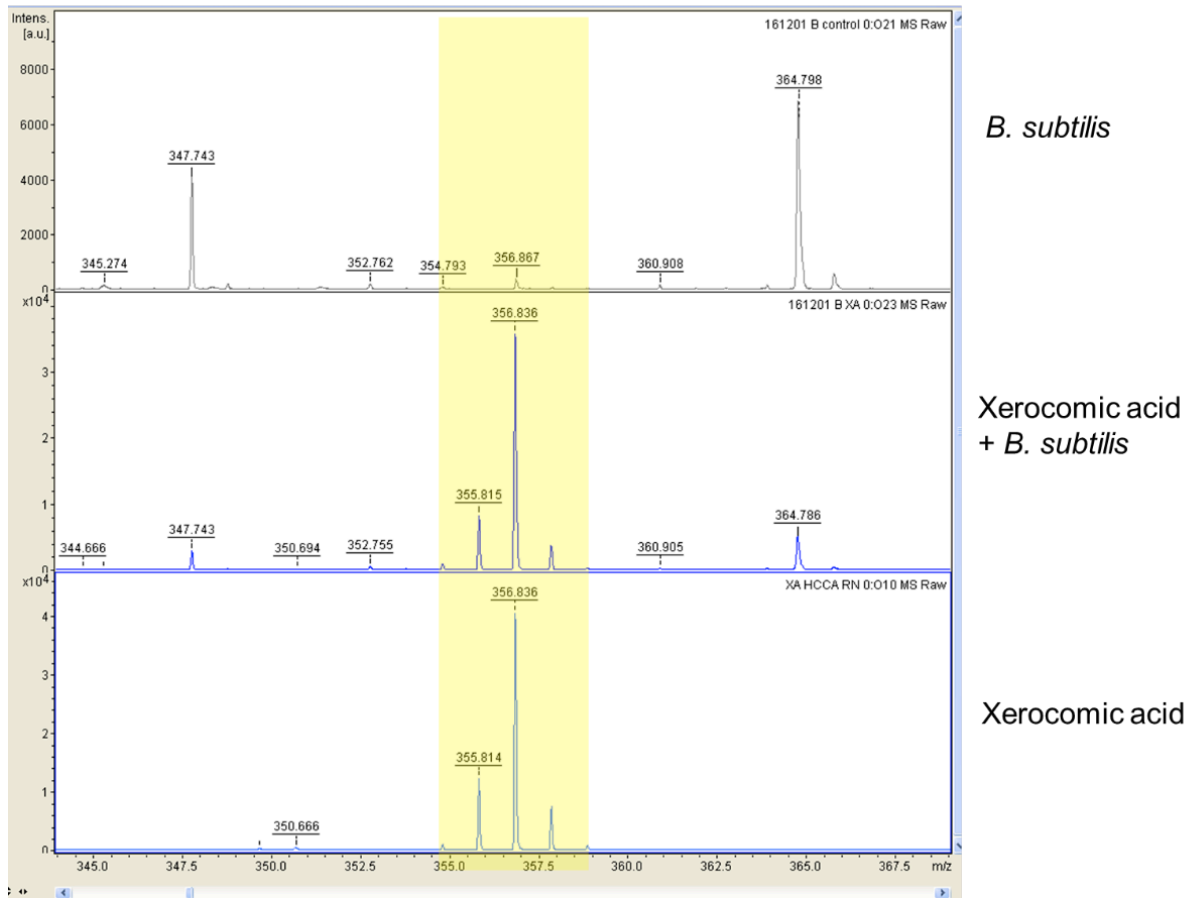


Figure 3-5: MALDI-TOF-MS analysis of *B. subtilis* incubated with 10 µg xerocomic acid (experimental sample) or methanol (control) and only xerocomic acid (reference). The ionized masses for xerocomic acid were identified in the experimental sample and reference. A similar mass was found in the control at a lower intensity as was the case in all other samples, indicating that this mass derived from the bacterium itself.

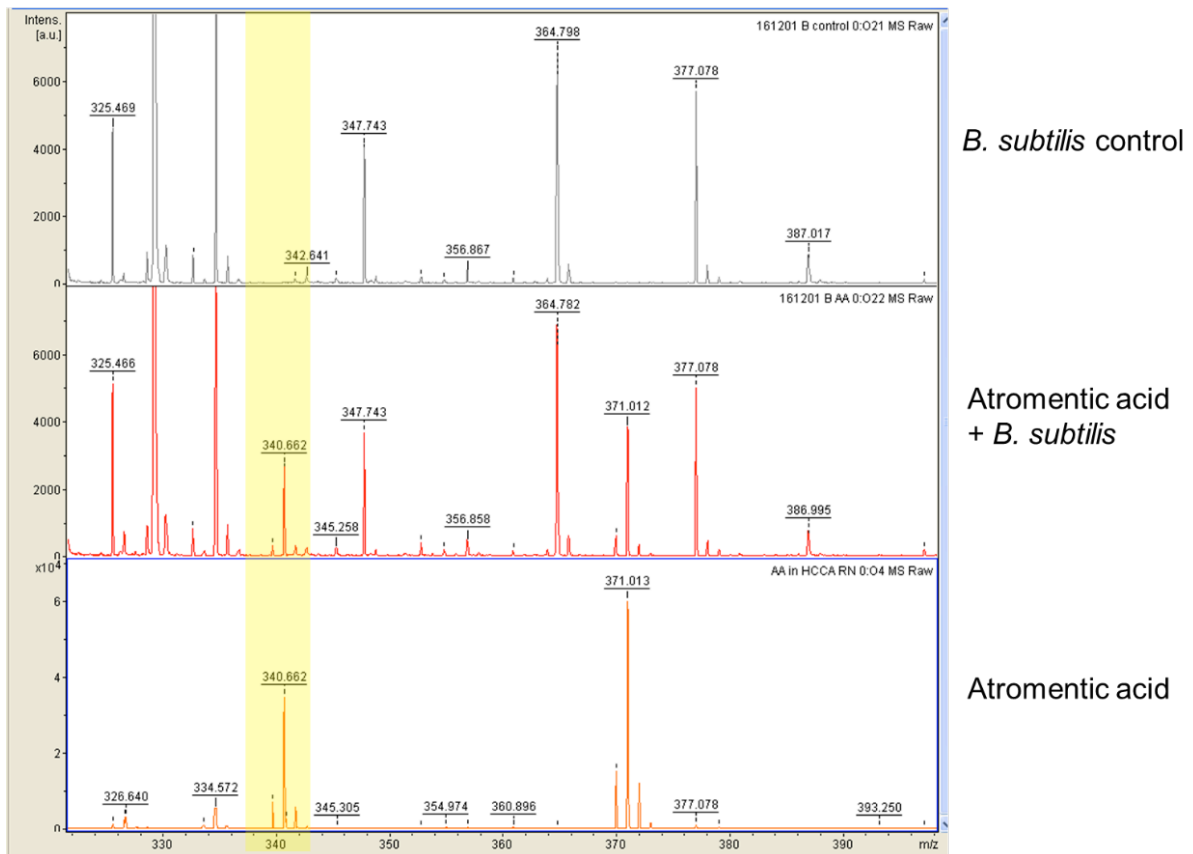


Figure 3-6: MALDI-TOF-MS analysis of *B. subtilis* incubated with 10 µg atromentic acid (experimental sample) or methanol (control) and only atromentic acid (reference). The ionized masses for atromentic acid were identified in the experimental sample and reference but were absent in the control.

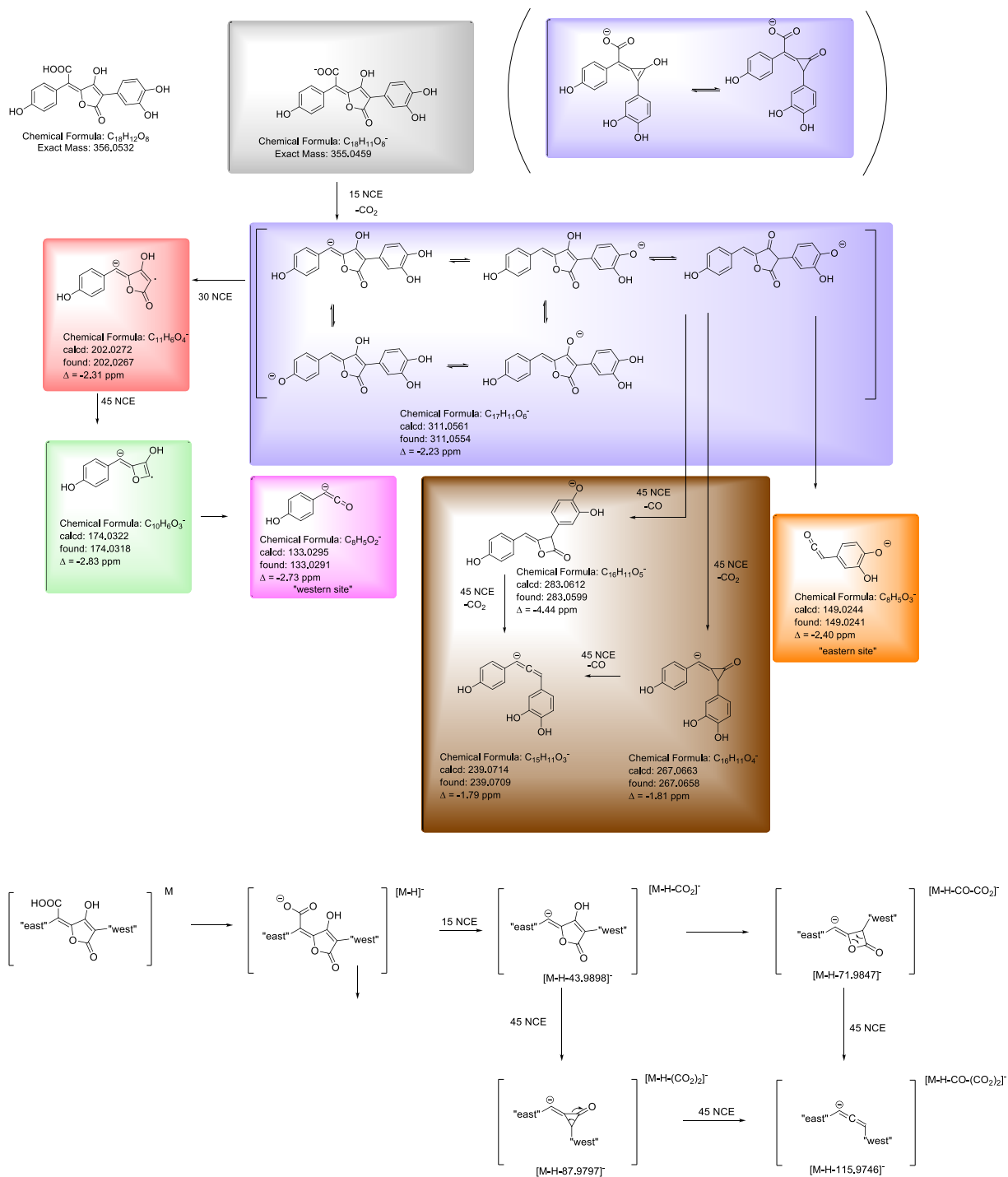


Figure 3-7: Orbitrap MS² measurements of xeroomic and variegatic acids. The proposed decomposition by MS² of xeroomic acid is shown in the colored diagram. Variegatic acid, which is shown in brackets below the schematic for xeroomic acid,

shared a similar decomposition. For each proposed structure, the calculated chemical mass is compared to what was found.

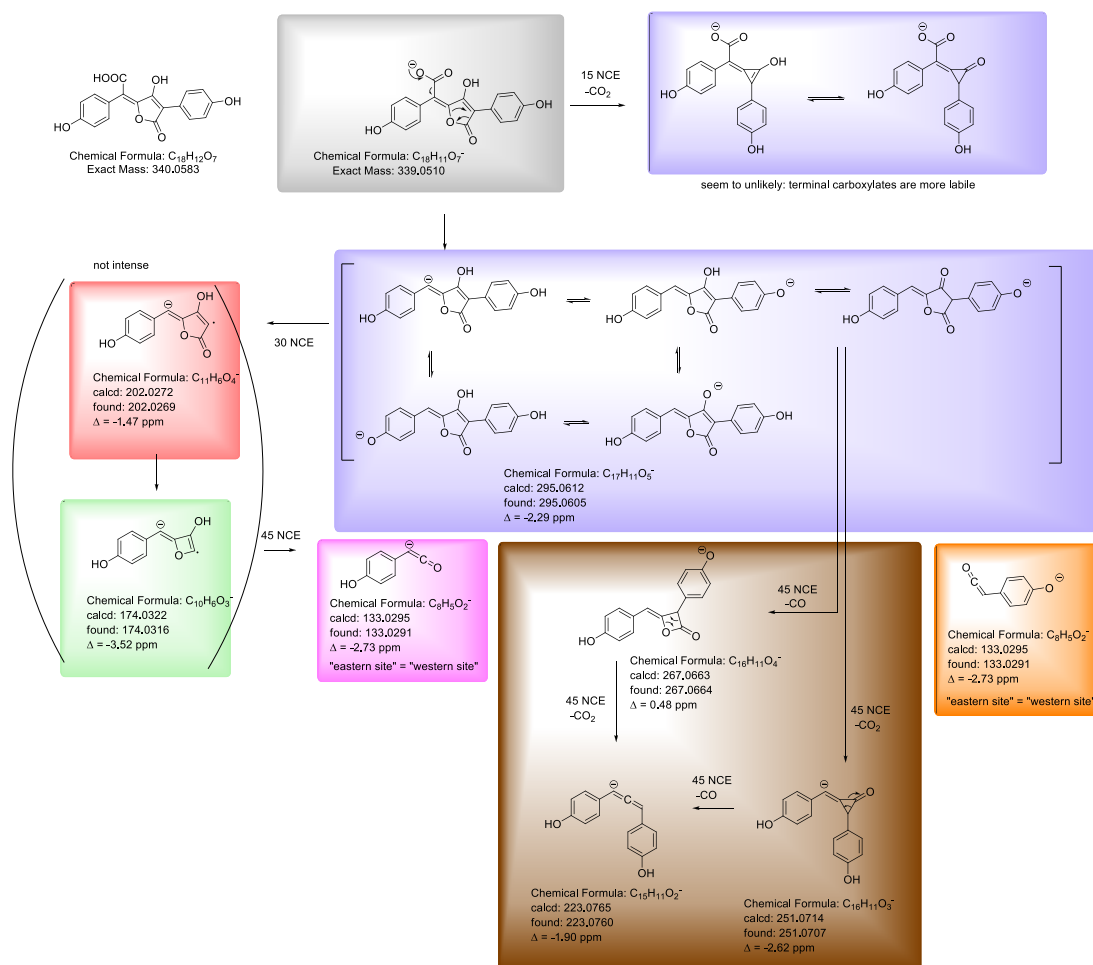


Figure 3-8: Orbitrap MS² measurements of atromentic acid, similar to the other two pigments noted beforehand. For each proposed structure, the calculated chemical mass is compared to what was found.

4. Discussion

4.1. Role and induction of natural products during co-culturing

By understanding the role, regulation and flux of natural products in complex biosystems, we can gain an understanding of the chemical language that is used between organisms and their consequences. With the focus on basidiomycetes, *Serpula lacrymans* (brown rotter) was co-incubated with 13 different bacteria from five distinct taxonomic groups, each of which induced pigmentation when compared to axenic fungal controls that showed no pigmentation (manuscripts, 2.3. and 2.4.). This work was later facilitated with Raman spectroscopy for quicker pigment identification during co-culturing (manuscript, 2.5.). Co-incubation work with *Paxillus involutus* (mycorrhiza-forming) did not produce a similar pigmentation response. Also, media with organic nitrogen content was previously found to induce pigmentation in each fungus (92, 94). Conversely, inorganic nitrogen in a ten-fold excess did not cause pigmentation, and it did not negate *B. subtilis*' effect on the fungus (manuscript, 2.4.). Because both high organic nitrogen content and bacteria induced pigmentation in *S. lacrymans*, from which the latter response was not observed in *P. involutus*, we then investigated the bioactivity of the atromentin-derived pigments from each fungus. Bioactivity tests would help support hypotheses of whether dissimilar pigmentation was merely an overlapping response to a nutritional cue, or if the pigments had a specific role against the bacterium. For example, dissimilar yet overlapping cues for fungal secondary metabolite production were described, such as bikaverin and gibberellins produced by *Gibberella fujikuroi*.

Both compounds were inducible under depleted nitrogen conditions, but nitrate conditions led to varying production of each (107).

The atromentin-derived pigments from *S. lacrymans* and *P. involutus* showed no antibacterial or antifungal activity (manuscripts, 2.3. and 2.4.). Previous literature (reviewed (5)) did not cite extensive research into the microbial bioactivity of atromentin and atromentin-derived pigments, presumably because there has been no discernable bioactivity from screening the pigments. Key mentions though are for atromentin, which inhibits an enoyl-ACP reductase of *Streptococcus pneumoniae* yet is nonetheless not antibacterial (108) and for variegatic, xerocomic and atromentic acids, which are non-specific inhibitors of four different cytochrome P450s (109). This unspecific activity may be because the compounds can act as iron-reductants as previously noted for Fenton chemistry (92).

Given the lack of antimicrobial bioactivity by the pigments, phenotypic changes of a bacterium that the pigments may cause were tested. The model system *S. lacrymans* – *B. subtilis* was chosen as the model interaction system because: *B. subtilis* is itself a model organism with a huge mutant library; it has well described phenotypes; its simplicity of growth conditions; inter-microbial interactions between this bacterium and fungi have already been described (110, 111); and, as described in this work, it induced excessive pigmentation in *S. lacrymans*.

In collaboration with Drs. Ramses Gallegos-Monterrosa and Ákos T. Kovács (JSMC), variegatic acid and xerocomic acid, but not atromentic acid, inhibited the spread of biofilm formation, and involutin and atromentin showed no bioactivity (manuscript, 2.4.). Additionally, variegatic acid and xerocomic acid inhibited/delayed the swarming motility of *B. subtilis*. Thus, we observed dissimilar bioactivity. This was the first sign that the pigment response may be specific to the bacterium rather than only

overlapping with nutrition. Indeed, other natural products have shown similar effects. Here, quorum sensing small compounds from *Pseudomonas aeruginosa* (e.g. 2-heptyl-4-quinolone and 2-heptyl-4-quinolone) did not kill *Bacillus atrophaeus* but were determined to be mild to potent anti-biofilm and anti-swarming compounds (112). Other community modulations via natural products come from two recent examples: i) lipopeptides from *Pseudomonas protegens* can immobilize *Chlamydomonas reinhardtii* (green alga), presumably so the bacterium can feed (113); and ii) antagonism between *Ralstonia solanacearum* (bacterium) and *Aspergillus flavus* is mediated via natural products from each (lipopeptides and imizoquins (tripeptide-derived alkaloid), respectively; (114)). The latter instance is particularly interesting because the lipopeptide ralstonin selectively suppresses the gene cluster that produces the imizoquins, perhaps in anticipation of the fact that the imizoquins will suppress bacterial growth. An additional example of microbes controlling one another comes from the basidiomycete *Coprinopsis cinerea*. This fungus is able to enzymatically cleave gram-negative quorum sensing compounds, and thus this basidiomycete is also modulating its surrounding community by disruption of compounds used for communication (115). Therefore, modulation of other co-inhabiting organisms by natural products or enzymes and its effect on signaling systems, virulence and survival appear to be an important defense or domineering feature across kingdoms.

While investigating a possible mechanism of action of the bioactive pigments from *S. lacrymans*, it was observed that the pigments may be binding to a cell wall component of bacteria (unpublished, 3.2.). We analyzed bacterial cells that were incubated *in vitro* with variegatic, xerocomic or atromentic acid by MALDI-TOF-MS. This was done in collaboration with Drs. María García-Altres Pérez and Christian Hertweck (HKI). The pigments were identified by ionized masses in the bacteria-pigment reactions and absent from the controls (unpublished, 3.2.).

Based on the MALDI-TOF-MS results, the pigments must somehow be associating with the bacterial cells, possibly attaching to the cell wall, the cell membrane or an associated cell wall protein. Polyphenols (a class that these pigments fall into) are well known to bind to proteins and have been well studied in food science because polyphenols are antioxidants (116). In fact, several hypotheses about dietary polyphenols state that their bioactivity against bacteria lies in the fact that they have the capacity to bind to the lipid bilayer or to create metal ion complexes, and thus impacting the bacterium itself or the surrounding environment, respectively (117). Therefore, the binding of the pigments to the bacterial cells is plausible to assume given their known binding capacity and the MALDI-TOF-MS results, and that their binding capacity may be the reason for the swarming delay and subsequent altered biofilm phenotypes.

Alternatively, the pigments may somehow interfere with the exopolymeric substances (EPS) and quorum sensing of *B. subtilis*, which in turn would affect swarming and biofilm formation (118). Given the conceivable lack of interest in the pulvinic acid-type pigments because no antimicrobial activity was described, our new results should spark ecological interest, and possibly even a “post-antibiotic, virulence-targeted” human-centric interest, of these pigments (112).

In addition to pigment induction by bacteria, we also observed that enzymatic (lytic enzymes and proteases, but not lysozymes) in the absence of any bacteria also induced pigmentation in *S. lacrymans*. Mechanical damage as a control did not induce pigmentation as was the case in an unrelated basidiomycete, “BY1” (81). Following up on the results of enzymatic induction, the co-culture of *B. subtilis* with *S. lacrymans* was also manipulated: i) *B. subtilis* amended with a general protease inhibitor cocktail or ii) heat-killed bacteria. Both conditions significantly

reduced pigmentation, indicating that secreted proteases were also part of the elicitation. Since external proteases are involved in swarming motility, this may be an alternative reason for weakened pigment induction (119). Alternatively, pigmentation was triggered by enzymatically released peptides or cell wall components from the fungus itself or from exo-proteins. As a parallel, co-incubation systems of different *Trichoderma* spp. showed that released peptides from the prey fungus were stimulating increased nitrogen metabolism in the predator fungus. This showed that during competition released peptides can induce metabolic changes (120). In these co-cultures, proteases were also involved in the degradation of the fungal cell wall during mycoparasitism (121). Additionally, the predator fungus *Trichoderma harzianum* can respond to cell wall debris (122). The response by merely cell debris was inconsistent with not only our results (autoclaved bacteria did not induce pigmentation) but also another well documented co-culture system: *Aspergillus-Streptomyces* (123). Based on the above information, we formed the hypothesis that the protease(s) or lytic enzymes were damaging the cell wall of *S. lacrymans* or degrading exo-proteins and thereby releasing peptides, which in turn would be the actual eliciting factors that induce pigmentation. This would also parallel that excessive organic nitrogen, but not inorganic nitrogen, induced pigmentation (92). Although we have laid the foundation, future work is required to determine the exact eliciting factor as well as correlations to nitrogen/ amino acid metabolism, which would identify more precisely the discreteness of pigment induction.

4.2. Genetic regulation and bioprospecting of natural products in co-cultures

We determined certain natural products that were secreted from *S. lacrymans* during co-incubation as well as the bioactivities of these pigments. This provided insight into the role of basidiomycete chemical mediators during confrontation with bacteria. We chose to then focus on the transcriptional regulation of the atromentin gene cluster as well as other natural product genes during co-culturing (manuscript, 2.3.). The focus on the transcriptional regulation of the atromentin-derived pigments (*i.e.*, the atromentin gene cluster) and other natural product genes would provide: i) first insight into the (co-)regulation of a basidiomycete natural product gene cluster, and ii) additional clues of other natural products that may be involved during co-incubation. The atromentin cluster contains the atromentin synthetase gene (*NPS3*), aminotransferase gene (*AMT1*), and alcohol dehydrogenase gene (*ADH2*). *NPS3* was characterized in this work (manuscript, 2.3.). From three separate *S. lacrymans* - bacterium co-cultures, qRT-PCR confirmed co-regulation of *NPS3* and *AMT1*, and that *ADH2* was barely up-regulated, suggesting its role in atromentin production was not essential.

We chose to use the co-culture with *Streptomyces iranensis* to look for additional inducible natural product genes in *S. lacrymans* because this bacterium not only showed prolonged gene induction in *S. lacrymans* but also was a model bacterium that induced a silent orsellinic acid (polyketide) gene cluster in *Aspergillus nidulans* (123). The genome of *S. lacrymans* contains 15 NRPS(-like) genes and 9 PKS / PKS-NRPS hybrid genes (92). Despite the unusually high number of annotated natural product genes (on average, genomes within the Agaricomycotina contain only

four PKS genes (124)), only three groups of natural products have been isolated from *Serpula* spp.: pulvinic acid-type family (58); fungicidal/fungistatic himanimides (azole polyphenolic compounds; (125)); and polyine acids (acetylenes; (126)). For each, the complete genetic and enzymatic basis remains unknown, thus exciting curiosity to bioprospect inducible natural product genes and find their respective natural products during co-culturing.

Some natural product genes were slightly up-regulated, and no gene was significantly down-regulated. Uncharacterized *NPS10* and *NPS11* (putative adenylate-forming reductases); *NPS1* (NRPS); and *NPS8* (PKS-NRPS hybrid) were up-regulated. The HPLC chromatograms for each respective qRT-PCR time point revealed no obvious difference between the co-culture and control other than the pulvinic acid-type pigments that may reveal new compounds corresponding with the up-regulated natural product genes. This could have been due to various factors such as biased extraction protocols, unoptimized HPLC gradients, compound degradation, lack of absorbance by the compound, or just not enough gene induction.

Some progress has been made that will help characterize the natural product repertoire of *S. lacrymans*. *NPS9* and *NPS11* were partially characterized (44). The preferred substrate of each's adenylation domain was characterized using an ATP- (³²P)-pyrophosphate exchange assay (l-threonine and benzoic acid, respectively); however, the final product remains unknown (44). *NPS1* has been annotated as a NRPS with the heptadomain structure A-T-C-A-T-C-T. This resembles NRPSs that produce gliotoxin in *Aspergillus fumigatus* (Figure 1-1; (127, 128)) and sirodesmin in the plant pathogenic fungus *Leptosphaeria maculans* (129). This background

information could facilitate the discovery of the natural product from NPS1. NPS8 is annotated as a hybrid and without further, reliable information.

Using *S. lacrymans* – *B. subtilis* as the other model co-incubation system, we chose RNA-sequencing (RNA-seq) to monitor a global transcriptional response during co-incubation. This would help facilitate new natural product discoveries as well as further insight into the peculiarities of the fungus during co-incubation like changes in primary metabolism or activated stress-related genes. A preliminary analysis of the top up- and down-regulated genes has shed some interesting insight into the fungal response to the bacterium (unpublished, 3.1.). As expected, the atromentin synthetase (*NPS3*) and aminotransferase (*AMT1*) were both up-regulated. The putative adenylate-forming reductase (*NPS10*) that was originally found up-regulated in the *S. lacrymans* – *Streptomyces iranensis* co-culture was also found up-regulated in this co-culture which indicated an overlapping response. The genome contains 15 annotated putative adenylate-forming reductases genes (92), and despite the overwhelming diversity of different compounds modified by these NRPS-like enzymes (43, 44), it would appear that *NPS10* has a particular role in the response to different bacteria. As no final natural product by these enzymes is yet described and thus no interpretation of their role for the basidiomycete can be made, further investigation and refinement of co-cultures is warranted to discover new and exciting compounds therefrom.

Other natural product genes that were initially excluded from our qRT-PCR work due to their classification (*i.e.*, not a NRPS, PKS or hybrid) were found to be up-regulated, thus highlighting a benefit of RNA-seq. Most notably, a putative terpene cyclase (*CYC6*) that was essentially unexpressed before the addition of bacteria was found up-regulated. Basidiomycete terpenes have pharmacologically relevant bioactivities

(130). It was observed that the diterpene lepistal from *Lepista sordida* can induce human cell lines to differentiate into different cells, and lepistal is also antibacterial and antifungal (131). Erinacines A-C isolated from *Hericium erinaceus* showed promise to curb dementia because of their ability to stimulate the biosynthesis of nerve growth factors (132). More ecologically and industrially related research has been done on gibberellic acids produced by ascomycetes. They are labdane-related/bicyclic diterpenoids (Figure 1-1). Gibberellic acids are phytohormones that can regulate plant growth and are biosynthesized from a presumably ancient pathway that is also used in plants to produce these compounds (130, 133). Future investigation into CYC6, which is otherwise silent without the introduction of bacteria, may reveal a highly bioactive terpene involved in microbial communication or defense.

Various other annotated genes that were found up-regulated were oxidoreductases, a laccase, monooxygenases, a ferritin-like gene, isocitrate lyases and a 2-oxoglutarate dehydrogenase. Oxoglutarate dehydrogenase is part of the citric acid cycle, and isocitrate lyase is a bridging enzyme between this cycle and the glyoxylate cycle; both cycles are involved in the production of oxalate in wood rot fungi (134). Oxalate, ferritin, and hydroquinones could together control the movement of iron (iron is necessary for brown rot). Appropriately, imaging data showed that *S. lacrymans* controls iron movement when colonizing wood (135). Altogether, it is interesting to see that pigment production due to bacteria coincided with what appeared to be an overlapping or coordinated response to the initial attack of wood (136). To rule out another possibility, it could be plausible that the glyoxylate cycle is induced by influxes of carbon (134). However, in the *S. lacrymans* co-cultures the fungus was not releasing carbon from wood nor was the fungus introduced to any new carbon source. It remains to be determined if the metabolic change is correlated with the

movement of iron during wood colonization or the bacterium itself was contributing new metabolites or inducing a core metabolic response.

The several up-regulated monooxygenase genes could be part of a xenobiotic metabolic response or modifying enzymes in conjunction with the up-regulated natural product genes (137). They also could in fact be the sought after unknown biocatalysts that transform atromentin into its derivatives.

RNA-seq experiments provided valuable information in other fungal defense systems. Co-culture RNA-seq experiments focusing on the model basidiomycete *Coprinopsis cinerea* confronted with either mechanical wounding (abiotic), or different consortia of nematodes or bacteria (biotic), including a co-culture of all three antagonists, showed that *C. cinerea* had specific responses to each confrontation. This demonstrated that the fungus recognized and appropriately defended itself from environmental cues (138).

Other techniques may also facilitate new discoveries as well as improve the workflow of studying natural products (e.g. heavily reduce sample preparation). Raman spectroscopy is a vibrational spectroscopy technique that can fingerprint compounds, and it was successfully repurposed and applied in this work to study basidiomycete pigments (manuscript, 2.5.). This technique was helpful in non-destructively and quickly identifying induced pigments on a hyphal-scale level in the interaction zones between two or three basidiomycetes, and basidiomycetes introduced to different bacteria. During confrontations there was a pigmentation response which appeared to be a ubiquitous fungal (defense) response. This was regardless if the pigment was a terphenylquinone-derived compound, a polyene or a styrylpyrone, with each conferring a dissimilar bioactivity. Raman spectroscopy also assisted in fingerprinting three new polyene or polyene-like pigments, of which two were isolated from *P.*

involutus. Insufficient amounts hindered NMR structure elucidation, but one of the polyenes, termed “Pax polyene 2,” was speculated (by MS² data) to contain nitrogen from (iso)leucine. The hybrid compound would add to the known nitrogen-containing fungal polyenes like the alkaloid antifeedant (iso)chalciporon (58); melanocrocin (139); and the antibacterial mycenaaurin A (140). The genome of *P. involutus* contains two annotated putative PKS-NRPS hybrid enzymes (JGI protein IDs 171130 and 155215), which may link a polyene with an amino acid, that have yet to be characterized (141). Other techniques have garnered attention for their capacity to quickly identify natural products *in situ*, including during inter-microbial communication, like applying nanospray desorption electrospray ionization mass spectrometry directly to growing bacteria on petri plates (142). Here, *Streptomyces coelicolor* confronted with *B. subtilis* showed varying metabolic profiles. For example, actinorhodin, an antibacterial polyketide pigment, was produced by *S. coelicolor* where the colony was closest to *B. subtilis* and not elsewhere. Altogether, a combinatorial approach of sequencing and non-invasive spectroscopy will improve the research of basidiomycete natural products, their respective genes, and with a spatial and temporal resolution.

4.3. Bioinformatics and cellular regulation of natural product gene clusters

The success of studying the natural products of basidiomycetes will combine both bench and *in silico* work. Bioinformatics, especially with the increase in available sequence data (7), has had profound impacts on studying the evolution of mycorrhizal symbiosis (141); the transcriptional regulation of active genes (e.g.

methylation; (143, 144)); the evolution of pathogenicity (e.g. horizontal gene transfer; (72)); and also fungal cellular responses (e.g. signaling pathways and transcription factors; (145, 146)). Therefore, we took an *in silico* approach to better understand the atromentin gene cluster. In collaboration with Dr. Ekaterina Shelest (HKI), we analyzed the atromentin gene clusters and respective promoter regions of 23 atromentin-producing basidiomycetes using the motif tool MEME (147, 148). The rationale behind examining the upstream regions of the genes was that the atromentin genes were co-regulated, and it was presumed that there was a shared transcription factor that recognizes similar DNA motifs, as this is a feature in other fungal natural product gene clusters (149). A search using only two of the essential atromentin biosynthesis genes would likely provide no meaningful promoter motif, so the search was bolstered to include 23 orthologous atromentin gene clusters (103, 150-152). This first and foremost showed high conservation of the gene cluster in and of itself, even in distantly related species (manuscript, 2.4.). Supporting the clusters' conservation, the promoter regions of the *NPS* (nucleotide sequence) followed essentially the same evolutionary path as their cognate *NPS* (amino acid sequence) as determined by tanglegrams from independently curated trees (manuscript, 2.4.). MEME searches showed that within the clusters there was a common promoter motif in *NPS* and *AMT* which was absent in almost all cases for the *ADH*, and two more motifs were observed only in the gene clusters for ectomycorrhizal fungi (manuscripts, 2.3. and 2.4.). Therefore, the combined results suggested that *NPS* and *AMT* were co-regulated, and that there may be additional regulatory mechanisms like co-transcription factors. This was congruent with qRT-PCR results and dissimilar pigment induction, respectively (manuscripts, 2.3. and 2.4.). In addition, mycorrhizae appeared to have duplication events of their *NPS*s like in *P. involutus* (55) and *Suillus luteus* (153). The results of dissimilar pigment induction by fungal lifestyle

appeared to parallel the current hypotheses that saprophytes are more competitive in nature than ectomycorrhizae. For example, ectomycorrhizae associate with more bacteria than do saprophytes and ectomycorrhizae allow for biofilm formation on their hyphae, *e.g.*, ectomycorrhizae appear more passive to prokaryotes (154-156). This may be due to the competitive nature of saprophytes for a carbon source, as they do not have a plant partner with whom to exchange nutrients (4).

The amount of research on regulatory mechanisms of natural products for ascomycetes outpaces that for basidiomycetes. For example, *in vitro* and *in vivo* evidence for basidiomycete transcription factors in natural product regulation is essentially undescribed when compared to ascomycetes. Transcription factors generally recognize specific sequences of DNA (“motifs”) and are primary regulatory proteins that control gene expression (157), thus investigation of said proteins can assist in natural product bioprospecting and understanding a cell’s regulatory systems. As a unique example for basidiomycete natural product regulation, a putative transcriptional gene, termed *urbs1* and annotated as a zinc-like GATA-binding transcription factor, was identified in *Ustilago maydis*, a widely-studied and uniquely genetically tractable basidiomycete. A genetic knockout of *urbs1* caused constitutive production of a siderophore under conditions that would normally suppress its production (158). Here, however, there was no direct evidence to verify the regulatory protein. Within this pathway for siderophore regulation and production, there is also the first catalysis step of a hydroxylation of L-ornithine by an L-ornithine N5-oxygenase (Sid1; (159)). There is evidence for binding of *urbs1* to a distal promoter motif of *sid1* (at least to one of the two G/TGATAA sequences; (160, 161)). The binding of the transcriptional repressor Urbs1, however, does not completely repress siderophore production. A ‘DNA looping’ notion that Urbs1 stretches across the promoter regions by binding to distal and proximal GATA sequences was

proposed; this would block other yet-to-be described transcription factors that are required for transcription. This provided an exemplar and rare insight into basidiomycete natural product gene regulation. This may draw parallels to the possibility of co-transcriptional regulation of atromentin biosynthesis because there exists also multiple (distant) motifs preceding the atromentin synthetase gene.

A more prominent example of a well described transcription factor involved in secondary metabolite production, albeit for ascomycetes, is AfIR that binds to known palindromic promoter sequences (5'-TCG(N₅)GCA) of clustered genes and controls the regulation of aflatoxin and sterigmatocystin in *Aspergillus* spp. (162). AfIR is a Zn(II)₂Cys₆ protein. Indeed, the motif searches preceding the atromentin synthetase genes identified a conserved palindromic sequence making this site a very plausible stretch of DNA to where a homodimeric transcription factor would bind. AfIR as well as many other well-described transcription factors involved in HC-toxin, penicillin and trichothecene production are pathway-specific transcription factors. In the case of atromentin production, it is likely that there exists a shared transcription factor that is not only pathway-specific (*i.e.*, it positively only activates atromentin production), but is part of a global regulatory system (*i.e.*, nutrition and bacterial cues overlap). This parallels to other well-described Cys₂His₂ zinc finger global transcription factors like CreA, AreA or PacC that co-regulate carbon, nitrogen or pH, respectively, alongside the aforementioned secondary metabolites of aflatoxin, sterigmatocystin, gibberellin, and penicillin (163). Much research was devoted to understanding the regulatory processes of these harmful or helpful secondary metabolites, which was facilitated by the genetic tractability of the examined fungi. Hopefully these regulatory processes for basidiomycetes will someday be equally understood by, for example, utilizing the genetic tool-kit of *Ustilago* spp. or *Aspergillus* spp. for recombinant production and manipulation of atromentin biosynthesis.

The three larger families of fungal transcription factors are the 'C₆ Zn cluster,' 'C₂H₂ Zn finger' and 'HD-like' proteins (146). Canonically, the former is a fungal-type N-terminal cysteine-rich protein that requires zinc to bind to DNA sequences, and the second is a protein containing repeating cysteine-histidine motifs that, with zinc, bind to DNA. In fact, the DNA motifs to which transcription factors bind can be inferred from the amino acid sequence of the transcription factor's DNA binding domain (157). This includes predictions for fungi and especially the well-studied yeast *Saccharomyces cerevisiae*. This algorithm is a very useful tool because only ~1% of eukaryotic transcription factors actually have verified DNA binding motifs. That said, the Zn family has progressively increased its distribution during the evolution of fungi, and this family is considered the most common family that regulates fungal gene clusters (146, 162). A preliminary examination of significantly up-regulated genes from *S. lacrymans* – *B. subtilis* RNA-seq data showed three transcription factor gene candidates (unpublished, 3.1.). One is annotated 'Zn(2)-Cys(6)' and two are annotated 'C₂H₂-type.' Therefore, the Zn family is highly plausible to be responsible for the regulation of atromentin biosynthesis.

Beyond transcription factors, there is a similar lack of evidence describing a global regulator, like LaeA (a methyltransferase-domain protein involved in regulating many processes like secondary metabolism and development) in basidiomycetes, although, for example, Velvet domain-containing protein homologs (proteins associated with LaeA) have been noted in *Coprinopsis cinerea* as well as in most of the fungal kingdom (164-166). For atromentin production, it was clear that there were overlapping stimulants for pigment production (both nitrogen and bacteria), and thus this was indicative of shared regulator proteins. Further support comes from the fact that the atromentin gene cluster contains no regulatory protein genes. Shared

regulatory processes parallel a few examples, such as the multi-stimulant production of bikaverin from *Fusarium fujikuroi* (167) and sterigmatocystin in *Aspergillus* spp. (166).

Delving even further and examining epigenetics, which is a 'higher-order' regulatory system that can govern transcription by altering DNA accessibility, provides further insight into natural product production. For example, chromatin remodeling alters the biosynthesis of secondary metabolites like penicillin, sterigmatocystin, and terrequinone A in *Aspergillus nidulans* (168). This was especially evident for the first time during fungal co-incubations when the intimate interaction between *Aspergillus nidulans* and *Streptomyces rapamycinicus* led to the induction of an otherwise silent gene cluster to produce polyketides (123) and led to the bacteria-dependent reorganization of the Saga-Ada complex (*i.e.*, increased histone acetylation via histone acetyltransferases; (169)). Similar results from a co-culture using *Aspergillus fumigatus* and the same bacterium were also found (170). In both cases, it was observed that there was a global epigenetic response in the fungal partner. This highlighted that such microbial communications have a broader impact on the interacting partner than merely activating one natural product gene cluster. Chemical epigenetic modifiers can also lead to the production of secondary metabolites that were otherwise not produced under axenic laboratory conditions. These chemicals can provide an additional inexpensive tool to unleash cryptic natural products. As an example, the introduction of 5-azacytidine, which disrupts DNA methylation, to the ascomycete *Diatrype* sp. led to the isolation of two new glycosylated polyketides (171). Here, autoclaved *E. coli* also induced production of these compounds. These results highlight the importance of modifying axenic laboratory growth conditions, including use of environmental cues. As a last epigenetic topic, methylation of promoters and genes is also an epigenetic feature for fungal gene cluster regulation

(143, 149). Use of the atromentin gene cluster may facilitate the understanding of basidiomycete epigenetic regulation. Overall, motif searches using genetically intractable basidiomycetes provided first-hand evidence of widely conserved basidiomycete promoter sequences that are likely involved in secondary metabolite biosynthesis, and may also be involved in global regulatory processes.

Three other topics on the peculiarities of the atromentin gene cluster are worthwhile to discuss: the assembly of gene clusters, glycoside hydrolase genes, and stress transcriptional elements. There are three speculated evolutionary routes to assemble gene clusters: i) horizontal gene transfer (HGT) of an existing cluster from one genome to the next; ii) a cluster duplication event from an ancestor; and iii) *de novo* assembly of genes in a genome into a cluster (172). After a gene cluster acquisition or formation, a further alteration of the cluster is possible, e.g., single nucleotide polymorphism of its genes, gene gain/loss, complete cluster loss, fusion of two clusters, idiomorphic cluster arrangements on different alleles, or the mobilization of the whole cluster (these phenomena were well described for the secondary metabolite clusters in *Aspergillus fumigatus*; (173)). HGT events of fungal gene clusters were described, and are speculated to have either derived from prokaryotes or fungi and possibly even via hyphal anastomoses (174-176). HGT is usually a transfer of contiguous fragments of DNA, and the “selfish operon model” states that transfer of such clustered arrangements is beneficial for the survival of the gene cluster (177). This would be an alternative to pass on a set of important genes to confer an evolutionary advantage to the organism (174). Such an evolutionary advantage can be observed from two examples where natural product gene clusters have been presumably transferred by HGT. The genome of the pathogenic fungus

Mycosphaerella populorum contains a HGT-obtained PKS-NRPS hybrid which is implicated in its evolution to become pathogenic in order to infect poplar (72). Secondly, the cluster that confers for the biosynthesis of the phytohormone gibberellic acid is presumed to be spread to different fungi by HGT (130).

One could speculate that the atromentin cluster may have had HGT events. For the atromentin gene cluster, not only is the cluster well conserved, the promoters are similarly conserved and evolved with their respective genes. This is also the case for the unessential alcohol dehydrogenase gene. There is a possibility that transposable elements (TE) flank the clusters, and TE are described to flank HGT clusters (72). Also, earlier-diverging brown rotters showed complete clusters, whereas in the later-diverging *Paxillaceae*, there were many duplication events of the atromentin synthetase genes including with their promoters, in addition to disruption of the gene cluster and loss of function of some atromentin synthetases. The level of aforementioned conservation, especially for the promoters, also extends to two unrelated atromentin-producing basidiomycetes that have a disrupted cluster, similar to *Paxillaceae*. The progressive 'disorder' of the atromentin gene cluster may parallel the evolutionary history of the persistent gene cluster responsible for HC-toxin. The NRPS-derived HC-toxin is produced by the plant pathogenic fungus *Cochliobolus carbonum* and the fungus *Alternaria jesenskae* (174, 178). Here, the NRPS gene cluster was presumed to have been transferred to *Cochliobolus* via HGT as a complete cluster, and at some point *A. jesenskae* received the cluster from *Cochliobolus* by HGT. Divergent *Cochliobolus* species also show disrupted clusters and duplication events. Interesting to note, however, that irrespective of where the gene would lie in the chromosome, the transcription factors should still regulate HC-toxin production, as would be the case for redundant atromentin production via conserved promoters. Conversely, if one assumed vertical transmission of the genes

then one would expect an evolution of the promoters of the atromentin synthetase genes, especially for the divergent basidiomycetes. This was not the case for the conserved motifs. Such promoter conservation could have been due to HGT or such a strong selective pressure on the motifs that point mutations were not permitted or were in fact eliminated. At the moment, it remains uncertain whether the cluster was transferred individually (e.g., HGT after speciation), or whether the cluster was there before speciation from a common ancestor and the cluster was merely well preserved with progressive rearrangements.

Concerning the second topic, an additional interesting observation was made when collecting data from the various atromentin gene clusters. It was observed that a glycoside hydrolase gene was usually located near the atromentin gene cluster. Variegatic acid is speculated to be involved in the initial attack of wood (92). It is known that glycoside hydrolases are also involved but at a later stage (92). Both qRT-PCR and RNA-seq data congruently supported the notion that the adjacent glycoside hydrolase gene was not co-regulated with the atromentin synthetase gene during co-incubation with bacteria. This is thus congruent with the current model of staggered, delayed induction. This, though, assumes that induction by bacteria is related to the fungus' attack of wood, which could be based on the aforementioned RNA-seq data. Although the gene location may not be coincidental, at the moment it is only speculative, and there is the possibility that the pigment response has no relation to the breakdown of plant material.

Lastly, stress-related transcriptional elements are known to be involved in transcription. We searched for ungapped motifs preceding the atromentin genes; however, we did not search for other stress-related transcriptional elements. Such known transcriptional elements are putative stress response elements (STRE),

metal response elements (MRE), xenobiotic response elements (XRE), heat shock element (HSE), antioxidant response elements (ARE), and AP1-binding elements (TRE). These were investigated in the promoters of stress-induced quinone reductases in the brown rotter *Gloeophyllum trabeum* using special software (179, 180). Such drawbacks, though, come from several avenues: i) these motifs are usually very short which generally leads to many insignificant motifs; ii) there is no basidiomycete-supported database of known stress elements; and iii) popular tools like TomTom (181) for cross-checking newly identified motifs against a database of transcription factor-associated motifs leads to, again, uncertain results due to lack of verified basidiomycete data. Therefore, although interesting to note that stress-related elements may exist and could provide clues to the reason behind multi-stimulated atromentin regulation, the current knowledge gap favors other *in silico* approaches.

The combined results show that the atromentin gene cluster is a good model to further investigate natural product regulation in basidiomycetes. This is because: i) gene induction was possible, in particular by inter-kingdom interactions; ii) the induction was able to be modulated; and iii) the gene cluster and promoter motifs were highly conserved in at least 23 basidiomycetes. Additionally, the fungal-derived pigments showed the potential to impact the basidiomycete's surrounding community. Further comprehension of fungal natural product regulation and biosynthesis will also further advance our understanding of pharmacologically relevant compounds and pathobiology. Successful advancements will combine both generated sequence data and complementary bench work to identify global regulatory proteins, epigenetic factors, transcription factors, and signaling transduction pathways in basidiomycetes.

5. References

1. O'Brien HE, Parrent JL, Jackson JA, Moncalvo JM, & Vilgalys R (2005) Fungal community analysis by large-scale sequencing of environmental samples. *Appl Environ Microbiol* 71(9):5544-5550.
2. Frohlich-Nowoisky J, *et al.* (2012) Biogeography in the air: fungal diversity over land and oceans. *Biogeosciences* 9(3):1125-1136.
3. Stajich JE, *et al.* (2009) The fungi. *Curr Biol* 19(18):R840-845.
4. Pellitier PT & Zak DR (2017) Ectomycorrhizal fungi and the enzymatic liberation of nitrogen from soil organic matter why evolutionary history matters. *New Phytol.* 10.1111/nph.14598.
5. Zhou ZY & Liu JK (2010) Pigments of fungi (macromycetes). *Nat Prod Rep* 27(11):1531-1570.
6. Fleming A (1929) On the Antibacterial Action of Cultures of a *Penicillium*, with Special Reference to their Use in the Isolation of *B. influenzae*. *Br J Exp Pathol* 10(3):226–236.
7. Grigoriev IV, *et al.* (2011) Fueling the future with fungal genomics. *Mycology* 2(3):192-209.
8. Grigoriev IV, *et al.* (2014) MycoCosm portal: gearing up for 1000 fungal genomes. *Nucleic Acids Res* 42(Database issue):D699-704.
9. Stadler M & Hoffmeister D (2015) Fungal natural products-the mushroom perspective. *Front Microbiol* 6:127.
10. Nielsen KF & Larsen TO (2015) The importance of mass spectrometric dereplication in fungal secondary metabolite analysis. *Front Microbiol* 6:71.

11. Henke MT & Kelleher NL (2016) Modern mass spectrometry for synthetic biology and structure-based discovery of natural products. *Nat Prod Rep* 33(8):942-950.
12. Sugano SS, *et al.* (2017) Genome editing in the mushroom-forming basidiomycete *Coprinopsis cinerea*, optimized by a high-throughput transformation system. *Sci Rep* 7(1):1260.
13. Schmidt-Dannert C (2016) Biocatalytic portfolio of Basidiomycota. *Curr Opin Chem Biol* 31:40-49.
14. Gelber IB, de Vries RP, & Tsang A (2017) Microbial Interactions. *Fungal Genet Biol* 102:1-3.
15. Bertrand S, *et al.* (2014) Metabolite induction via microorganism co-culture: A potential way to enhance chemical diversity for drug discovery. *Biotechnology Advances* 32(6):1180-1204.
16. Hartmann T (2008) The lost origin of chemical ecology in the late 19th century. *Proc Natl Acad Sci U S A* 105(12):4541-4546.
17. Jones CG & Firn RD (1991) On the Evolution of Plant Secondary Chemical Diversity. *Philosophical Transactions of the Royal Society of London Series B-Biological Sciences* 333(1267):273-280.
18. Firn RD & Jones CG (2009) A Darwinian view of metabolism: molecular properties determine fitness. *J Exp Bot* 60(3):719-726.
19. O'Brien J & Wright GD (2011) An ecological perspective of microbial secondary metabolism. *Curr Opin Biotechnol* 22(4):552-558.
20. Romero D, Traxler MF, Lopez D, & Kolter R (2011) Antibiotics as Signal Molecules. *Chem Rev* 111(9):5492-5505.
21. Arnison PG, *et al.* (2013) Ribosomally synthesized and post-translationally modified peptide natural products: overview and

- recommendations for a universal nomenclature. *Nat Prod Rep* 30(1):108-160.
22. Moss MO (2001) *Fungal Metabolites* (John Wiley & Sons, Ltd.).
 23. Harvey AL, Edrada-Ebel R, & Quinn RJ (2015) The re-emergence of natural products for drug discovery in the genomics era. *Nat Rev Drug Discov* 14(2):111-129.
 24. Soukup AA, Keller NP, & Wiemann P (2016) Enhancing Nonribosomal Peptide Biosynthesis in Filamentous Fungi. *Methods Mol Biol* 1401:149-160.
 25. Walsh CT, Brien RVO, & Khosla C (2013) Nonproteinogenic Amino Acid Building Blocks for Nonribosomal Peptide and Hybrid Polyketide Scaffolds. *Angewandte Chemie-International Edition* 52(28):7098-7124.
 26. Strieker M, Tanovic A, & Marahiel MA (2010) Nonribosomal peptide synthetases: structures and dynamics. *Curr Opin Struct Biol* 20(2):234-240.
 27. Fricke J, Blei F, & Hoffmeister D (2017) Enzymatic Synthesis of Psilocybin. *Angew Chem Int Ed Engl* 56(40):12352-12355.
 28. Kosentka P, *et al.* (2013) Evolution of the toxins muscarine and psilocybin in a family of mushroom-forming fungi. *PLoS One* 8(5):e64646.
 29. Chen H & Du L (2016) Iterative polyketide biosynthesis by modular polyketide synthases in bacteria. *Appl Microbiol Biotechnol* 100(2):541-557.
 30. Brandt P, Garcia-Altare M, Nett M, Hertweck C, & Hoffmeister D (2017) Induced Chemical Defense of a Mushroom by a Double-Bond-Shifting Polyene Synthase. *Angew Chem Int Ed* 56(21):5937-5941.

31. Heddergott C, Calvo AM, & Latge JP (2014) The volatome of *Aspergillus fumigatus*. *Eukaryot Cell* 13(8):1014-1025.
32. Arcamone F, *et al.* (1969) Adriamycin, 14-hydroxydaunomycin, a new antitumor antibiotic from *S. peuceetius* var. *caesius*. *Biotechnol Bioeng* 11(6):1101-1110.
33. Scharf DH, *et al.* (2012) Biosynthesis and function of gliotoxin in *Aspergillus fumigatus*. *Appl Microbiol Biotechnol* 93(2):467-472.
34. Baccile JA, *et al.* (2016) Plant-like biosynthesis of isoquinoline alkaloids in *Aspergillus fumigatus*. *Nat Chem Biol* 12(6):419-424.
35. van der Velden NS, *et al.* (2017) Autocatalytic backbone N-methylation in a family of ribosomal peptide natural products. *Nat Chem Biol*.
36. Sterner O, Etzel W, Mayer A, & Anke H (1997) Omphalotin, a new cyclic peptide with potent nematocidal activity from *Omphalotus olearius*. II. Isolation and structure determination. *Natural Product Letters* 10(1):33-38.
37. Sehgal SN, Baker H, & Vezina C (1975) Rapamycin (AY-22,989), a new antifungal antibiotic. II. Fermentation, isolation and characterization. *J Antibiot (Tokyo)* 28(10):727-732.
38. Aparicio JF, *et al.* (1996) Organization of the biosynthetic gene cluster for rapamycin in *Streptomyces hygroscopicus*: analysis of the enzymatic domains in the modular polyketide synthase. *Gene* 169(1):9-16.
39. Keating TA, *et al.* (2001) Chain termination steps in nonribosomal peptide synthetase assembly lines: directed acyl-S-enzyme breakdown in antibiotic and siderophore biosynthesis. *Chembiochem* 2(2):99-107.

40. Bloudoff K & Schmeing TM (2017) Structural and functional aspects of the nonribosomal peptide synthetase condensation domain superfamily: discovery, dissection and diversity. *Biochim Biophys Acta* 1865(11 Pt B):1587-1604.
41. Lackner G, Bohnert M, Wick J, & Hoffmeister D (2013) Assembly of melleolide antibiotics involves a polyketide synthase with cross-coupling activity. *Chem Biol* 20(9):1101-1106.
42. Gao X, *et al.* (2012) Cyclization of fungal nonribosomal peptides by a terminal condensation-like domain. *Nat Chem Biol* 8(10):823-830.
43. Kalb D, Lackner G, & Hoffmeister D (2014) Functional and phylogenetic divergence of fungal adenylate-forming reductases. *Appl Environ Microbiol* 80(19):6175-6183.
44. Brandenburger E, *et al.* (2016) Multi-genome analysis identifies functional and phylogenetic diversity of basidiomycete adenylate-forming reductases. *Fungal Genet Biol.*
45. Xu HY, Andi B, Qian JH, West AH, & Cook PF (2006) The alpha-amino adipate pathway for lysine biosynthesis in fungi. *Cell Biochemistry and Biophysics* 46(1):43-64.
46. Ehmann DE, Gehring AM, & Walsh CT (1999) Lysine biosynthesis in *Saccharomyces cerevisiae*: mechanism of alpha-amino adipate reductase (Lys2) involves posttranslational phosphopantetheinylation by Lys5. *Biochemistry* 38(19):6171-6177.
47. Pospiech A, Bietenhader J, & Schupp T (1996) Two multifunctional peptide synthetases and an O-methyltransferase are involved in the biosynthesis of the DNA-binding antibiotic and antitumour agent

- saframycin Mx1 from *Myxococcus xanthus*. *Microbiology* 142 (Pt 4):741-746.
48. Geib E, *et al.* (2016) A Non-canonical Melanin Biosynthesis Pathway Protects *Aspergillus terreus* Conidia from Environmental Stress. *Cell Chem Biol* 23(5):587-597.
49. Schneider P, Bouhired S, & Hoffmeister D (2008) Characterization of the atromentin biosynthesis genes and enzymes in the homobasidiomycete *Tapinella panuoides*. *Fungal Genet Biol* 45(11):1487-1496.
50. Wackler B, *et al.* (2011) Ralfuranone biosynthesis in *Ralstonia solanacearum* suggests functional divergence in the quinone synthetase family of enzymes. *Chem Biol* 18(3):354-360.
51. Pauly J, Nett M, & Hoffmeister D (2014) Ralfuranone Is Produced by an Alternative Aryl-Substituted gamma-Lactone Biosynthetic Route in *Ralstonia solanacearum*. *J Nat Prod* 77(8):1967-1971.
52. Brachmann AO, Forst S, Furgani GM, Fodor A, & Bode HB (2006) Xenofuranones A and B: phenylpyruvate dimers from *Xenorhabdus szentirmaii*. *J Nat Prod* 69(12):1830-1832.
53. Schuffler A, Liermann JC, Opatz T, & Anke T (2011) Elucidation of the biosynthesis and degradation of allantofuranone by isotopic labelling and fermentation of modified precursors. *Chembiochem* 12(1):148-154.
54. Balibar CJ, Howard-Jones AR, & Walsh CT (2007) Terrequinone A biosynthesis through L-tryptophan oxidation, dimerization and bisprenylation. *Nat Chem Biol* 3(9):584-592.

55. Braesel J, *et al.* (2015) Three redundant synthetases secure redox-active pigment production in the basidiomycete *Paxillus involutus*. *Chem Biol* 22(10):1325-1334.
56. Wackler B, Lackner G, Chooi YH, & Hoffmeister D (2012) Characterization of the *Suillus grevillei* quinone synthetase GreA supports a nonribosomal code for aromatic alpha-keto acids. *Chembiochem* 13(12):1798-1804.
57. Tauber JP, Schroeckh V, Shelest E, Brakhage AA, & Hoffmeister D (2016) Bacteria induce pigment formation in the basidiomycete *Serpula lacrymans*. *Environ Microbiol* 18(12):5218-5227.
58. Gill M & Steglich W (1987) Pigments of fungi (Macromycetes). *Prog Chem Org Nat Prod* 51:1-317.
59. Hermann R (1980) Untersuchungen zur Konstitution, Synthese und Biosynthese von Pilzfarbstoffen. (Rheinische Friedrich-Wilhelms-Universität Bonn, Germany).
60. Schneider P, Weber M, Rosenberger K, & Hoffmeister D (2007) A one-pot chemoenzymatic synthesis for the universal precursor of antidiabetes and antiviral bis-indolylquinones. *Chem Biol* 14(6):635-644.
61. Roth K (2015) Pilzragout nach Chemiker Art. *Chemie in unserer Zeit* 49(3):196–212.
62. Frisvad JC, Andersen B, & Thrane U (2008) The use of secondary metabolite profiling in chemotaxonomy of filamentous fungi. *Mycological Research* 112:231-240.
63. Welti S, *et al.* (2015) Oxygenated lanostane-type triterpenes profiling in laccate *Ganoderma* chemotaxonomy. *Mycological Progress* 14(7).

64. Davoli P & Weber RW (2002) Simple method for reversed-phase high-performance liquid chromatographic analysis of fungal pigments in fruit-bodies of Boletales (Fungi). *J Chromatogr A* 964(1-2):129-135.
65. Thörner W (1878) Ueber einen in einer Agaricus-Art vorkommenden chinonartigen Körper. *Ber. Dtsch. Chem. Ges.* 11:533– 535.
66. Gill M (1994) Pigments of fungi (Macromycetes). *Nat Prod Rep* 11(1):67-90.
67. Gill M (2003) Pigments of fungi (Macromycetes). *Nat Prod Rep* 20(6):615-639.
68. Gruber G (2002) Isolierung und Strukturaufklärung von chemotaxonomisch relevanten Sekundärmetaboliten aus höheren Pilzen, insbesondere aus der Ordnung der Boletales. Dissertation (Ludwig-Maximilians-Universität München, München).
69. Netzker T, *et al.* (2015) Microbial communication leading to the activation of silent fungal secondary metabolite gene clusters. *Front Microbiol* 6:299.
70. Spiteller P (2015) Chemical ecology of fungi. *Nat Prod Rep* 32(7):971-993.
71. Halbwachs H, Simmel J, & Bassler C (2016) Tales and mysteries of fungal fruiting: How morphological and physiological traits affect a pileate lifestyle. *Fungal Biology Reviews* 30(2):36-61.
72. Dhillon B, *et al.* (2015) Horizontal gene transfer and gene dosage drives adaptation to wood colonization in a tree pathogen. *Proc Natl Acad Sci U S A* 112(11):3451-3456.

73. Edwards RL & Elsworthy GC (1967) Variegatic acid, a new tetronic acid responsible for the blueing reaction in the fungus *Suillus (boletus) variegatus* (Swartz ex Fr.) *Chem. Commun. (London)* 0:373b-374.
74. Kögl F & Deijs WB (1935) Untersuchungen über Pilzfarbstoffe XI. Über Boletol, den Farbstoff der blaue entlaufenden Boleten. *Liebigs Annalen der Chemie* 515(10).
75. Nelsen SF (2010) Bluing components and other pigments of boletes. *Fungi* 3(4):11-14.
76. Zhou Q (2010) Natural Diterpene and Triterpene Quinone Methides: Structures, Synthesis, and Biological Potentials. *ChemInform.* 41(10).
77. Besl H, Krump CH, & Schefcsik M (1987) Die Wirkung von Pilzfruchtkörpern auf Drosophila-Maden. *Zeitschrift für Mykologie* 53(2):273-282.
78. Besl H & Blumreisinger M (1983) Die Eignung von Drosophila melanogaster zur Untersuchung der Anfälligkeit Höherer Pilze gegenüber Madenfrass. *Zeitschrift für Mykologie* 49(2):165-170.
79. Spiteller P (2008) Chemical defence strategies of higher fungi. *Chemistry* 14(30):9100-9110.
80. Mueller SO, *et al.* (1999) Occurrence of emodin, chrysophanol and physcion in vegetables, herbs and liquors. Genotoxicity and anti-genotoxicity of the anthraquinones and of the whole plants. *Food Chem Toxicol* 37(5):481-491.
81. Schwenk D, *et al.* (2014) Injury-induced biosynthesis of methyl-branched polyene pigments in a white-rotting basidiomycete. *J Nat Prod* 77(12):2658-2663.

82. Lang M, Spiteller P, Hellwig V, & Steglich W (2001) Stephanosporin, a "Traceless" Precursor of 2-Chloro-4-nitrophenol in the Gasteromycete *Stephanospora caroticolor*. *Angew Chem Int Ed* 40(9):1704-1705.
83. Holighaus G & Rohlf M (2016) Fungal allelochemicals in insect pest management. *Appl Microbiol Biotechnol* 100(13):5681-5689.
84. Miethke M & Marahiel MA (2007) Siderophore-based iron acquisition and pathogen control. *Microbiol Mol Biol Rev* 71(3):413-451.
85. Neilands JB (1952) A Crystalline Organo-Iron Pigment from a Rust Fungus (*Ustilago-Sphaerogena*). *Journal of the American Chemical Society* 74(19):4846-4847.
86. Garibaldi JA & Neilands JB (1955) Isolation and Properties of Ferrichrome-A. *Journal of the American Chemical Society* 77(9):2429-2430.
87. Welzel K, Einfeld K, Antelo L, Anke T, & Anke H (2005) Characterization of the ferrichrome A biosynthetic gene cluster in the homobasidiomycete *Omphalotus olearius*. *FEMS Microbiol Lett* 249(1):157-163.
88. Haas H (2014) Fungal siderophore metabolism with a focus on *Aspergillus fumigatus*. *Nat Prod Rep* 31(10):1266-1276.
89. Haas H (2003) Molecular genetics of fungal siderophore biosynthesis and uptake: the role of siderophores in iron uptake and storage. *Applied Microbiology and Biotechnology* 62(4):316-330.
90. Moree WJ, *et al.* (2012) Interkingdom metabolic transformations captured by microbial imaging mass spectrometry. *Proc Natl Acad Sci U S A* 109(34):13811-13816.

91. Rasmussen ML, Shrestha P, Khanal SK, Pometto AL, 3rd, & Hans van Leeuwen J (2010) Sequential saccharification of corn fiber and ethanol production by the brown rot fungus *Gloeophyllum trabeum*. *Bioresour Technol* 101(10):3526-3533.
92. Eastwood DC, *et al.* (2011) The plant cell wall-decomposing machinery underlies the functional diversity of forest fungi. *Science* 333(6043):762-765.
93. Zhu Y, *et al.* (2017) Fungal variegatic acid and extracellular polysaccharides promote the site-specific generation of reactive oxygen species. *J Ind Microbiol Biotechnol* 44(3):329-338.
94. Shah F, *et al.* (2015) Involutin Is an Fe³⁺ Reductant Secreted by the Ectomycorrhizal Fungus *Paxillus involutus* during Fenton-Based Decomposition of Organic Matter. *Appl Environ Microbiol* 81(24):8427-8433.
95. Rineau F, *et al.* (2012) The ectomycorrhizal fungus *Paxillus involutus* converts organic matter in plant litter using a trimmed brown-rot mechanism involving Fenton chemistry. *Environ Microbiol* 14(6):1477-1487.
96. Aumann DC, Clooth G, Stejfan B, & Steglich W (1989) Komplexierung von Caesium-137 durch die Hutfarbstoffe des Maronenrohrlings (*Xevecornus badius*) *Angew. Chem.* 4(495-496).
97. Avery SV (1995) Caesium accumulation by microorganisms: uptake mechanisms, cation competition, compartmentalization and toxicity. *J Ind Microbiol* 14(2):76-84.
98. Kasuga A, Aoyagi Y, & Sugahara T (1995) Antioxidant Activity of Fungus *Suillus bovinus* (L: Fr.) O. Kuntze. *J Food Sci* 60(5):1113-1115.

99. Dörfelt H & Görner H (1989) *Die Welt der Pilze* (Urania-Verlag).
100. Buller AHR (1922) *Researches on Fungi* (Longmans, Green and Co., London).
101. Bleuler-Martinez S, *et al.* (2017) Dimerization of the fungal defense lectin CCL2 is essential for its toxicity against nematodes. *Glycobiology* 27(5):486-500.
102. Kauserud H, *et al.* (2007) Asian origin and rapid global spread of the destructive dry rot fungus *Serpula lacrymans*. *Mol Ecol* 16(16):3350-3360.
103. Brakhage AA & Schroeckh V (2011) Fungal secondary metabolites - Strategies to activate silent gene clusters. *Fungal Genetics and Biology* 48(1):15-22.
104. Wick J, *et al.* (2015) A Fivefold Parallelized Biosynthetic Process Secures Chlorination of *Armillaria mellea* (Honey Mushroom) Toxins. *Appl Environ Microbiol* 82(4):1196-1204.
105. Kukurba KR & Montgomery SB (2015) RNA Sequencing and Analysis. *Cold Spring Harb Protoc* 2015(11):951-969.
106. Singhal N, Kumar M, Kanaujia PK, & Viridi JS (2015) MALDI-TOF mass spectrometry: an emerging technology for microbial identification and diagnosis. *Front Microbiol* 6:791.
107. Giordano W, Avalos J, Cerda-Olmedo E, & Domenech CE (1999) Nitrogen availability and production of bikaverin and gibberellins in *Gibberella fujikuroi*. *Fems Microbiology Letters* 173(2):389-393.
108. Zheng CJ, Sohn MJ, & Kim WG (2006) Atromentin and leucomelone, the first inhibitors specific to enoyl-ACP reductase (FabK) of *Streptococcus pneumoniae*. *J Antibiot (Tokyo)* 59(12):808-812.

109. Huang YT, Onose J, Abe N, & Yoshikawa K (2009) *In vitro* inhibitory effects of pulvinic acid derivatives isolated from Chinese edible mushrooms, *Boletus calopus* and *Suillus bovinus*, on cytochrome P450 activity. *Biosci Biotechnol Biochem* 73(4):855-860.
110. Stanley CE, *et al.* (2014) Probing bacterial-fungal interactions at the single cell level. *Integr Biol (Camb)* 6(10):935-945.
111. Benoit I, *et al.* (2015) *Bacillus subtilis* attachment to *Aspergillus niger* hyphae results in mutually altered metabolism. *Environ Microbiol* 17(6):2099-2113.
112. Reen FJ, Shanahan R, Cano R, O'Gara F, & McGlacken GP (2015) A structure activity-relationship study of the bacterial signal molecule HHQ reveals swarming motility inhibition in *Bacillus atrophaeus*. *Org Biomol Chem* 13(19):5537-5541.
113. Aiyar P, *et al.* (2017) Antagonistic bacteria disrupt calcium homeostasis and immobilize algal cells. *Nat Commun* 8(1):1756.
114. Khalid S, *et al.* (2017) NRPS-derived isoquinolines and lipopeptides mediate antagonism between plant pathogenic fungi and bacteria. *ACS Chem Biol*.
115. Stockli M, *et al.* (2017) *Coprinopsis cinerea* intracellular lactonases hydrolyze quorum sensing molecules of Gram-negative bacteria. *Fungal Genet Biol* 102:49-62.
116. Papadopoulou A & Frazier RA (2004) Characterization of protein-polyphenol interactions. *Trends in Food Science & Technology* 15(3-4):186-190.

117. Kemperman RA, Bolca S, Roger LC, & Vaughan EE (2010) Novel approaches for analysing gut microbes and dietary polyphenols: challenges and opportunities. *Microbiology* 156(Pt 11):3224-3231.
118. Marvasi M, Visscher PT, & Martinez LC (2010) Exopolymeric substances (EPS) from *Bacillus subtilis*: polymers and genes encoding their synthesis. *Fems Microbiology Letters* 313(1):1-9.
119. Connelly MB, Young GM, & Sloma A (2004) Extracellular proteolytic activity plays a central role in swarming motility in *Bacillus subtilis*. *J Bacteriol* 186(13):4159-4167.
120. Seidl V, et al. (2009) Transcriptomic response of the mycoparasitic fungus *Trichoderma atroviride* to the presence of a fungal prey. *Bmc Genomics* 10.
121. Gruber S & Seidl-Seiboth V (2012) Self versus non-self: fungal cell wall degradation in *Trichoderma*. *Microbiology* 158(Pt 1):26-34.
122. Geremia RA, et al. (1993) Molecular characterization of the proteinase-encoding gene, *prb1*, related to mycoparasitism by *Trichoderma harzianum*. *Molecular Microbiology*. 8(3):603-613.
123. Schroeckh V, et al. (2009) Intimate bacterial-fungal interaction triggers biosynthesis of archetypal polyketides in *Aspergillus nidulans*. *Proc Natl Acad Sci U S A* 106(34):14558-14563.
124. Lackner G, Misiek M, Braesel J, & Hoffmeister D (2012) Genome mining reveals the evolutionary origin and biosynthetic potential of basidiomycete polyketide synthases. *Fungal Genet Biol* 49(12):996-1003.

125. Aqueveque P, Anke T, & Sterner O (2002) The himanimides, new bioactive compounds from *Serpula himantoides* (Fr.)Karst. *Zeitschrift Fur Naturforschung C*. 57(3-4):257-262.
126. Hearn MTW, Jones ERH, Pellatt MG, Thaller V, & Turner JL (1973) Natural acetylenes. Part XLII. Novel C7, C8, C9, and C10 polyacetylenes from fungal cultures. *J. Chem. Soc., Perkin Trans. 1*. 5(8):2785-2788.
127. Balibar CJ & Walsh CT (2006) GliP, a multimodular nonribosomal peptide synthetase in *Aspergillus fumigatus*, makes the diketopiperazine scaffold of gliotoxin. *Biochemistry* 45(50):15029-15038.
128. Cramer RA, Jr., et al. (2006) Disruption of a nonribosomal peptide synthetase in *Aspergillus fumigatus* eliminates gliotoxin production. *Eukaryot Cell* 5(6):972-980.
129. Gardiner DM, Cozijnsen AJ, Wilson LM, Pedras MS, & Howlett BJ (2004) The sirodesmin biosynthetic gene cluster of the plant pathogenic fungus *Leptosphaeria maculans*. *Mol Microbiol* 53(5):1307-1318.
130. Schmidt-Dannert C (2015) Biosynthesis of terpenoid natural products in fungi. *Adv Biochem Eng Biotechnol* 148:19-61.
131. Mazur X, Becker U, Anke T, & Sterner O (1996) Two new bioactive diterpenes from *Lepista sordida*. *Phytochemistry* 43(2):405-407.
132. Kawagishi H, Shimada A, Shirai R, & Okamoto K (1994) Erinacines A, B and C, strong stimulators of nerve growth factor (NGF)-synthesis, from the mycelia of *Herichium erinaceum*. *Tetrahedron Letters* 35(10):1569-1572.

133. Gupta R & Chakrabarty SK (2013) Gibberellic acid in plant: still a mystery unresolved. *Plant Signal Behav* 8(9).
134. Munir E, Yoon JJ, Tokimatsu T, Hattori T, & Shimada M (2001) A physiological role for oxalic acid biosynthesis in the wood-rotting basidiomycete *Fomitopsis palustris*. *Proc Natl Acad Sci U S A* 98(20):11126-11130.
135. Kirker G, *et al.* (2017) Synchrotron-based X-ray fluorescence microscopy enables multiscale spatial visualization of ions involved in fungal lignocellulose deconstruction. *Sci Rep* 7:41798.
136. Presley GN, Zhang J, & Schilling JS (2016) A genomics-informed study of oxalate and cellulase regulation by brown rot wood-degrading fungi. *Fungal Genet Biol.*
137. Lah L, *et al.* (2011) The versatility of the fungal cytochrome P450 monooxygenase system is instrumental in xenobiotic detoxification. *Mol Microbiol* 81(5):1374-1389.
138. Plaza DF, Schmieder SS, Lipzen A, Lindquist E, & Kunzler M (2015) Identification of a Novel Nematotoxic Protein by Challenging the Model Mushroom *Coprinopsis cinerea* with a Fungivorous Nematode. *G3 (Bethesda)* 6(1):87-98.
139. Aulinger K, Besl H, Spiteller P, Spiteller M, & Steglich W (2001) Melanocrocin, a polyene pigment from *Melanogaster broomeianus* (Basidiomycetes). *Z Naturforsch C* 56(7-8):495-498.
140. Jaeger RJ & Spiteller P (2010) Mycenaaurin A, an antibacterial polyene pigment from the fruiting bodies of *Mycena aurantiomarginata*. *J Nat Prod* 73(8):1350-1354.

141. Kohler A, *et al.* (2015) Convergent losses of decay mechanisms and rapid turnover of symbiosis genes in mycorrhizal mutualists. *Nat Genet* 47(4):410-415.
142. Watrous J, *et al.* (2012) Mass spectral molecular networking of living microbial colonies. *Proc Natl Acad Sci U S A* 109(26):E1743-1752.
143. Mondo SJ, *et al.* (2017) Widespread adenine N6-methylation of active genes in fungi. *Nat Genet* 49(6):964-968.
144. Tisserant E, *et al.* (2013) Genome of an arbuscular mycorrhizal fungus provides insight into the oldest plant symbiosis. *Proc Natl Acad Sci U S A* 110(50):20117-20122.
145. Corrochano LM, *et al.* (2016) Expansion of Signal Transduction Pathways in Fungi by Extensive Genome Duplication. *Curr Biol* 26(12):1577-1584.
146. Shelest E (2017) Transcription Factors in Fungi: TFome Dynamics, Three Major Families, and Dual-Specificity TFs. *Front Genet* 8:53.
147. Bailey TL, *et al.* (2009) MEME SUITE: tools for motif discovery and searching. *Nucleic Acids Res* 37(Web Server issue):W202-208.
148. Bailey TL & Elkan C (1994) Fitting a mixture model by expectation maximization to discover motifs in biopolymers. *Proc Int Conf Intell Syst Mol Biol* 2:28-36.
149. van der Lee TAJ & Medema MH (2016) Computational strategies for genome-based natural product discovery and engineering in fungi. *Fungal Genet Biol* 89:29-36.
150. Wolf T, Shelest V, Nath N, & Shelest E (2016) CASSIS and SMIPS: promoter-based prediction of secondary metabolite gene clusters in eukaryotic genomes. *Bioinformatics* 32(8):1138-1143.

151. Fischbach MA & Walsh CT (2006) Assembly-line enzymology for polyketide and nonribosomal Peptide antibiotics: logic, machinery, and mechanisms. *Chem Rev* 106(8):3468-3496.
152. Hoffmeister D & Keller NP (2007) Natural products of filamentous fungi: enzymes, genes, and their regulation. *Nat Prod Rep* 24(2):393-416.
153. Shah F, *et al.* (2016) Ectomycorrhizal fungi decompose soil organic matter using oxidative mechanisms adapted from saprotrophic ancestors. *New Phytol* 209(4):1705-1719.
154. de Carvalho MP, Turck P, & Abraham WR (2015) Secondary Metabolites Control the Associated Bacterial Communities of Saprophytic Basidiomycotina Fungi. *Microbes Environ* 30(2):196-198.
155. Guennoc CM, Rose C, Labbe J, & Deveau A (2017) Bacterial Biofilm Formation On Soil Fungi: A Widespread Ability Under Controls. *bioRxiv* 130740.
156. Pent M, Poldmaa K, & Bahram M (2017) Bacterial Communities in Boreal Forest Mushrooms Are Shaped Both by Soil Parameters and Host Identity. *Front Microbiol* 8:836.
157. Weirauch MT, *et al.* (2014) Determination and inference of eukaryotic transcription factor sequence specificity. *Cell* 158(6):1431-1443.
158. Voisard C, Wang J, McEvoy JL, Xu P, & Leong SA (1993) *urbs1*, a gene regulating siderophore biosynthesis in *Ustilago maydis*, encodes a protein similar to the erythroid transcription factor GATA-1. *Mol Cell Biol* 13(11):7091-7100.
159. Mei B, Budde AD, & Leong SA (1993) *sid1*, a gene initiating siderophore biosynthesis in *Ustilago maydis*: molecular

- characterization, regulation by iron, and role in phytopathogenicity. *Proc Natl Acad Sci U S A* 90(3):903-907.
160. An Z, Mei B, Yuan WM, & Leong SA (1997) The distal GATA sequences of the *sid1* promoter of *Ustilago maydis* mediate iron repression of siderophore production and interact directly with Urbs1, a GATA family transcription factor. *EMBO J* 16(7):1742-1750.
161. Basse CW & Farfsing JW (2006) Promoters and their regulation in *Ustilago maydis* and other phytopathogenic fungi. *Fems Microbiology Letters* 254(2):208-216.
162. Yin W & Keller NP (2011) Transcriptional regulatory elements in fungal secondary metabolism. *J Microbiol* 49(3):329-339.
163. Yu JH & Keller N (2005) Regulation of secondary metabolism in filamentous fungi. *Annu Rev Phytopathol* 43:437-458.
164. Plaza DF, Lin CW, van der Velden NS, Aebi M, & Künzler M (2014) Comparative transcriptomics of the model mushroom *Coprinopsis cinerea* reveals tissue-specific armories and a conserved circuitry for sexual development. *BMC Genomics* 15:492.
165. Bayram O & Braus GH (2012) Coordination of secondary metabolism and development in fungi: the velvet family of regulatory proteins. *FEMS Microbiol Rev* 36(1):1-24.
166. Brakhage AA (2013) Regulation of fungal secondary metabolism. *Nat Rev Microbiol* 11(1):21-32.
167. Wiemann P, *et al.* (2009) Biosynthesis of the red pigment bikaverin in *Fusarium fujikuroi*: genes, their function and regulation. *Mol Microbiol* 72(4):931-946.

168. Macheleidt J, *et al.* (2016) Regulation and Role of Fungal Secondary Metabolites. *Annu Rev Genet* 50:371-392.
169. Nutzmann HW, *et al.* (2011) Bacteria-induced natural product formation in the fungus *Aspergillus nidulans* requires Saga/Ada-mediated histone acetylation. *Proc Natl Acad Sci U S A* 108(34):14282-14287.
170. Konig CC, *et al.* (2013) Bacterium induces cryptic meroterpenoid pathway in the pathogenic fungus *Aspergillus fumigatus*. *Chembiochem* 14(8):938-942.
171. Williams RB, Henrikson JC, Hoover AR, Lee AE, & Cichewicz RH (2008) Epigenetic remodeling of the fungal secondary metabolome. *Org Biomol Chem* 6(11):1895-1897.
172. Khaldi N & Wolfe KH (2011) Evolutionary Origins of the Fumonisin Secondary Metabolite Gene Cluster in *Fusarium verticillioides* and *Aspergillus niger*. *Int J Evol Biol* 2011:423821.
173. Lind AL, *et al.* (2017) Drivers of genetic diversity in secondary metabolic gene clusters within a fungal species. *PLoS Biol* 15(11):e2003583.
174. Walton JD (2000) Horizontal gene transfer and the evolution of secondary metabolite gene clusters in fungi: an hypothesis. *Fungal Genet Biol* 30(3):167-171.
175. Khaldi N, Collemare J, Lebrun MH, & Wolfe KH (2008) Evidence for horizontal transfer of a secondary metabolite gene cluster between fungi. *Genome Biol* 9(1):R18.
176. Slot JC & Rokas A (2011) Horizontal transfer of a large and highly toxic secondary metabolic gene cluster between fungi. *Curr Biol* 21(2):134-139.

177. Ballouz S, Francis AR, Lan R, & Tanaka MM (2010) Conditions for the evolution of gene clusters in bacterial genomes. *PLoS Comput Biol* 6(2):e1000672.
178. Wight WD, Labuda R, & Walton JD (2013) Conservation of the genes for HC-toxin biosynthesis in *Alternaria jesenskae*. *BMC Microbiol* 13:165.
179. Cohen R, Suzuki MR, & Hammel KE (2004) Differential stress-induced regulation of two quinone reductases in the brown rot basidiomycete *Gloeophyllum trabeum*. *Applied and Environmental Microbiology* 70(1):324-331.
180. Womble DD (2000) GCG: The Wisconsin Package of sequence analysis programs. *Methods Mol Biol* 132:3-22.
181. Gupta S, Stamatoyannopoulos JA, Bailey TL, & Noble WS (2007) Quantifying similarity between motifs. *Genome Biology* 8(2).

6. Acknowledgments

This work was supported by the Deutsche Forschungsgemeinschaft (DFG)/ Sonderforschungsbereiche (SFB) under the Collaborative Research Center 1127 (phase I) umbrella project. I am appreciative of the special collaborative efforts that were encouraged.

I thank my supervisor, all the collaborators, and technical assistants who made my projects possible: Prof. Dirk Hoffmeister, Dr. Ekaterina Shelest, Dr. Ákos T. Kovács, Dr. Ramses Gallegos-Monterrosa, Dr. Volker Schroeckh, Prof. Axel A. Brakhage, Dr. Christian Matthaeus, Dr. Nico Ueberschaar, Dr. María García-Altare Pérez, Julia Greßler, Christiane Weigel, Dr. Jana Braesel, JGI personnel, Claudius Lenz, Dr. Daniel Braga de Lima, and Andrea Perner. In particular, I would like to express my appreciation to Prof. Hoffmeister for passing on his enthusiasm of the fungal universe and for always being available; to Dr. Shelest for putting up with bombardments of emails (but I suspect it was not so bad because the very last email usually started with, “ignore the previous emails”), and to Dr. Matthaeus for introducing me to the best coffee machine on the campus.

I am forever grateful to my parents for their lifelong support that allowed me to follow any aspiration that I wanted. I am also similarly grateful to my fiancée for her love and support.

In particular, I give a shout out to Daniel, mainly because he understood all meaningful references (“that’s a lot of potatoes!”). I also enjoyed the BBQ sessions and talks with Derek, Jacob, Rob, and Matan. Also, I give a shout out to Jonas who was always curious to learn the armpit of the English language.

Eigenständigkeitserklärung

Hiermit versichere ich, dass mir die Promotionsordnung der Biologisch-Pharmazeutischen Fakultät der Friedrich-Schiller-Universität Jena bekannt ist. Ich habe die vorliegende Dissertation eigenhändig verfasst und dabei weder Textabschnitte aus einer eigenen Prüfungsarbeit oder von dritten ohne Kennzeichnung übernommen. Die von mir verwendeten Hilfsmittel, persönliche Mitteilungen und Quellen sind in der Arbeit gekennzeichnet. Bei der Auswahl und Auswertung von Material sowie bei der Herstellung des Manuskripts haben mich keine anderen, als die in der Danksagung erwähnten Personen unterstützt. Personen, die an der Anfertigung von Publikationen beteiligt waren, sind in der Publikationsliste angegeben. Die Hilfe eines Promotionsberaters habe ich nicht in Anspruch genommen. Ebenso wenig haben Dritte von mir unmittelbar oder mittelbar geldwerte Leistungen erhalten, die im Zusammenhang mit dem Inhalt der vorliegenden Dissertation stehen. Ich habe die Dissertation noch nicht als Prüfungsarbeit für eine staatliche oder andere wissenschaftliche Prüfung eingereicht. Außerdem habe ich weder die gleiche, noch eine in wesentlichen Teilen ähnliche oder eine andere Abhandlung bei einer anderen Hochschule als Dissertation eingereicht.

James Patrick Tauber